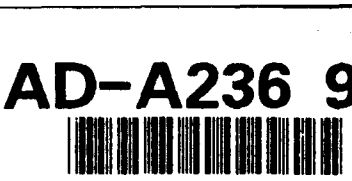

(2)

FINAL TECHNICAL REPORT

for

HIGH FLUX NEUTRAL BEAMS

ONR Contract No. N00014-88-K-0437

July 1, 1988 - March 31, 1990

Principal Investigators

Norman Rostoker, Amnon Fisher and J. Carl Leader

Department of Physics

University of California

Irvine, California 92717

TABLE OF CONTENTS

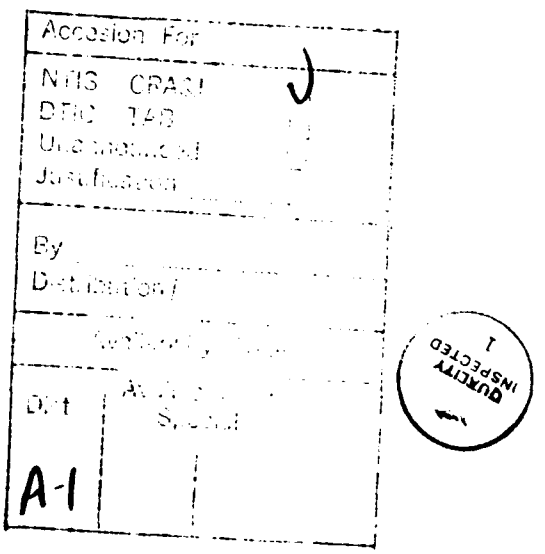

UNIVERSITY OF CALIFORNIA

Irvine

Production of Intense Negative Ion Beams In Magnetically Insulated Diodes

A dissertation submitted in partial satisfaction of the requirements

for the degree of Doctor of Philosophy in Physics

by

Hayim Lindenbaum

Committee in charge:

Professor Norman Rostoker, Chair

Professor Amnon Fisher, Co–Chair

Professor Gregory A. Benford

1988

Contents

List of Tables

List of Figures

Acknowledgements

I wish to thank my dissertation committee, Professors Norman Rostoker, Amnon Fisher, and Gregory Benford, for guiding me so patiently through this work.

I am grateful to all of the Physics Department faculty for their lectures and discussions which have given me the theoretical background necessary for this work, and to all my friend at the UCI plasma beam lab for their daily support and help. Special thanks to Dr. Fan Ruyu with whom I worked hand by hand on this experiment for more than a year.

I am grateful to Prof. Amnon Fisher. His daily interest support and advice made this experiment possible.

I am grateful for the financial support of the University of California Division of Graduate Studies and Research, for whom I worked during this project. I wish to thank the Office of Naval Research and McDonnell Douglas corporation R&D for financial support of this experiment.

Curriculum Vitae

Hayim Lindenbaum

February 16,	1947	Born Hadera, Israel
	1969	B.Sc. in Physics, Technion, Israel Institute of Technology
	1975	M.Sc in Physics, Technion, Israel Institute of Technology
	1988	Ph.D in Physics, University of California, Irvine

Publications

"H^- Ion Source and High Flux Neutral Beams" *International society for optical Engineers SPIE, Innovative Science and Technology Symposium, Los-Angeles(1988).*

"Intense Pulsed Source of Negative Ions" 6^{th} *International Conference on High Power Particle Beams, Kobe(1986).*

ABSTRACT OF THE DISSERTATION

Production of Intense Negative Ion Beams In Magnetically Insulated Diodes

by

Hayim Lindenbaum

Doctor of Philosophy in Physics

University of California, Irvine, 1988

Professor Norman Rostoker, Chair

Professor Amnon Fisher, Co–Chair

A lot of effort has been put in the last few years in development of intense high energy positive ion beams. Ion-beam sources were built for use in inertial confinement fusion,magnetic confinement fusion and beam propagation studies. Most of these ion sources use magnetically insulated diodes. In these diodes a plasma is produced on the anode's surface and ions are extracted and accelerated by a high voltage pulse to produce a beam. Electrons are prevented from reaching the anode by applying a magnetic field in the high voltage gap, thus creating what is called a "magnetic insulation".

Power losses in magnetically insulated diodes led to the suggestion, which was first made by a group at UCI ,that negative ions,produced in the cathode's plasma are responsible for these losses. Preliminary experiments at UCI showed negative ion currents of 10^{-3} times the space charge limited value. A detailed work followed by a group at Sandia National Labs. who studied H^- production

in magnetically insulated transmission lines (MITL) [2 – 4]. These works gave rise to the hope of producing intense beams of H^- ions in high power diodes. Following this approach,a group at the Lebedev institute in Moscow reported a series of experiments in a cylindrical symmetric coaxial magnetically insulated diode,in which H^- ion beams with current densities of $200 A/cm^2$ and energy of a few hundred Kev were produced. They reported that a high voltage prepulse was necessary to get these high current densities. Independent efforts at at Ecole polytechnique in France and at Tomsk to reproduce and understand the Lebedev results have had no success in producing high current densities.

Our purpose was to study the production of intense negative ion beams in magnetically insulated diodes, and to develop an understanding of this process by measuring the ion beam parameters as a function of diode and cathode plasma conditions in different magnetically insulated diodes. We tried a coaxial diode, a racetrack diode and an annular diode. We used the UCI APEX pulse line that has a nominal output of 1MV, 140kA under matched conditions with a pulse length of 50nsec. Negative ion intensity and divergence were measured with Faraday–cups and CR–39 track detectors. Cathode plasma was produced by passive dielectric cathodes and later, by an independent plasma gun. This plasma gun was introduced in order to be able to control cathode plasma parameters and production time.

Negative ion currents had an intensity of a few A/cm^2 with a divergence ranging between a few tenths milliradians for an active TiH_2 plasma gun and 300 milliradians for a passive polyethelene cathode. Negative ions were usually emitted from a few "hot spots" on the cathode surface. These "hot spots" are believed to cause transverse electrical fields in the diode gap responsible for the beam divergence. Mass spectrometry measurements showed that the ion beam consists of mainly H^- ions when using a polyethelene or a TiH_2 cathodes, and mainly of negative carbon ions when using a carbon cathode. About 10% of the negative ions produced were due to residual gas molecules adsorbed on the cathode surface. This was checked by using a bare aluminum cathode. Negative

ion production in the cathode plasma seems to be insensitive to the type of diode used. Beam properties on the other hand, are of course sensitive to diode geometry.

The above results are discussed in connection with other measurements done on magnetically insulated diodes by other groups. The most interesting relation is with neutral particles density measurements done on cathode and anode plasmas. This is because the highest cross section for negative ion production is through a collision of an electron with a highly vibrationally excited neutral molecule. We then also discuss the "hot spot" phenomena in our experiment in connection with a similar phenomena regarding electron emission from a few sites on the cathode surface in magnetically insulated diode. A model is suggested in which negative ions are produced by collision of neutrals and electrons at the low density interface between the cathode plasma and the electron negative charge layer.

Chapter 1 INTRODUCTION

1.1 Background

1.1.1 Significance and uses of negative ion beams.

The development of pulsed power technology during the last 30 years made it possible to produce high intensity ion and neutral particle beams. Machines have been built which can produce very high energy short time pulses. A typical pulse has a voltage of a few megavolts with a duration of a few tens of nanoseconds and a current of tens to hundreds of kiloamperes.

High intensity neutral beams have a broad variety of applications. The main goal towards which the research in this area has been aimed is the production of high intensity neutral beams for fusion purposes. The beam is needed in order to heat a magnetically confined plasma to the 10 keV temperatures required for fusion. A high intensity neutral beam can also be used for directed energy weapon purposes as well as for research in different types of beam propagation and beam–plasma interaction studies.

Much of the research effort in this area has been directed towards producing high intensity positive ion beams and passing them through a neutralizing cell in order to get a high intensity neutral beam. The positive ion beam is usually produced in a magnetically insulated diode. In this types of diode a plasma is produced on the anode surface. Ions are extracted from this plasma and accelerated by a high voltage pulse to produce a beam. Electrons are prevented from reaching the anode by applying a magnetic field in the high voltage gap, thus creating what is called *magnetic insulation.*

Power losses in magnetically insulated diodes led to the suggestion, which was first made by a group at UCI [1], that negative ions produced at the cathode plasma are responsible for these losses. The existence of these ions in the cathode plasma led to the idea of using magnetically insulated diodes for intense negative–ion beam production.

The intense research which was carried out in order to produce positive ion beams brought with it new types of magnetically insulated diodes. People got a better understanding of the physical phenomena occurring at these diodes. Intense positive ion beams with beam intensities of the order of a few thousand ampers per square centimeter have been produced. An excellent review of the research done on positive ion production in magnetically insulated diodes was written by Humpheris [2].

In order to convert the intense positive ion beam to a neutral beam neutralizing cells have been used. The problem with this scheme is that the efficiency of the neutralizing cell is very low for positive ions with energy above 80 keV as can be seen from FIG. 1–1.

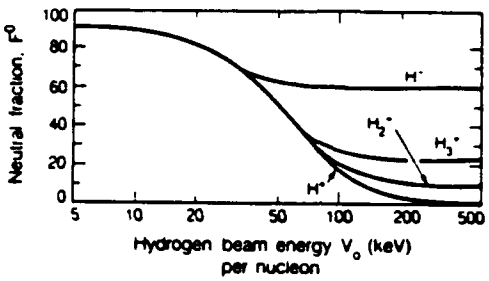

FIG 1–1: Neutralizing gas–cell efficiency for negative hydrogen ion–beam (after Fink [3]).

The binding energy of the outer electron in a hydrogen atom is 13.6 eV while the outer electron in a negative hydrogen ion has a binding energy of 0.7 eV. As we shall see later, it is much simpler and easier to neutralize a negative hydrogen ion, than to do the same for a positive one. It looks thus very attractive to combine the technology of high voltage magnetically insulated diodes with the production of high intensity negative ion beams in order to produce high intensity neutral beams.

1.2 Description of the Experiment

1.2.1 Experimental goal

The objective of the work reported here is to measure the production of negative ion beams in different magnetically insulated diodes configurations. Plasma in these diodes is created close to the cathode surface and negative ions are extracted from it and accelerated via a high voltage (1–2 MeV) short time (50–75 nsec) pulse. Our objective is to identify the favorable conditions for negative ion production. By this we mean the we intend to investigate the effect of cathode dielectric material, cathode shape, presence of a high voltage prepulse or any other factor which could effect the cathode plasma in which these ions are believed to be produced. The effect of cathode plasma parameters could be checked by building an independent plasma gun that could produce the cathode plasma. Plasma parameters, including density, temperature and creation time could be controlled and their effect on negative ion creation be checked. We also intended to see how the diode shape effects negative ion production by working with three different types of magnetically insulated diodes. Physical properties of the beam, including beam divergence, homogeneouty, and ion mass composition were measured. As we shall see later, we tried to measure many other physical phenomena which could clarify the physical picture. These include taking x–ray picture of the dio[illegible], measuring x–ray and visible light intensity as a function of time and takin[illegible]R–39 ion track pictures of the cathode.

The experiments described here have of course the practical goal of producing intense negative ion beams. But they also have the goal of understanding the production mechanizm of negative ions in the cathode plasma. The cathode plasma consists usually of *hot spots* from which high electron currents are drawn. The emission of negative ions might be related to these hot spots. By measuring the intensity of negative ion emission from the cathode surface we can understand better the behaviour of the cathode plasma and the production of negative ions in it.

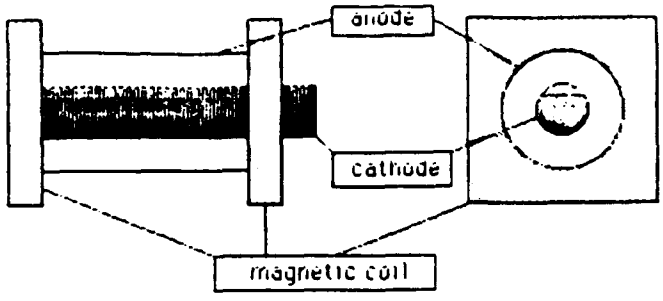

a: Cylindrically symmetric coaxial diode.

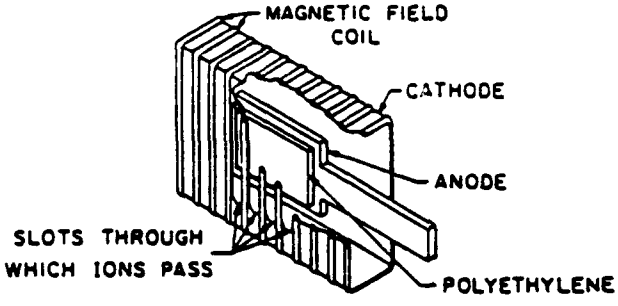

b: Racetrack diode.

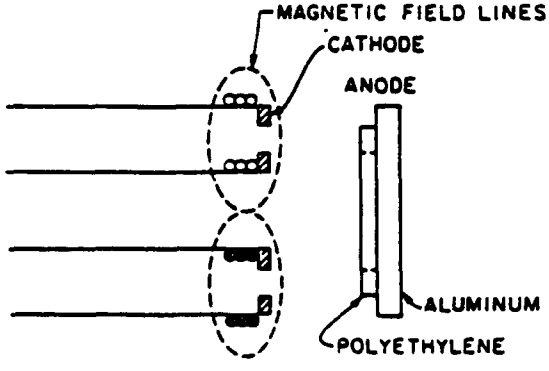

c: Annular diode.

Figure 1–2: Different types of magnetically insulated diodes used in this work.

1.2.2 Experiment description

We studied negative ion beams from three types of magnetically insulated diodes. The first diode is a cylindrically symmetric *coaxial diode*. The diode consists of an inner cathode made of a conducting cylinder coated with dielectric material and an outer wire–mesh cylinder which serves as the anode (see figure 1–2 **a**). The diode was adapted to the UCI APEX pulse line that has a nomonal output of 1 MV 140 kA under matched conditions with a pulse length of 50 nsec. An axial magnetic field of 14 kGauss prevents the electrons from crossing the high–voltage gap. Beam intensity, divergence, and mass composition were traced via a CR–39 track detector. Electrical measurements of the beam current with a Faraday–cup were unsuccessful in this case due to the beam divergence in the vertical direction. Cathodes made of carbon, aluminum and polyethelene coated aluminum with different shapes were tried. CR–39 pictures of the beam at the wire mesh were taken. These pictures were used to check the plasma uniformity and negative ion production in it. Pictures of the diode using an x–ray pinhole camera gave us information about the behavior of the electrons in the diode and the effectiveness of the magnetic insulation.

Another diode configuration we tried is called the *racetrack–diode*. The cathode has a paddle shape and is located at the middle of a wire mesh box which serves as the anode. The same box is used to hold the magnetic field coil turns (see figure 1–2 **b**). Ion beam intensity was measured with a Faraday cup charge collector and track counting using a CR–39 track detector. CR–39 pinhole camera pictures were used to measure beam divergence as well as plasma homogeneity. We tried cathodes made of TiH_2, carbon, and polyethelene covered aluminum. The results indicated that the APEX machine prepulse affects the production of negative ions in the diode. The APEX machine has a prepulse of about 2% when using a resistive supressor, and about 10% when the resistor is disconnected. To simulate the effect of the prepulse we have built a prepulsed plasma generator which produces plasma in the high voltage gap before the high

voltage pulse arrives. Plasma density as well as time of production could be controlled. The plasma gun timing was measured with a light collecting optical fiber connected to a photomultiplier. The plasma gun flashboard cathode has a circuit creating arcs across 120 groves on the cathode surface. We filled this groves with TiH_2 and also tried epoxy filled groves. We put different types of wire meshes in front of the flashboard to see how they effect the plasma homogeneouty as well as negative ion production.

The last type of diode investigated is called an *annular-diode*. Two concentric cylindrical coils produce a radially magnetic field in the anode cathode gap. The anode consists of two coplanar carbon rings attached to one edge of the coils. The cathode consists of another ring spaced parallel to the two carbon rings. All rings are aligned perpendicular to the coils axis (see figure 1–2 **c**). We measured the negative ion production in this diode using a cathode made of carbon brushes and also a polyethelene coated cathode. We then built a prepulsed annular plasma gun and measured the production of negative ions under different plasma parameters and with different types of wire mesh in front of the plasma gun. Ion measuring techniques were very similar to the ones used in the racetrack diode experiment and included Faraday cup charge collectors together with CR–39 track detectors.

1.3 Thesis Outline

We start the thesis by reviewing previous work done on production of intense negative ion beams. This review is the subject of chapter 2. The same chapter also reviews related work like research on negative ion production in transmission lines or discharge negative ion sources. Chapter 3 deals with general experimental techniques used. These include Faraday cup measurements, CR–39 track detectors, Langmuir probe measurements of plasma parameters, and x–ray emission measurements. This chapter also includes a description of the APEX machine together with the vacuum system and diode high voltage and current measurements. Chapter 4 describes the prepulsed plasma gun. It contains a

description of the electronic circuit, the construction of the flashboard cathode and the light measuring system used mainly to measure the plasma gun timing.

Chapters 5,6 and 7 describe experiments on three types of magnetically insulated diodes. Chapter 5 describes the experiments done on a cylindrically symmetric coaxial diode. The chapter contains a discussion of the physical phenomena occurring in this diode and how they could effect the production of negative ions in it. Chapter 6 contains the results of experiments done on a racetrack type diode with a discussion, and chapter 7 contains results and discussion for an annular diode.

Chapter 8 deals with models that could explain how negative ions are produced and accelerated in magnetically insulated diodes. The chapter explains how the cathode plasma is produced through what is called *explosive emission* during which negative ions can be created. It explains how similar phenomena occur in an arc discharge (which is the phenomena occurring in the prepulsed plasma gun). It also deals with the conditions under which negative ions exist in a plasma. Chapter 9 summarizes the conclusions of this thesis.

Chapter 2 REVIEW OF PREVIOUS WORK

2.1 Introduction

This chapter contains a review of negative ion physics and production. It begins with a general description of the properties of negative ions and then describes what are the main physical mechanisms through which negative ions are produced and destroyed. Then there are a few examples of discharge type negative ion sources.

We next describe the work done on producing high intensity negative ion beams in magnetically insulated diodes. This part also contains work on magnetically insulated transmission lines in regard to negative ion production. This phenomena was investigated since negative ions cross the high voltage gap despite the insulating magnetic field and cause leakage current in transmission lines.

2.2 Negative ions production and properties

2.2.1 Negative ions and how they are formed

Because of the expansion of knowledge about negative ions their influence on the nature of physical phenomena in which they are concerned has been understood in much greater detail. This applies to light absorption in stellar, including solar atmospheres, and to electric discharge and breakdown phenomena in electronegative gases and in the terrestrial ionosphere. Negative ions are employed in tandem and circular particle accelerators and in various types of gas discharge sources for producing neutral beams. A few review works have been written about the large variety of experiments performed with negative ions. The books of Massey [4] and Smirnov [5] include an extensive background of the subject. Since in our experiment we tried to get beams of hydrogen or carbon we shall restrict this background survey to these ions.

ion	E(eV)
H^-	0.76
Li^-	0.34
B^-	0.12
C^-	1.37
CH^-	0.74
C_2^-	3.50
OH^-	1.83
O^-	1.80
O_2^-	0.47
Al^-	-0.16
Si^-	0.60
Cl^-	3.7

Table 2–1. Values of electron affinities of a few common negative ions. (after Smirnov [4])

Table 2-1 gives the electron affinity values of a few negative ions. Notice that carbon makes a very stable negative ion. The negative hydrogen ion has a quite low affinity (0.76 eV). It will lose the extra electron very easily. Residual molecules which exist in oil pumped vacuum systems can also make negative ions. These include O_2 molecules as well as CH molecules.

The unbound states of negative ions form a continuum just as do the corresponding states for neutral atoms. However whereas the unbound electron in the latter case moves in a field which falls off asymptotically at large distances from the nucleus as r^{-1}, for negative atomic ions the interaction falls off much faster due to polarization effects. This fact together with the low binding energies make it unlikely that any of these atomic ions have any excited states. There is some evidence however that a metastable state of C^- exists with detachment energy of 0.03eV [6]. Molecular ions do have metastable states. Resonance states of H_2^- have been observed in an energy range extending from 11.15 eV above the ground state of H_2 [7]. C_2 has an excited state lying 2.0 eV above the ground state–which seems to be stable [8].

Negative ions are formed through a few collision processes. The first process is called ***bound electron capture.*** It happens when two neutral atoms or molecules collide through a reaction of the type:

$$X + Y \longrightarrow X^- + Y^+ \tag{2.1}$$

or

$$X^+ + Y \longrightarrow X^- + Y^{++} \tag{2.2}$$

Negative hydrogen ions are produced usually through the reactions:

$$H + H_2 \longrightarrow H^- + H_2^+ \longrightarrow H^- + H^+ + H \tag{2.3}$$

or

$$H + H_2 \longrightarrow H + H^+ + H^- \tag{2.4}$$

Cross section for this reactions is around 10^{-17} cm^2 for hydrogen atoms with energies peaked around 10 keV as can be seen from FIG. 2–1 .

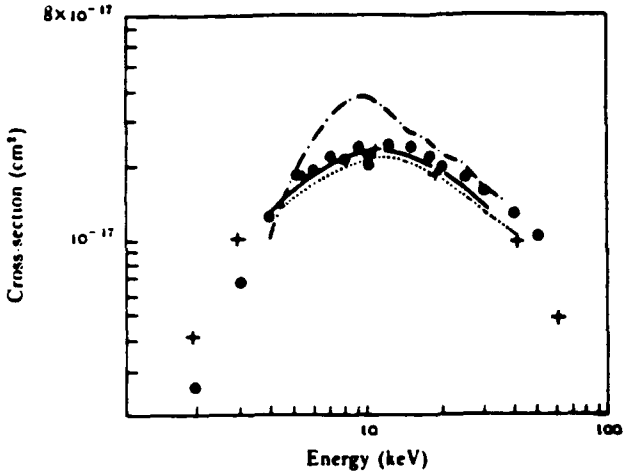

Figure 2–1: Cross section for electron capture by a hydrogen atom (after Massey [9]).

The most important processes are the *dissociative* processes. They are separated into reactions of the type:

$$XY + e \longrightarrow X + Y^- \tag{2.5}$$

called *dissociative attachment* processes, and reactions of the type:

$$XY + e \longrightarrow X^+ + Y^- + e \tag{2.6}$$

called *polar dissociation.*

In 1960 Ehlers [10] had successfully extracted a current of 5mA of negative ions from a Penning type hydrogen ion source and attributed these ions to polar dissociation. Since then much work has been done on investigating the reactions which lead to such high current densities. In 1984 York [11] was able to extract 35 mA H^- from what is called a *multicusp source.* The processes which take part in an electrical discharge in hydrogen gas, and can produce negative ions

are [12]:

$$e + H_2 \longrightarrow H^- + H \ \ (E = 3.75eV \ ; \ \sigma = 1.5 \times 10^{-21} \ cm^2) \qquad (2.7)$$

$$e + H_2 \longrightarrow H^- + H \ \ (E = 10.0eV \ ; \ \sigma = 1.4 \times 10^{-20} \ cm^2) \qquad (2.8)$$

$$e + H_2 \longrightarrow H^- + H^* \ \ (E = 14.2eV \ ; \ \sigma = 3.5 \times 10^{-20} \ cm^2) \qquad (2.9)$$

$$e + H_2 \longrightarrow H^- + H^+ + e \ \ (E > 17.6eV \ ; \ \sigma = 2 - 3 \times 10^{-20} \ cm^2) \qquad (2.10)$$

It is believed today [13] that dissociative attachment to highly excited molecular energy levels (2.9) is the most probable source of negative ions in hydrogen discharges, with the active portion of the vibrational spectrun occuring above $\nu" = 5$. Indeed, a calculation done by Wadera et. al. [14] shows high cross section for dissociative attachment by highly vibrationally excited mulecules as can be seen in table 2–2 and in FIG. 2–2.

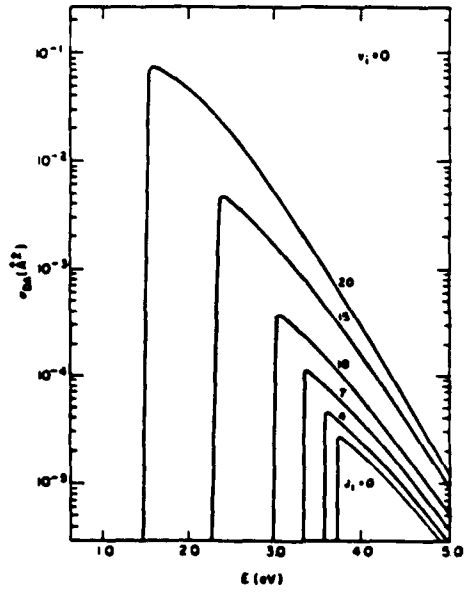

Figure 2–2: Dissociative attachment cross section for various rotational levels of the ground vibrational state of H_2 (after Wadera [14]).

ν	E(eV)	$\sigma_{DA}(cm^2)$
0	3.75	2.8×10^{-21}
1	3.23	8.3×10^{-20}
2	2.75	1.0×10^{-18}
3	2.29	7.5×10^{-18}
4	1.86	3.8×10^{-17}
5	1.46	1.2×10^{-16}
6	1.08	2.9×10^{-16}
7	0.74	4.3×10^{-16}
8	0.42	3.2×10^{-16}
9	0.14	4.3×10^{-16}

Table 2–2. Attachment cross sections near threshold for several vibrational levels of hydrogen (after Vaciera [14]).

2.2.2 Negative ions destruction

For each of the processes of negative ion formation there is a corresponding inverse reaction which involves destruction of the negative ions. We mentioned in chapter 2.2.1 only the reactions which have a high cross section for producing negative hydrogen or carbon ions. We shall do the same in this chapter and outline only the the most probable ways by which these ions are destroyed.

The first reaction is called *photodetachment*:

$$A^- + h\nu \longrightarrow A + e \tag{2.11}$$

The cross section for this reaction was measured in hydrogen by Smith and Burch [15] and is around 10^{-17} cm^2 in the infrared, visible and UV range of photon energy (FIG 2-3).

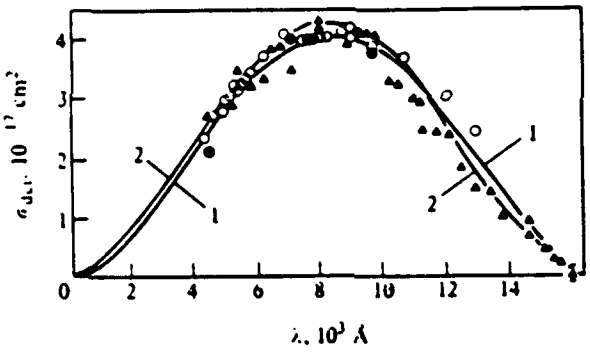

Figure 2-3: Photodetachment cross section of the hydrogen ion (after Smirnov [16]).

When we apply a high voltage pulse to a magnetically insulated diode, electron leakage currents hit the electrode and chamber surfaces emitting x-ray and ultraviolet radiation. Photodetachment can play an important role in destruction of negative ions, and we shall come back to this problem later in chapter 9. The same photodetachment process is used to produce high intensity neutral particle beams. Neutralizing cells based on photodetachment are very

simple to use and can neutralize a negative ion beam without changing its divergence [3]. Since pulsed sources compress the negative ion beams to bursts with relatively high particle density ($10^{12}/cm^3$), the mean free path of a photon in the beam is about 10^3 m. If the beam is 1 m wide and a 10 pass system through a 1 m deep source region is assumed, a photodetachment neutralization efficiency of at least 90% might be achieved with a pulsed light source which provides 10–20 J over 100 nsec beam duration. The use of photodetachment would eliminate the need for elaborate pumping systems involved with gas stripping cells.

Photodetachment from negative carbon ions has a much lower cross section since this ion is much more stable (see 2.1.1). Fig. 2–4 describes cross section measurements for this ion.

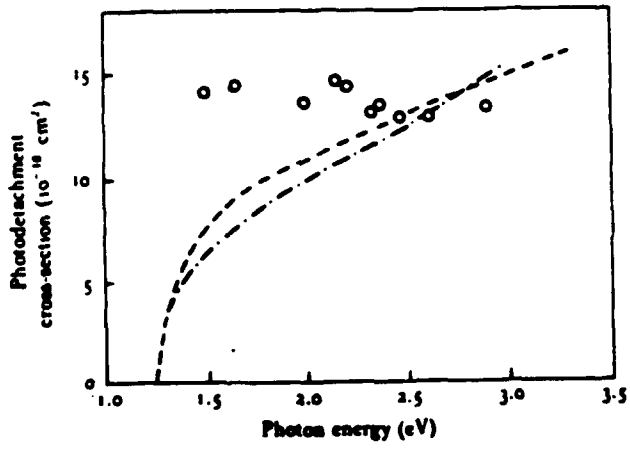

Figure 2–4: Photodetachment cross section of C^- (after Massey [17]).

Another type of reaction which leads to destruction of negative ions is *destruction by electron impact*:

$$e + H^- \longrightarrow 2e + H \tag{2.12}$$

The cross section for this reaction is around 10^{-15} cm^2 for negative ions with energies between 5–9 keV as can be seen from part a of FIG. 2–5. The cross

section has the same order of magnitude when the negative hydrogen ions have a very low energy between 0–30 eV (FIG. 2–5 part **b**).

Collision between a negative ion and another atom or ion can lead to detachment of the extra electron. The reaction in which a negative ion collides with a positive ion is called *associative detachment*;

$$H^+ + H^- \longrightarrow H_2^+ + e \tag{2.13}$$

The cross section for this reaction is shown in FIG. 2–6. The cross section is around 10^{-17} cm^2 for hydrogen ions with energies around 1–5 eV, and goes up to 10^{-13} cm^2 for ion energies around 10^{-3} eV.

This picture would not be complete without mentioning two other reactions. The first reaction does not lead to destruction of a negative ion and is called *charge exchange*:

$$H^- + H^+ \longrightarrow H + H^- \tag{2.14}$$

The cross section is around 10^{-16} cm^2 and is shown in FIG 2–7. The other important reaction is called *double electron detachment*:

$$H^- + H \longrightarrow H + H^+ + 2e \tag{2.15}$$

This reaction was used in our experiment in order to distinguish between negative ions and electrons. When a beam of negative ions is passed through a thin foil of mylar (about 2μ thick for 1 MeV ions) most of them are converted into positive ions as seen in equation (2.15). This processes is sometimes called *stripping*. A similar beam of electrons would suffer no change in charge sign. The cross section for this reaction is around 10^{-16} cm^2 and is shown in FIG 2–8.

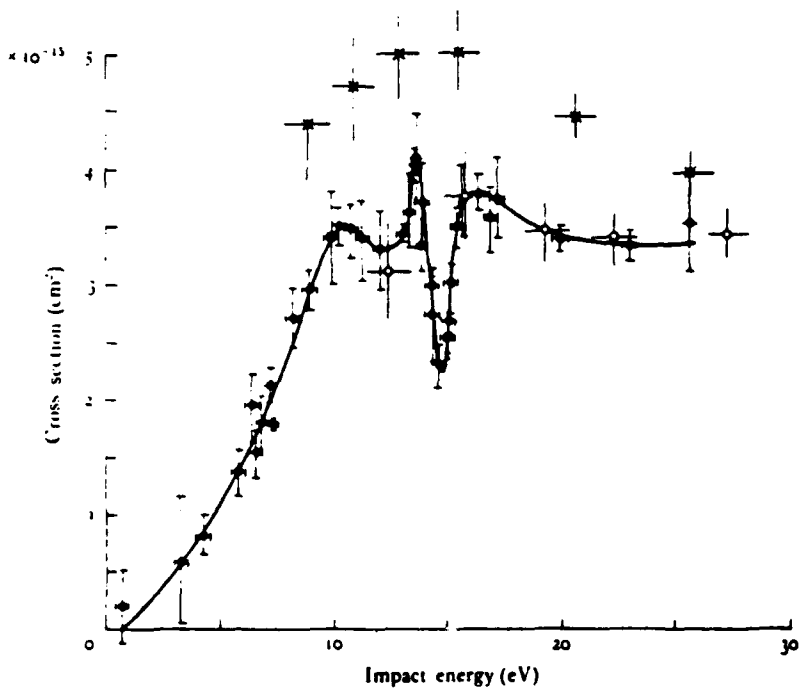

Figure 2–5 **a**: Cross section for detachment of electron from H^- by electron impact, at low impact energies (after Massey [18]).

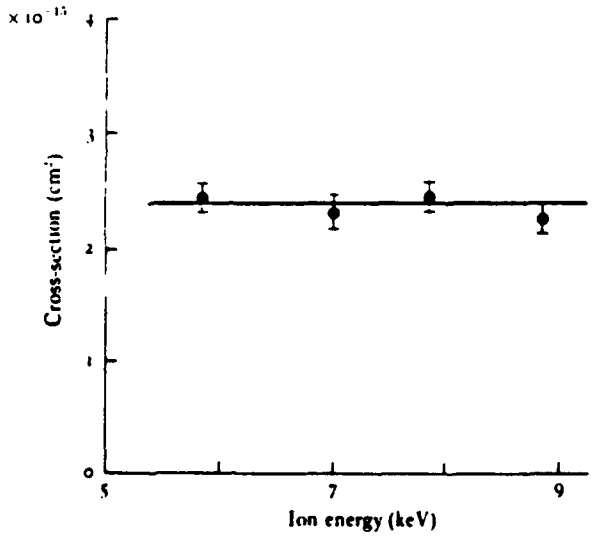

Figure 2–5 **b**: cross section for detachment of electron from H^- by electron impact, at high impact energies (after Peart [19]).

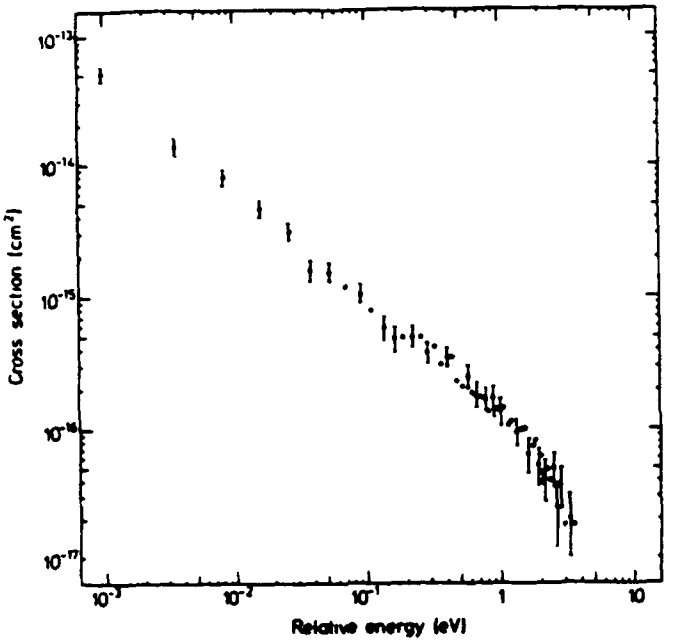

Figure 2–6: Cross section for associative ionization of hydrogen (after Poulaert [20]).

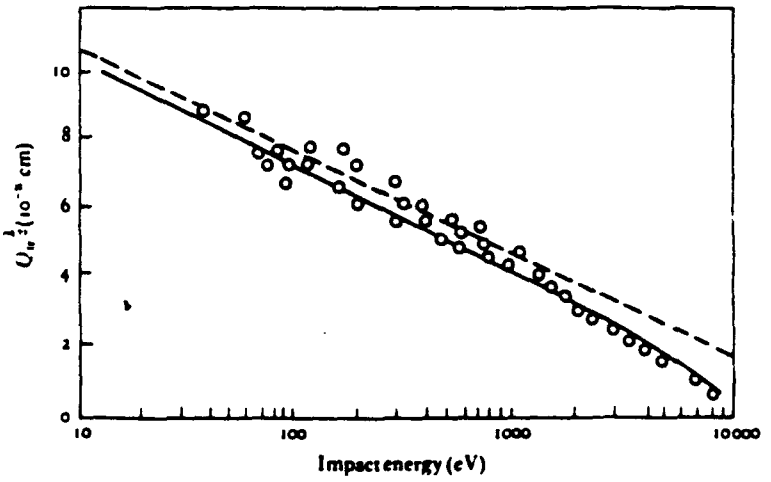

Figure 2–7: Cross section for charge transfer processes in hydrogen (after Massey [21]).

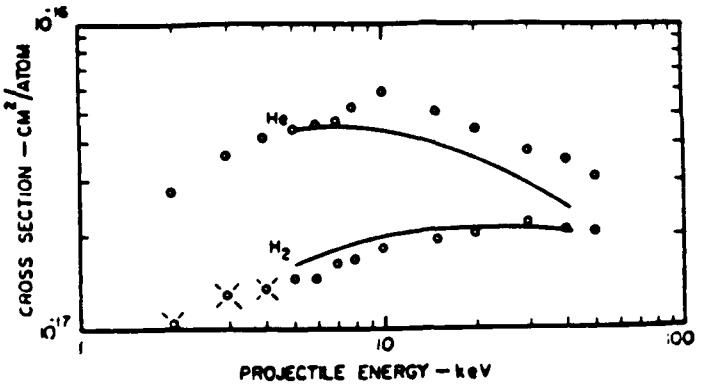

Figure 2–8: Double electron loss cross section in hydrogen negative ion (after Williams [22]).

2.2.3 Gas discharge negative ion sources

Much effort has been put lately in research aimed to develop new gas discharge negative ion sources. The results gained from this research can help us understand better the negative ion production phenomena which takes place in a high voltage magnetically insulated diode. The ion sources are usually grouped into *surface production* ion sources and *volume production* ion sources. The surface production source contains usually a hydrogen glow discharge plasma generator. Ions and neutrals from the plasma impinge upon a low work function surface. The return particle flux contains negative ions. It was found that by using a low work-function surface (usually the surface is made of a transition metal covered with Cs layer) caused the negative ion current to increase by two orders of magnitude compared to a bare metal surface [23, 24]. Currents densities of $2mA/cm^2$ with a total current of about 1A have been produced with this type of source [25]. Usually cesium is added to the hydrogen taking part in the glow discharge, and gets adsorbed on the transition metal surface. The surface itself is heated to lower its work-function. As we shall see later we have tried to follow some of these ideas in our experiment. We added to the

plasma producing dielectric material in our experiment some alkali metal salts in order to lower the work function and get more negative ions.

Volume discharge negative ion sources usually use a Penning low pressure glow discharge as a plasma source. A whole variety if ion source geometries was used for volume negative ion production. One of the most successful is the tandem ion source [26]. The source is divided into two parts between which there is a magnetic filter (see figure 2–9).

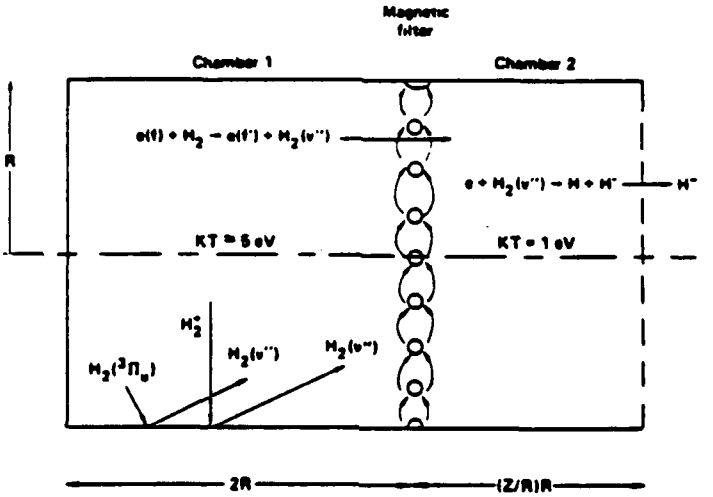

Figure 2–9 : Tandem discharge negative ion source (after Hiskes [26]).

Vibrationally excited molecules are generated in chamber 1 and dissociative attachment to these molecules to form negative ions occurs in chamber 2. The magnetic filter supports a relatively large concentration of fast electrons, E > 25eV in chamber 1 , while maintaining a low temperature, kT $\approx$ 1eV thermal electron bath in the second chamber. Currents of 35 mA/cm^2 have been produced with this source [11].

Gas discharge ion sources are clearly limited to a total current of a few amperes. They also have a high gas loading due to the nature of the source. This problem limits the aperture of the beam, requires differential pumping, limits

the beam current and requires a multistage accelerating system. Magnetically insulated diodes used as a negative ion source are much simpler and produce much higher current densities. We shall now review the work done on this sources.

2.3 Work done on magnetically insulated diode negative–ion beam sources.

2.3.1 Work done at the Lebedev institute in Moscow.

A series of experiments was conducted during the last 10 years at the Lebedev institute at Moscow on the production of negative ion beams in magnetically insulated diodes [27, 28, 29]. The only diode geometry used was the cylindrically symmetric coaxial diode (see figure 2–10 **a**). the experiments were performed on the ERG accelerator (voltage 600–1000 kV, current 30–40 kA, pulse duration 100–200 nsec). The dielectric materials used as a cathode coating plasma production materials were polyethelene, teflon, and polymethylacrylate. A magnetic field of 7–19 kGauss was used for electron insulation. Slots or round holes were cut in the anode to pass the negative ion current. Ion current was measured by graphite activation $^{1}2C(p,\gamma)^{13}N(\beta^{+})^{13}C$ having a threshold of 457 keV and a half life time of 9.96 minutes. The graphite consisted of a few bars surrounding the anode. In a modified geometry the ion current was measured by electrical means (see figure 2–10 **b**). A metal plate collected the ion current which was passed then through a shunt resistor and recorded on a scope. As mentioned by the authors, the current was obstructed by leakage electron current from the cathode. This problem did not appear when a metallic cathode was used. The same leakage current caused intense brehmsstrahlung which obstructed the γ rays from the activation measurements.

One of the main results mentioned was that it is essential for the high voltage generator to have a prepulse in order to be able to measure any negative ions. This prepulse is caused by the capacitive coupling through the output switch of the high voltage machine. The prepulse in this experiment had a duration

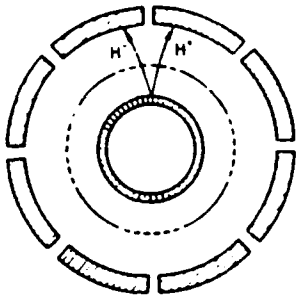

a: Coaxial diode and graphite activation system.

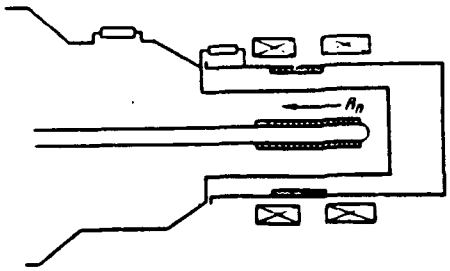

b: Electrical ion current measuring system.

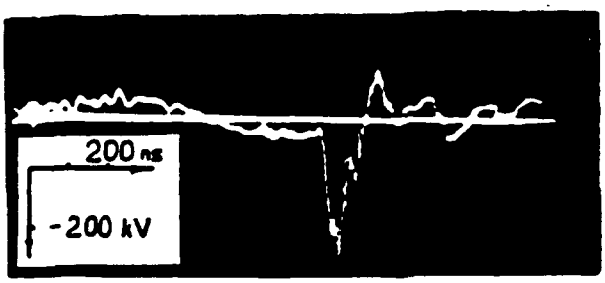

c: Shape of the high voltage pulse.

Figure 2–10: Experiment construction at the Lebedev institute (see Kolomenski [28]).

of 1 μsec and consisted of a positive and a negative halfwaves. Many more negative ions were formed in the presence of the negative part of the prepulse. The minimum width of the prepulse which generated negative ions was 100 nsec. Elongation of the prepulse to 400 nsec did not enhance the negative ion current. The negative ion currents reported reached 200 A/cm^2 with a total current of 5kA. Presence of H^- ions was recorded by track formation on aluminized mylar foil.

In an effort to simulate the effect of the prepulse, a laser with energy of 5J and a pulse duration of 20 nsec was used. The laser irradiated the polyethelene coated cathode at a given time before the high voltage was applied to the diode. Maximum negative ions were produced for a time interval of 150–200 nsec between the laser and the high voltage pulse. Activation of the graphite target corresponded in this experiment to 10^{13} particles. The reported current of 200 A/cm^2 is much higher than the Child–Langmuir limit which is estimated by the authors to be around 20–30 A/cm^2 for the full diode gap. The explanation mentioned is that the effective gap could be much smaller due to plasma expansion into it.

2.3.2 Work at Sandia national laboratory on transmission lines

Magnetically insulated transmission lines are used to transfer energy from a high voltage generator to a diode. These diodes are usually used for ion beam production for inertial confinement fusion. The insulating magnetic field in the lines is created by the line current. Negative ions produced in the cathode plasma of the line are not insulated by the magnetic field because of their relatively large mass. They cause a leakage current which can effect the power flow in the line. The phenomena of negative ion production in a MITL was investigated at Sandia Natl. Labs. [30, 31, 32, 33, 34]. This work gives us much insight into the physical phenomena of negative ion production in magnetically insulated diodes.

The first set of measurements was aimed to measure the negative ion beam intensity and its atomic mass composition. The line pulse had a peak of about

2MV and was 100 nsec long. It was preceeded by a prepulse of 240 kV for 15 nsec. The main pulse had a $dV/dt=10^{15}V/s$. Negative ion mass and current density were measured with a time of flight mass spectrometer using a magnetic deflector to sweep electrons out of the drift tube. Negative ion current varied from shot to shot. Ion current of a few A/cm^2 were measured. Time of flight spectra were consistent with H^-, H_2^-, O_2^- and C_2^- ions. A Thomson parabola mass spectrometer was then used to analyze the ion–beam mass composition. H^- ions with a typical intensity of 0.25 A/cm^2, C^- with 1 A/cm^2 and C_2^- with intensity of 0.75 A/cm^2 were measured. Typical parabola traces are shown on figure 2–11 **a**. Negative ion currents seemed to be source limited and were strongly dependent on cathode surface condition.

Another set of experiments was aimed to measure the cathode plasma behavior in the line. The plasma formation was studied using laser–schlieren photography, time resolved visible light photography, and and visible light spectroscopy. This part of the work was done on the THOR 0.5 MV, 2Ω accelerator with a 50 nsec voltage pulse. The measurements revealed the existence of a cathode plasma sheath which extended about 0.2 cm from the cathode surface, with a density of 10^{15}–$10^{16}/cm^3$ and a temperature of a few electron–volts. The plasma had a monotonically increasing density gradient from the edge of the cathode plasma sheath to the cathode surface, of 1×10^{17} to 1×10^{18} cm^{-4} (see figure 2–11 **b**). Plasma expansion velocities of 1-2 $cm/\mu sec$ were measured, which corresponds to the thermal velocity of a 2eV hydrogen plasma. With visible light spectroscopy dominant lines of singly ionized states of Carbon, Silicon and Oxygen were measured.

2.3.3 Work done by other groups on negative ion production.

The high negative ion current densities obtained at the Lebedev institute were followed by other groups trying to reproduce the results.

The first group was at Ecole Polytechnique in France. They used a 1.5 MV, 43Ω, 20 nsec PULSRAD generator with a racetrack type diode [35]. Various

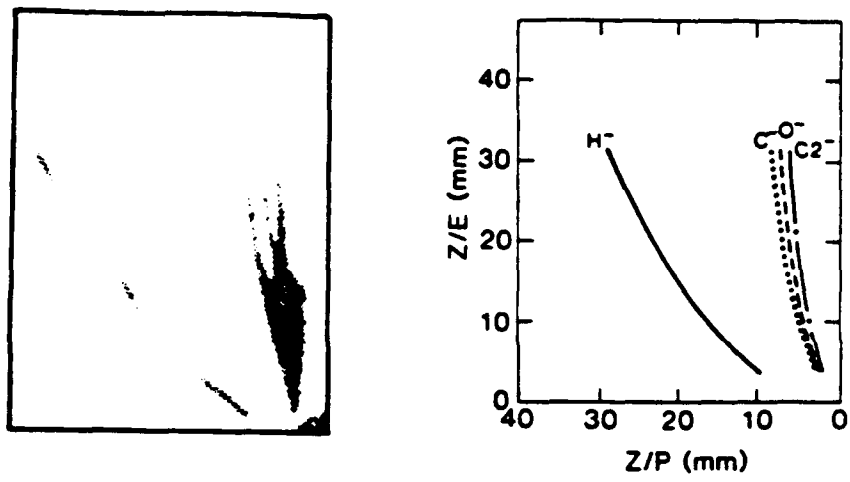

A: Thomson parabola negative ion traces.

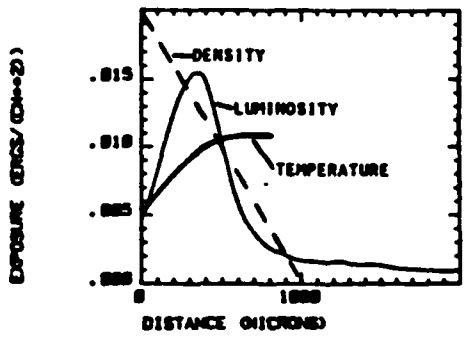

B: Luminosity, density, and inferred temperature profiles of the cathode plasma.

Figure 2–11: Experimental results on negative ion production in MITL (after Stinnet [31]).

cathode coating have been tried including polyethelene, epoxy resin and vaselin oil. Ion beam diagnostics was performed using a Faraday-cup and graphyte nuclear activation. No high energy H^- activation has been detected with or without a prepulse (no details are given about the prepulse shape but it is mentioned that this prepulse was much shorter than the one used at the Lebedev institute).

Another interesting experiment was performed by a group at Tomsk [36]. The diode had a coaxial shape with a thin film installed in its medium plane (see figure 2-12). The inner cylinder served as an anode and was pulsed via the 8Ω 80nsec 500 kV VERA accelerator.

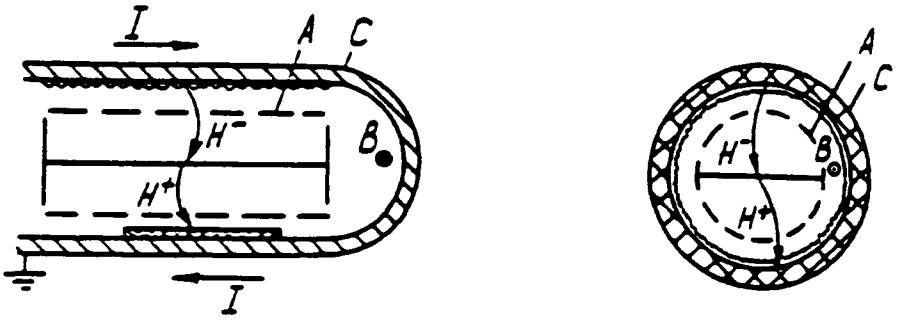

Figure 2-12: Diode construction at the Tomsk experiment (after Bistritsky [36]).

The VERA machine has a prepulse of 250 nsec duration and 60-80 kV amplitude. Ion current was measured by the usuall carbon activation technique. In this diode, the H^- ions generated in the first A-C gap were initially accelerated towards the anode, then stripped to H^+ in the thin anode film, and postaccelerated in the second gap (see figure 2-12). The total energy of the ions incident on the target was almost twice the anode voltage. This experimental scheme was chosen to exclude the possibility of positive ions accelerated because of voltage reversal or collective phenomena.

Ion currents reported were on the $(0.25\pm0.15)A/cm^2$ level at 10 GW power levels and electron cathode current densities in the (0.5–1) kA/cm^2 range. This values of negative ion currents correspond to (0.5–2)% level of H^- percentage in the A–C plasma. These negative ion current densities were the same with or without the prepulse.

2.4 Summary.

The large variety of experiments done on negative ion sources reflects the wide interest in this subject. Contradictory results have been obtained in production of negative ion beams using magnetically insulated diodes. This thesis aimed to resolve these contradictions as well as to try and understand the negative ion production phenomena in these diodes.

Chapter 3 GENERAL EXPERIMENTAL ARRANGEMENT

3.1 Introduction.

In this chapter we shall review the general experimental techniques used by us in this research. We shall start by giving a brief description of the high voltage APEX machine, together with the voltage and current measurement systems. We shall then go through the diode set up, including vacuum system and magnetic insulation. At last we shall review the diagnostics systems used. These include Faraday cup charge collectors, CR-39 ion track detectors, Langmuir probes, x-ray camera and brehmsstrahlung intensity measurements. Additional specific techniques will be reviewed shortly at the next chapters, whenever such a technique is used.

3.2 The APEX machine.

The APEX machine consists of a 1MV, 50 nsec Marx generator, and a 7Ω coaxial transmission line. The Marx consists of 24 stages, each containing a 0.2μF capacitor, a pressurized spark gap, and assorted charging resistors. The transmission line has an electrical length of 25 nsec. A self firing pressurized gas switch connects the line to the load. The Marx pressurized gaps were filled with dry air, and the line gap was filled with SF_6. The dry air in the gaps limited the voltage on each stage to about 30 kV, with an output signal of about 700 kV, and a total energy of 90 Joule. More details about Marx generators can be found in a review article by Nation [38].

The first two Marx gaps are triggered with a midplane trigger electrodes, and the remaining gaps are triggered by the rising voltage pulse on the Marx and the electrical noise from the triggered gaps. A triggered vacuum gap switches a 60 kV trigger signal to the first gaps. The APEX machine has a built in triggering circuit used to trigger the vacuum gap from a pushbutton or a delay unit. In our experiment we wanted the APEX machine to have a low jitter in

order to be able to match its timing with a plasma creating prepulsed plasma gun–both triggered by a delay unit. Marx delay between this triggering signal and the high voltage at the line output was about 1.4μsec with a jitter of about 0.2μsec.

The Marx output current was monitored using a small pickup loop the sensitivity of which is 10v/4kA. The voltage was measured via a ring shaped capacitive divider with a sensitivity of 10v for every 550 kV machine pulse. We did not use inductive correction since the diode inductance effected the monitored pulse only at the first 10nsec. Figure 3–1 shows typical voltage–current traces.

A 300Ω resistor was used at the line output to suppress the APEX prepulse. When the resistor was connected there was a prepulse of about 2% of the main pulse, compared to about 10% when the resistor was disconnected.

3.3 Diode chamber and vacuum system.

The diode chamber is a stainless–steel cross shaped chamber (see figure 3–2) with four openings. One of the openings was connected to the outer side of the APEX line interface and the three others were closed with aluminum flanges. Using aluminum enabled us to use an x–ray camera "through" the flanges to record the areas on the diode chamber where electrons are stopped and brehmsstrahlung is emitted. Faraday cup charge collectors were installed through Wilson seals in the aluminum flanges. A high–current feedthrough was used for transferring energy from a capacitor bank to the insulating magnetic field coils.

The chamber was evacuated with a vacuum system consisting of a 6" 1200 l/s diffusion pump and a 360 l/m forepump. This vacuum system was able to evacuate the diode chamber to a pressure of about 10^{-5} Torr which was the usual working pressure. Pressure monitoring was done with a regular Bayard–Alpert air calibrated ionization gauge.

The cathode was mounted on a 4" diameter, 30" long hollow shank. This

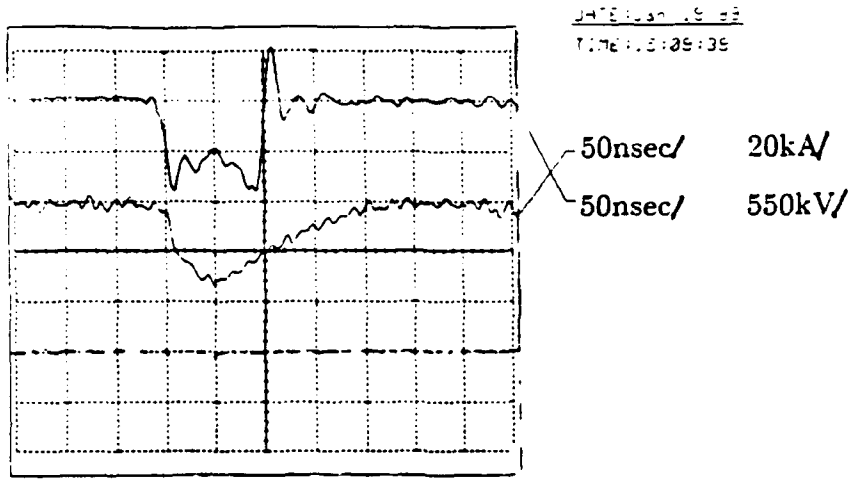

a:Voltage current traces for a normal shot.

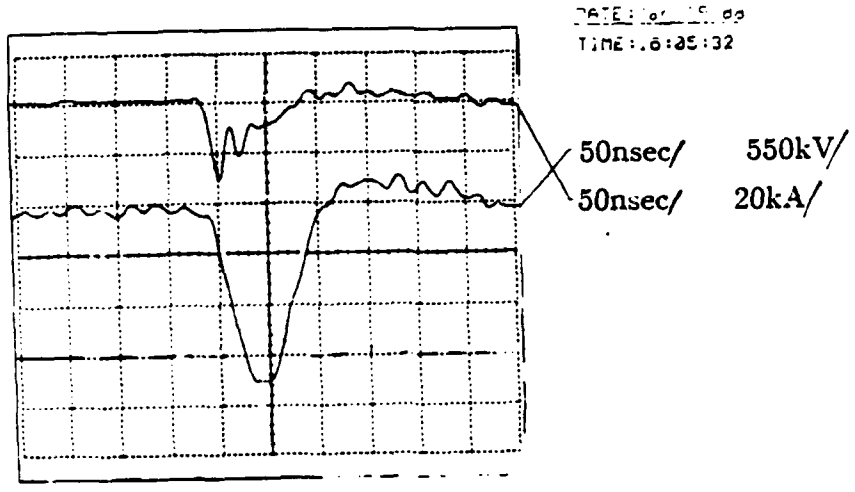

b:voltage current traces for a low diode impedance.

Figure 3–1 :Typical voltage current traces of a magnetically insulated diode.

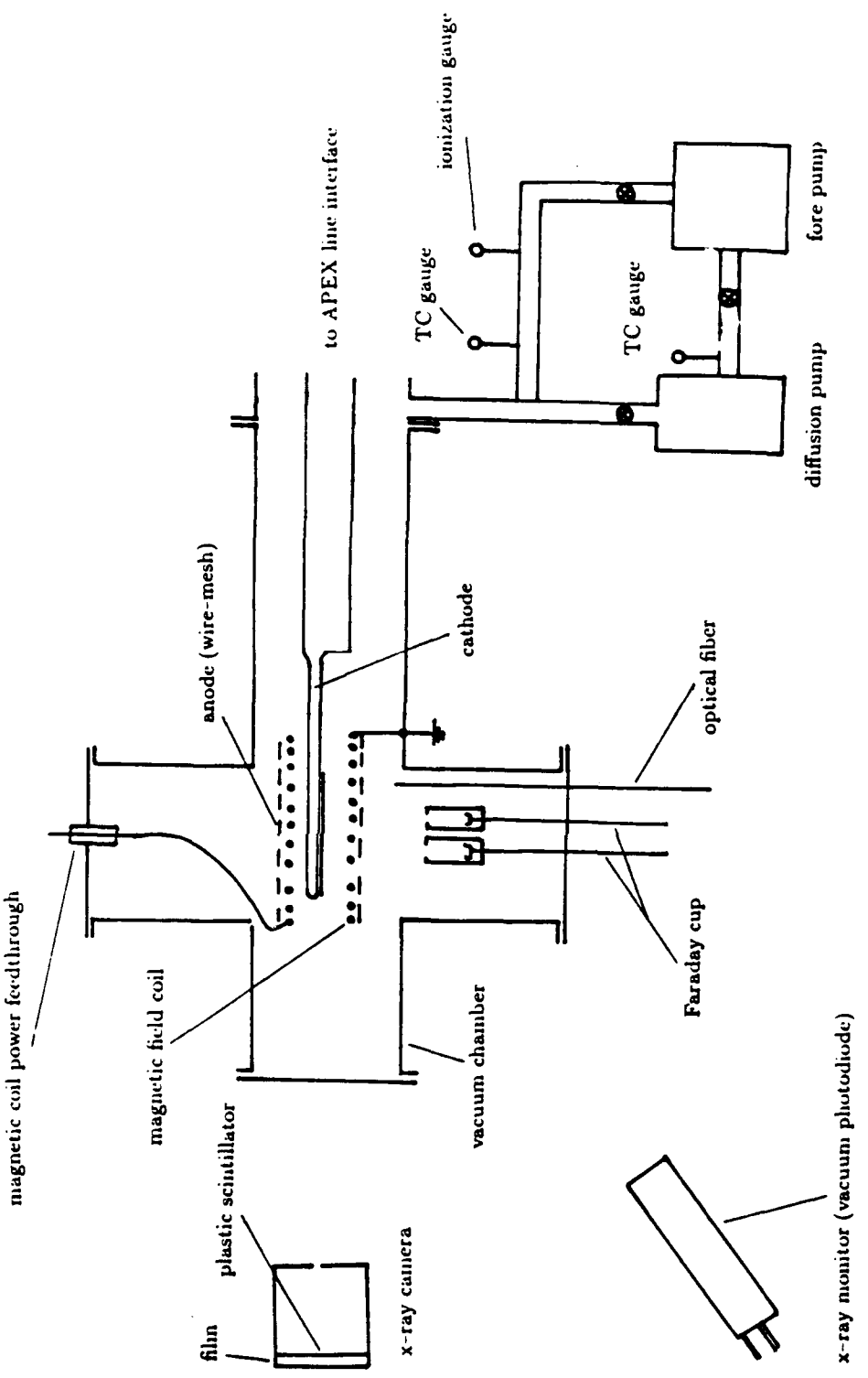

Figure 3–2: Diode chamber and vacuum sustem.

was done mainly in order to have enough space to put the prepulsed plasma gun in. This arrangement caused also a high mechanical load at the vacuum–oil interface where sealing had to be improved by adding an external additional "O" ring.

3.4 Magnetic insulation.

3.4.1 General principles.

Magnetically insulated diodes used to produce intense ion beams were first proposed by Winterberg [39]. At field stresses of about 1MV/cm electrons are emitted from whisker explosions in the cathode surface [40]. The cathode then, can be considered to be an unlimited source of electrons. By the Child–Langmuir space charge limited current law [41, 42], only 2% of the current in the diode would be carried by ions due to the smaller mass of the electrons. For a planar geometry the Child–Langmuir current density is given by:

$$j = 0.05(Ze/m)^{1/2}V^{3/2}d^{-2} \tag{3.1}$$

where Ze/m = charge–to–mass ratio of the particle, V = gap potential and d = gap spacing in cgs–emu units. Electron flow in the diode is supressed by applying a sufficiently high magnetic field parallel to the surface of the electrodes. The critical field necessary is given by [2]:

$$B^* = (1/d)(2eV/r_e)^{1/2}(1 + eV/2m_ec^2))^{1/2} \tag{3.2}$$

where d = gap spacing, r_e = classical electron radius, m_e = electron mass and V = gap voltage. This expression is derived from the conservation of canonical momentum and energy for a particle in the diode gap. The critical field for a gap of about 1cm with a voltage of 1MV is about 4–5 kGauss.

When a high enough magnetic field is applied electrons do not cross the gap but are forced into a drift along the cathode in a $\vec{E} \times \vec{B}$ direction. This is sometimes called *Hall drift* resembling the equivalent famous solid state effect.

We always have a small transverse electrical field component in the diode gap. This component causes the Hall drifting electrons to move along magnetic field lines. Some of the electrons reach the cathode and some drift along magnetic field lines to the vacuum chamber walls or other parts of the diode. The effectiveness of magnetic insulation is usually measured by the diode perveance, $P = I/V^{3/2}$, where I and V are the diode voltage and current, respectively. By following the reduction in the perveance as a function of applied magnetic field, the degree of electron current supression is obtained. In some cases perveance reduction by more than a factor of 300 have been obtained.

Although electron current can be dramatically supressed, some leakage current remains. It has been observed that for finite geometries, two other criteria must be fulfilled to maximize the insulation. First, insulating magnetic field lines must not connect electrically stressed cathode surfaces to higher potential (anode) surfaces: otherwise electrons can flow along field lines to these surfaces. The second criterion is that the electron Hall current, driven by the perpendicular electric and magnetic fields in the diode, must flow in a closed path to insure equilibrium and increase diode efficiency. This efficiency is usually defined as the ion current divided by the total diode current. The Hall current path is determined by electrode shaping in a manner consistent both with extraction requirements and with the diode magnetic field geometry.

Due to the slow rise time of the magnetic field in our experiment (about 100μsec in our case) the magnetic field penetrates into the metal cathode. The penetration depth is given by:

$$\delta = \left(\frac{2}{\mu\omega\sigma}\right)^{1/2} \tag{3.3}$$

where δ is the skin depth, ω is the field frequency and σ is the conductivity. This equation is in MKS units. For our case of magnetic field with an aluminum cathode the skin depth is equal to about 2 mm . This penetration deforms the magnetic field lines and is an undesired effect in our case. Deformed field lines can connect the anode to the cathode. Electrons drifting along such a line could

cause diode shorts. Magnetic field penetration can cause a deflection of the ion–beam. If we had a case of a magnetic field which does not penetrate into the cathode the canonical momentum of a particle moving in this field would be conserved with no effect of the field on the beam direction. But a particle moving in a field penetrating the cathode will be deflected. This deflection will be larger for particles with a small mass. It will be much higher for hydrogen than it is for carbon ions. This is one of the reasons why carbon ions make a much more parallel beam in magnetically insulated diodes.

3.4.2 Magnetic insulation experimental setup.

The magnetic insulation in the high voltage diode gap was established by discharging a high energy capacitor bank through a low inductance coil which supplied the field. We tried to build coils with as low inductance as possible to get small field penetration as explained in 3.4.1.

The capacitor bank consisted of two groups of 9 capacitor each having a capacitance of 280μF. Each such group has a capacitance of 2160μF (see figure 3–3). One of the capacitor groups was charged to +3kV and the other to -3kV. An ignitron switch (triggered from a pushbutton and a standard krytron circuit) connected the two capacitor groups to supply a 6kV pulse to the coil. The peak current was a function of the coil inductance. Figure 3–4 shows the currents for a coaxial, racetrack and annular diode coil cases. The point in time at which the APEX was fired is also shown. It corresponds usually to the point where the magnetic field reaches its peak. Magnetic field intensity was measured at each diode configuration using a Hall effect probe and also with a small search coil. Details of the coil shapes used, together with field intensity measurements results will be given in chapters 5, 6 and 7 when discussing the different diodes used.

3.5 Ion–beam diagnostic techniques.

3.5.1 Faraday cup charge collectors.

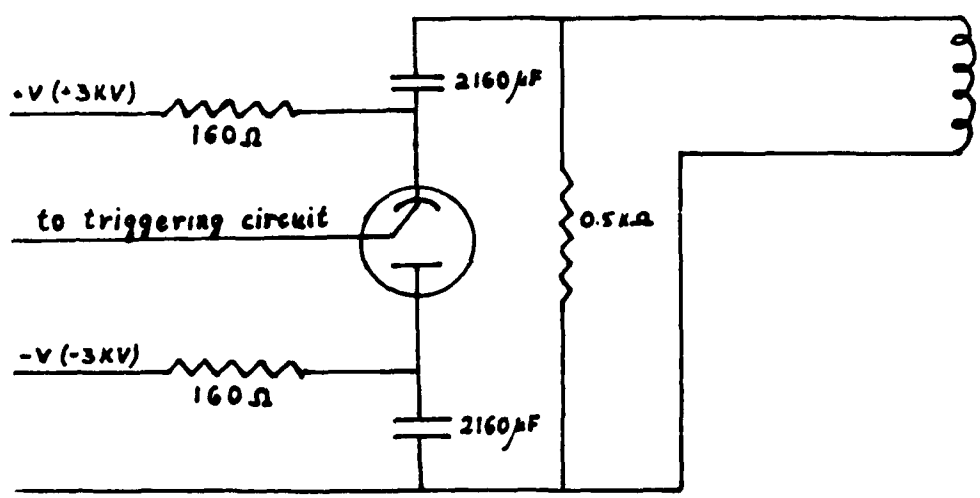

Figure 3–3: Magnetic field electrical circuit.

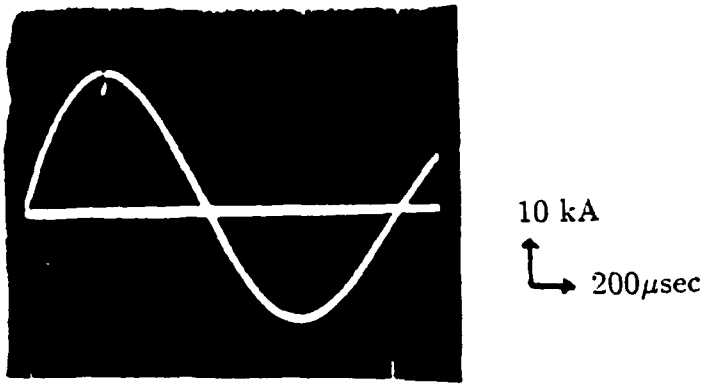

a: Coaxial diode coil current.

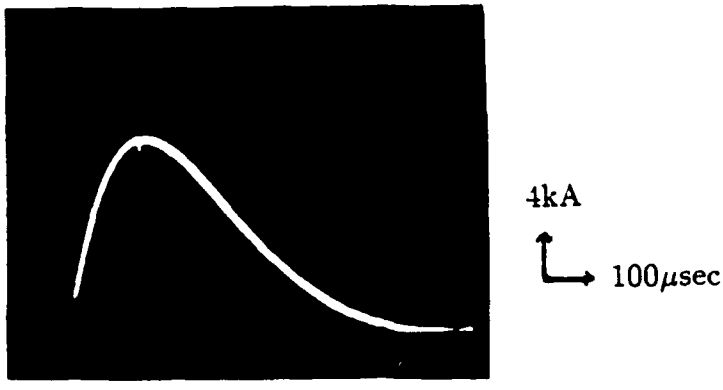

b: Racetrack diode coil current.

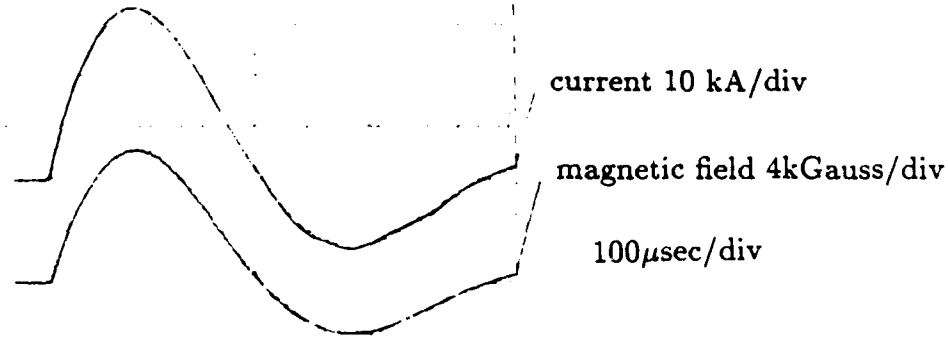

c: Annular diode coil current.

Figure 3–4: Magnetic coil current and field shape.

The Faraday cup charge collector is a standard device for measuring electron and ion beam currents [43, 44]. This simple instrument does have limitations that must be considered in its use and in the interpretation of the data. A typical Faraday cup used is seen in figure 3–5. It consists of a 2" diameter Copper tubing with a charge collector inside. The tubing has a 0.5" diameter aperture at its end. The charge collector has a cup shape to reduce the problem of secondary electrons emitted from it. Small Samarium–Cobalt magnets provide a field of about 1.6 kGauss.

In this experiment the negative ion beam current was measured. Electrons which diffuse along the magnetic insulation field lines have an energy of about 0.7meV. These electrons are sometimes backscattered towards the Faraday cup. The main problem is to get rid of these extra electrons. One of the possible solutions is to put an insulating magnetic field along the distance d between the cup aperture and charge collector (see figure 3–5). Ions are less affected by this field. But by getting rid of the electrons, the low energy ions are also lost (see figure 3–6). Since electrons have the same charge sign, we usually checked that what we measure is ions by putting a sheet of 25μ thick mylar in front of the Faraday cup. This mylar stops any ion created in the diode since the maximum energy for such ions is about 0.7 MeV. Electrons penetrate this layer easily. A final check was done by putting a 2μ thick mylar in front of the Faraday cup. Ions with energies of more than 200 keV can penetrate this film (see figure 3–7) losing two electrons. This is the "stripping" process discussed in chapter 2.2.2. If indeed the measured current did change its sign when the thin mylar was put in front of the Faraday cup we were sure that we measure negative hydrogen ions. This procedure could not be carried on for Carbon ions since their range is in mylar is shorter than 2μ.

In some cases we did measure electrons together with negative ions on the Faraday cup. This was done by placing the Faraday cup at a distance of about 20 cm from the diode and put a thin piece of mylar in front of it. The difference in time of flight would be such that the electron and ion current signals would

with carbon cathode with polyethelene cathode

Ion tracks on faraday cup collector.

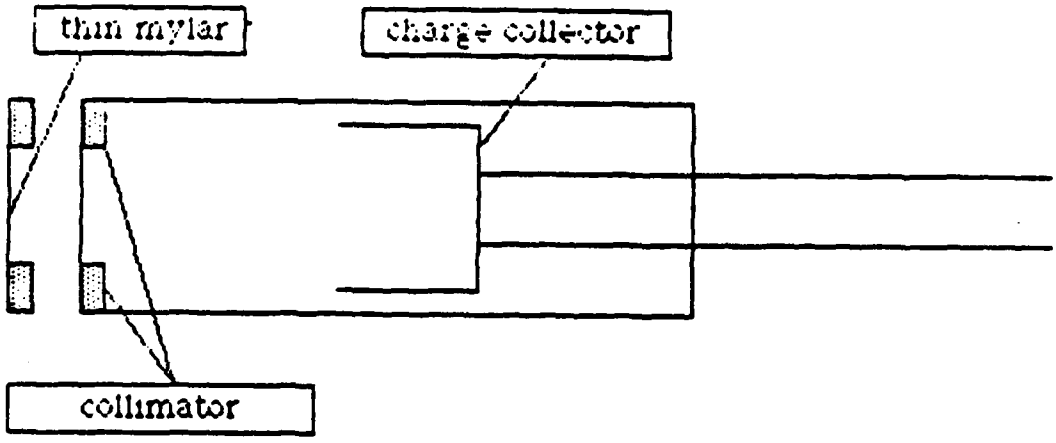

Figure 3-5: Faraday cup.

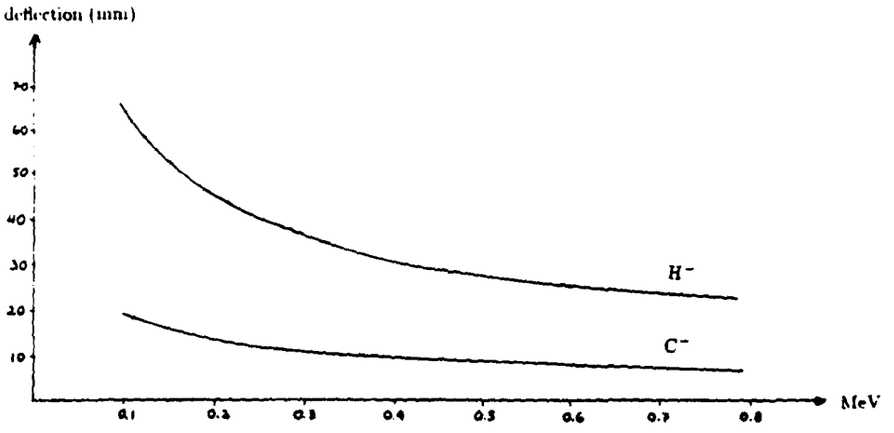

a: Radial deflection of an ion entering the cup parallel to its axis.

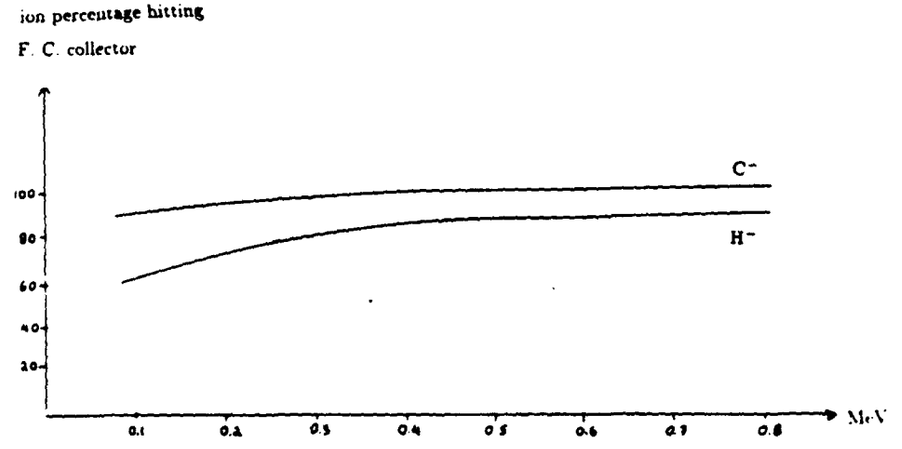

b: Relative ion current measured by the charge collector due to magnetic deflection inside the Faraday cup.

Figure 3-6: Effect of Faraday cup magnetic field on ion current measurments.

not interfere with each other (see figure 3–8). In a few cases we did bias the cup with a small voltage. Usually the Faraday cup is biased when measuring a beam of positive ions. These ions drag electrons with them. The cup is then biased negatively to repel the electrons. The electrons have about the same velocity as the ions , and since their mass is much smaller their energy is also small and the bias voltage needed is at most a few hundred volts. In our case the electrons hitting the cup have a very high energy and could not be repelled by a bias voltage. Nevertheless we did use bias in cases when the geometry was such that no electrons hit the Faraday cup (and this was the case with the annular diode as shall be explained in chapter 7). There was then no need for magnets around the Faraday cup. The bias voltage was used in this case only to make sure that no secondary electrons leave the cup collector in absence of a magnetic field. In any case we always checked the current with the thick and thin pieces of mylar as described above.

3.5.2 CR–39 track detectors.

CR–39 as a particle track detector was first used in 1978 [46]. CR–39 is a clear plastic material the chemical name of which is *ethyl diglycol carbonate.* Particles which hit it cause a local damage track. When the material is put in an etching solution there is a difference in the bulk etching rate and the track area etching rate. This difference leaves a "picture" of the areas were particles caused damage. We usually used a 6 mole solution of NaOH heated to 80° celsius as an etching solution. The etching time was about 1 hour. In figure 3–9 a one can see the etching rate for a proton track compared to the bulk etching rate for different energies. As can be seen the CR–39 "sensitivity" (the ratio of track to bulk etching rates) is highest for low energy particles. The range of these particles in the CR–39 is obviously small, and leaving the CR–39 in the etching solution for a while will cause tracks of low–energy particles to disappear. In our case we were able to see proton tracks with energies as low as 70 keV for etching times of 1 hour. Another interesting feature is that

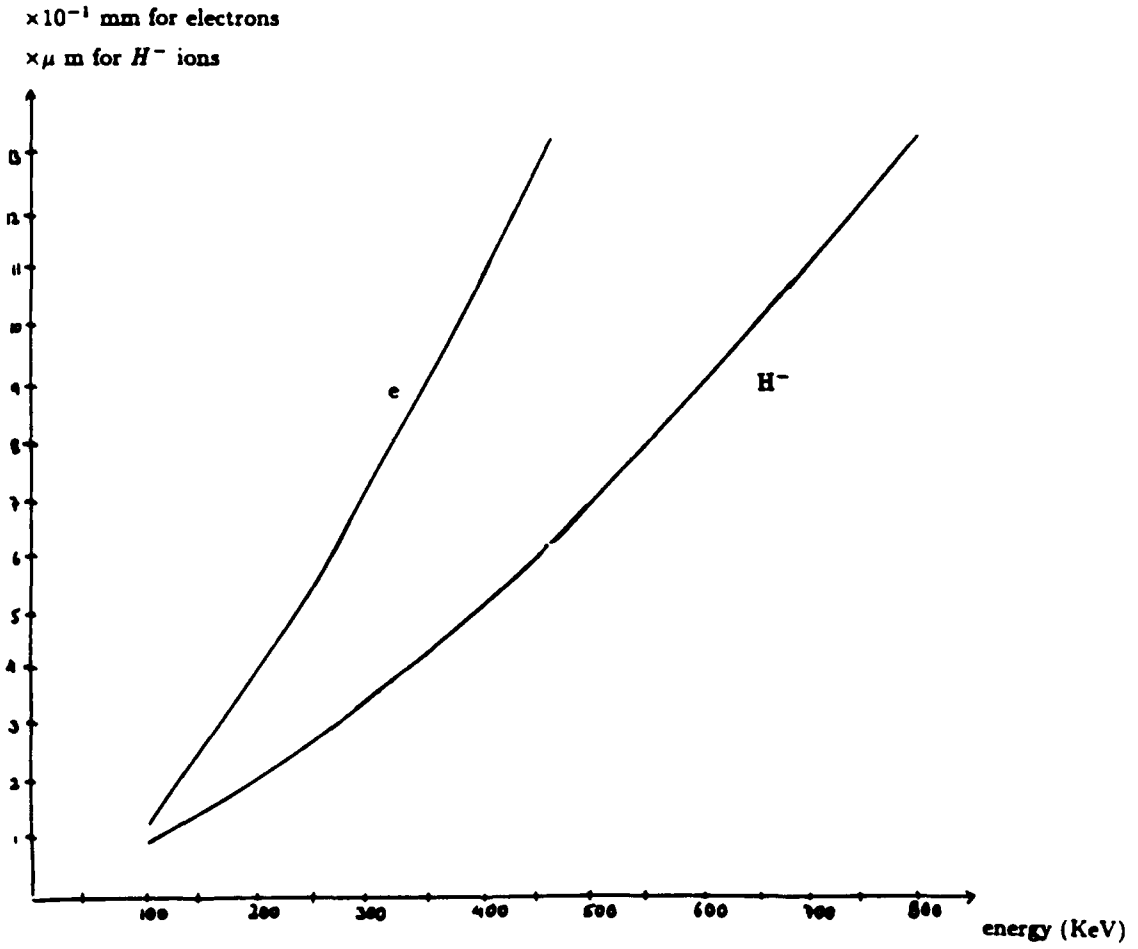

Figure 3–7: Penetration depth of ions and electrons in mylar (after Janni [40]).

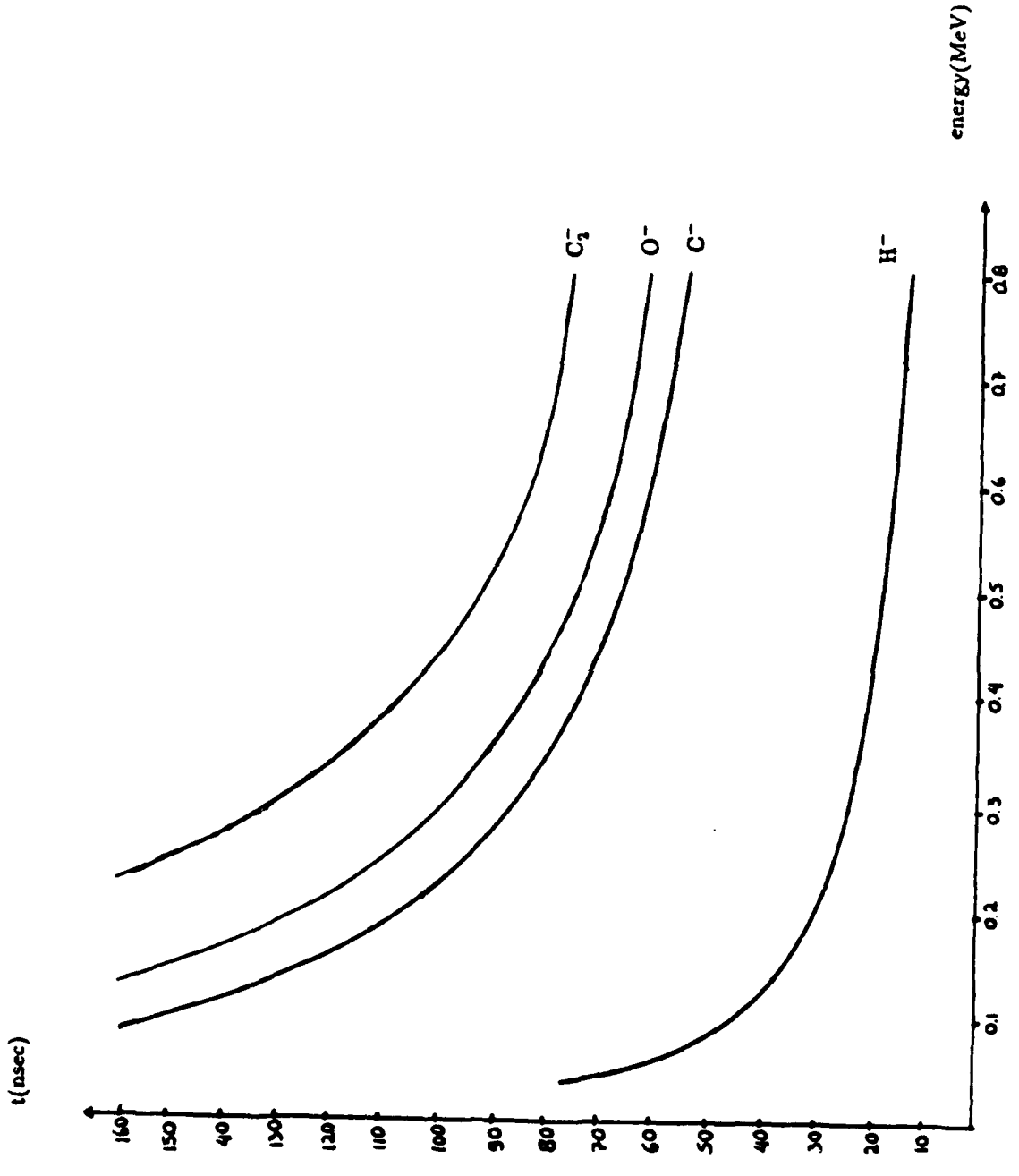

Figure 3–8: Time of flight along 20 cm for different negative ions.

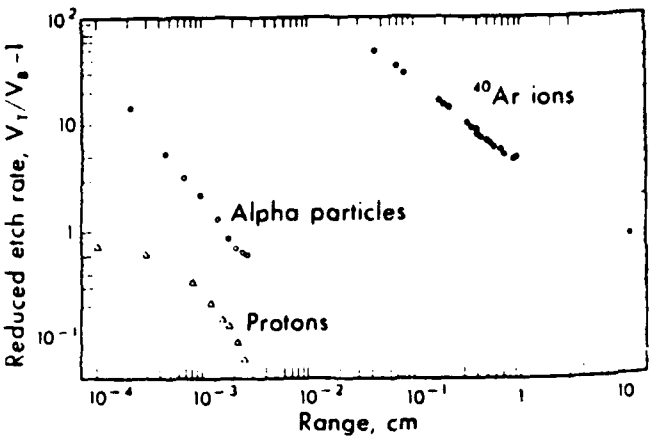

a: CR–39 sensitivity (after Cartwright [46])

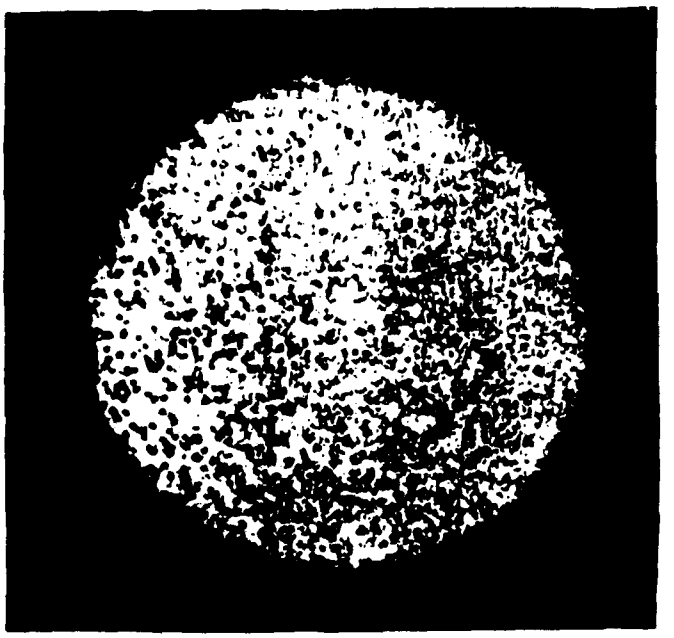

b: A typical CR–39 picture showing H^- and C^- tracks.

Figure 3–9: CR–39 sensitivity and track pattern.

different ions have different track sizes. Carbon, for instance has a lower range in the CR–39, but the damage it causes is larger (see figure 3–9 **b**). Carbon tracks usually have about twice the damage track size of hydrogen with the same energy. Combinations of CR–39 with different thickness mylar films on it were used to scan different particle energy ranges (see figure 3–7). A nice review article about CR–39 properties and uses was written by Somogyi [47]. The CR–39 was purchased from American acrylic co. in Strattford Connecticut. Two types of this material were used by us. We used a 0.025" thick CR–39 which is defined by this company as "highest quality proton detection" material. We also used a 0.040""regular quality". The 0.025" CR–39 had a shelf life of about one year, after which it showed an inhomogeneous etching behaviour. Some areas were etched quicker than the others, which distorted the ion track picture. We did not have any problems with the 0.040" CR–39.

3.6 x–ray measurements.

3.6.1 x–ray camera.

Most of the diode current consists of electrons which drift along magnetic field lines and hit the chamber walls. These high energy electrons emit x–rays when they are stopped or slowed at the walls. In order to see the exact points where the electrons hit the chamber we used an x–ray camera. The camera was made of a lead box with a 4 mm hole in it. A $CaWO_4$ scintillator (we used a regular medical x–ray intensifier) was put 12 cm from the hole with a film attached to it. X–ray pictures were taken each shot (see figure 3–10). We were able to see by this method if the electron flow is symmetric. A symmetric electron flow means that the diode electrodes and magnetic field coils are aligned correctly. We were also able to see if a high current is caused by a short outside the diode gap (for instance at the shank or the line interface). By changing the camera distance from the diode we were able to figure out where the electrons hit the chamber. This information could be used to understanding the electron flow in the diode.

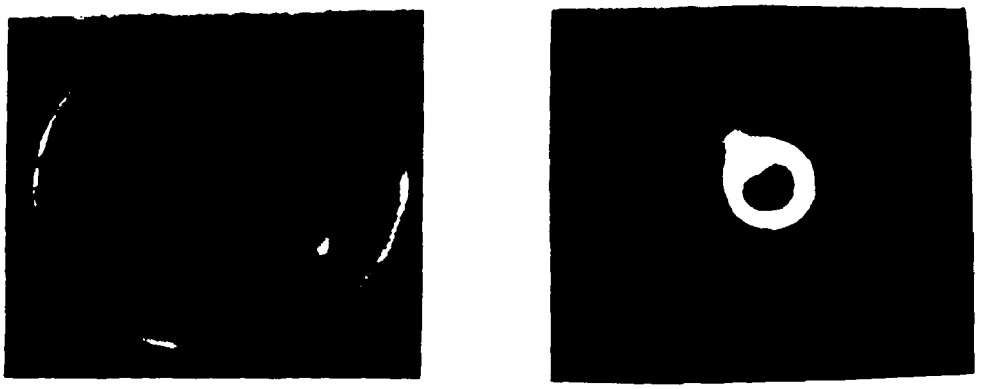

a: Coaxial diode.

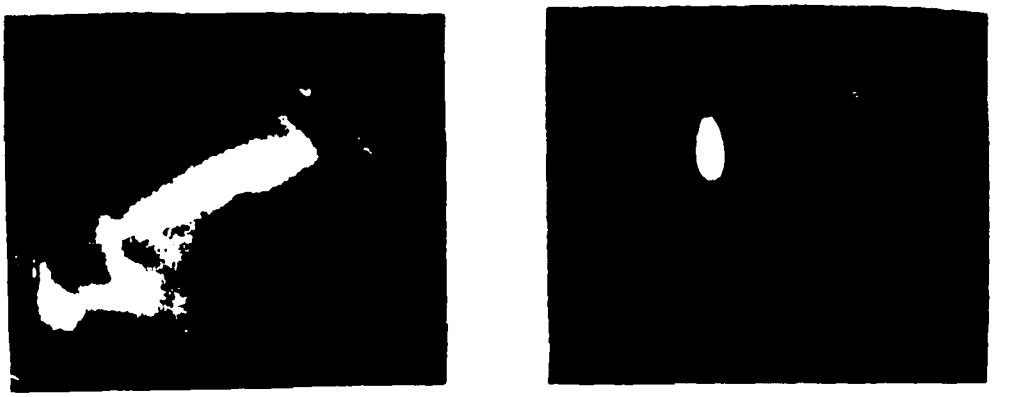

b: Racetrack diode.

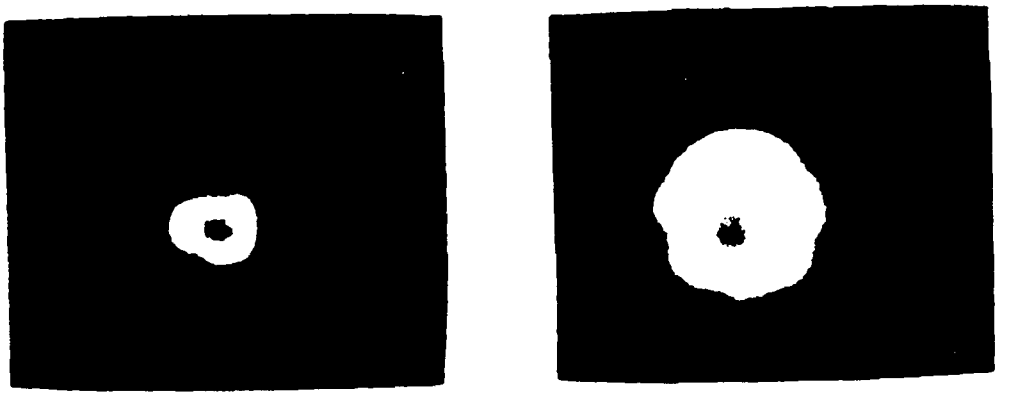

c: Annular diode.

Figure 3–10: X–ray pictures of normal shots (left) and shorts (right) with different diode configurations.

3.6.2 Brehmsstrahlung measurements.

The time dependence of the x–ray emission from the chamber walls was measured with a FW114 vacuum photodiode made by ITT. The diode had an NE–102 plastic scintillator connected to it. Typical x–ray pulse shape are shown in figure 3–11 together with the diode circuit.

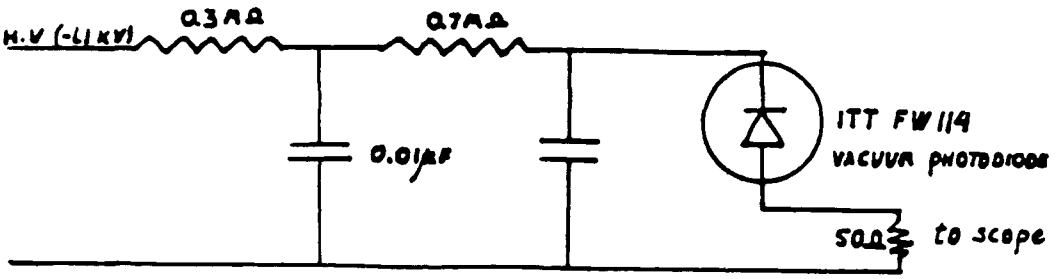

a: Diode circuit.

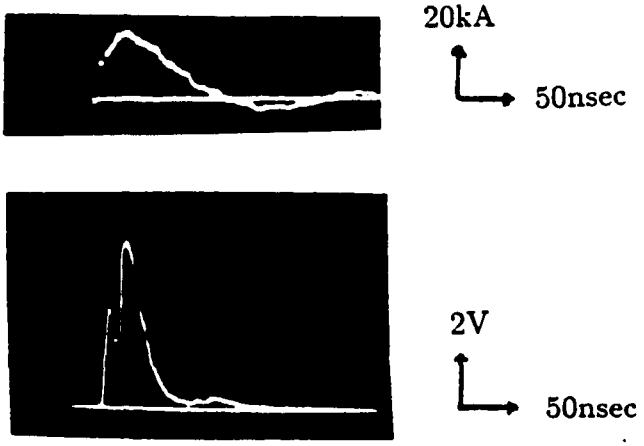

b: A typical x-ray emission trace (below) together with a diode current trace (above).

Figure 3-11: X-ray diode circuit and typical pulse shape.

Chapter 4 PLASMA PRODUCTION

4.1 Introduction

Plasma is usually produced in high voltage diodes using what is called a *passive flashboard*. This is done by putting a thin layer of dielectric material on one of the electrodes. If a beam of negative particles is desired the dielectric material is put on the cathode surface to produce a cathode plasma. All previous work on negative ion production was done using this plasma production method (see chapter 2). We have tried many kinds of passive cathodes in our experiment. However, the work done at the Lebedev institute (see chapter 2.3.1) and some results we got in an early stage of the experiment pointed at the fact that the APEX prepulse voltage had a dominant effect on the production of negative ions. Since the APEX prepulse could not be controlled we decided to build an independent prepulsed plasma gun. The idea was to inject a plasma into the high voltage diode gap at a given time before applying the main high voltage pulse. This should simulate the effects of the APEX prepulse. We wanted to be able to control the plasma temperature, density and production time. A special plasma gun was built for these purposes. It consists of a driving circuit powered by batteries, and a plasma creating flashboard. Plasma is created on 120 arcing points across the flashboard surface.

The physical processes involved in plasma production in the case of the passive flashboard and in the case of the active plasma gun are discussed in chapter 4.2. The next chapters deal with plasma gun details. The plasma gun driving circuit is embedded in the cathode shank and has to be able to float on the APEX high voltage. The driving circuit is discussed in chapter 4.3. The flashboard was designed to produce a homogeneous plasma over a large cathode area. It is described in chapter 4.4. Since high voltage switching circuits have always some jitter, the real time lag between firing the plasma gun and the APEX high voltage pulse was measured via a light detecting fiber optics and

photomultiplier system the details of which are given in chapter 4.5. The last chapter deals with plasma measurements. Plasma density and temperature were measured with a Langmuir probe. The results are discussed in chapter 4.6.

4.2 Physical processes of plasma production

Plasma source requirements for intense beam injectors are quite severe. The plasma must be localized to a thickness smaller than the gap width and may have to supply ion fluxes of the order tens and hundreds of A/cm^2 over an area of hundreds of square centimeters. The most commonly used plasma source is the passive flashboard. This plasma source is just a sheet of insulator (usually with holes or metal metal pins in it), attached to the cathode surface. Plasma is produced by formation of vacuum ballasted breakdowns on the insulator surface (see figure 4–1). The exact process by which plasma is formed when such an insulator is put on one of the electrodes is not clear. Insulating surfaces in vacuum exposed to tangential electric fields of the order of 100–200 Kv/cm will go an avalanche breakdown that produces a dense plasma. The breakdown appears to be initiated at the *triple point* where insulator, conductor and vacuum meet. The strong fields along the insulator surface are produced by direct charging of the insulator from electron flow in the gap, and by the existence of a fringing field due to the holes and pins in the insulator. The surface breakdown mechanism affects only a thin surface layer, so plasma can be produced with small energy investment. Flashboards are used in almost all present intense ion beam experiments. If the insulator contains hydrocarbon molecules (as is the case in polyethelene), a mixed plasma is produced containing both hydrogen and carbon ions. The hydrogen usually diffuses to the plasma surface rapidly. In positive ion experiments beams of 80% protons are typically obtained [48]. As was mentioned in chapter 1, carbon makes very stable negative ions. By using a hydrocarbon insulator we shall usually get a plasma which contains both H^- and C^- ions.

The physical processes involved in plasma formation in the case of a passive

dielectric flashboard are quite involved. The plasma starts to build up at electric fields of about 100–200kV/cm. This fields are not high enough to free electrons from the potential barrier that binds them in the cathode material. However, at the surface of the cathode, the local electric field can be enhanced by factors of more than 100 over the value of the macroscopic electric field. This is because the actual cathode surface contains many microprotrusions or whiskers. These whiskers have typical heights and diameters of 100 and 10μm respectively [49]. Another reason for field enhancement are dielectric materials or microparticles present on the cathode surface [50]. These dielectric materials have usually a high dielectric constant. This fact enhances the local fields at the triple point, which starts the field emission process.

For several nanoseconds the electron current buildup is determined by the field emission process. As the emitted electron density increases the whiskers through which the current flow become hot because of Joule heating. When the local current density reaches a value of 10^7–10^8 A/cm^2, the heated whiskers explode and form a local burst of vaporized material [51]. This phenomena was termed *explosive emission.* A similar phenomena occurs when we use a metal cathode. Plasma is created close to small dielectric microparticles on the cathode surface.

The material in the vapor bursts is quickly ionized, resulting in the formation of local plasma flares in the neighbourhood of the exploded whiskers. These individual flares quickly expand and merge into a plasma cloud that spreads over the entire cathode surface. If a strong magnetic field is present the plasma remains confined over localized points on the cathode surface.

The capacitively coupled surface breakdown source is simple and useful but has a few disadvantages. There is almost no control over plasma density and temperature. Since the flashboard must be located in the accelerating gap it is subject to damage which limits the repetition rate and cleanliness of the system. It is advantageous to use a separate plasma gun. There is much more control over plasma temperature, density and creation time. A separate plasma gun

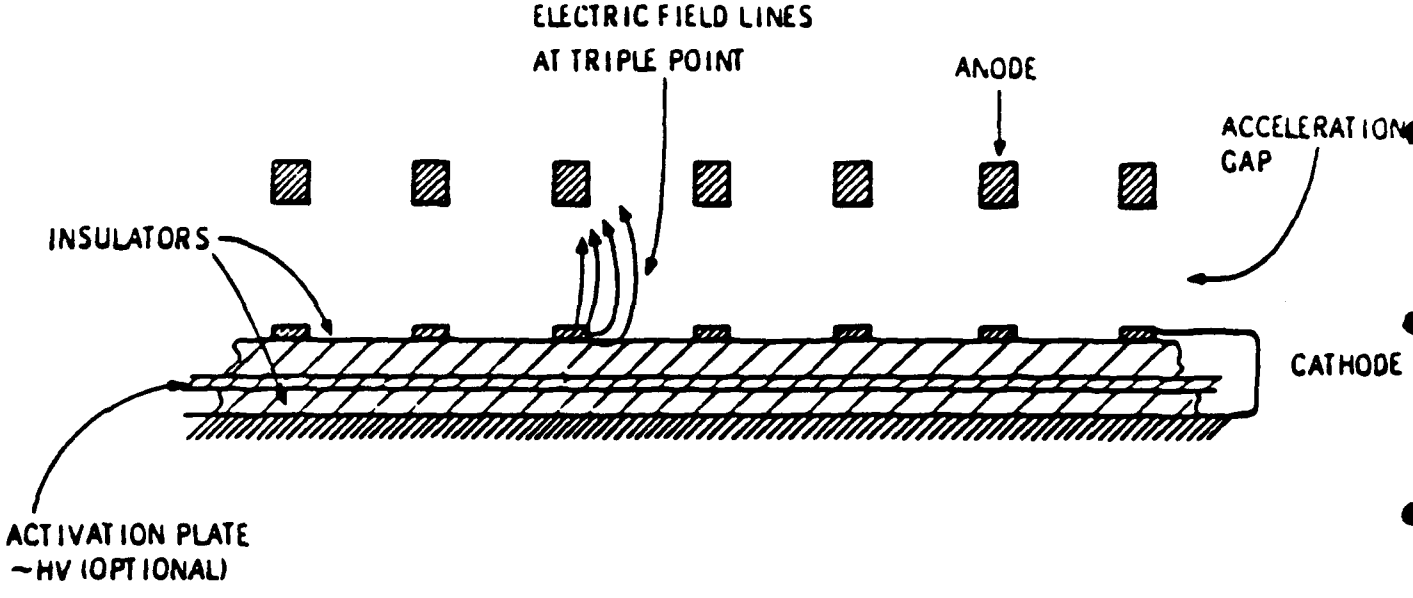

Figure 4-1: A passive flashboard plasma gun.

can also produce a much more uniform plasma.

The plasma gun we used created arcs across 120 points on the cathode surface. Each arc was produced along a thin layer of TiH_2 powder (see figure 4–2). The high current density of the arc caused some of the TiH_2 to evaporate and ionize [52]. The physical processes are very similar to the whisker explosion case. The main difference is that the current through each plasma gun arcing point can be controlled. We chose TiH_2 since it contains much hydrogen, and since Ti does not produce negative ions. We shall discuss plasma formation and negative ion production in more details in chapter 8.

4.3 Plasma gun driving circuit

The plasma gun general setup is shown in figure 4–3. The gun was triggered by an outside light signal supplied by a flashtube. The flashtube was driven by a standard krytron circuit switching a capacitor through the flashtube. The krytron was triggered directly from a 400V signal from the delay unit *D1*. This delay unit was triggered by the insulating magnetic field trigger pulse. Another delay unit (*D2*) triggered the main high voltage pulse, by supplying a 400V trigger signal to the APEX vacuum gap.

The plasma gun circuit consists of a high voltage part triggered by a low voltage circuit (see figure 4–4). The high voltage part of the circuit supplies the energy to the flashboard through an output transformer. The transformer was introduced to get higher output voltages if necessary, and to insulate the driving circuit from high voltage noise caused by the main pulse in the flashboard area. The energy discharged is first stored in a high voltage capacitor (C1). Six rechargeable NiCd batteries supply energy to a DC to DC convertor, the output of which is connected to the capacitor C1 through a 5MΩ resistor. A magnetic on/off switch starts the charging procedure. The switch is in a normally closed position when it senses a magnetic field. A rod with a small samarium–cobalt magnet on its edge was installed in the diode chamber to activate the switch. The rod could be moved through a Wilson seal to touch the diode shank and

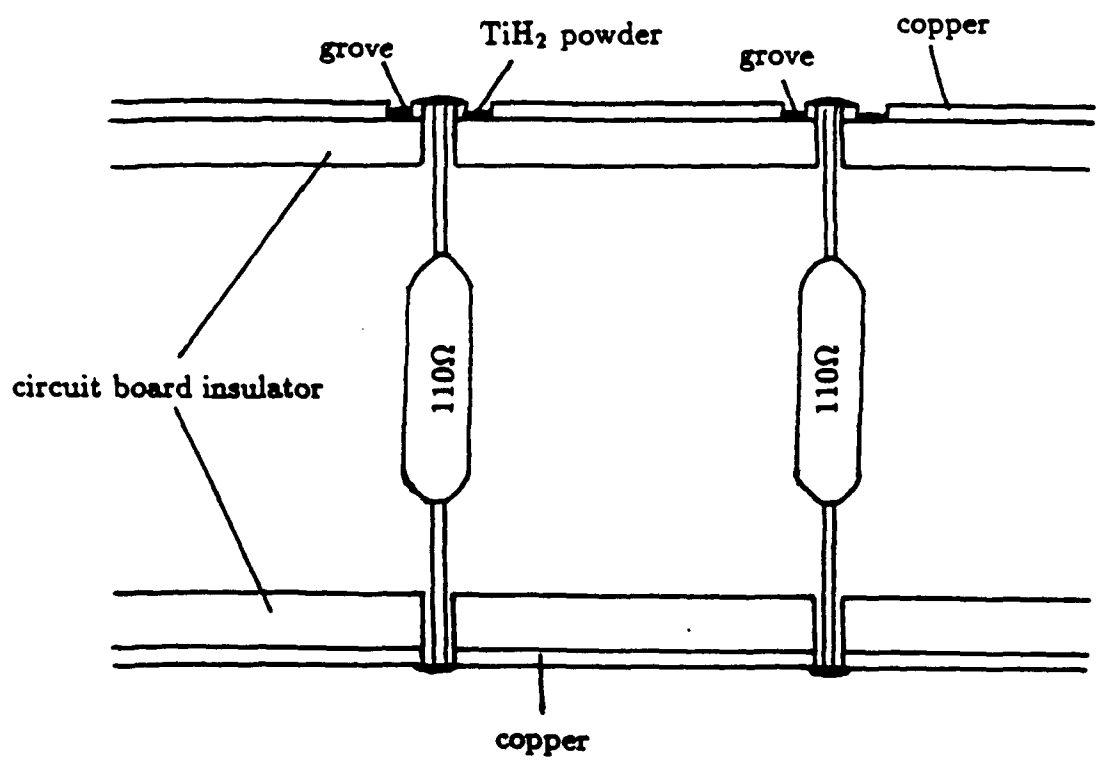

Figure 4–2: Plasma creation with an arc plasma gun.

deactivate the inside circuit. The batteries were connected in series to supply 8 volts to the convertor. The convertor's output voltage was about 2.7 kV under these conditions.

Two high voltage switches were used. The capacitor is discharged through a CP CLARE TG–1457 triggered spark gap. The spark gap is triggered by a 3m RG–174 line charged to 2.7 kV and discharged through an EG&G KN–6 krytron. The krytron is triggered by a low voltage triggering circuit through a 1:30 transformer. This transformer insulates the low voltage part of the circuit from the high voltage part, protecting the low voltage components.

The low voltage circuit is triggered by a flashtube external light source. The flashtube supplies a high intensity light pulse to a photodiode in the low voltage triggering circuit through a clear window in the diode vacuum chamber (see figure 4–3). The photodiode triggers an SCR through a field emission transistor. A small capacitor (C2) charged by a 9V battery discharges through the SCR into the primary of the 1:30 transformer.

The circuit was mainly operated in a high output current mode or in a low output current mode. In the low output current mode we used a 0.25μF capacitor discharged into a 1:2 output transformer. The total output current was 500A. The current pulse shape is shown in figure 4–5 **a**. The flashboard has 120 arcing points on its surface, so the average current in each arc was about 3A.

In the high output current mode the circuit was operated with a 2μF capacitor charged to 2.7 kV and discharged to the flashboard through a low inductance 1:1 transformer. The transformer consisted of 3 turns of RG–174 cable, the inner core of which was used as a primary, and the outer as a secondary. The output current reaches a value of 3.2 kA, with an average current of about 270 A per arcing point (see figure 4–5 **b**).

4.4 The plasma creating flashboard

The flashboard is the part of the system which converts the power supplied

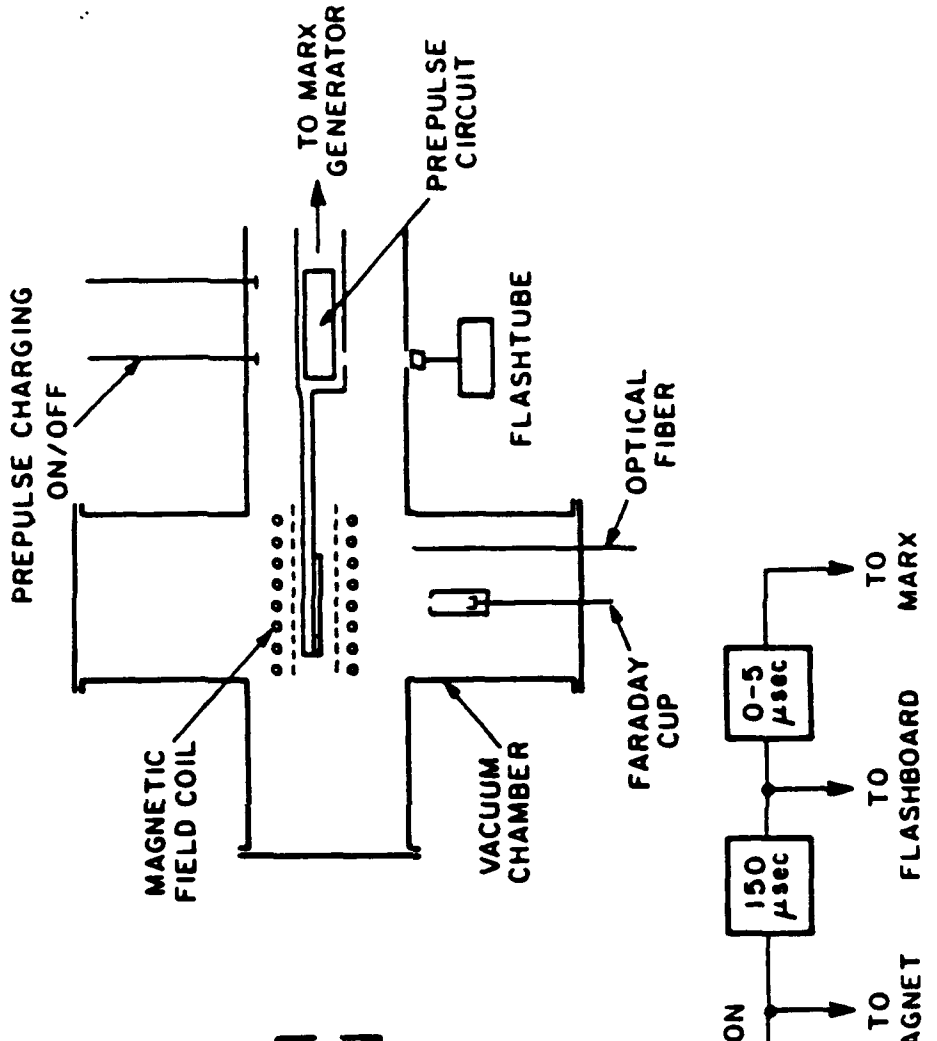

Figure 4-3: Prepulsed plasma gun general layout.

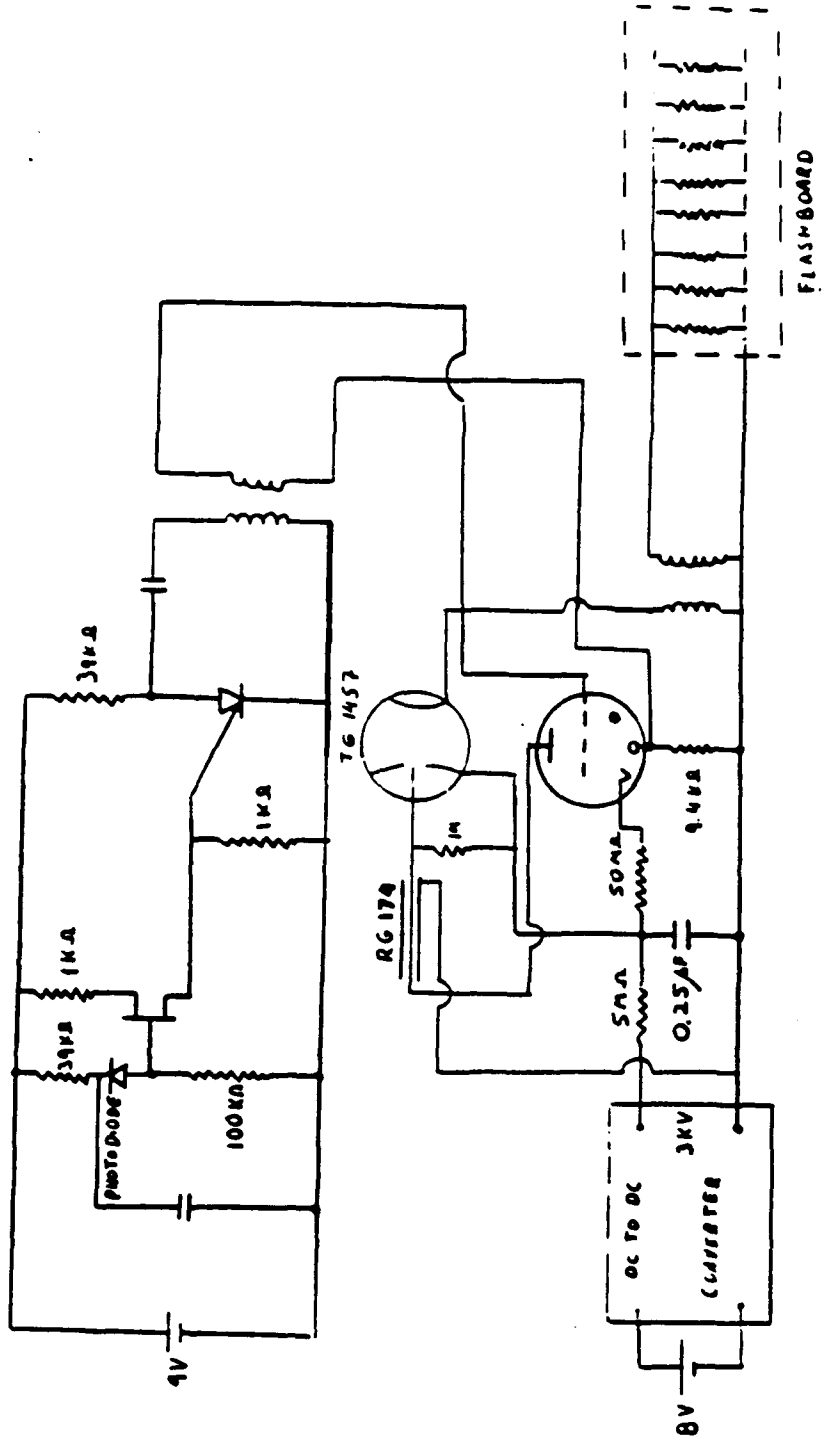

Figure 4–4: Prepulsed plasma gun driving circuit.

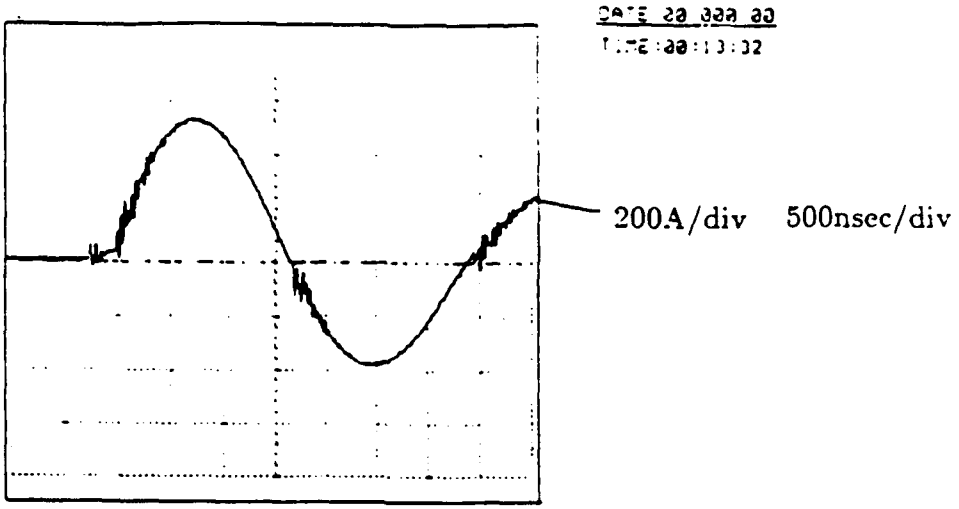

a: Output current with a 0.25μF capacitor and a 1:2 output transformer.

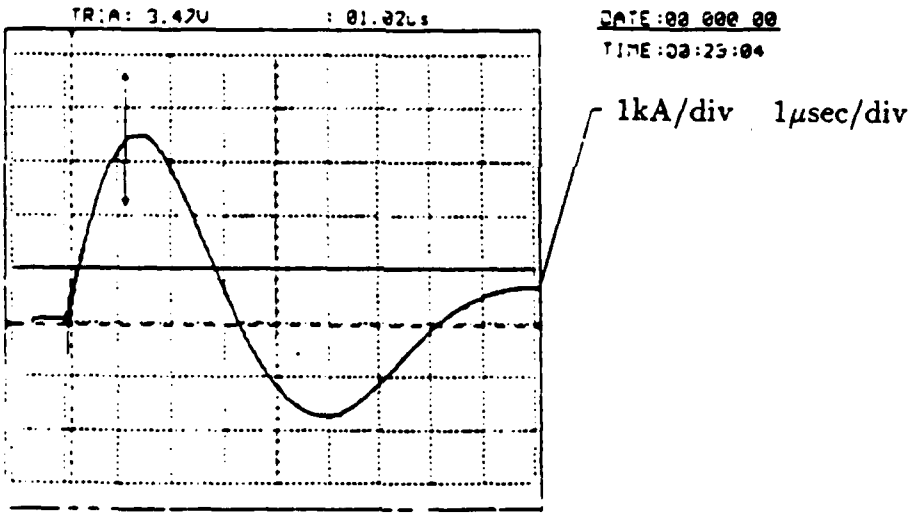

b: Output current with a 2.0μF capacitor and a 1:1 low inductance transformer.

Figure 4-5: Plasma gun driving circuit output current.

by the electrical circuit into a plasma. Once a plasma is created, it usually can supply the electron current extracted by the high field in the diode gap. The plasma surface then behaves very much like a cathode surface with a low work function consisting what is called a *virtual cathode* [2]. This name is usually associated with reflex diodes, but it is also used to describe the fact that the existing cathode plasma replaces the real metal cathode surface in regards to the electric field in the diode. The plasma surface shape can modify the electric field line shape in the diode high voltage gap. An inhomogeneous plasma could create high localized electric fields which could cause ion beam divergence or even diode breakdown. The flashboard has to be able to create a homogeneous cathode plasma.

The flashboard was built from an array of 120 arcing points as can be seen in figures 4–6 and 4–7. Figure 4–6 shows the flashboards used in a racetrack diode, and figure 4–7 shows the flashboard used in an annular diode. Figure 4–8 and figure 4–9 show pictures of the visible light emitted during flashboard operation. Each arcing point consists of a cental metal pin surrounded by a TiH_2 powder filled grove. The powder was bound to the grove with a sodium–silicate binder. The current through each arcing point was limited by a 110Ω 0.25 Watt resistor. The total resistance of the flashboard was about 0.9Ω which did not effect the circuit current. This arrangement assured a homogeneous dissipation of the circuit current over the flashboard area.

An arc created in vacuum evaporates some of the electrodes material. This material is ionized and a plasma of electrons and positive ions (some of them double or triple ionized) is created. As will come out of this work, negative ions also exist in this plasma. The arc plasma is then driven forwards by diffusion forces and by the arc current magnetic field. The plasma surface should look like 120 discrete points immediately after firing the plasma gun. But at a later time the plasma expands and should create a more homogeneous surface. This should be true haven't we had an insulating magnetic field. This field could confine the plasma. We shall return to the problem of plasma homogeneouty

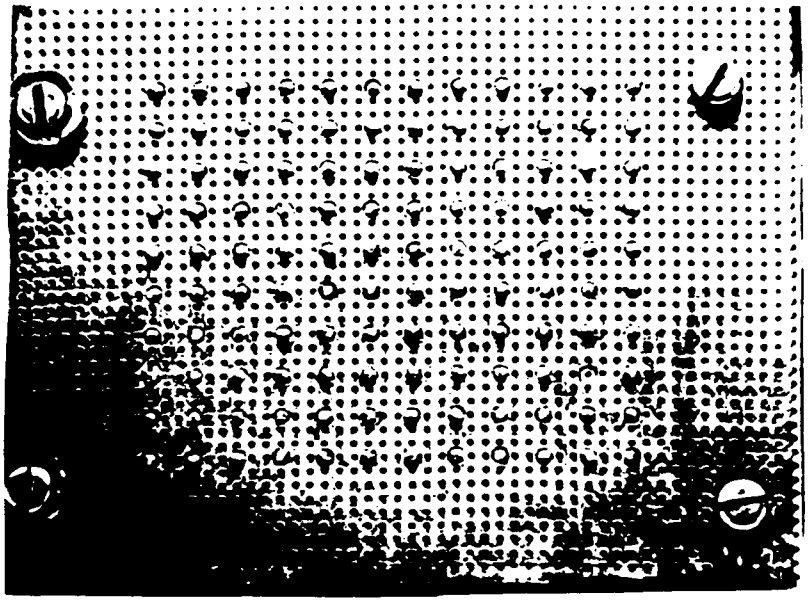

a: Regular flashboard–front view.

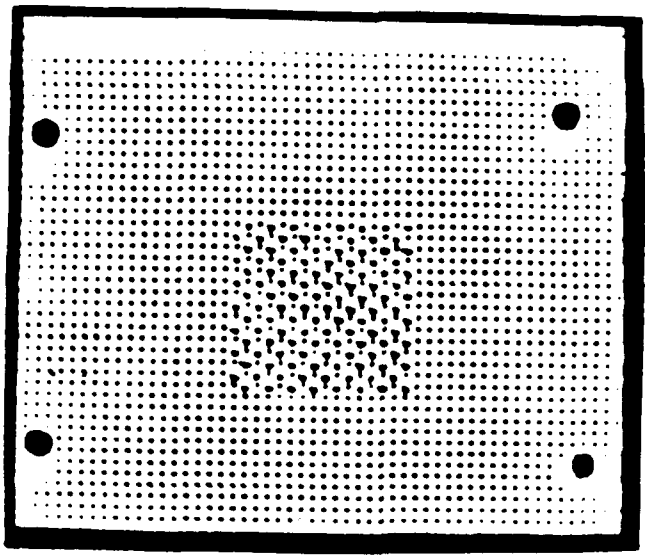

b: Dense array point flashboard.

Figure 4–6: Racetrack diode flashboard.

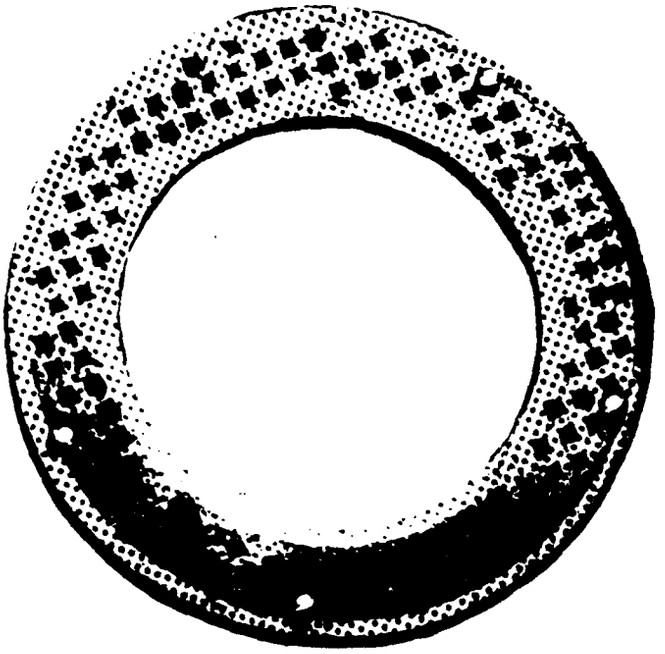

a: Flashboard front wiew.

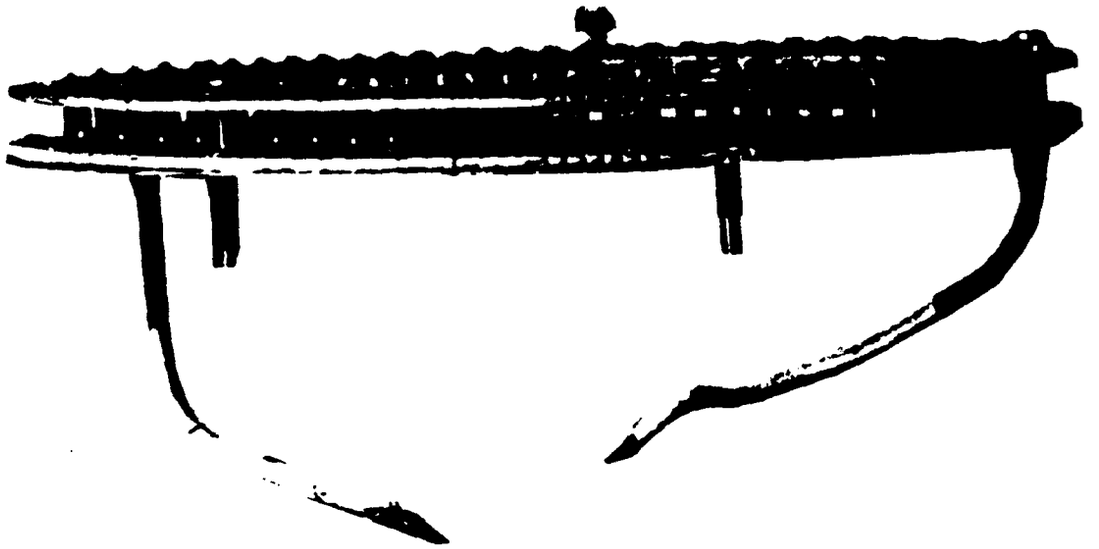

b: Flashboard side view.

Figure 4–7: Annular diode flashboard.

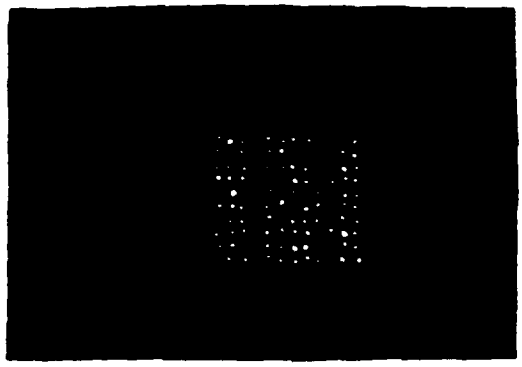

Figure 4–8: Light emitted from a racetrack flashboard.

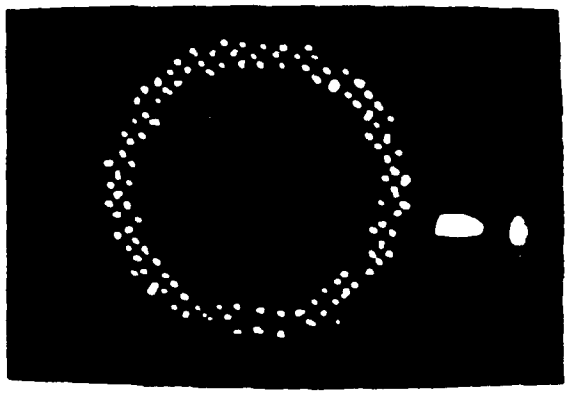

Figure 4–9: Light emitted from an annular diode flashboard.

and expansion in a high voltage insulated diode in chapter 8.

4.5 Light measuring system

The light measuring system was introduced in order to measure the actual time lag between plasma gun firing and application of the high voltage pulse to the diode. An optical fiber was put into the diode vacuum chamber collecting light emitted from the cathode surface. The light was transferred through the fiber to a photomultiplier, the output of which was recorded by a scope. The light signal gave us information about the flashboard operation conditions. Sometimes a low amplitude light signal meant that the batteries have to be recharged, and sometimes it meant that the flashboard was contaminated with metal deposits created in the diode vacuum chamber, causing some of the arcing points on the flashboard to short.

Examples of light signals measured are shown in figure 4–10. Light measurements show clearly the flashboard current frequency and light amplitude. One can easily see that the magnetic field confines the plasma since with this field the second and third light amplitudes are about the same.

4.6 Langmuir probe plasma measurements

Plasma parameters were measured using a double Langmuir probe. All plasma measurement were performed on a racetrack diode geometry, without applying a high voltage or a magnetic field. When we tried to measure the plasma parameters with a magnetic field, no signal was recorded by the Langmuir probe indicating that the plasma was confined by the field. The experiment setup is shown in figure 4–11, and the Langmuir probe circuit is given in figure 4–12.

Probe measurements were made under low and high plasma gun output current conditions. The probe was made from two metallic thin rods with an exposed area of $7.8 \times 10^{-6} m^2$. The rods were embedded in a copper tubing sealed with epoxy and connected to the chamber flange through a Wilson seal.

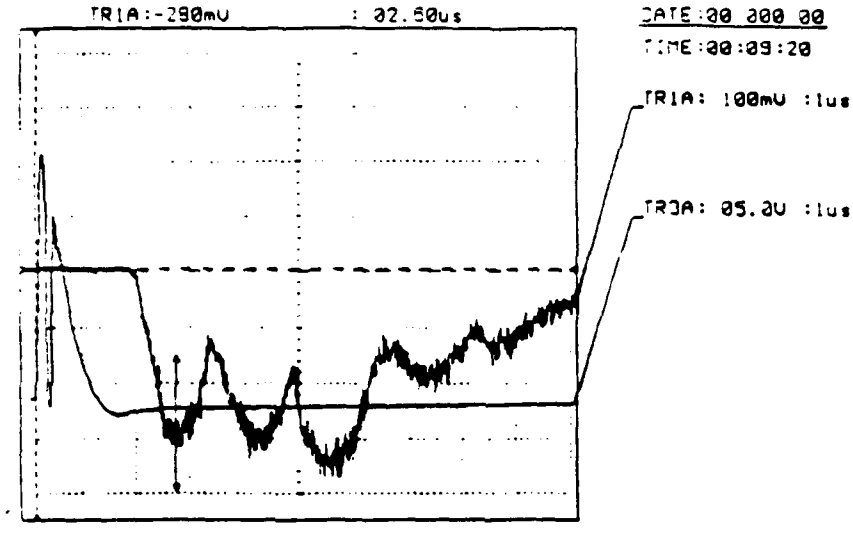

a: Magnetic field = 3.1 kgauss.

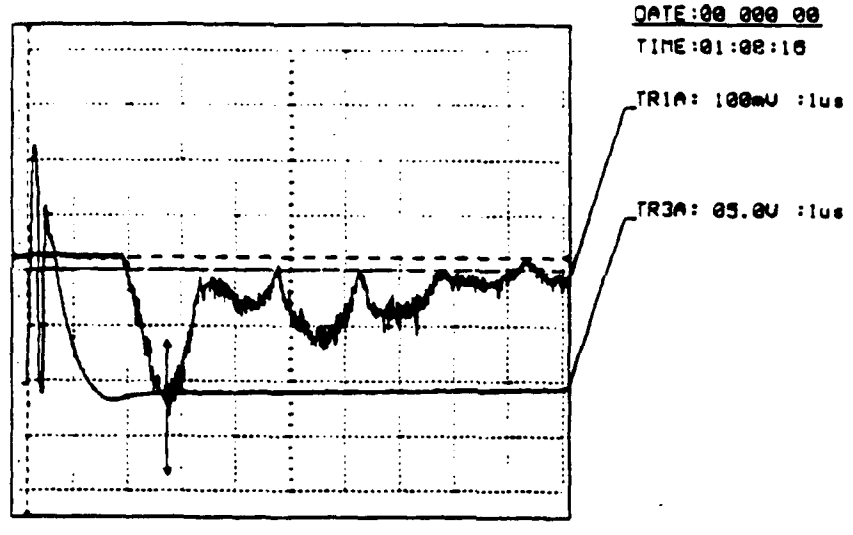

b: Magnetic field =0

Figure 4–10: Photomultiplier light signal together with plasma gun triggering signal for a 0.25μF capacitor, 1:2 output transformer in diferrent insulating magnetic fields.

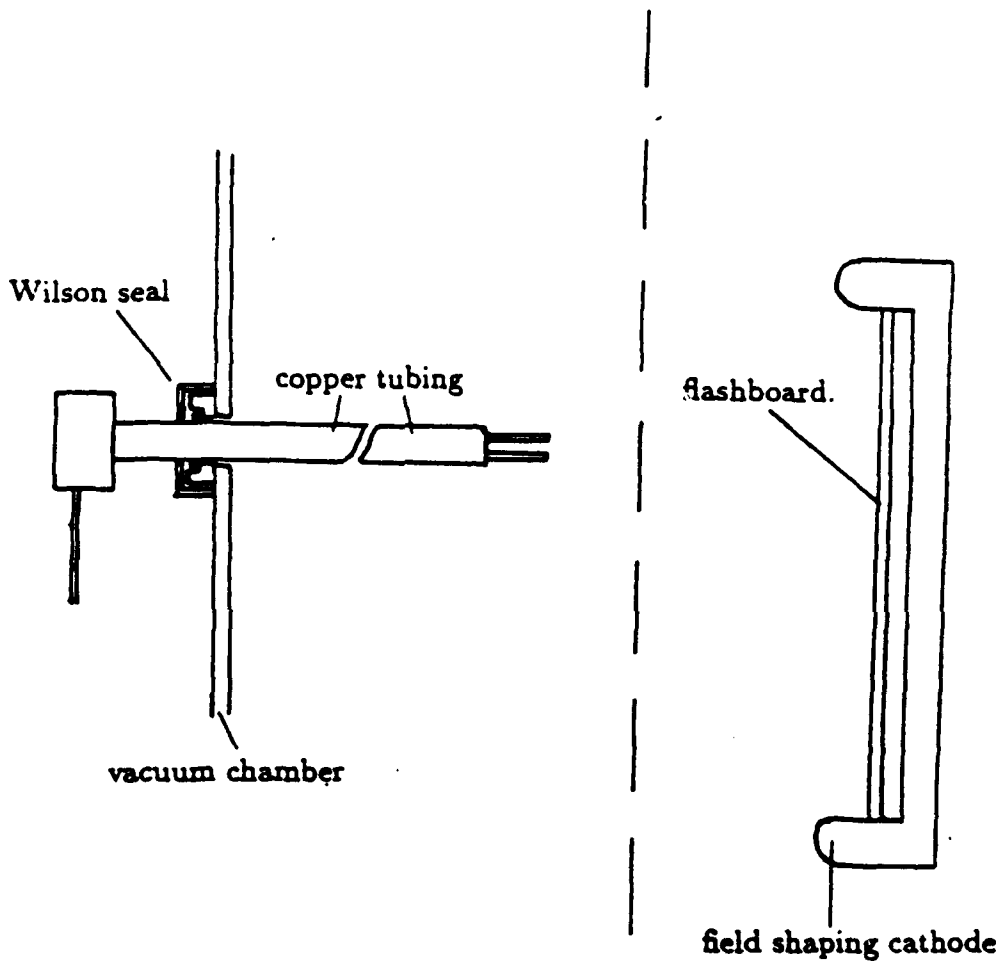

Figure 4-11: Langmuir probe plasma measurments setup.

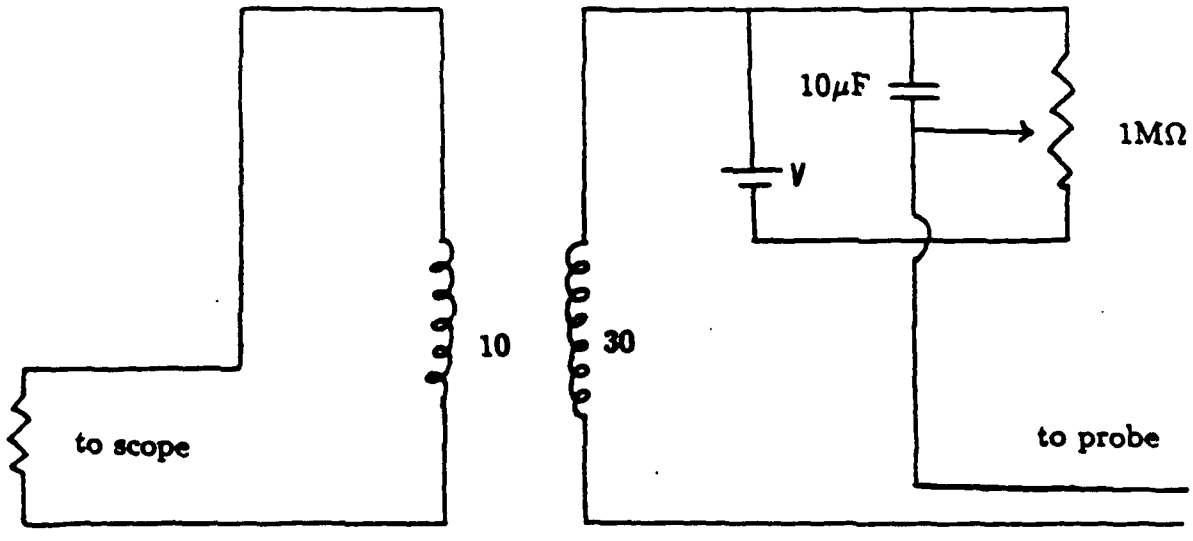

Figure 4-12: Langmuir probe electrical circuit.

The voltage difference on the probe was changed with a 30 volt battery and a potentiometer (see figure 4–12). Probe signal was passed through an 10:30 insulating transformer and recorded on a scope. In order to be able to calculate the plasma parameters a graph of probe current versus probe voltage has to be drawn [53]. The plasma temperature can be found by measuring the slope of the graph at the origin:

$$\left.\frac{dI}{dV}\right]_0 = \frac{e}{kT_e}\frac{i_{1+}i_{2+}}{i_{1+}+i_{2+}} \tag{4.1}$$

Where I is the probe current, V is the probe voltage, T_e is the plasma electron temperature, and i_{1+} and i_{2+} are the probe saturation currents for a negative and a positive voltage respectively. Once the temperature is known we can use it to calculate the electron density using the equation:

$$i_+ = \frac{1}{2}n_0 eA\left(\frac{kT_e}{m}\right)^{1/2} \tag{4.2}$$

Where A is the probe exposed area, n_o is the plasma electron density, m is the plasma ion mass, and i_+ is the saturation current. An example of the probe current together with the light pulse collected by the optical fiber is shown in figure 4–13 for a plasma gun with high current conditions. Probe current has a delay of about 0.5μsec compared to the light pulse indicating that the front part of the plasma has an expansion velocity of about 8.0 cm/μsec. This velocity was also measured by putting a Faraday cup at a distance of 13.0 cm from the cathode surface. Faraday cup current is shown in figure 4–14. The expansion velocity of the plasma front is indeed about 8.0 cm/μsec. It is to be remembered that these measurements were done without an insulating magnetic field present. We repeated the measurement with an insulating magnetic field of about 3.0 kGauss. The results are shown in figure 4–14 **b**. No current was measured by the Faraday cup. It is clear that even this small magnetic field confines the plasma produced by the gun under high current conditions. The high expansion velocity of the plasma is probably caused by the magnetic field produced by the

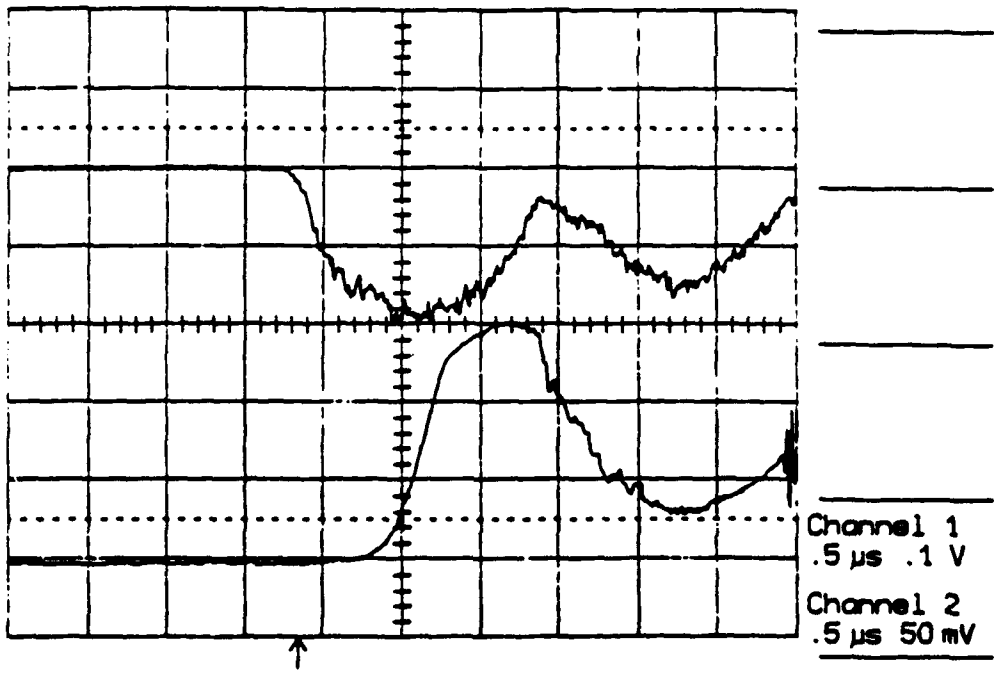

Figure 4-13: Typical Langmuir probe current and light pulse from a plasma gun operating under high current conditions.

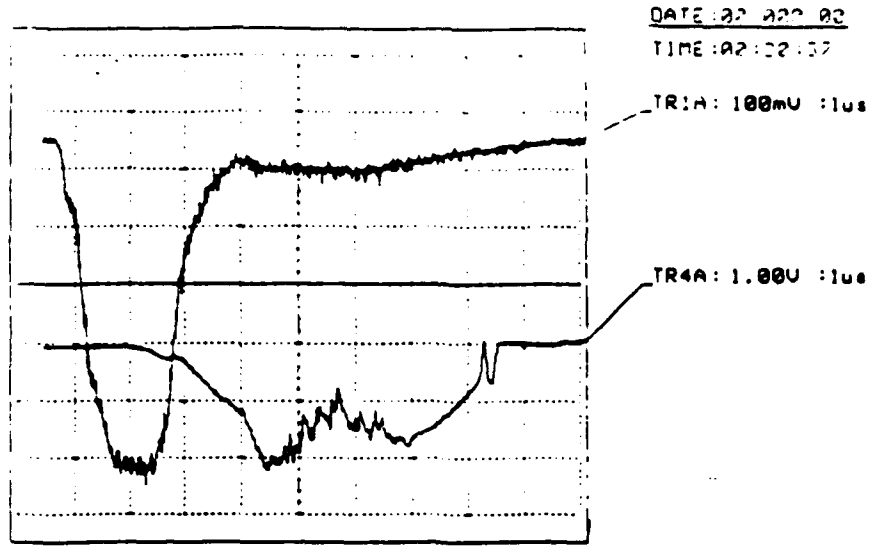

a: Magnetic field=0

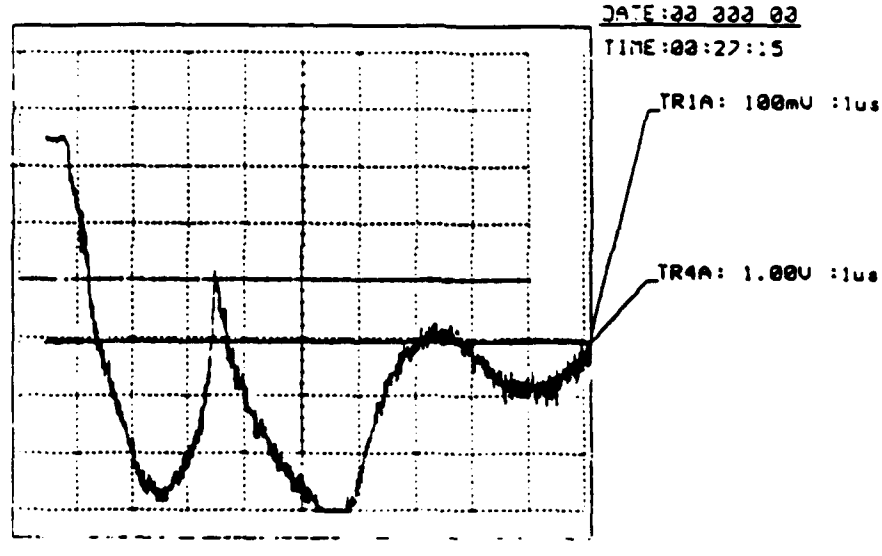

b: Magnetic field =3.0 kGauss.

Figure 4–14: Current collected by a Faraday cup 13.0 cm from the plasma gun.

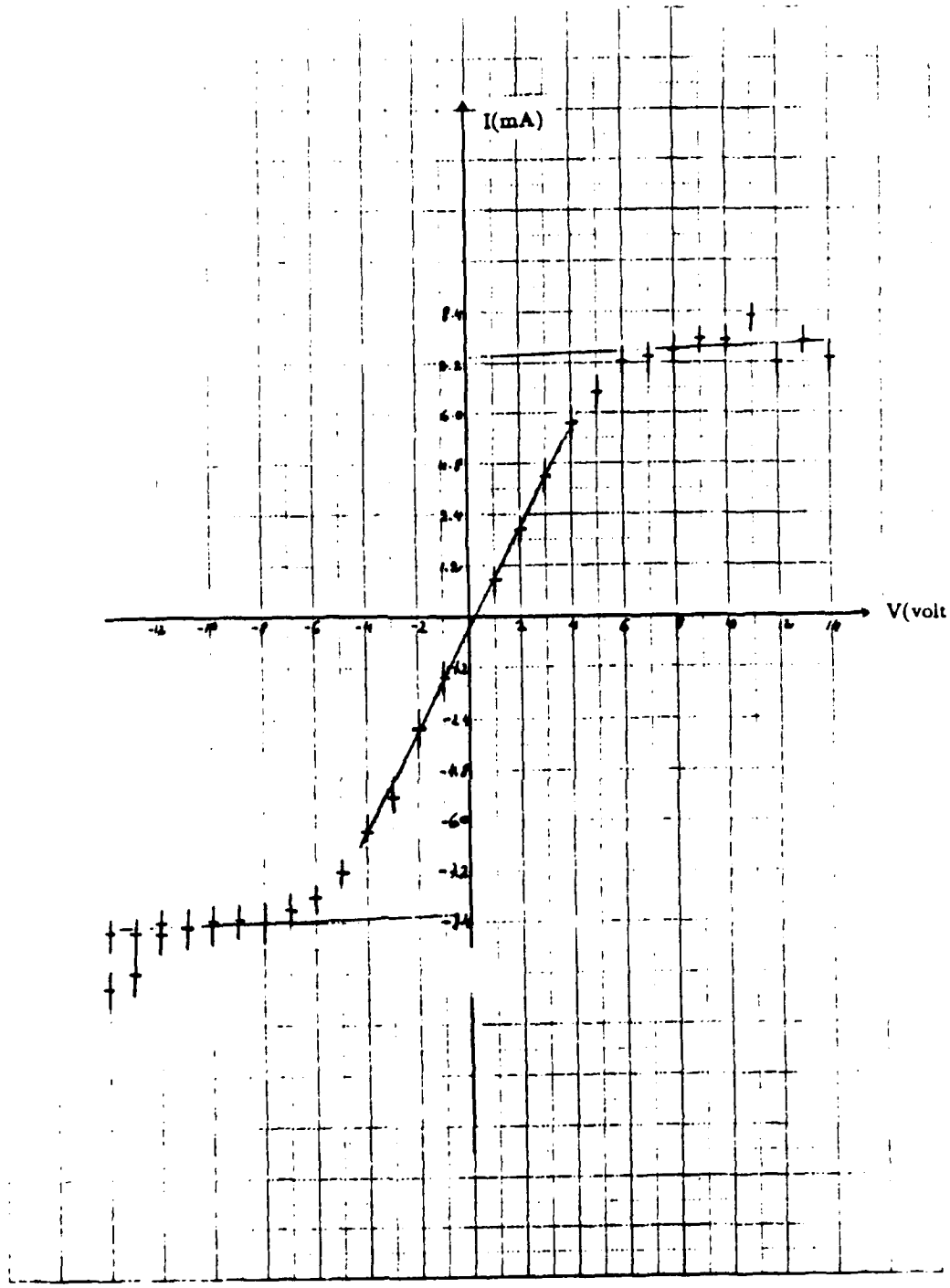

Figure 4–15: A typical Langmuir probe current voltage graph for low current plasma gun conditions.

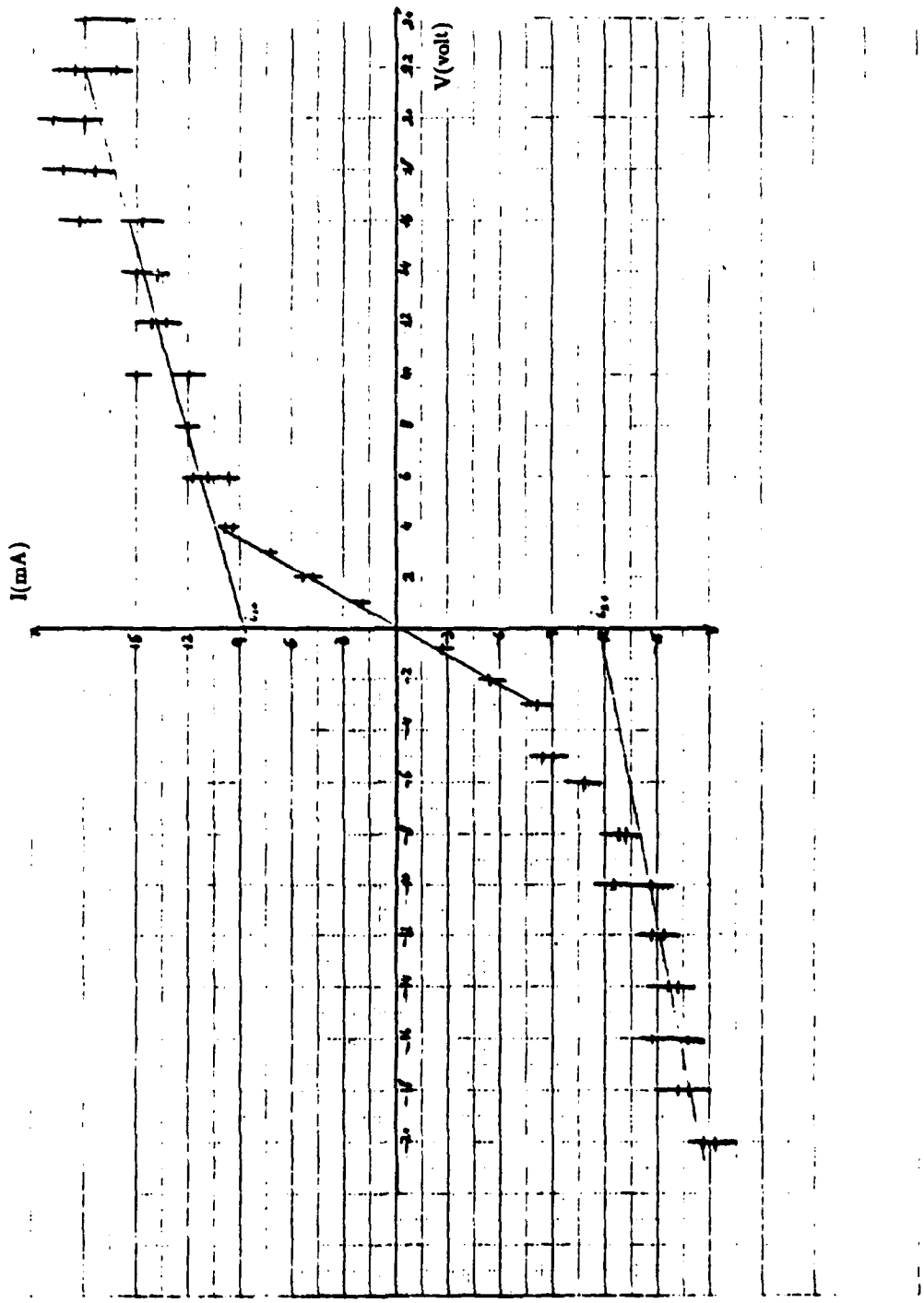

Figure 4–16: A typical Langmuir probe current voltage graph for high current plasma gun conditions.

flashboard arc current. This field drives the arc plasma forwards. This is what we call a *Bostick plasmoid* [54]. Since the plasma behavior is different whenever we have an insulating magnetic field we shall not discuss it any more.

Typical Langmuir probe current–voltage graphs are shown in figure 4–15 for the low current conditions and in figure 4–16 for the high current plasma gun conditions. One can easily measure the saturation current and the graph slope at the origin. Table 4–1 contains the probe measurement results. typical plasma densities are around $3 \times 10^{11}/\mathrm{cm}^3$ for low current conditions, and around $1.3 \times 10^{12}/\mathrm{cm}^3$ for the high current conditions. Plasma temperature is around 3.3 eV for the low current case and around 1.6 eV for the high current case. Plasma density and temperature were measured at the center of the cathode and at two points each 3.0 cm from the cathode center. Plasma density was a little lower at the center. This difference could be attributed to the fact that the probe was about 2.0 cm from the cathode surface. Since the gun consists of 120 distinct points there might be a small plasma density difference. The calculations are based of the assumptions that we have only positive hydrogen ions in the plasma. We could take into account the effect of two positive mass species by looking at equation 4.2 and introducing an effective mass:

$$\frac{1}{\sqrt{m}_{eff}} = \frac{c_1}{\sqrt{m}_1} + \frac{c_2}{\sqrt{m}_2} \tag{4.3}$$

Where m_1 and m_2 are the ion masses, and c_1 and c_2 are their concentrations respectively, where $c_1 + c_2 = 1$. If we assume a plasma of 50% hydrogen and 50% carbon ions we get a plasma density which is about 13% lower than the numbers given in table 4–1. Gas load was estimated by the chamber pressure rise to be about 10^{15} particles per pulse under high current plasma gun conditions. This did in some cases impose a too high load on the diode and we had to put a 50% fine screen in front of the gun. The plasma on the screen surface was much more homogeneous as could be inferred from beam divergence measurements. We could not measure its parameters because the signal to noise ratio of the probe

distance(cm)	position	density ($1/cm^3$)	temperature (eV)
4.0	center	4.3×10^{11}	3.4
4.0	center	7.9×10^{11}	3.5
7.0	center	3.3×10^{11}	3.3
7.0	center	3.5×10^{11}	3.0
10.0	center	3.7×10^{11}	3.9
4.0	right	6.3×10^{11}	2.9
4.0	top	6.7×10^{11}	2.6
*4.0	center	1.3×10^{12}	1.6

Table 4–1: Plasma temperature and density measurments with a Langmuir probe at different position and distances, under low current plasma gun conditions

***this measurment was done with high current plasma gun conditions.**

was too low in this case. The gas load in the case of low current gun condition did not cause any problems in all diode configurations. We shall discuss this problem further when dealing with results of the separate diodes investigated.

4.7 Summary

The problem of plasma production in a high voltage beam producing diode was discussed in this chapter. A new plasma gun was developed to simulate the effects of the machine prepulse and to produce a more homogeneous plasma into the diode gap. The plasma gun was operated for a few hundred shots by now. The only problem was contamination of the flashboard surface which appeared once due to material evaporated in the diode during breakdowns. The flashboard was cleaned with isopropyl alchohol and new Ti powder put in the groves. The plasma gun is very reliable and has a very good timing and plasma production reproducibility.

Chapter 5 EXPERIMENTS WITH A CYLINDRICALLY SYMMETRIC COAXIAL DIODE

5.1 Diode geometry

The cylindrically symmetric coaxial diode consists of an inner cylindrical cathode and an outer cylindrically shaped wire–mesh anode (figure 5–1). This diode geometry is very simple, and the high symmetry provides a good magnetic insulation (we shall discuss this point in section 5.2). The cathode was made from a conducting material, which sometimes was coated with a thin dielectric layer (we tried polyethelene, diffusion pump oil or parafine). We tried cathodes made of aluminum and carbon. Cathodes with diameters varying between 25mm and 70mm were tried. The cathode was mounted on an aluminum tubing connected to the APEX output. Cathodes could be easily interchanged without changing the diode coaxial alignment. The anode was made of a 4" diameter stainless steel wire mesh with a 50% transparency. The wire mesh was attached to two epoxy casted magnetic field coils. It was electrically grounded to the vacuum chamber through four conductors to lower the coil and diode inductance. The best diode high voltage holdoff was achieved when we used a cathode with a radius of 1/e of the anode. In this case the diode had less breakdowns since the field on the cathode surface is minimal. All the measurements done on the coaxial diode were performed with the APEX prepulse resistor disconnected. Typical voltage current traces can be seen in figure 5–2. The voltage was peaked around 700 kV and the current was usually around 30 kA.

This diode resembles very much the *magnetron*. The magnetron is an instrument used among other things to create negative ions and measure their affinity [55]. It consists of an electron emitting hot filament surrounded by a grid and an anode in a cylindrically symmetric coaxial arrangement. An axial magnetic field of a few hundred gauss prevents the electrons from reaching the anode. A low pressure gas is allowed into the instrument. Gas atoms ionized

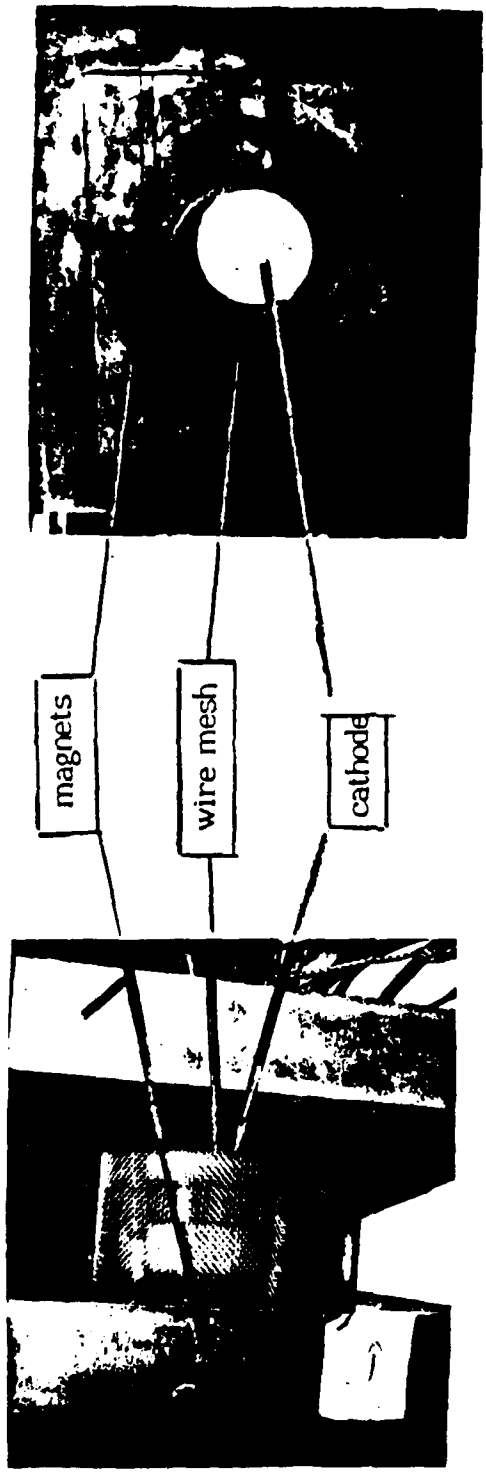

Figure 5–1: Cylindrically symmetric coaxial diode.

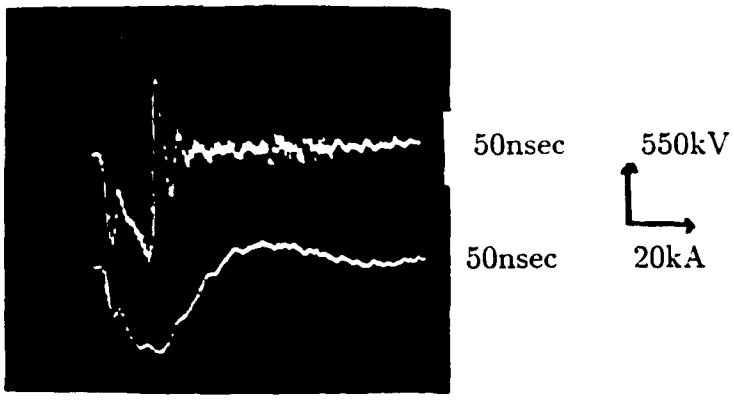

a: Anode cathode distance=15 mm.

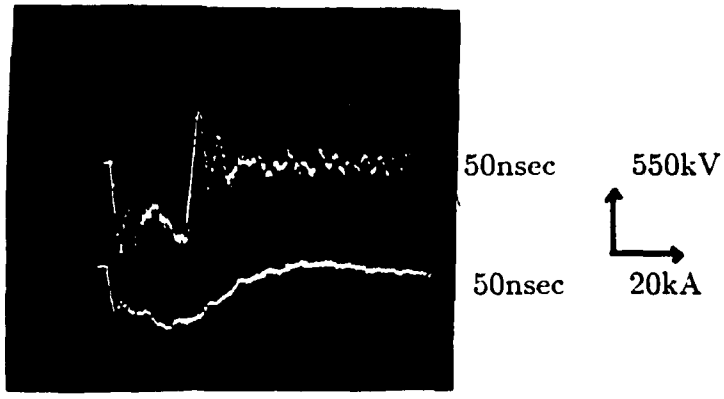

b: Anode cathode distance=20 mm.

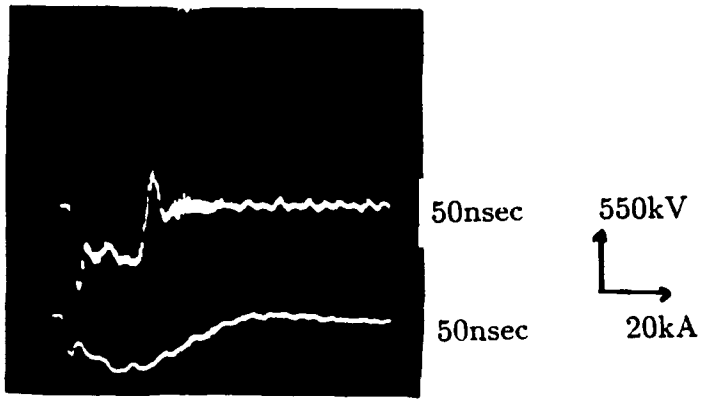

c: Anode cathode distance=25 mm.

Figure 5-2: Voltage-current traces for a cylindrical diode.

by the electrons emitted, create negative ions. Electrons are prevented from reaching the anode by the grid and the axial magnetic field. The total current (ion + electron) is measured in the absence of the magnetic field, and the ion current alone in its presence. It is then possible to compare the fluxes of ions and electrons out of a small volume near the filament surface. The flux of neutral species into this element of volume may be calculated by the kinetic theory of gases and, if fluxes into the volume are identified with concentrations, the equilibrium constant for ion formation, at the assumed temperature of the filament surface, may be calculated, and the heat of reaction, which is the required electron affinity, may be evaluated by methods of statistical mechanics. The geometry and operation of this instrument is basically similar to the coaxial diode. The interesting point here is that it was necessary to put a grid to collect electrons and prevent the creation of the negative space charge near the cathode. The high voltage diode in our case does not have, however an electron collecting grid like in the magnetron case. The electron cloud around the cathode can create a space charge which might prevent negative ions from leaving the cathode plasma and reach the acceleration gap.

The cylindrically symmetric coaxial diode was investigated at the Lebedev institute (see chapter 2). Currents of the order of 200 A/cm^2 have been measured. Ion current was measured using carbon nuclear activation by the beam protons. However, the results of the Lebedev institute group could not be reproduced by other researchers. A review of the Lebedev institute group work, as well as of other groups is given in chapter 2.

Due to its geometry, the coaxial diode cannot produce a unidirectional beam. Ions accelerated by the electrical field move basically in a radially outwards direction. As we shall see in chapter 5.2, the insulating magnetic field causes the ions to have an azimuthal deflection. The ions going out of this diode will not move in the same direction and will probably not meet the definition of what we call a "beam". This diode is certainly useless for fusion or beam propagation purposes. However, because of its simple configuration,

and in order to try and reproduce the Lebedev group results we decided to investigate this diode.

5.2 The insulating magnetic field and its use for ion mass spectrometry

The insulating magnetic field was supplied by two magnetic coils. The field was parallel to the diode axis. The two coils were connected in series to a capacitor bank through the circuit described previously in figure 3–3. The magnetic field was 14.0 kGauss when the capacitor bank was charged to its maximum voltage of ±3.0 kV. Magnetic field pulse shape was similar to current shape shown in figure 3–4a. The coils inductance was about 20μHenry. Field intensity was calculated using the EFFI code [56]. Field direction and intensity were measured as a function of the distance from the diode axis with a small search coil and also with a small Hall–effect probe. The results are shown in figure 5–3. The EFFI code calculations agree quite well with the search coil measurements.

We used this insulating magnetic field to perform mass spectrometry of the ion beam. This was done by tracing the particle trajectory with a CR–39 film and compare it to a calculated trajectory. This way we were able to find out what ion species does our beam contain, and even to see what their energies are. First let us see what is the trajectory of a particle emitted from the cathode under the combined influence of the electric and magnetic fields. We shall use the single particle approximation and assume that the particle is not affected by space charge of other particles around when it crosses the high voltage gap. We shall first describe the equations of motion for the case of a parallel plates gap and then modify the equations to the cylindrical case.

Charged particles ejected from the cathode are subject to an $\vec{E} \times \vec{B}$ drift [57]. The equation of motion of a particle in the presence of electric and magnetic fields is:

$$m\frac{d\vec{v}}{dt} = q(\vec{E} + \vec{v} \times \vec{B}) \tag{5.1}$$

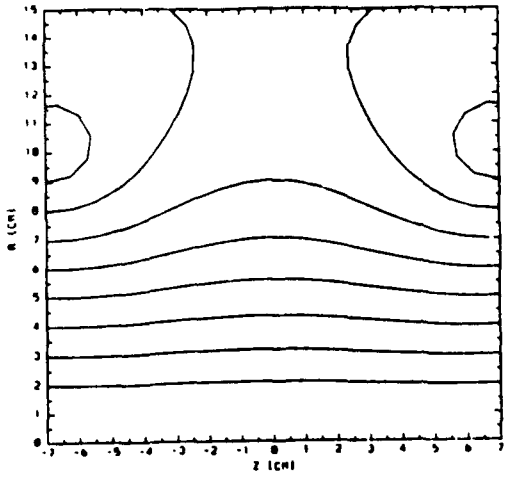

a: Magnetic field lines.

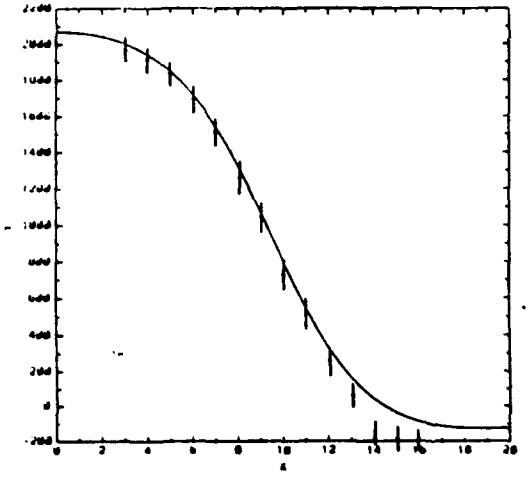

b: Field intensity at the diode center as a function of distance from the axis.

Figure 5–3: Insulating magnetic field for a cylindrical diode.

For a homogeneous magnetic field along the $\hat{z}$ axis, an electric field along the $\hat{x}$ axis and a particle with initial velocity in the x–y plane we get:

$$\frac{dv_x}{dt} = \frac{q}{m}E_x \pm \omega_c v_y \tag{5.2}$$

$$\frac{dv_y}{dt} = \mp\omega_c v_x \tag{5.3}$$

Where ω_c is the *cyclotron frequency*:

$$\omega_c = \frac{\mid q \mid B}{m} \tag{5.4}$$

The particle motion is composed of drifting circular orbits. The drift velocity is :

$$\vec{v}_{drift} = \frac{\vec{E} \times \vec{B}}{B^2} \tag{5.6}$$

The drift velocity is independent of the particle mass or energy. The radius of each drifting circle is the *Larmor radius*:

$$r_L = \frac{mv_\perp}{\mid r \mid B} \tag{5.7}$$

And $v_\perp$ is the particle velocity in the x–y plane. The Larmor radius for electrons is much smaller than it is for ions. Electrons are prevented therefore from crossing the high voltage gap, and ions do cross it. Actually relativistic effects should be taken into account when dealing with electrons, but the above equation are correct for ions. Magnetic insulation was checked by taking x–ray pictures of the diode at different magnetic fields (see figure 5–4). It is clearly seen that we get a good magnetic insulation even at fields as low as 4 kGauss for a high voltage gap of 20 mm and a voltage of about 750 kV.

In our case the diode has a cylindrical symmetry. We have a magnetic field along the diode axis, and an electric field in the radial direction. We shall assume that both fields are a function of the radial distance r, but are homogeneous along the diode axis. We then get the equations of motion:

$$\frac{dv_r(r;t)}{dt} = \frac{q}{m}E_r(r) \pm \frac{\mid q \mid B(r)}{m}v_\theta(r;t) \tag{5.8}$$

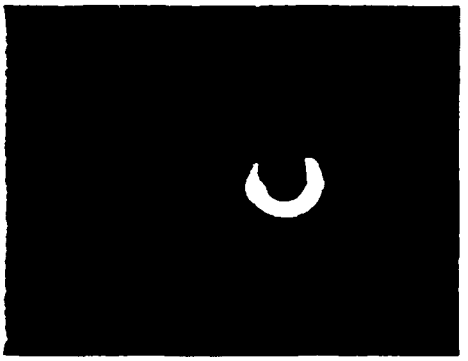

Magnetic field = 0 kGauss.

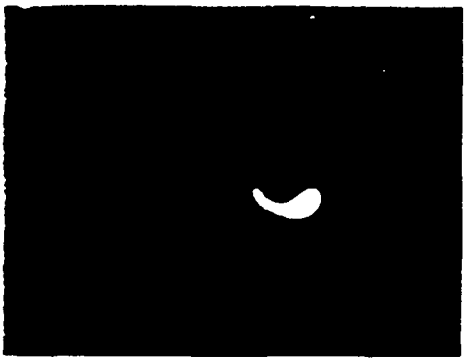

Magnetic field =2.0 kGauss.

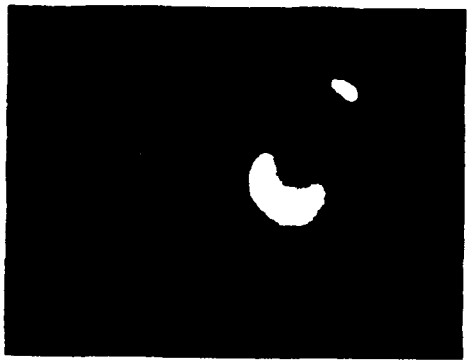

Magnetic field =3.7 kGauss.

Magnetic field =5.1 kGauss.

Figure 5-4: X-ray pictures for different magnetic field values.

$$\frac{dv_\theta(r;t)}{dt} = \mp\frac{\mid q \mid B(r)}{m} \tag{5.9}$$

We solved this set of equation numerically on a computer. The electric field was introduced under the assumption that the plasma layer is very thin such that the field is given by the diode geometry only. The magnetic field was introduced to the equations by taking the field measurements results and fitting a polynomial to them by minimizing the mean square deviation. Particle trajectories were calculated for hydrogen and carbon ions for different values of diode voltage and magnetic field (see figure 5–5). A box with two 1.0 mm holes in it was put around the anode wire mesh. The box was covered with a CR–39 track detector (see figure 5–6). A similar idea was used at Cornell for investigating a positive beam ion mass composition [58]. We designed the box such that hydrogen ions would be deflected to the lower part of the box and carbon or higher mass negative ions would be deflected to the back side. A piece of CR–39 was also put at the top side to try and detect positive ions. However, in none of the experiments performed with this box were any positive ions detected. The box itself is shown in figure 5–7. It is estimated that this method could not detect hydrogen ions with energy less than 80 KeV due to the finite thickness of the lower box cover in which the hole was drilled. Such ions would impinge on the box at a low angle and hit the hole walls.

A few kinds of experimental errors can happen when using the above method. Ion tracks on the CR–39 were sometimes etched so that they could not be seen in the microscope. This usually happened when ions impinge on the track detector with low angle. They then penetrate the CR–39 to a smaller distance. When the material is etched (we usually etched it for one hour at 80° C) a bulk of material is removed (see chapter 3), and the tracks disappear. An example can be seen in figure 5–9.

The EFFI code does not take into account the fact that the magnetic field penetrates only a few millimeter into the cathode. When calculating the different ion trajectories we take into account mainly the magnetic field intensity in the

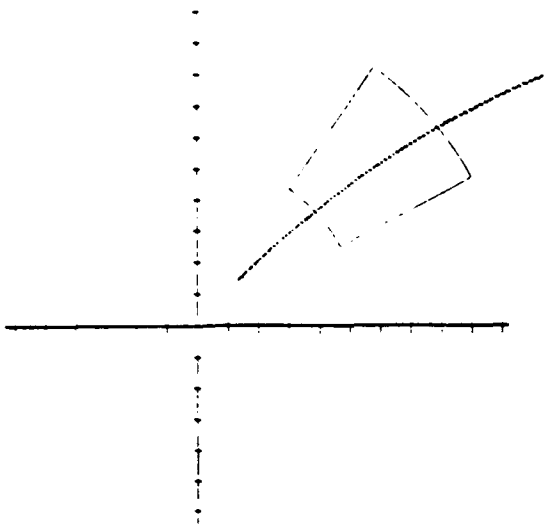

700 keV C^- ions

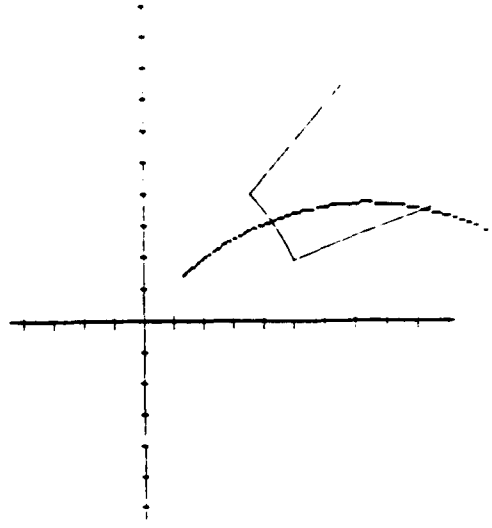

100 keV C^- ions

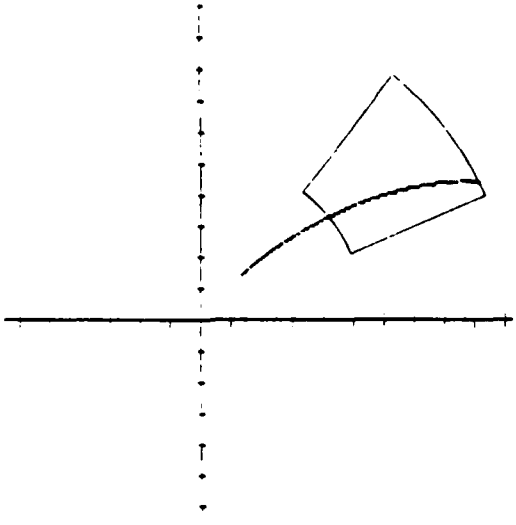

700 keV H^- ions

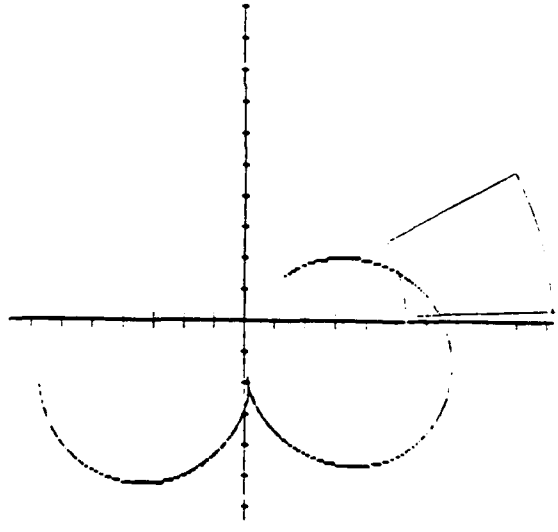

100 keV H^- ions

Figure 5-5: Calculated ion trajectories.

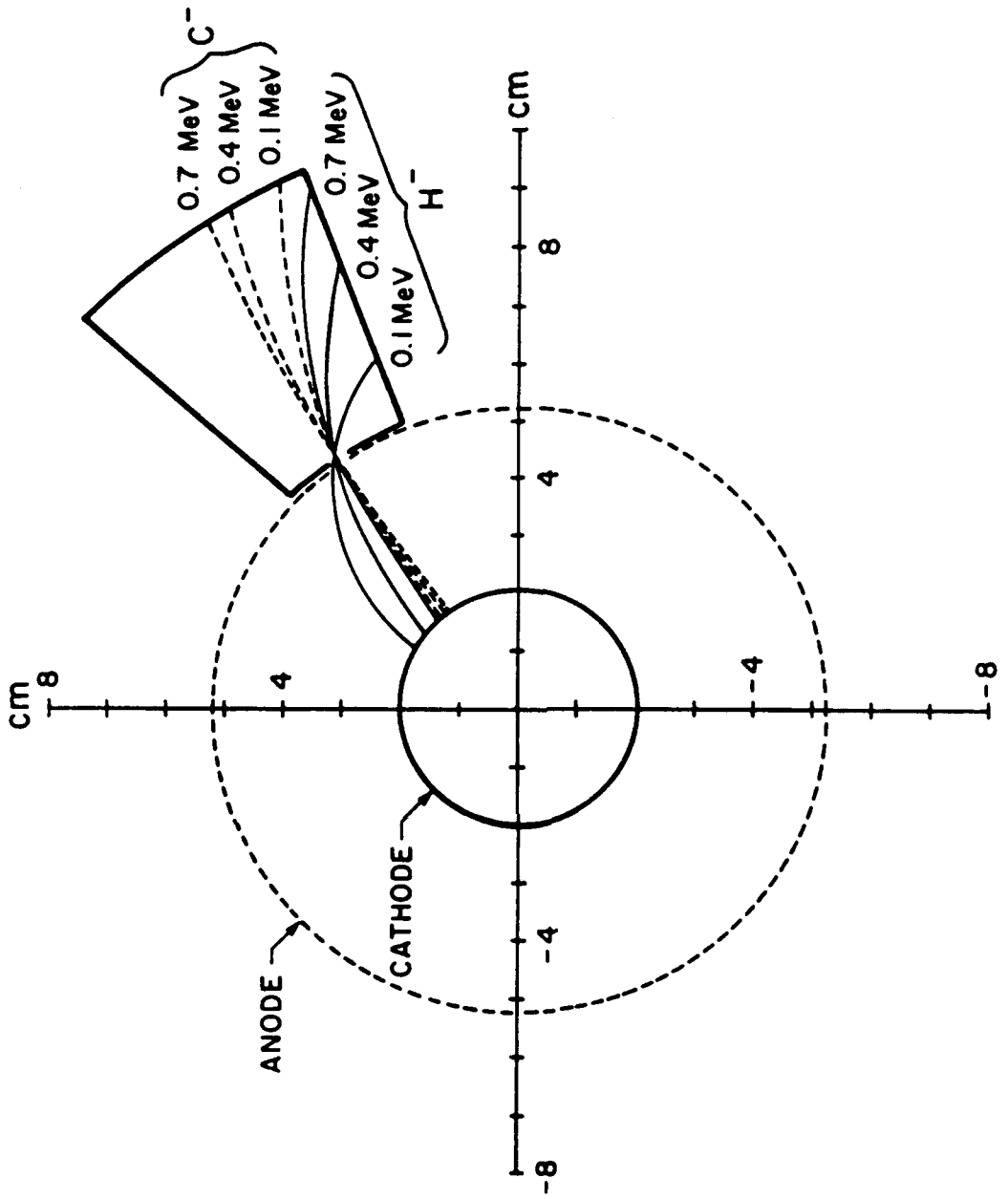

Figure 5–6: Ion mass spectrometry experiment layout.

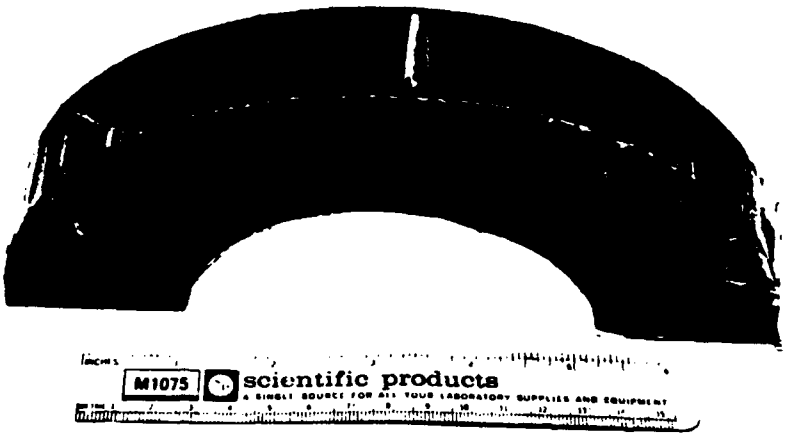

Figure 5–7: Ion track detecting box for mass spectrometry.

a: Polyethelene coated cathode.

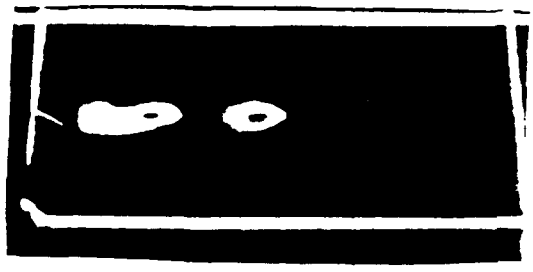

b: Carbon cathode.

c: Aluminum cathode.

Figure 5-8: CR-39 ion tracks for different 63 mm diameter cathodes.

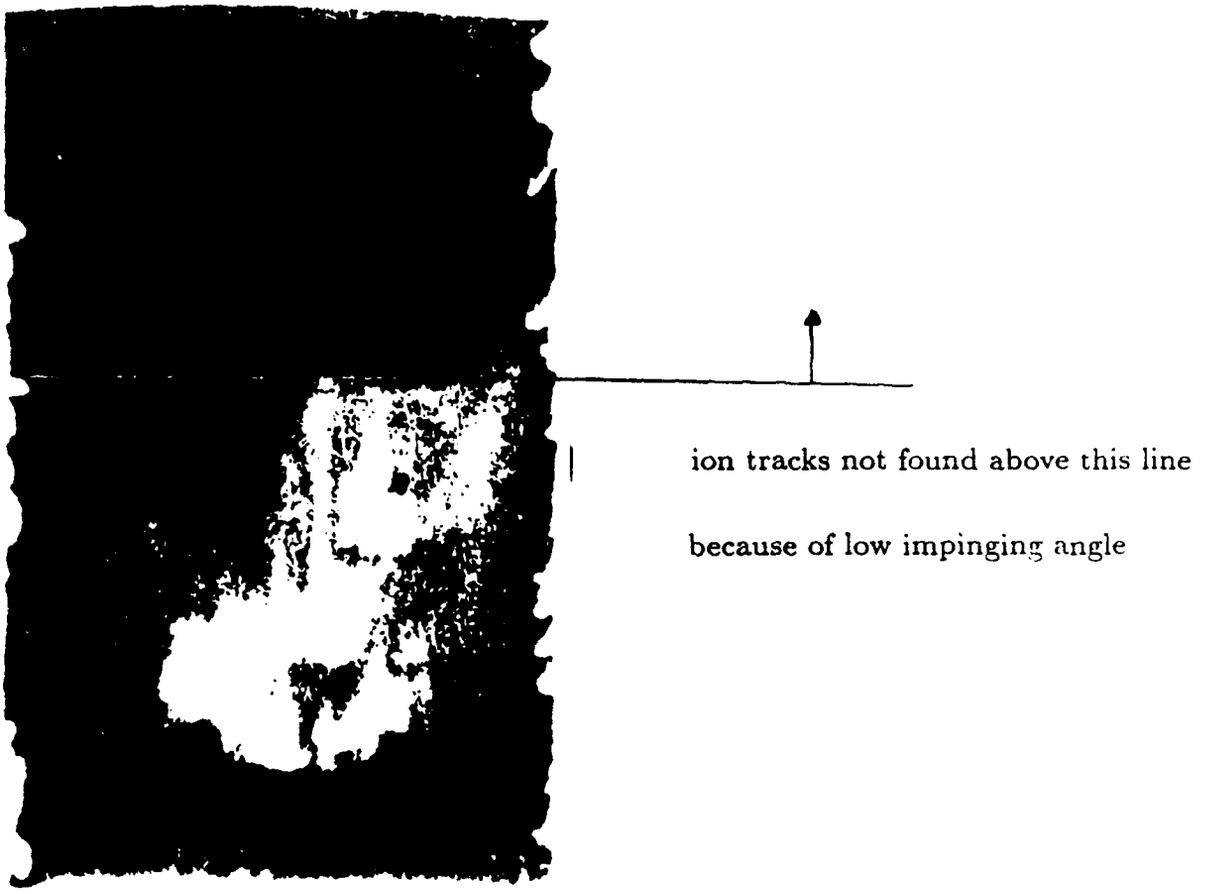

Figure 5–9: Effect of low impinging angle on CR–39 ion tracks.

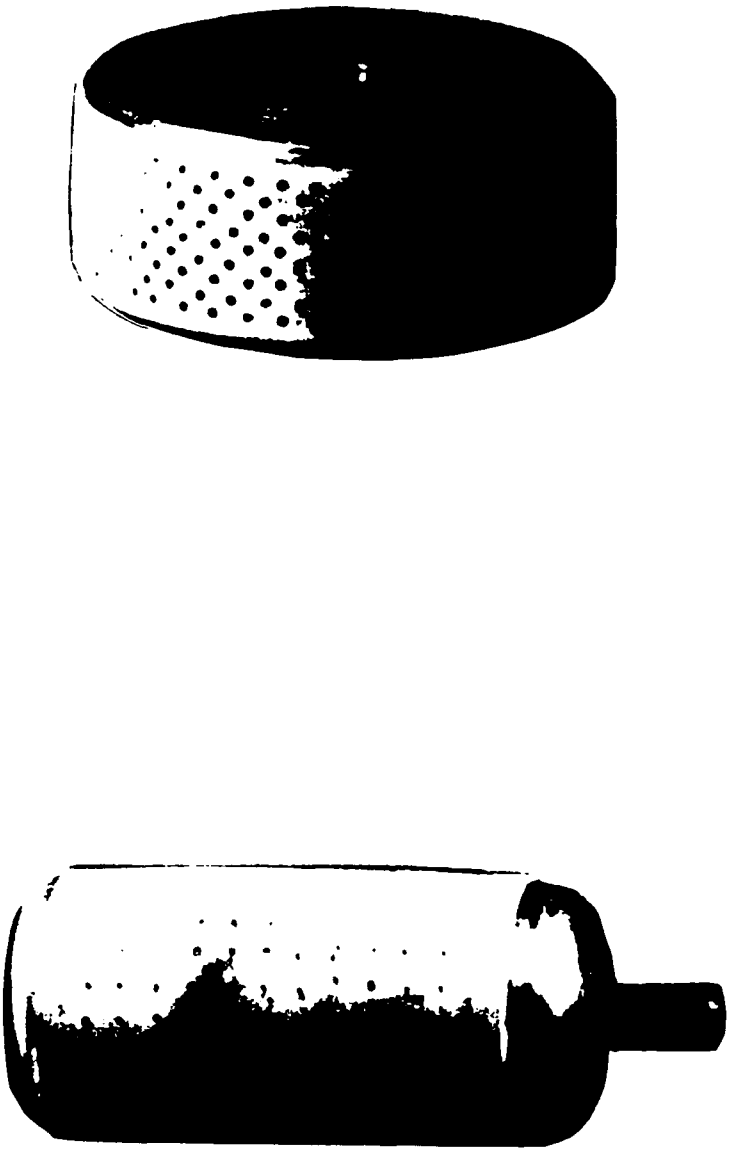

Figure 5–10: Different types of polyethelene covered cathodes.

high voltage gap. This field would be higher due to the exclusion of the magnetic field from the cathode. We calculated ion trajectories taking into account a 20% higher magnetic field. This did cause the different ion trajectories to change. Taking this effect into account enabled us to identify ion species like hydrogen and carbon for which the mass difference is large. These ion trajectories agreed very well with the calculated ones. However we could not decide about a higher mass peak if it is C_2^- or O^-.

When we calculated the ion trajectories we assumed that both magnetic and electric fields are homogeneous along the diode axis. In this case, ion tracks on the CR–39 should follow a straight line. An example of such a line is shown in figure 5–8. Any inhomogeneouty in the electric or magnetic fields could cause the ions to deflect in the axial direction. Such a deflection could not be caused by any means by the initial velocity direction of the ion when it leaves the plasma. The energy of the ions in the plasma is a few electron volts, and the velocity or direction at which they leave the plasma has no effect on their trajectories at the high voltage gap.

5.3 Experiments with polyethelene covered cathodes

5.3.1 Pinhole camera pictures

The polyethelene covered cathode was usually made of an inner aluminum rod covered with a thin layer (1–2 mm) of polyethelene (see figure 5–10). The polyethelene was drilled with 2mm holes and then sandpapared and cleaned with methanol. Cathodes were used for tens and hundreds of shots without any significant damage.

Pinhole camera pictures of the cathode show an interesting phenomena. Emission of negative ions was localized to a few spots on the cathode surface (see figure 5–11) . Both high and low energy ions were emitted from these spots. This was revealed by covering the CR–39 with a 2.5μm of mylar film. This mylar stops hydrogen ions with energy less then 250 kV. It also stops heavier ions over our whole energy range (see chapter 3). The fact that both low and high energy

ions are emitted from the same spots leads to the conclusion that the spots are active over most of the high voltage pulse period. It also leads to the conclusion that the spots are created at about the same time. The *hot spots* phenomena is very typical to electron emission from the cathode. This is the first time that a similar phenomena is associated with negative ion emission from the cathode.

The initiation of cathode hot spots was discussed in chapter 4. These spots are formed as a consequence of the explosion of microprojections on the cathode after reaching the critical field–emission current density. The places of appearance of this hot spots fluctuate on the cathode surface of a high voltage diode [59]. These place fluctuations were not observed in our case. This is just a conclusion based on the fact that we get both low and high energy ions from the same spot. This means that during the high and low voltage parts of the pulse the spot stayed at the same position. This is true within a few millimeters. A typical CR–39 spot picture has a diameter of about 2–3 mm which is equivalent to a diameter of 5–8 mm on the cathode surface. We would not therefore observe spot place fluctuations within a distance of a few millimeters.

Ions with transverse deflection angle of about 100 milliradians can be seen in figure 5–11. Without this transverse deflection we should have gotten a straight line picture. It looks like the plasma created at the few spots seen deforms the electrical field in the acceleration gap causing this deflection. The large spot diameter together with the small number of spots leads to the conclusion that plasma created at the spots expands very quickly and shields the rest of the cathode area from the electric field in the gap. Once this happens no more spots can be created on the cathode by field emission. A similar phenomena was observed by Hinshelwood [60]. The fact that we get negative ion emission only from a few spots on the cathode area will be the subject of the theoretical discussion in chapter 8. These hot spot dense plasma points distort the electric field in the high voltage gap and create large ion deflection. As we shall see later, this phenomena was typical to polyethelene cathodes in all types of diode configuration investigated.

Figure 5–11: Pinhole camera picture of a polyethelene cathode.

We can use the pinhole camera picture to count the number of particles emitted from a hot point. The average number counted in figure 5–11 was about 3×10^7 particles per spot. This is equivalent to a current density of about $25 A/cm^2$ averaged on the spot. Taking into account that the spots cover about 20% of the cathode area we get an average current of about $5 A/cm^2$ over the whole cathode.

The fact that we get negative ion emission from a small random area on the cathode, together with the fact that the electric field in the gap is distorted creates a problem. We lose a significant amount of ions which are deflected by the transverse fields. These fields also can cause problems when a second stage accelerating system is used since the whole beam optics is distorted. This lowers the efficiency of the magnetic insulation, and causes power loss to the diode. And the really bad thing here is that the transverse fields are of random nature and it is not possible to overcome the problem they create.

5.3.2 Wire mesh CR–39 pictures

We used CR–39 to take pictures of ion emission from all diode parts. This was done just by covering the whole anode with small pieces of CR–39 track detector. Sometimes we covered the CR–39 with thin layers of mylar to see the picture at different ion energies. This technique gave us information about ion emission from all diode parts in a single shot.

Figure 5–12 is a CR–39 wire mesh picture of ion emission from a diode. With ions accelerated radially outwards we should get a clear square wire mesh picture with square holes. With ions deflected in the azimuthal direction only (such in the case of homogeneous electric and magnetic fields) we should get a wire mesh with rectangular holes with their long edge in the azimuthal direction. This edge should be clear, but the other edge (in the axial direction) should not be very well defined in the pictures since ion energy changes during the pulse. This is caused by the azimuthal magnetic deflection. A typical picture is shown in figure 5–12 a. When transverse electric field in the diode deflect ion beam

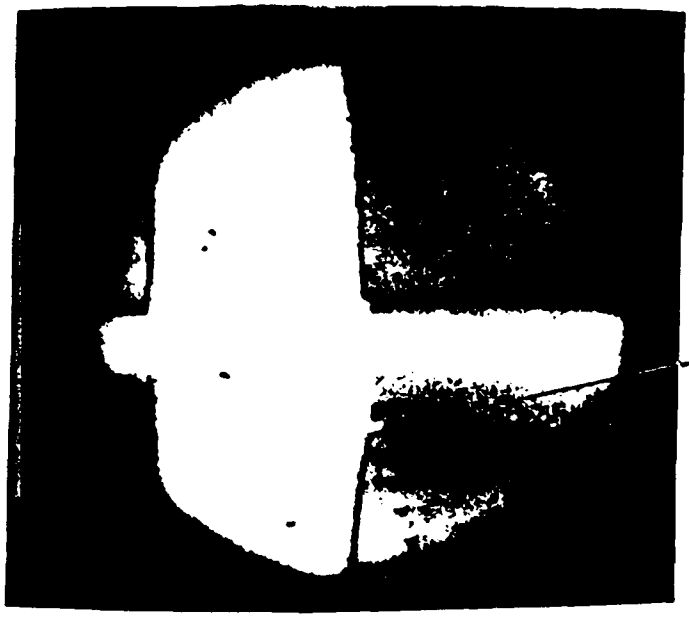

a: Undistorted wire mesh picture.

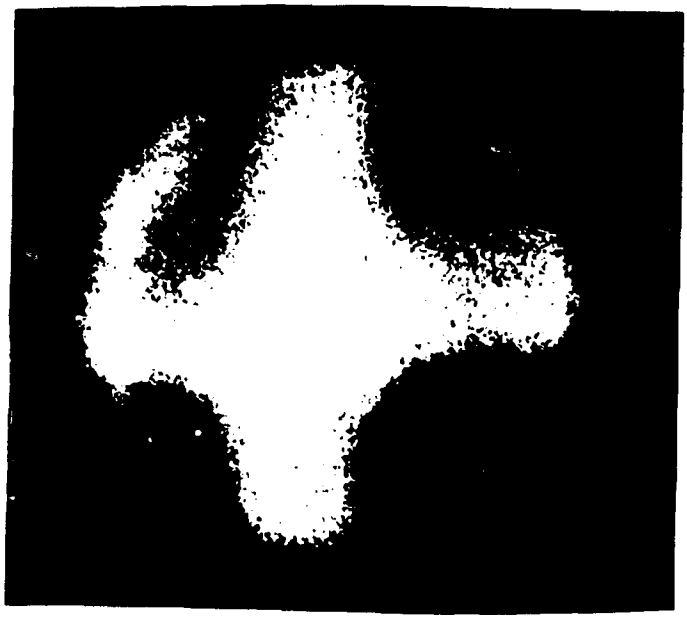

b: Distorted wire mesh picture.

Figure 5–12: Microscope wiew of CR–39 wire mesh pictures.

trajectories, and when this happens in many places over the cathode area we get a distorted wire mesh picture (figure 5–12 **b**).

Figure 5–13 describes a wire mesh picture of a 63 mm polyethelene cathode. There are some areas where the wire mesh looks the way it is supposed to look, and some other areas where the whole mesh picture is distorted. This distortion could be associated with the hot spots phenomena discussed in 5.3.1. It is clearly seen that at areas where the picture is distorted we get higher ion emission both in the high energy case (picture with mylar on it) and in the low energy case. The fact that we get high energy ions from all over the cathode means that during the pulse the plasma spreads all over this area. Trajectories of negative ion emitted from this "expanded" plasma areas are less deflected by transverse fields. The location of the hot spots is quite random, and we could not associate them with any particular part of the cathode.

Looking at the CR–39 pictures in the microscope shows that a large amount of ions hit the CR–39 at low angles. A rough estimate is that about 30% of the ions have an energy of 200 keV or less. This ions could be emitted either at the end or at the beginning of the pulse. As we shall see later, some of the ions are created from residual gas molecules on the cathode surface. These ions are probably created sometime at the beginning of the high voltage pulse. Since in this type of diode we were not able to measure the ion current with a Faraday cup, we could not check when these low energy ions were created.

5.3.3 Magnetic field mass spectrometry

Mass spectrometry of the ions created by this diode was performed via the insulating magnetic field mass spectrometer (see chapter 5.2). The traces are of H^- ions and about an equal amount of C^- ions (see figure 5–8). Hydrogen ions with energy as low as 80 keV which is the lowest detection limit of this spectrometer, were measured. CR–39 traces have a wide axial spread which is probably caused by the transverse fields in the diode gap. The higher energy ions have a smaller axial spread. Beam divergence for H^- ions in the axial

Figure 5–13: Wire mesh CR–39 picture of a polyethelene cathode.

direction was 0.3 radians at an energy of 100 keV and about 70 milliradians at an energy of about 500 keV. The identification of H^- traces was confirmed by putting 2.5μ mylar on the CR-39. The mylar stopped all ions heavier than H^-. Another important fact is that no positive ions were detected. These ions would be easily detected on the back side of the CR-39 box especially for the case of hydrogen where the magnetic deflection is the largest. It is quite difficult to draw any more conclusive conclusion in this case because of the large axial deflection.

5.4 Experiments with carbon cathodes

5.4.1 Pinhole camera pictures

The carbon cathode was just a 63 mm diameter rod of graphite with small 2mm holes drilled in it. These holes were drilled to create some field inhomogeneouty on the cathode surface in order to create the field emission necessary for cathode plasma production. Pinhole camera pictures taken on a CR-39 track detector had a straight line shape. Beam divergence was around 40 milliradians with an estimated intensity of about 1-3A/cm^2 on the cathode surface. This estimate is based on etch pit counting of the CR-39 track detector. The fact that we get a straight narrow line means that in this case the azimuthal deflection is small and the high voltage field in the diode gap is homogeneous. It also means that the cathode plasma is homogenous. No hot spots were seen on the CR-39 pictures.

5.4.2 Wire mesh CR-39 pictures

The wire mesh picture of the carbon cathode negative ions is very homogeneous. The wire mesh can be clearly seen all around the diode (see figure 5-14). The same picture taken with 2.5μ mylar on the CR-39 had only a small amounts of ions on it. It looks like most of the ions in this case are carbon ions. The small amount (about 5%) of ions passing through the mylar could only be negative hydrogen ions with energy above 250 keV. Checking track size in the

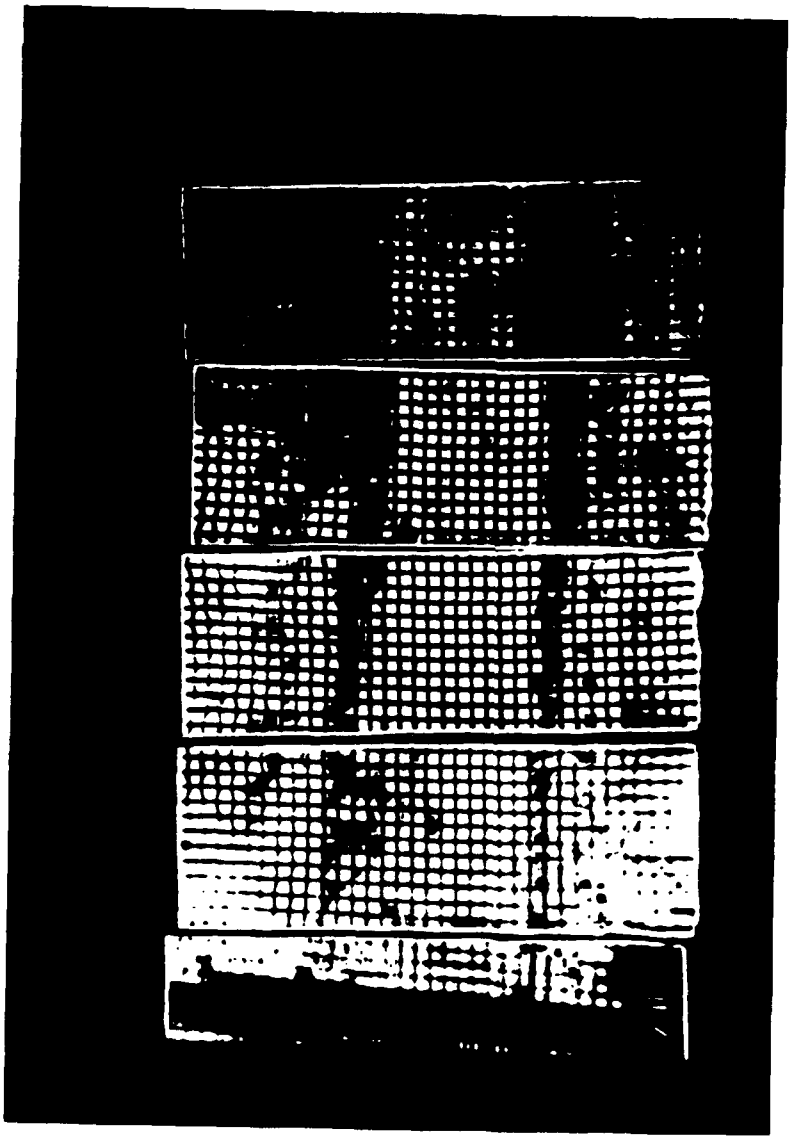

Figure 5–14: Wire mesh CR–39 picture of a carbon cathode.

microscope revealed the existence of a small number of tracks with a smaller etched diameter. These tracks correspond to negative hydrogen ion tracks (see chapter 3).

5.4.3 Magnetic field mass spectrometry

Magnetic field spectroscopy revealed the experimental facts above. The spectrometer box picture had a straight line shape with most of the ions in the carbon area (see figure 5–8). Tracks of heavier ions (which might be C_2^- or O^-) are also clearly seen (see figure 5–8). It is estimated that about 10% of the ions in this case are H^- ions and the rest consists of comparable amounts of C^- ions and heavier ions (probably C_2^-). Identification of H^- ion traces was performed with a 2.5μ mylar on the CR–39 film. Lowest carbon ion energy is estimated to be around 100 keV. Since ion tracks follow a straight line transverse electric fields do not probably exist in the acceleration gap. As we shall see later, this behaviour was typical to all conducting cathodes (meaning cathodes not covered with any insulating material). No positive ions were seen on the CR–39.

5.5 Experiments with aluminum cathodes

Aluminum cathodes were introduced into this experiment in order to check the effect of residual gases on negative ion production. We used cathodes made of bare aluminum which of course does not produce negative ions. The cathodes were sanded and cleaned with isopropyl–alchohol before installed in the diode. The pressure in our vacuum system was around 10^{-5} Torr. At this pressure we have a few monolayers of adsorbed gases on the cathode surface [61]. One monolayer of hydrogen molecules, for instance, contains about 10^{15} adsorbed background gas molecules per cm^2. These molecules can be removed from the cathode surface by low energy electrons and some positive ions hitting the cathode surface. If only a few tenths of a percent of these molecules create negative ions it could account for current densities of a few A/cm^2.

Wire mesh pictures revealed a very homogeneous beam of ions (see figure 5–15). Ion current density was estimated to be about $0.5A/cm^2$. Beam divergence

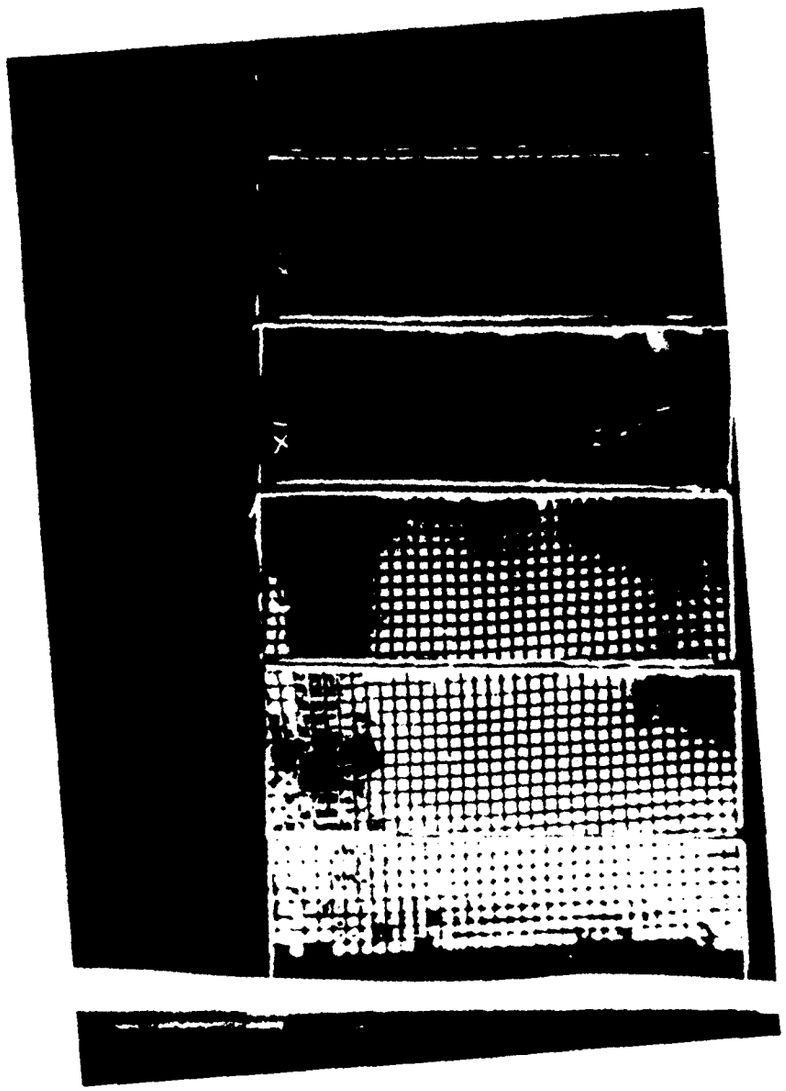

Figure 5-15: Wire mesh CR-39 pictures of an aluminum cathode.

was about 40 milliradians in the axial direction. No hot spots were seen on the CR-39 pictures. Magnetic mass spectrometry (see figure 5–8) shows tracks of about equal amounts of C^- and C_2^- ions. Only a small amount of H^- ions (about 10%) was detected. No damage signs were seen on the cathode after a few tens of shots.

5.6 Experiments with other types of diodes

During this set of experiments on the cylindrically symmetric diode we also tried some special cathode configurations. Our aim was to try and get more negative ions with these cathodes. Not always did we make a complete set of measurements. We shall describe here the main types checked.

The first cathode was made of a carbon coated cylinder wrapped with carbon fibers. This cathode is shown in figure 5–16. We did check here only the current density using etch pit counting. The current was about $5A/cm^2$. No attempt was made to check the beam mass composition. We then coated the carbon fibers with a thin layer of wax. This did not change much the current density and it was about the same as before.

We also tried a cathode with a wide grove in it. The cathode is seen in figure 5–17. The outer sides of the cathode are coated with polyethelene in which we drilled 2mm holes in the usual manner. The wire mesh picture of this cathode is shown in figure 5–18. The interesting thing here is that we get a quite homogeneous emission of ions from all over the cathode above the cathode center. The current density at the edges (where we put polyethelene) is higher. Ions at the edges are deflected in a transverse direction showing the behavior of hot spots seen before. The field intensity at the cathode center is evidently much smaller than at the edges. We would then expect a much higher current intensity at the edges, since we have a dielectric material there, and also because the electric field there is higher. We also would expect some focusing of the beam. This is because of the electric field shape, and also because of the magnetic field lines shape close to the cathode. Since the the magnetic

Figure 5-16: Carbon fibers coated cathode.

Figure 5–17: Polyethelene cathode with a grove at the middle.

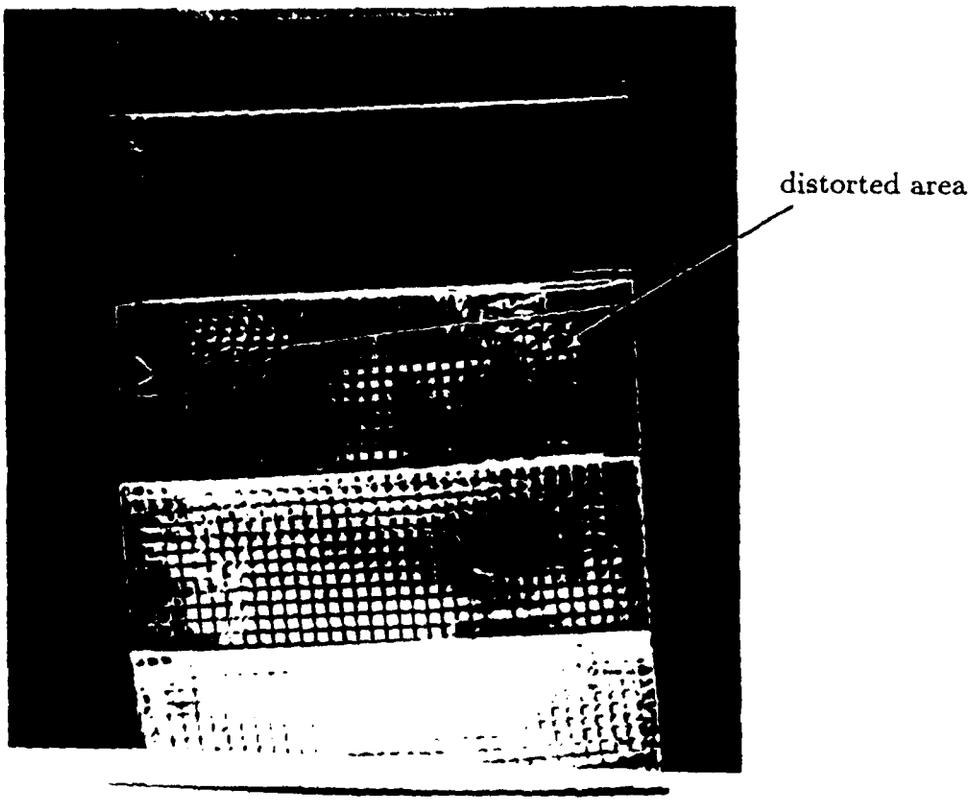

figure 5-18: Wire mesh picture of a polyethelene cathode with a grove.

field cannot penetrate the cathode to a distance larger than the skin depth, it should basically have a concave shape. Electrons follow magnetic field lines so we should have gotten focusing of the beam towards the cathode center. This behaviour was not detected.

The behaviour of this last cathode leads to a few conclusions. Plasma is first created by the explosive emission phenomena probably at the cathode edges. Electrons and ions from this plasma drift in the diode in the $\vec{E} \times \vec{B}$ direction. They hit the cathode surface and release adsorbed gas molecules which by collision create more negative ions. This usually happens when electrons with energy of at least a few hundred volts cause excitation of the adsorbate–substrate bond [62]. We then get plasma all over the cathode surface. Ions are then emitted from cathode areas which do not have a dielectric material cover. Once we have a plasma close to the cathode surface it changes the electric and magnetic field lines shape at the vicinity of the cathode. The electric and magnetic fields become more homogeneous. The focusing field created by the cathode shape is distorted by the plasma. This explanation is not conclusive. It is just a possible explanation to the ion track pictures we got with this cathode.

5.7 Summary

The results of negative ion production measurements using a cylindrically symmetric coaxial diode were presented in this chapter. The main points coming out of these experiments are:

- When using an insulator covered cathode (like polyethelene) negative ions are created mostly at a few hot spots on the cathode area. The spots have a circular shape with a 5mm diameter. Large axial ion deflection was measured in this case. This deflection is probably caused by transverse electric field caused by distortion of the gap field by the hot spots. It looks like these spots do not move within the time duration of the high voltage pulse.
- Both negative hydrogen and carbon ions are created from a polyethelene

cathode material	current density (A/cm^2)	divergence (radians)	composition
C_2H_2	5	70–300	
C	1–3	40	10% H^-;45% C^-;45% heavier
Al	0.5	40	10% H^-;45% C^-;45% heavier

Table 5–1: summary of results with coaxial diode configuration.

cathode. When using a carbon cathode we got mostly C^- ions with an equivalent amount of heavier ions, probably C_2^-.

- Negative ions are produced both from the bulk material and residual gases adsorbed on the cathode surface. It is estimated that about 10% of the ions originate from residual gas molecules.
- High energy ions have been emitted from all areas of cathodes only partly covered with dielectric material. It appears like the cathode plasma expands very rapidly along the cathode surface (expansion time estimated to be not more than 30 nsec), and releases surface molecules from all over the cathode. The electron and ion $\vec{E} \times \vec{B}$ drift velocity in our diode is about 6.6 m/μsec for the maximum diode voltage. This velocity is mass independent, and could explain the ion emission above. Positive ions and electrons drift in opposite directions, but if we have a few hot spots covering about 30% of the cathode area it the $\vec{E} \times \vec{B}$ drift could still explain the quick plasma coverage of the cathode.
- Current densities of about 5A/cm^2 have been measured. Beam axial divergence was about 40 milliradians for cathodes made of carbon or aluminum, and about 200–300 milliradians for polyethelene covered cathodes.

An obvious result is that we did not get the high current densities reported by the Lebedev group on a similar experiment. This experiment is discussed in chapter 2. The current densities reported by the Lebedev group reach 200 A/cm^2, while in our experiment we got about 5A/cm^2. A few reasons can account for this difference. One of them might be the ion beam current measuring system. Ion current density was measured at the Lebedev institute by nuclear activation of carbon by the beam protons. The whole wire mesh area was covered with carbon used for this measurement. This way ions were measured without having to take their trajectories into consideration. In our experiment we used etch pit counting using a small box which measures only a small area of the cathode at a time. With this method low angle ions are lost during the etching procedure when some of the material is removed.

The problem still appears to be when comparing the Lebedev results with the Child–Langmuir current limit (equation 3.1). This equation applies basically to two infinite parallel plane geometry. If we use the equation as an approximation to our cylindrical diode we see that for the voltage and spacing we used the current should be around 40 A/cm^2 for protons. If we take into account a beam containing about 50% carbon ions and 50% hydrogen ions the Child–Langmuir limit goes down to about 25 A/cm^2. The Lebedev current density reported looks very high compared to the Child–Langmuir limit. We have also to remember that this limit cannot be overcome in our case as it is for the case of a positive ion producing diode. Electrons drifting in the high voltage gap in the case of a positive diode, reduce the space charge of the positive ions and allows one to reach current densities much higher than the Child–Langmuir limit. Since we are dealing with negative ions, we need small mass positive particles to drift in the gap in order to overcome the Child–Langmuir limit. Such particles do not exist of course in our case.

Positive ions ejected from the anode plasma could reduce the space charge and allow a current of ions a little higher than the Child–langmuir limit. This is usually considered as a ***bipolar flow*** which in our case would refer to positive and negative ions (usually it refers to positive ions and electrons) [63]. In case that both charges reach the current limit it comes out that this limit is 1.86 higher than a single particle flow limit. This number could not explain the high current densities reported by the Lebedev group. We still have a high electron charge in the gap which also tends to reduce the negative ion current. We also do not have any anode plasma producing mechanism and probably the positive ion current will be well below the Child–Langmuir limit. We measured this positive ion current and it was really small.

We measured the positive ion current in our diode by using a hollow carbon cathode seen in figure 5–19. We drilled a 1mm hole in the cathode and put a small piece of CR–39 inside the cathode against the hole. The current measured was about 0.5A/cm^2 and consisted mainly of low energy ions. This

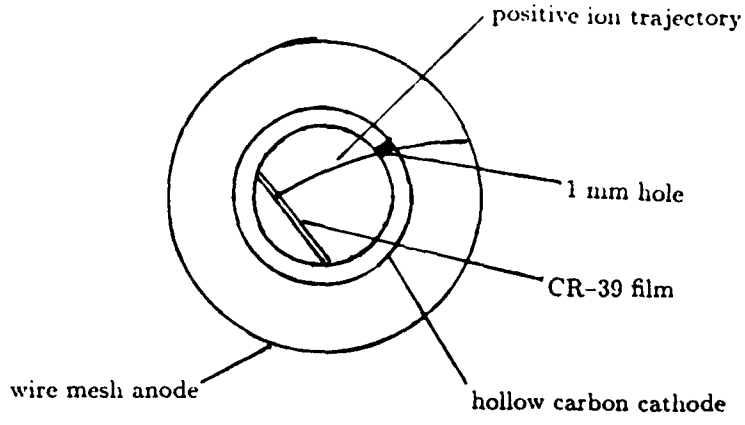

a: Hollow cathode experiment setup.

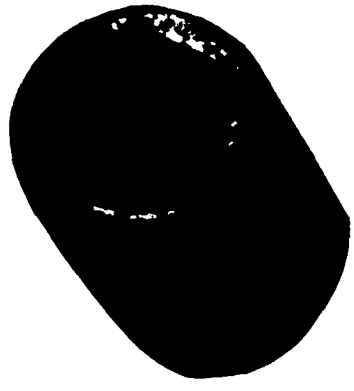

b: Picture of hollow cathode.

Figure 5-19: Hollow carbon cathode setup for measuring positive ion tracks.

was confirmed with a piece of thin mylar on the CR–39. We believe that these ions cross the gap at the end of the high voltage pulse. This pulse has a small polarity change at its end. We believe that these ions have no effect on negative charge space neutralization during the main pulse.

It could be of course, that the cathode plasma expands into the gap and the real gap is much smaller. A virtual gap three times smaller than the real diode gap makes the Child–Langmuir limit ten times larger. As we shall see later, the extracting field on the cathode plasma surface is small since it is shielded by the drifting electron cloud in the diode gap. This effect lowers the extracted current, and tends to "balance" the effect of a smaller gap. We could not find a satisfactory explanation for the large ion current reported by the Lebedev group. In our experiment we did not have the same prepulse used by the Lebedev group and described in chapter 3. Since we could not have any control of this prepulse we built a prepulse plasma creating gun. We were not able to build this gun with a cylindrical symmetry and it will be discussed in the next chapter which describes experiments with a racetrack diode.

Chapter 6 EXPERIMENTS WITH A RACETRACK TYPE DIODE

6.1 Diode geometry

The racetrack diode has an inner paddle shape cathode positioned at the center of an outer wire mesh box serving as the anode (see figure 6–1). This shape provides a closed current path for the electron Hall current created by the cathode, as well as a planar plasma surface from which the ion beam can be accelerated [64].

The insulating magnetic field was supplied by a 11 turns coil. Each turn was made of two 0.5" stainless steel rods soft soldered to two copper stripes at the upper and lower sides. The coil was mechanically supported by a G–10 epoxy glued box. The coil current was supplied by the capacitor bank and circuit described previously in chapter 3.4.2. Magnetic field had a peak value of about 9.6 kGauss when the capacitor was charged to ±3kV. Calculated field lines using the EFFI code are parallel to the diode axis. Magnetic field profile can be seen in figure 6–2. Electric field lines are basically perpendicular to the cathode surface (at least when this situation is not changed by the emitting plasma surface). Electrons are believed to drift in closed path trajectories in a $\vec{E} \times \vec{B}$ direction around the cathode. 20eV electrons drifting with the E/B velocity have a Larmour radius of tenths of a millimeter. The Larmor radius of electrons which gain the whole diode energy is about 2mm. Electrons would therefore drift around the cathode edges without being lost. The problem is that the transverse component of the electric field causes the electrons to drift along magnetic field lines and out of diode. If the magnetic field has a high degree of symmetry this process would be slow enough not to cause a high diode load during the pulse.

The magnetic field pulse shape followed the coil current shape seen in figure 3–4b. The pulse has a rise time of about 100μsec. This means that the magnetic

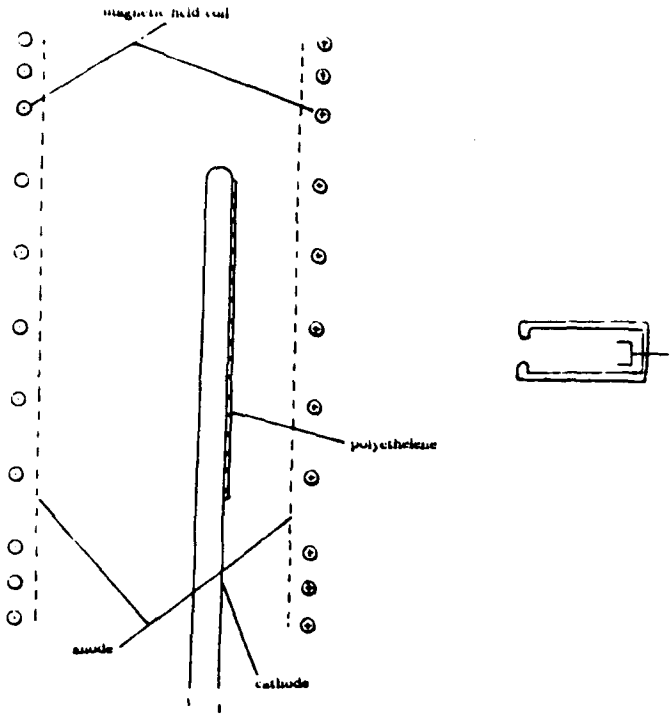

a: Diode geometry

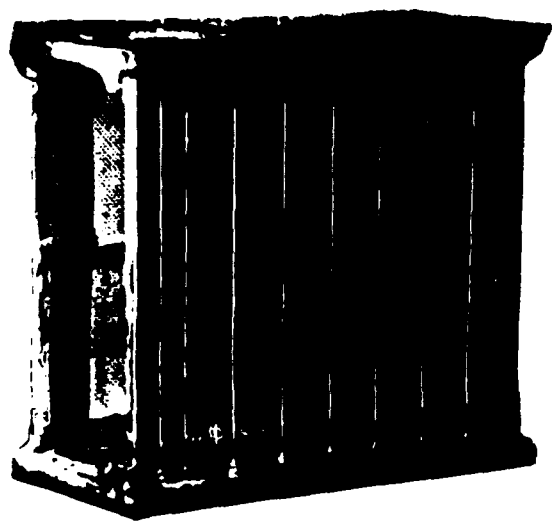

b: diode picture

Figure 6–1: Racetrack diode geometry.

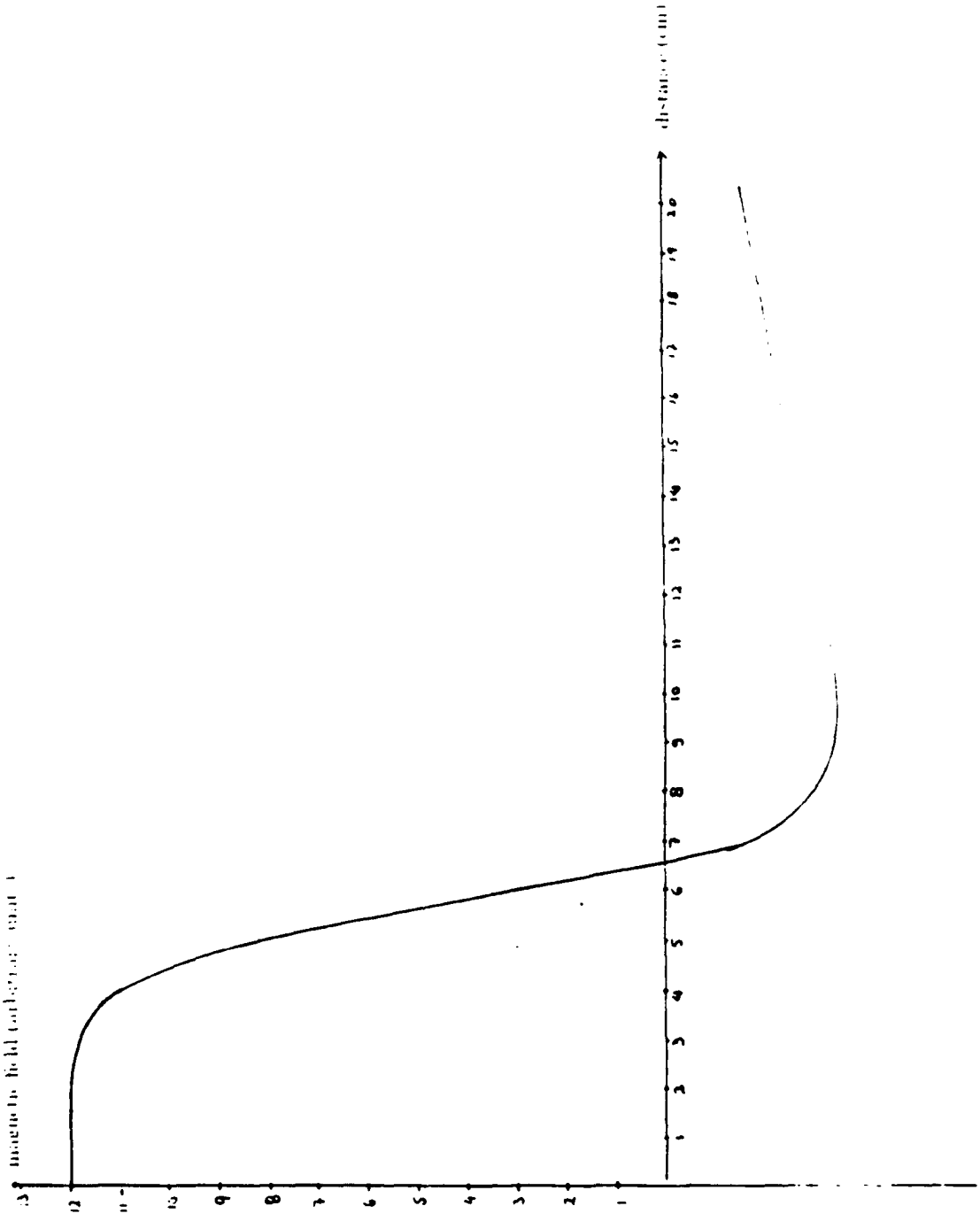

Figure 6-2: Magnetic field intensity profile in a racetrack diode.

field penetrated a few millimeters into the cathode. This field penetration is an undesired effect since it could distort the magnetic field lines. This could lower the stability of the Hall drifting electrons and create diode shorts when lines happen to connect the anode and cathode. Moreover, an ion accelerated through this magnetic field will suffer a transverse deflection since its canonical momentum is not conserved. Since we did want to maintain a high enough insulating field on all cathode area we had to use a many turns coil. This caused the higher inductance and slow rise time of the field pulse. The coil ohmic resistance was chosen to get a critically damped current signal as can be seen from the current shape. This was done by choosing the right length and diameter of the stainless steel rods. This coil structure was aimed to achieve high mechanical strength to withhold the high magnetic force shocks, and at the same time get maximum total beam current out of the coil box. The APEX was triggered to fire the high voltage pulse at peak magnetic field by a delay unit in a way described in chapter 3.4.2. The anode was made of a 50% transparent stainless steel wire mesh. The mesh had a box shape and was supported to the insulating magnetic field coil box through a few insulators. It was grounded to the diode vacuum chamber. The distance between the cathode and the wire mesh anode could be varied. This distance usually ranged between 10mm and 25mm.

A few types of cathodes have been tried. We first tried a few passive dielectric cathodes. These include aluminum cathodes covered with a thin layer of insulating dielectric material. We tried polyethelene ,wax and a few combinations of epoxy mixed with $NaBH_4$ salt or $CsBH_4$ salt. Cs is used in many low voltage discharge negative ion sources since it easily loses its extra electron by collision with other particles which then convert to negative ions. We then tried a cathode made of thin carbon brushes. This cathode was made actually so that we could coat the brushes with dielectric insulators like parafine or combinations of parafine with the Cs or Na salts. We found out that bare carbon brushes produce negative carbon ions and this possibility was also investigated.

Since we wanted to be able to control plasma production in the diode we built an active plasma producing cathode. This cathode was described in chapter 4. The plasma was basically produced by creating vacuum arcs across TiH_2 powder. The arcs were created by an independent circuit across 120 points on the cathode surface. We tried cathodes with varying arc current intensities and different arc point spacings. We even tried a cathode with arcing groves filled with epoxy instead of the TiH_2 powder. In some cases we put a fine metal screen in front of the cathode to avoid high diode load and electric field distortion created by the dense plasma ejected from the gun.

Diode voltage was measured via a capacitive voltage divider described in chapter 3. The voltage was usually peaked around 700 kV and diode current ranged between 15 kA without a plasma source in the gap, and up to 40 kA with a plasma source. X-ray camera pictures were taken every shot, but due to the diode geometry the information supplied was valuable mainly in cases of diode shorts where the shorting area could be identified (see figure 3-10). X-ray emission was measured with a vacuum photodiode described in chapter 3. The emission had usually a sharp peak timed about 40 nsec after the high voltage start (see figure 3-11). This is about where the voltage and current reach their peak. The signal shape was not sensitive to diode conditions, and we got about the same pulse shape for the different cathodes used.

6.2 Experiments with passive cathodes

6.2.1 Polyethelene cathodes

Polyethelene is most commonly used in magnetically insulated diodes as a passive plasma source. The usual polyethelene cathode we investigated was made of a 2mm thick polyethelene sheet glued to an aluminum paddle shaped cathode (see figure 6-3). Small holes were drilled in the polyethelene 10mm apart. The polyethelene was sandpapered and washed throughly with isopropanol before use.

Negative ion current was usually measured with a Faraday cup. The cup

was placed outside the wire mesh at a distance of about 20 cm from the cathode. Part of the beam entering the Faraday cup is lost before reaching the collector due to its deflection by the Faraday cup magnetic field (see figure 3–6 **A**). Nevertheless we should be able to see most of the ions entering the Faraday cup with energy more than 100 keV. The current measured by the Faraday cup is shown in figure 6–4 **a**. We get at first a low level current followed later by a large peak (and sometimes another later peak). The low level current is probably caused by electrons. Electrons are faster and appear first at the Faraday cup collector.These electrons are probably backscattered from the Faraday cup walls, since this is the only way they could overcome the cup magnetic field. This explanation was indeed confirmed by making the cup a little shorter and putting a 25μm thick piece of mylar in front of the cup. This made the current at the beginning of the pulse much larger, and the later current peaks to disappear. This is because the mylar stopped all ions but did not stop electrons. This current shape repeated itself in most of the shots we made with the polyethelene cathode. The current peak corresponds to a current density of about 5A/cm^2 of negative ions emitted from the cathode. When we put a 2.5 μm thick mylar in front of the Faraday cup we got a positive current signal with a similar shape (see figure 6-4 **b**). This polarity change is typical to H^- ions and was discussed in chapters 2.2.2 and 3.5.1. The fact that we get the same pulse shape with a thin mylar means that most of the ions created are H^- ions. These are the only ions able to penetrate this thickness of mylar. The time of arrival of the H^- ions corresponds to H^- ions with energy of about 250 keV.

The ion pulse then lasts for about 100 nsec. This pulse has a long timed tale corresponding to the low energy ions created at the end of the high voltage pulse. First ion peak time of flight corresponds to hydrogen ions with an energy of about 250 kV (probably this is the voltage at which the plasma is created by explosive emission). The diode reaches this voltage in about 10nsec due to the fast high voltage risetime. It looks like ions are then ejected from the cathode plasma as long as this plasma exists. The reversed polarity signal shape

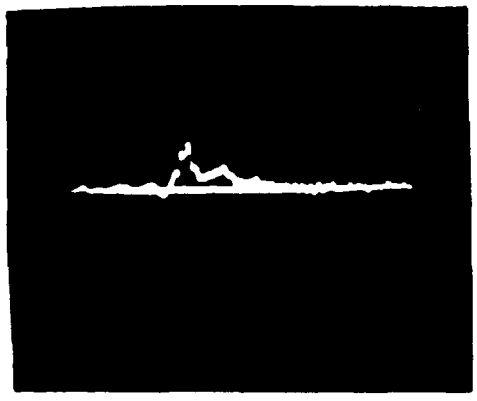

a: Without mylar on the Faraday cup.

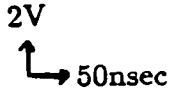

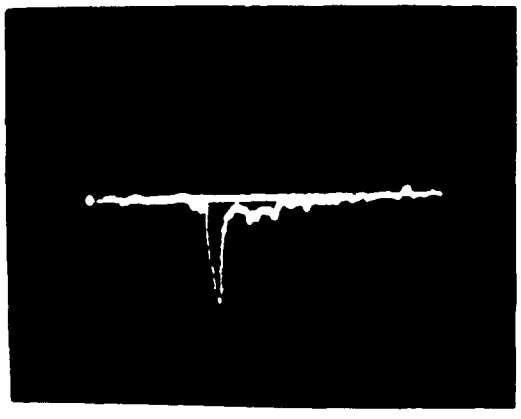

b: With 2.5μm thick mylar on the Faraday cup.

Figure 6–4: Current collected by the Faraday cup in case of a polyethelene cathode.

confirms that most of the ions in this case are H^- ions. We should expect an ion current peak at the beginning of the pulse created by accumulation of ions produced during the high voltage rise. It then happens that low energy ions created at an early stage arrive at the Faraday cup at the same time as high energy ions created later. The first peak is about four times larger than the average current collected later. This could happen when more ions are created at an early stage of the pulse. We could expect this behaviour since residual gas molecules adsorbed on the cathode surface could be detached from the surface by electron bombardment at an the beginning of the pulse. The thin mylar reduces the first peak relatively more than it reduces other parts of the pulse. This is probably because the first ions arriving are low energy ions. Hydrogen ions with energy less than 250 keV would not penetrate the mylar (see figure 3–7).

Current reduction with mylar could be attributed to the existence of carbon ions in the beam. To check this point we used the magnetic field for ion mass spectrometry in a similar way to what was described in chapter 5. We calculated different ion trajectories and compared it to the traces we got on a box with a CR–39 film at the back. We used the equations of motion 5.2 and 5.3. We used a minimum mean square deviation fit of a fourth order polynomial to get a functional form for the magnetic field profile described in figure 6–2. The experiment setup together with calculated ion traces is seen in figure 6–5. In most of the shots we did not get separate track areas for hydrogen and other ions. However, in one of the shots hydrogen and other ion tracks were separated on the CR-39 picture. The CR–39 picture is seen in figure 6–6. Two groups of ion traces were identified by the track size (measured in a microscope). These tracks correspond to hydrogen ions, and heavier ions, probable carbon. About 70% of the tracks were of hydrogen and the rest of them were carbon. However, in most of the shots we made, carbon and hydrogen traces overlapped and there was no way to distinguish between them.

We measured the ion beam uniformity by putting a piece of CR–39 in front

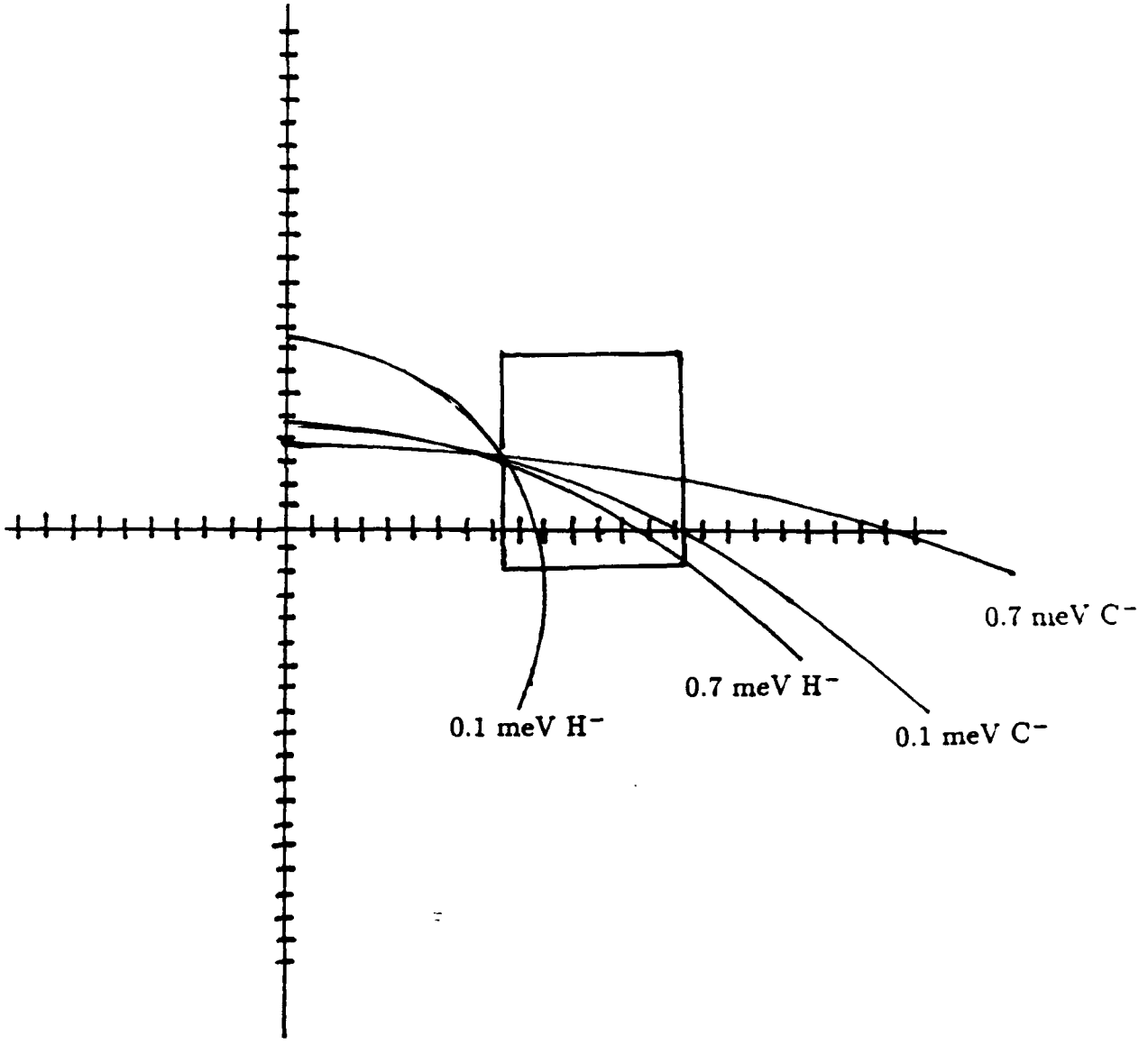

Figure 6-5: Magnetic field ion mass spectrometry experimental setup.

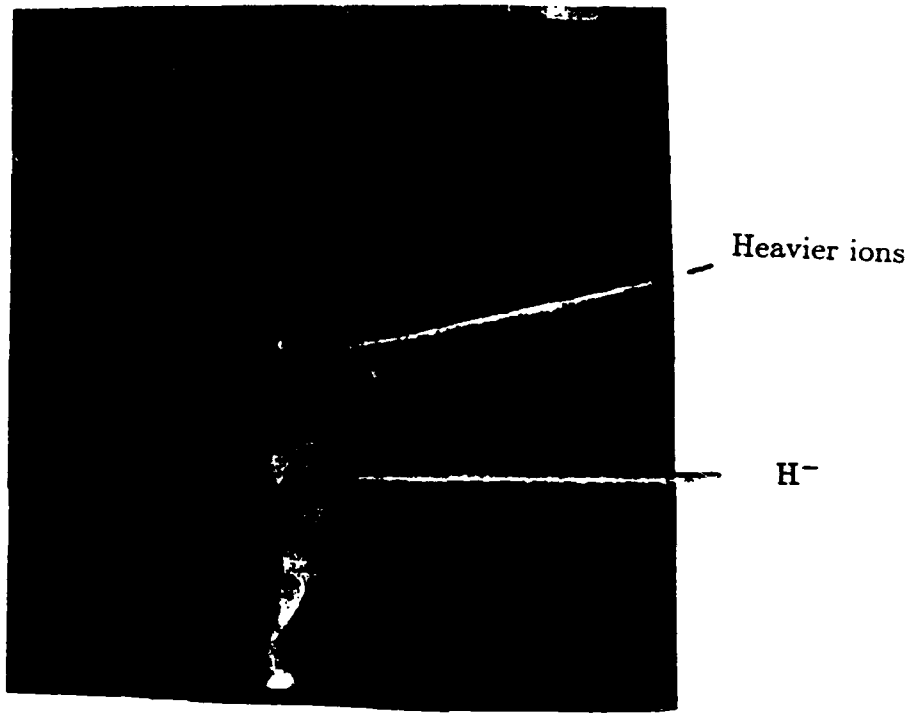

Figure 6-6: CR-39 traces of ions deflected by insulating magnetic field.

of the wire mesh. The same method was applied to the cylindrically symmetric diode and explained in details in chapter 5. The CR–39 picture is seen in figure 6–7. This figure shows that ion trajectories at some areas are distorted showing the hot–spot behaviour described in chapter 5. A CR–39 pinhole camera picture reveals the existence of these hot spots. Each spot had a diameter of about 5mm as in the coaxial diode case. Beam divergence measured was around 100 milliradians in the axial direction. Beam divergence in the azimuthal direction is very large due to ion deflection because of the insulating magnetic field. A typical pinhole camera picture is seen in figure 6–8. Ion beam current was estimated by etch pit counting to be around $5A/cm^2$.

We also tried a polyethelene cathode with small steel nails put in it. This was just a 2mm thick polyethelene glued to an aluminum cathode with nails put at a distance of about 1 cm from each other. We made Faraday cup measurements together with CR–39 pictures of this diode. It behaved in exactly the same way as the previous polyethelene cathode.

6.2.2 Carbon brushes cathodes

We built the carbon brushes cathode to check the effect of Cs and Na salts on negative ion production. The idea was to coat the brushes with these salts. Cs is used in low voltage gas discharge negative ion sources. It was found out (see chapter 2.2.3) that it adsorbs on the chamber walls and lowers the work function. Ion impinging on those walls catch an extra electron and become negative ions.

The carbon brushes cathode is seen in figure 6–9. It is made of a piece of carbon in which holes were drilled and carbon fibers put in. A piece of aluminum was attached with screws to the back side of the carbon and connected it to the high voltage shank. The salts we chose to put on the brushes were $CsBH_4$ and $NaBH_4$. These salts also contain four hydrogen per molecule which, it was hoped might enhance negative hydrogen ion production. Ion beam diagnostics was made in the usual way with Faraday cup measurements and CR–39 track

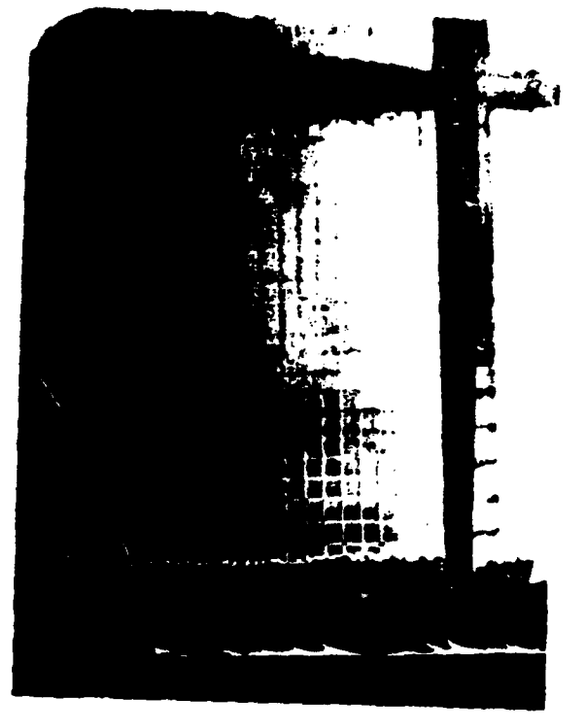

Figure 6–7: CR–39 wire mesh picture with a polyethelene cathode.

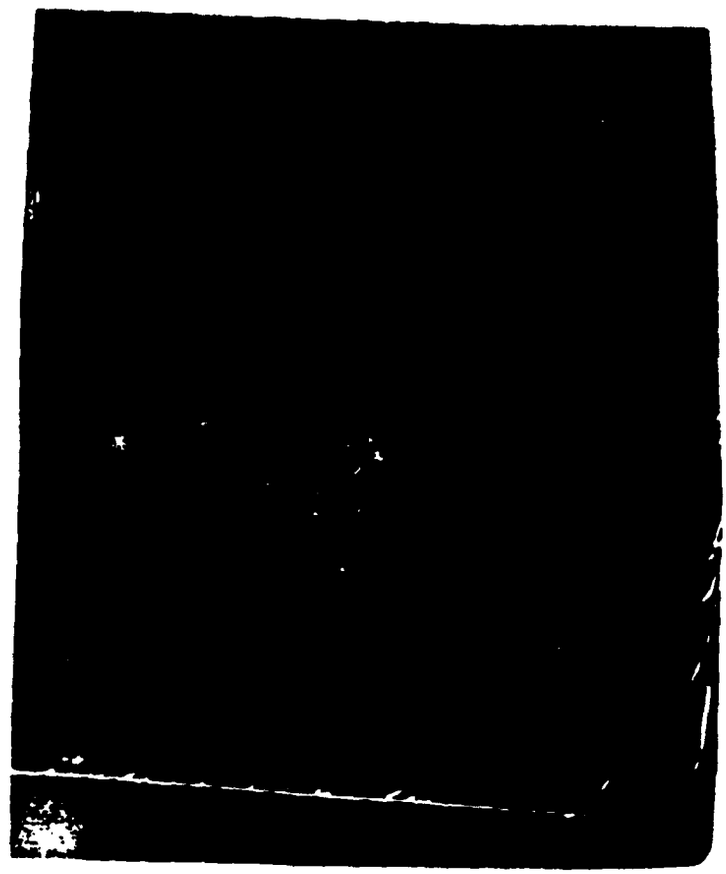

Figure 6–8: Pinhole camera picture of a polyethelene cathode.

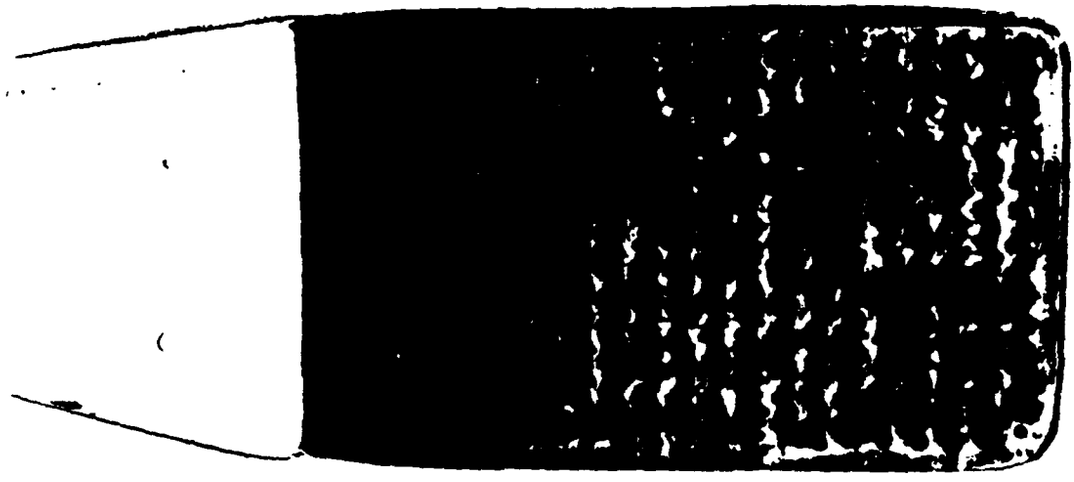

Figure 6-9: Carbon brushes cathode.

detectors.

A typical Faraday cup picture is seen in figure 6–10. There is a low current at the beginning of the pulse and then a high narrow peak with a width of about 25 nsec. This peak reached about 8–10A/cm^2. The ion current then goes down to about one third of its peak value with a long tail. The negative ion current pulse has a time duration larger than the high voltage pulse. This means that negative ions are emitted as long as there exists a high voltage to extracts them from the plasma. The ions accelerated at the end of the high voltage pulse have a lower energy and a larger time of flight which makes the current signal broader. When we put a 2.5μm thick mylar in front of the Faraday cup the current signal was very small (at the same level as the measured noise). The interesting phenomena was that we got the same current collected when we changed the salts or even when we tried a cathode without any salts on the brushes. We also tried to put parafine on the brushes and got the same current signal. We did repeat this measurements a few times with the same results.

The conclusion was very obvious. It looked like most of our current ion signal consisted of negative C^- or heavier ions. These could be either C_2^- or O^- ions. The amount of negative hydrogen ions was certainly small. If this was really the case then the first high peak corresponds to C^- ions with energy of about 200 keV. We can assume that at this voltage plasma starts to be created by the high field stress. This makes sense since it looks like plasma starts to be created on a polyethelene cathode at a voltage of about 250 kV. The carbon brushes cathode has sharper "edges" created by the brushes tips and it makes sense that the breakdown voltage is a little lower. Pinhole camera pictures showed a beam divergence of about 0.3 radians. This divergence In this case divergence could be caused by the fact that the cathode consists of brushes and not of a flat surface. It could be also caused by transverse fields created by dense hot plasma spots on the cathode area.

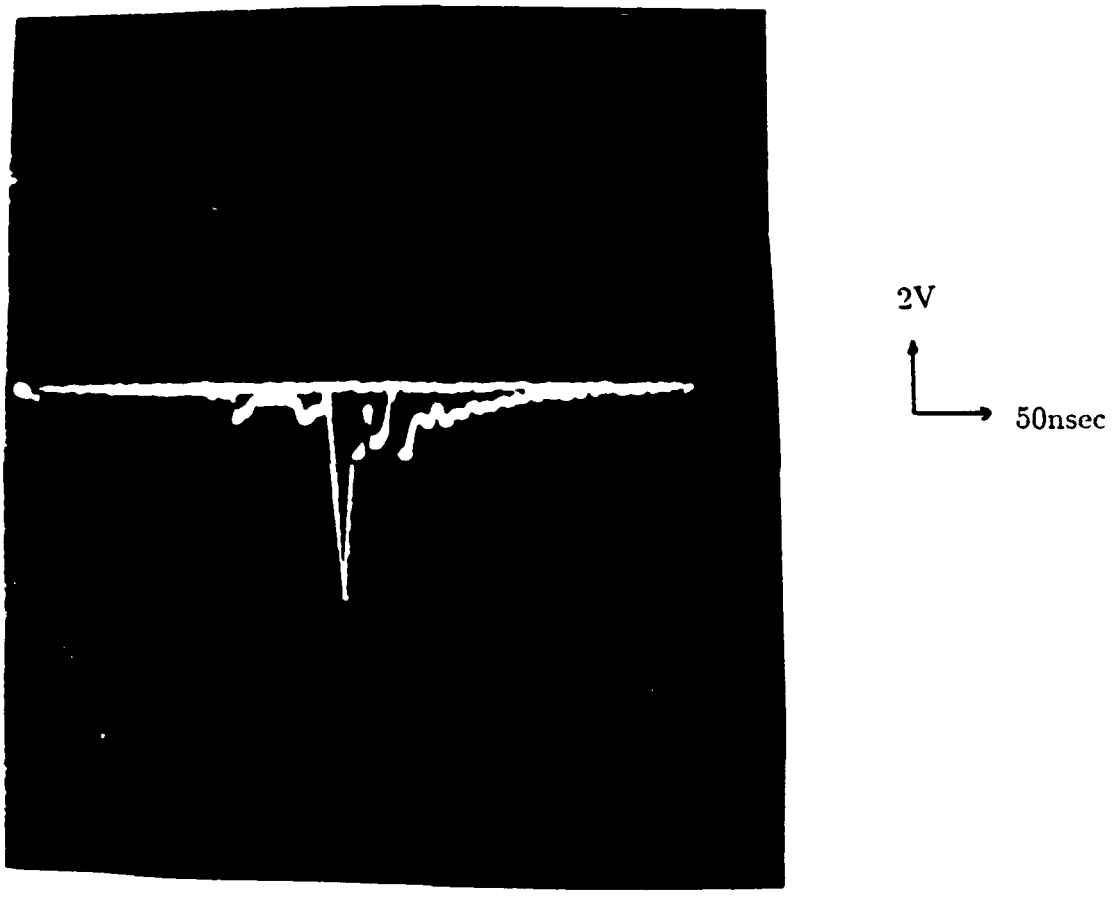

Figure 6–10: **Faraday cup signal from a carbon brushes cathode.**

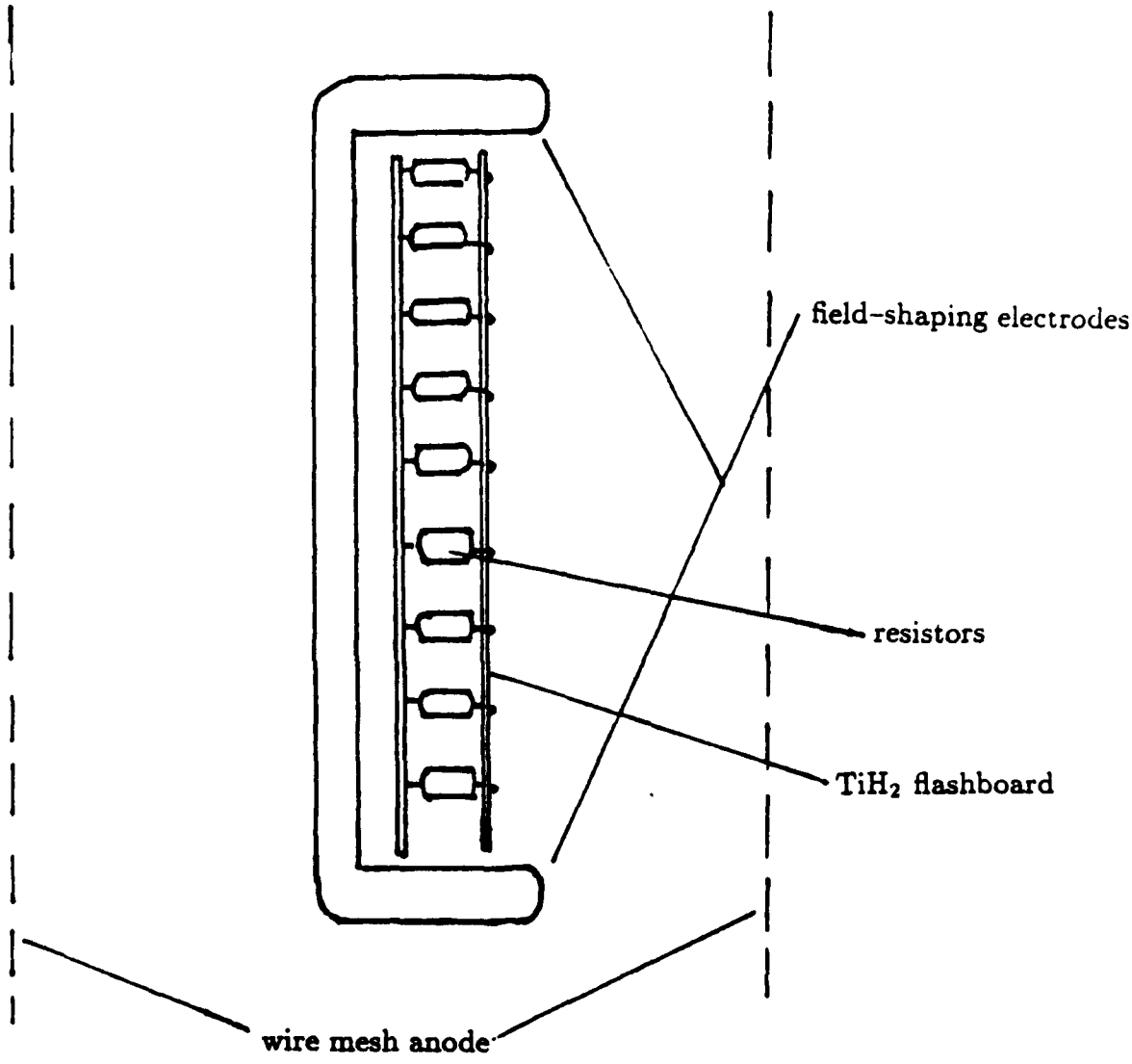

Figure 6-11: Diode geometry with a TiH_2 active cathode.

6.3 Experiments with active cathodes

6.3.1 TiH_2 cathode with low arc currents

The active cathode was introduced in order to be able to control plasma production and see its effect on the amount of negative ions produced. We also wanted to use the cathode to simulate the effect of a prepulse plasma production. The cathode and the driving circuit are described in details in chapter 4.

We started with a regular 120 points TiH_2 cathode shown in figure 4–6 **a**. The plasma gun circuit was operated under what we defined as *low-current* conditions. These conditions are described in chapter 4.3. The current through each arcing point on the plasma gun surface was about 5A and its pulse shape is shown in figure 4–5 **b**. Plasma density was measured under these condition (without a magnetic field) with a Langmuir probe (see chapter 4-6). Plasma electron density was around $10^{12}/cm^3$. Plasma electron temperature was around 3.3 eV (see table 4–1). The diode geometry is seen in figure 6–11. The plasma gun was was placed in a metal box with field shaping electrodes around. This created a focusing electric field geometry. Magnetic field lines have a concave shape since the cannot penetrate the field shaping electrodes (up to the skin depth of course). Since drifting electrons follow magnetic field lines, this geometry was also supposed to create a concave plasma emitting surface with a focusing effect. In addition, since the highest electric field stress was on the field shaping electrodes, these electrodes were supposed to protect the plasma gun from diode breakdowns.

The first parameter we changed was the delay between plasma production and the diode high voltage pulse. This delay was measured with a light measuring system described in chapter 4.5. Ion current was measured with a Faraday–cup. We had difficulties getting rid of electrons reaching the cup collector. To solve this problem we placed a thin film of mylar on the Faraday cup. This film changed the charge sign of negative ions, but left the electron sign unchanged. The film we used was transparent to hydrogen ions with energy

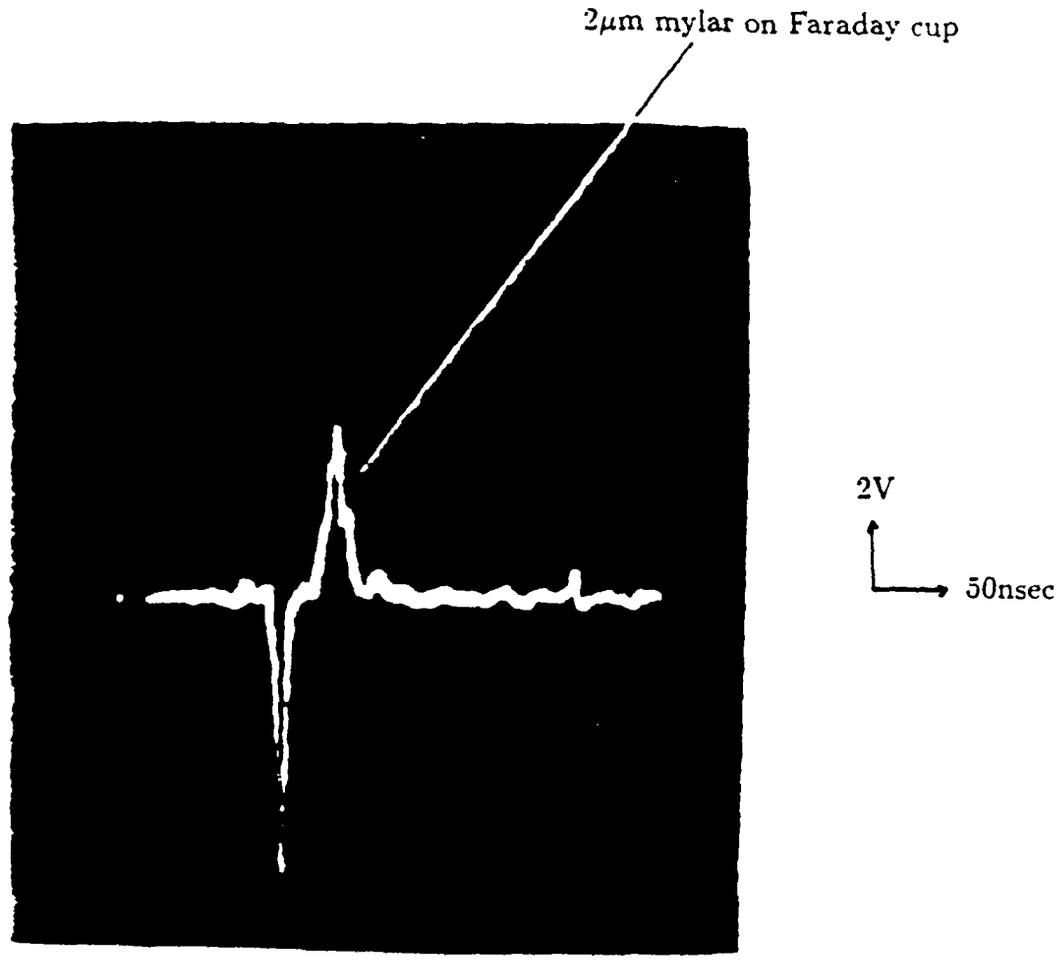

Figure 6–12: Faraday cup current signal from a low current TiH_2 active flashboard.

higher than 250 kV. Since we used TiH_2 powder in our plasma flashboard we did not expect any other negative ions anyhow.

We started with a zero delay between the plasma gun and the high voltage. We then gradually made the delay larger. Only at a delay of about 1μsec we started to record current signals on the Faraday cup. A typical Faraday cup current signal is shown in figure 6–12. The negative part of the signal is due to electrons and the positive part due to negative hydrogen ions. There is a minimum time of arrival difference between H^- ions and electrons of about 20 nsec. This is based on the assumption that the only electrons which would make it through the magnetic filter of the cup have energy of a few hundreds keV. Negative ion current has a peak of about $2A/cm^2$ and a width of about 80 n ec. It looks like ions are extracted from the cathode plasma as long as the high voltage exists. Negative ions were recorded for delay times ranging between 1.1μsec to 5.5μsec which was the largest delay we tried in this case. Typical diode voltage current traces under these conditions are see in figure 6–13 a.

Ion current density as a function of delay is shown in figure 6–14. The ion current is maximal for delay times of 1–2μsec and then goes down gradually. This could be caused by the fact that diode current is larger and the extracting voltage is lower due probably to plasma diffusion into the high voltage gap. The fact that we do not measure ions for the first 1 μsec could be explained by the fact that the flashboard is recessed inside the field shaping electrons. The plasma created is confined by the magnetic field (this fact was confirmed by the Langmuir probe measurements described in chapter 4) and it probably takes about 1 μsec till some of it diffuses along the magnetic field lines into higher electric stress area.

Beam divergence was measured with CR–39 box for a delay of 1.5μsec. Hot spots of high ion emission were identified. This time the spots probably correspond to arcing points on the flashboard surface. Beam divergence was about 100 milliradians in the axial direction.

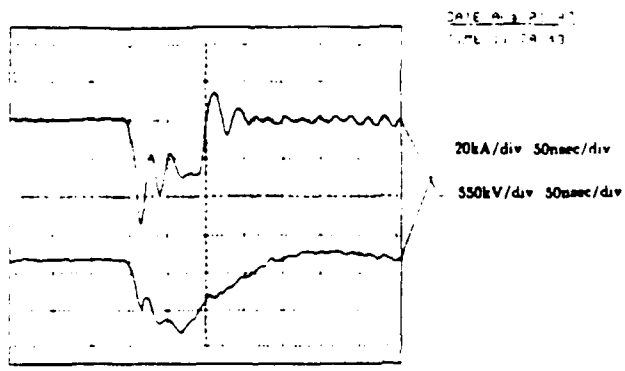

a: Low current conditions, delay=1.7μsec.

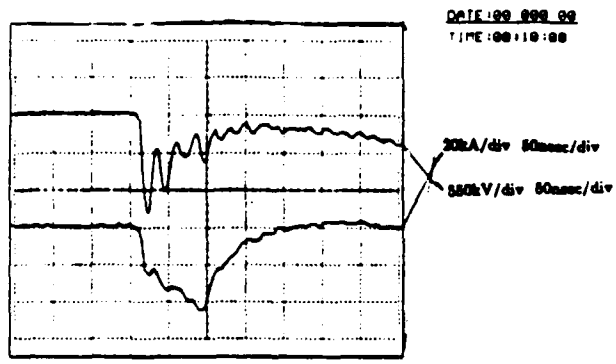

b: High current conditions, delay=1.7μsec.

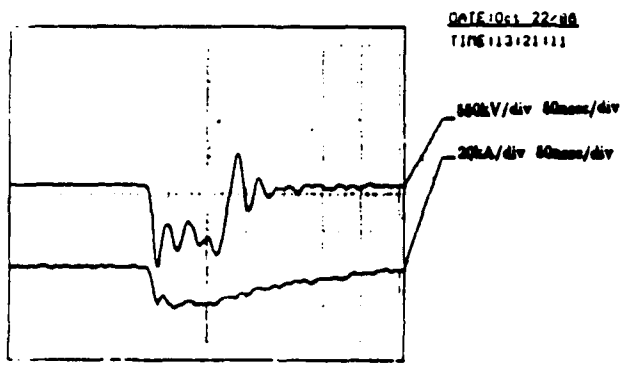

c: High current conditions with a fine mesh, delay=1.9μsec.

Figure 6–13: Voltage–current traces of a TiH_2 active cathode.

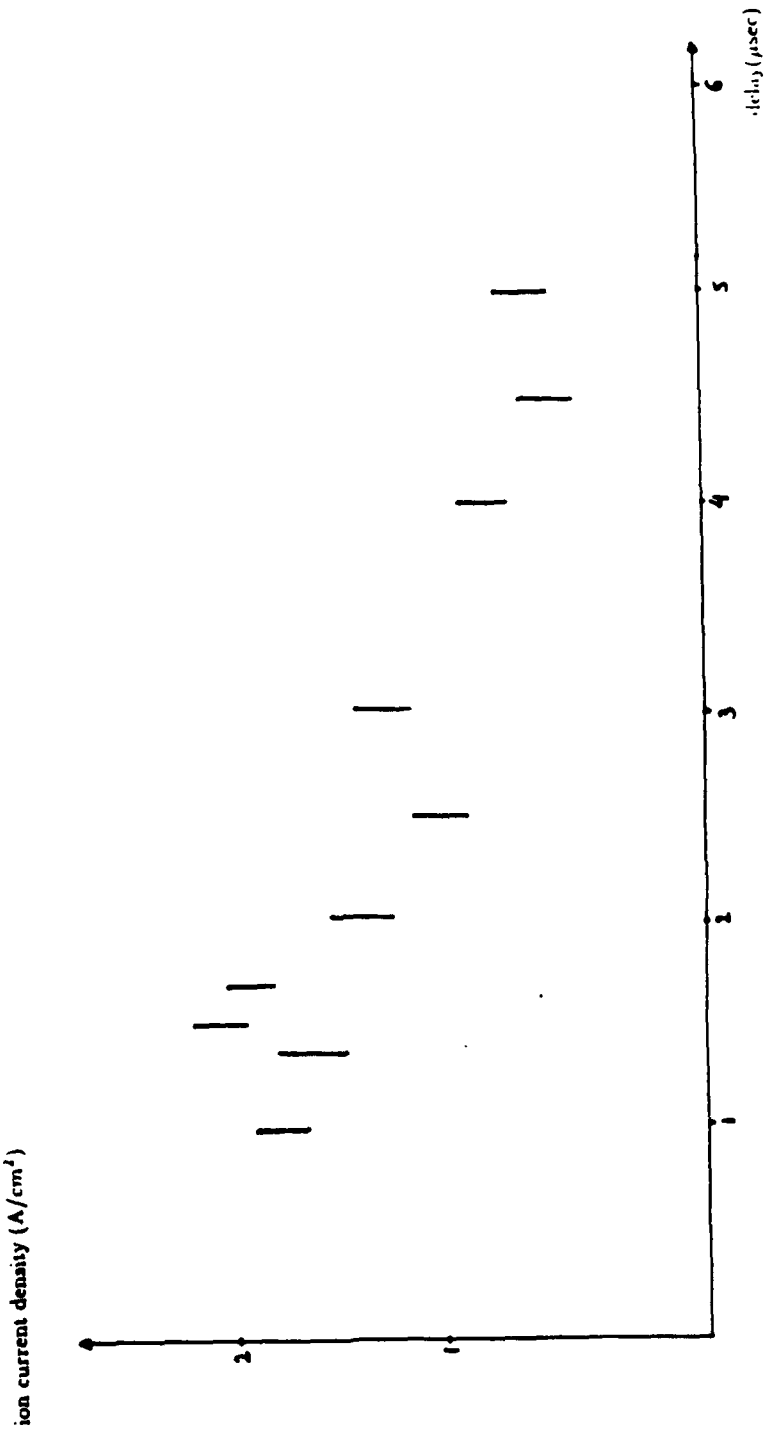

Figure 6-14: Faraday cup ion current as a function of delay for low current flashboard conditions.

6.3.2: TiH_2 cathodes with high arc currents

The next thing we did was to check the flashboard under what we defined in chapter 4 as the *high current* conditions. The diode geometry is the same as in figure 6–10 with exactly the same TiH_2 flashboard. Under these condition the plasma density as measured with a Langmuir probe was around $1.3 \times 10^{12}/cm^3$ with an electron temperature of 1.6 eV (see table 4–1). Under these conditions we got a very small negative ion current (comparable to the Faraday cup noise) and a higher diode current. The voltage was around 600 kV with a current of about 35 kA. When we took a CR–39 wire mesh picture we got traces of a very inhomogeneous beam (see figure 6–15). On the CR–39 are damage traces of electrons and a small number of ion traces. At the areas damaged by electrons there are no ions at all. This CR–39 picture is caused by a very inhomogeneous electric field in the diode gap. The electron damage means that at some areas of the diode the magnetic insulation did not work. At these areas negative ions were not extracted from the cathode plasma probable because of the high space charge of the extracted electrons. Without magnetic insulation the extracted ion current behaves according to the Child–Langmuir law. Since the electron mass is much smaller the extracted current is then dominated by electrons. The failure of the magnetic insulation at some diode areas could be caused by the dense plasma injected into the gap. This plasma could cause transverse electric fields in the gap with higher field stress that could cause higher extracted currents at some areas.

In order to lower the amount of plasma injected into the gap we put a fine wire mesh screen in front of the plasma gun. The screen was made of a 0.2mm sheath of stainless steel with a transparency of about 30%. We did not measure any ions for delay times less than 0.7μsec. The ion current density reached $0.5A/cm^2$ for delay times between 2–3μsec. The current density then decreased gradually. We measured ion beam axial divergence with a CR–39 box. Beam divergence was about 10 milliradians for a delay of 1.0μsec. With a delay of

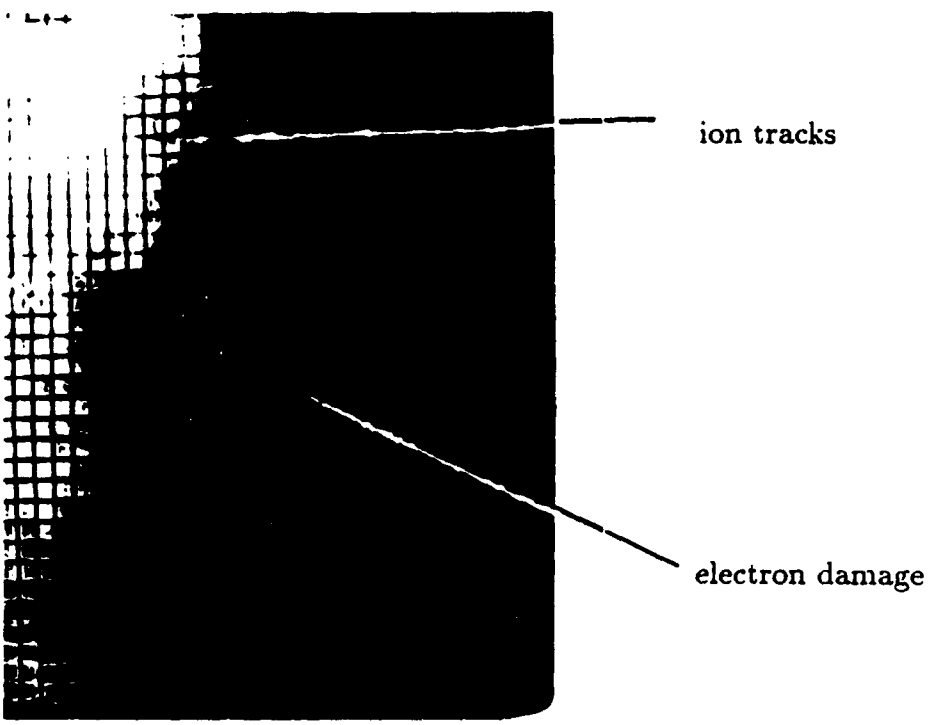

Figure 6–15: CR–39 beam divergence with high current conditions

2.5μ we got an axial divergence of 60 milliradians (see figure 6–16). CR–39 wire mesh pictures revealed a very homogeneous plasma.

6.3.3: Other active cathodes

The plasma in our gun is produced through creating arcs across groves on the flashboard. We usually worked with TiH_2 filled groves. The next step was to try filling the groves with other materials. We tried first to fill it with epoxy. Since the epoxy glue is a good insulator we mixed it with Ni powder before it cured. We tried this flashboard under high and low current conditions. Current density was about 20% lower than the TiH_2 case. This current was difficult to measure since we did want to measure carbon ions and we could not use the thin mylar Faraday–cup combination. We had to measure the current with the Faraday using a much longer magnetic insulated cup. This fact was taken into account in correcting the ion current measured. Beam divergence was the same as in the TiH_2 case.

The next thing we did was to spray this epoxy flashboard with AERODAG. This is just a fine carbon particles spray with a binder. The carbon layer was thin and would probably evaporate when passing a high current through it. This was checked by firing the cathode. The fact that we got light from all grove sites means that an arc was created and some material was evaporated by this arc. The current density was about 30% lower than with the TiH_2 case, and the beam divergence was the same.

In order to try and simulate the prepulse effect we did the following experiment. We put a thin layer of polyethelene on the flashboard stainless steel screen (see figure 6–17). This polyethelene layer was drilled with a few hundred holes in it. Without firing the flashboard this cathode looks and should behave the same as a passive polyethelene cathode. The idea was to use it first as a passive cathode, without firing the flashboard, and measure the negative ion current. Then we intended to create a prepulse plasma with the flashboard and see how it affects the negative ion current. We tried the plasma gun only

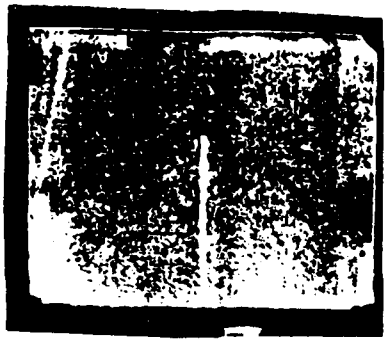

beam divergence=10 milliradians

a: Delay= 1.1μsec.

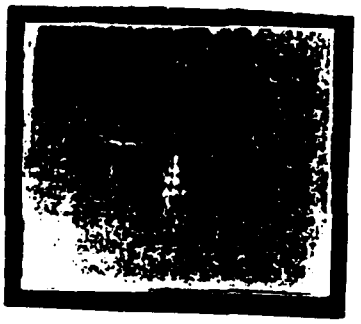

beam divergence=50 milliradians

b: Delay= 2.5μsec.

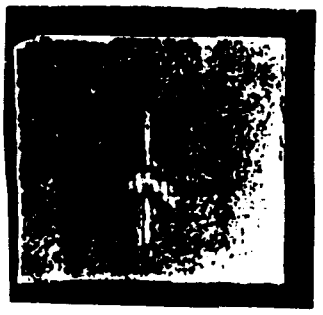

beam divergence=60 milliradians

c: Delay= 3.5μsec.

Figure 6–16: Beam divergence for diggerent delay times (high current gun + screen).

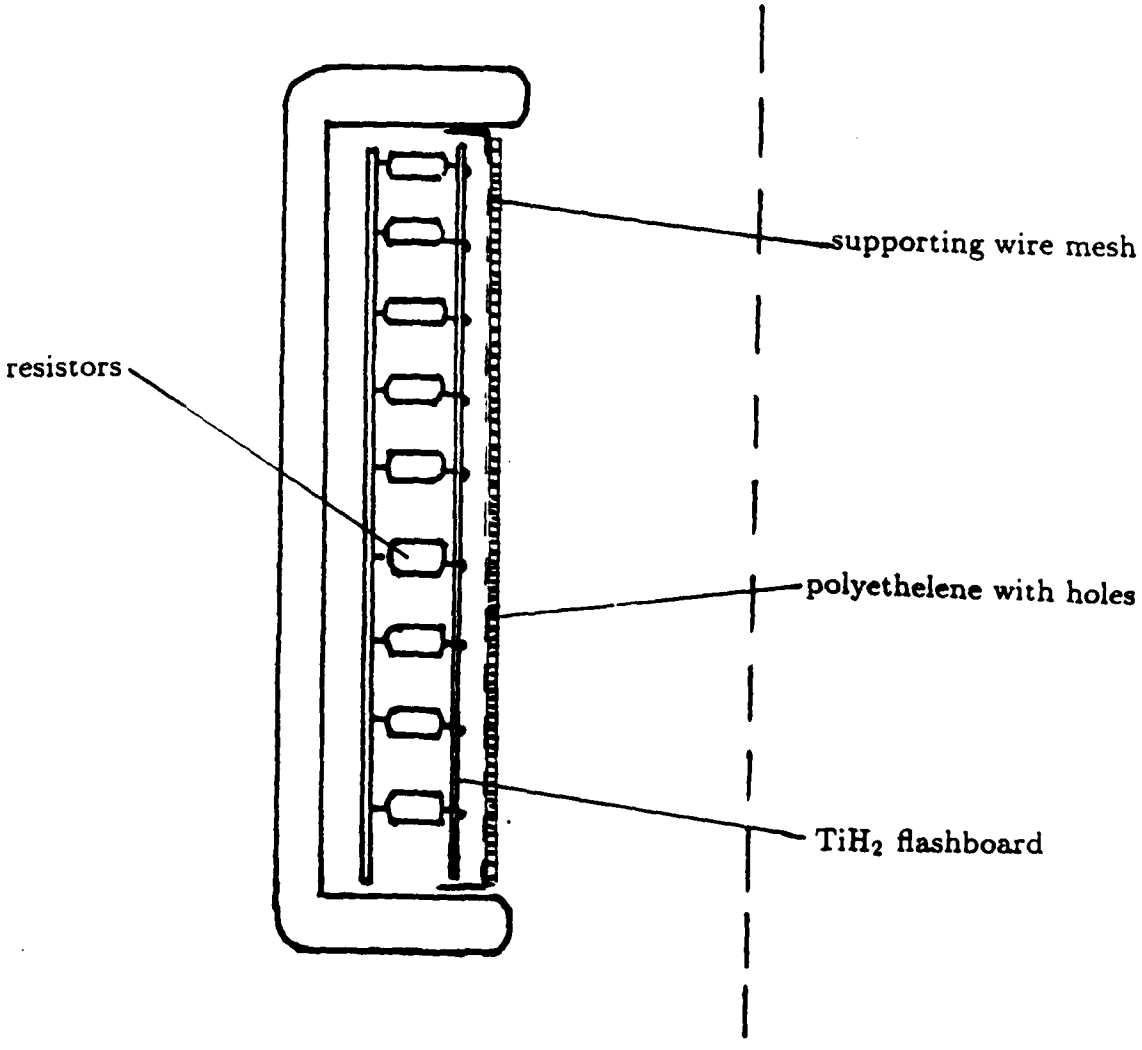

Figure 6-17: Active cathode with a polyethelene layer to simulate the prepulse effect.

under the low current conditions since under the high current condition the plasma gun polyethelene combination would load the diode and short it. The results were quite disappointing. With the prepulse we did get an ion current higher by about 20%, but the plasma was inhomogeneous showing the hot spot phenomena in both cases. The effect of this prepulsed plasma was checked up to delay times of 10μsec. In the Lebedev experiment this delay was about 300 nsec. The minimum delay we could reach is about 700 nsec which is the time it takes the plasma to move from the flashboard and reach the polyethelene layer. The effect of the prepulsed plasma in this case was small.

6.4: Summary

A few conclusions can be drawn from the experiments described in this chapter:

- When we used a passive polyethelene cathode we got a negative ion current density of about 5A/cm^2. This current consists of about 70% H^- ions and 30% heavier ions, probably C^- and C_2^-. Negative ions were extracted from the cathode plasma all along the high voltage pulse duration. Beam divergence was about 100 milliradians in the axial direction. Negative ions were emitted mainly from a few small area hot spots on the cathode surface.
- When we used a carbon brushes cathode we got a beam of 8-10A/cm^2 which consisted mainly of ions heavier than hydrogen, probably carbon. Beam divergence was about 0.3 radians in the axial direction. The large divergence might be caused by the fact that the cathode surface consisted of localized carbon brush fiber tips. Ion current was not affected much by putting Cs and Na salts on the brushes. It was also not affected by coating the brushes with a thin layer of parafine.
- An active plasma gun was used to create plasma in the high voltage gap before firing the APEX. Under low arc flashboard current cathode ion current was about 2A/cm^2 and had a divergence of about 100 milliradians. Ion current was not measured for delay times of less than 1μsec. The current

cathode material	current density (A/cm^2)	divergence (radians)	composition
C_2H_2	5	100	70% H^-;30% heavier
carbon brushes	8–10	300	
active TiH_2 (low current)	2	100	
active TiH_2 (fine screen)	0.5	10	

Table 6–1: summary of results with racetrack diode configuration.

had a maximum for delay times between 2–3μsec. When we tried to use the gun under high flashboard current conditions we got a very high diode load with a very small ion current. When we put a fine metal screen in front of the gun we got a beam divergence of 10 milliradians with a current density of 0.5A/cm^2. Beam divergence was a function of delay time and became larger for larger delay times.

- Filling the plasma gun groves with epoxy or spraying the groves with a carbon paint gave about the same current density and beam divergence.

The results obtained with the racetrack diode prove first of all the similarity between plasma created by explosive emission processes and plasma created by our arcing plasma gun. In both cases negative ions were emitted from hot spot areas of dense plasma. These hot spots are probably areas on the cathode surface where more plasma is created. These areas distort the electric field at the vicinity of the cathode surface. In cases this plasma was not homogeneous it created transverse fields that caused large beam divergence and even ruined the magnetic insulation causing high diode currents. The plasma gun was able to simulate plasma creation by passive cathodes. However, an attempt to cause a drastic enhancement of the ion current density by creating a prepulsed plasma on a passive polyethelene cathode failed. This prepulsed plasma made the ion current larger by not more than 20%. The highest current densities were achieved with carbon brushes cathodes, probably because the affinity of the negative carbon ion is larger.

Another interesting phenomena is the fact that we got a smaller amount of negative ions when we used the plasma gun with high current conditions. Under these conditions the plasma has a higher density. As we shall see in chapter 8, negative ions cannot exist in a dense plasma since the collision rate is higher.

Chapter 7 EXPERIMENTS WITH AN ANNULAR DIODE

7.1 Diode geometry

The annular diode geometry was a result of the diode physics understanding gained during the research done on positive ion racetrack diodes. The diode provides a stable electron cloud confinement over microsecond time scales [65].

This stable magnetic insulation is produced by a radial magnetic field. This radial field is supplied by two axially symmetric coaxial magnetic coils (see figure 7–1). The anode consists of two carbon rings attached to the coils. The cathode has a ring shape with an outer diameter similar to that of the bigger anode carbon ring, and an inner diameter similar to that of the smaller anode ring. All coils and electrodes are centered around the same axis. Ions are accelerated and emitted through the annular empty space between the two coils. A 50% transparent wire mesh was attached to the anode carbon rings between the coils to shape the electric field. We used different types of cathodes. These include passive polyethelene and carbon cathodes, and active TiH_2 and carbon cathodes. The coils together with the anode were attached to the diode chamber through a set of screws which enabled us to change the anode–cathode distance.

Electrons ejected from the cathode drift in an azimuthal direction creating closed circular drift paths. Since we always have some transverse electric field these electrons are forced to drift along the magnetic field lines. An electron layer is then created next to the cathode. This layer follows the magnetic field line shape and acts as a virtual cathode. The electric field near the cathode is perpendicular to this layer and is therefore shaped by the magnetic field lines. The preferred situation is when magnetic field lines have a slightly focusing shape with the focal axis parallel to the diode axis. The annular space between the coils is quite narrow, and any misalignment of the electric field would cause the beam to hit one of the coils. This could damage the coils. Another problem appears in cases when any magnetic line connects a high electric stress area on

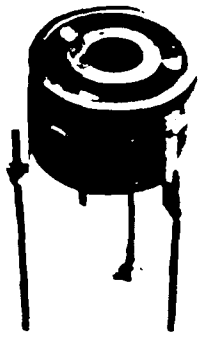

a: Coils structure with anode carbon rings

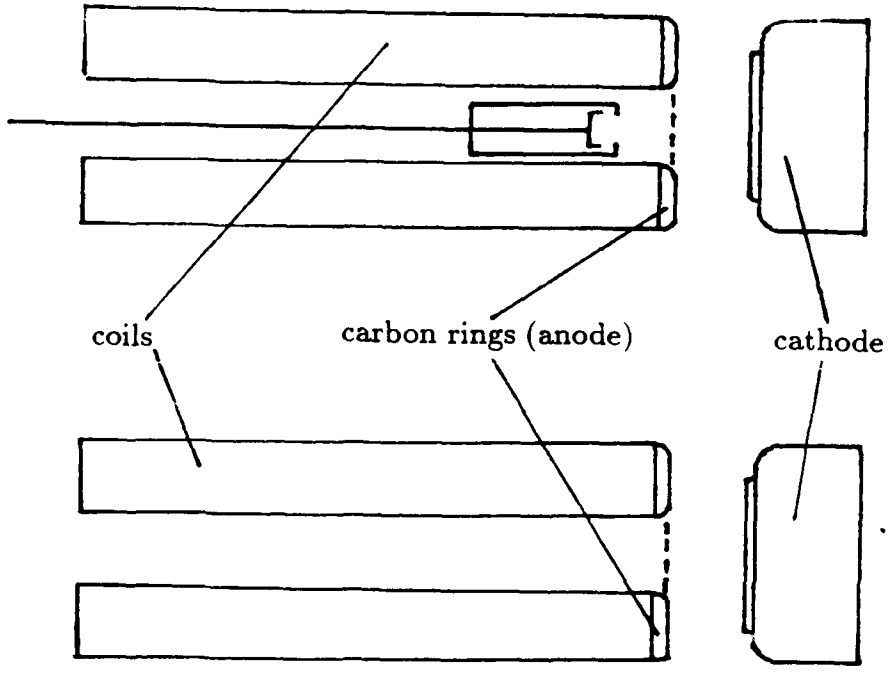

b: Diode geometry

Figure 7-1: Annular diode geometry.

the cathode to a ground potential area like the anode. Electrons drifting along magnetic field lines can cause diode closure. Magnetic field coils design had therefore to be done very carefully.

We used the EFFI code to design the magnetic field coils. This code, unfortunately does not take into account the limited penetration of the magnetic fields into the electrodes. The skin depth could reach a few millimeters with the pulse risetime we used (see chapter 3–7 figure 3–6 and figure 7–3). We used image coils in order to take into account the conducting electrodes effect. The results of this calculation are shown in figure 7–2. The best coil ratio turned to be with 3 turns in the inner coil, and 7 turns in the outer. This configuration gives a symmetric field at the high voltage gap with a slightly focusing shape near the cathode.

The coils were made of 0.5mm copper stripes with two layers of glass fiber cloth between the adjacent turns. They were vacuum casted in EPON 815 epoxy with a GENAMIDE catalyst. The two carbon rings used as an anode were electroplated with iron and soldered to copper stripes connecting them to ground. They were then glued to the coils. The inner and outer sides of the coil tubing were coated with a thin conducting layer of AERODAG to prevent insulator breakdown by accumulated charges.

We measured the coils magnetic field with a small Hall probe and also with two search coils. The search coils were about 5mm long and were connected perpendicular to each other on a small wooden stick. The idea was to measure magnetic field direction at the vicinity of the coils. The experiment was carried over with the coils and cathode in their final configuration. A typical search coil current trace is shown in figure 7–3. The agreement with the results of the EFFI code calculation was good. The spatial resolution however, was only about 5mm because of the finite size of the search coils.

As we did mention, electron drift along magnetic field lines. In our case most of the electron leakage current drifted along the lines into the empty space inside the inner coil. We had to put a thick piece of carbon there to prevent this

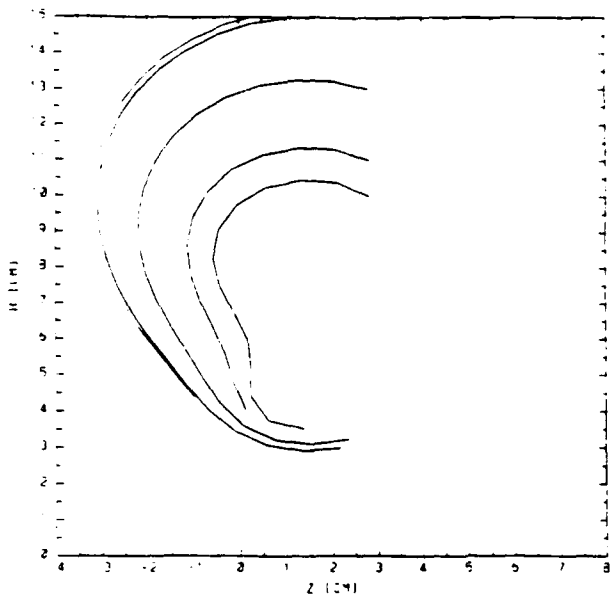

a: Magnetic field lines without image coils.

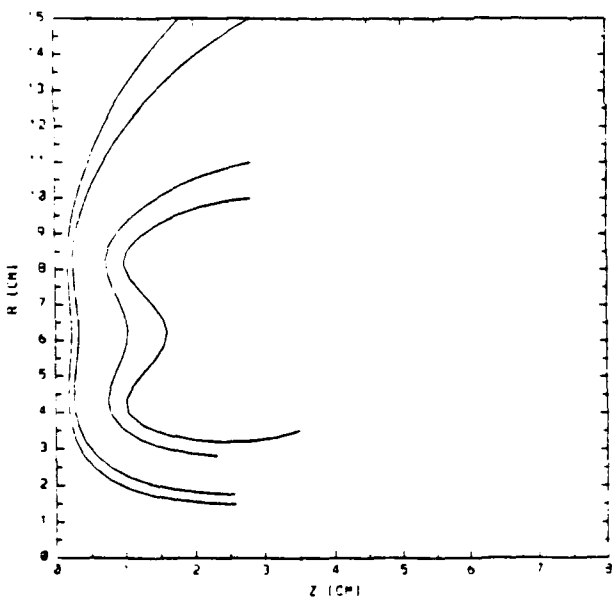

b: Magnetic field lines with a 3 turns outer coil, 7 turns inner coil and similar image coils.

Figure 7-2: EFFI magnetic field calculations.

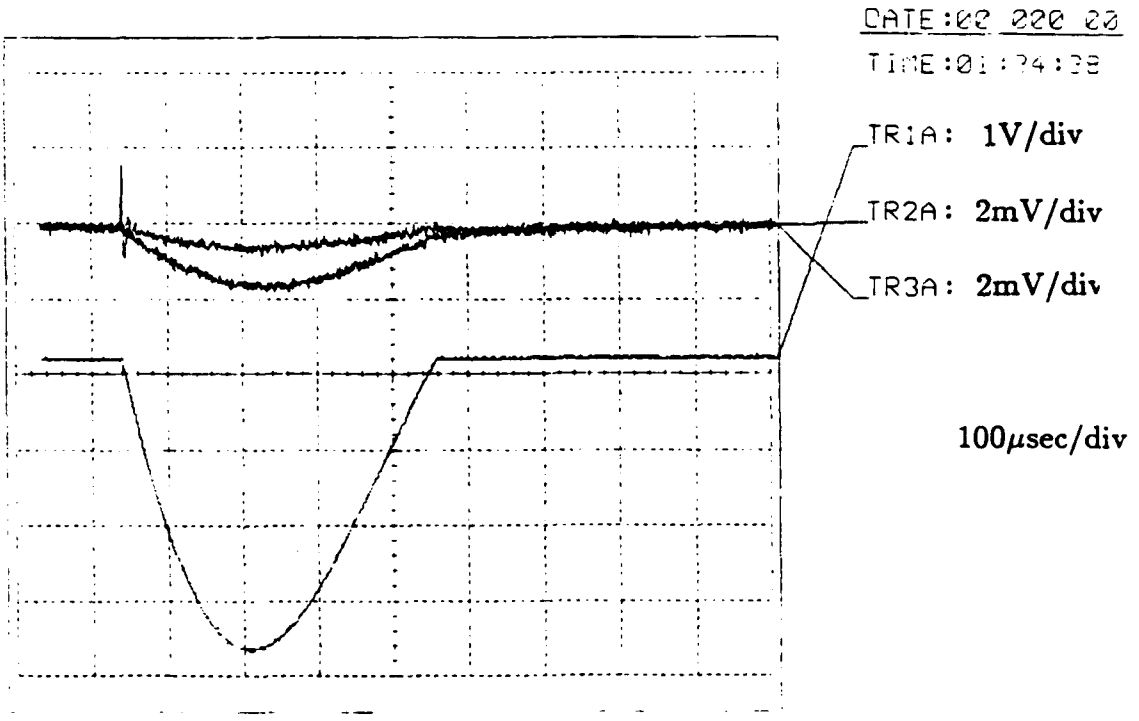

Figure 7–3: Typical search coil current traces (traces 2A and 3A) and Hall probe signal(trace 1A).

coil from damage caused by the high electron current. This is seen in the x-ray pictures of the diode (see figure 7-4). This picture shows a nice round ring of high intensity x-ray emission from the center of the inner coil. We changed the magnetic field capacitor voltage to see how the magnetic insulation builds up. At a field of 3 kGauss we had quite a good magnetic insulation as can be seen in figure 7-4. The diode voltage was usually around 700kV and the current around 20kA when no cathode plasma source was present.

Negative ion current was measured mainly with two Faraday cups put in between the two magnetic coils. Since most of the electrons drifted into the inner side of the smaller coil we rarely had any electron current reaching the Faraday cups. The fact that both cups were put in the narrow space between the coils also helped to get a Faraday cup current signal free of backscattered electrons. This was checked every few shots with a 25μm thick piece of mylar which could stop ions and not electrons. The Faraday cups were very short with a collector distance of about 1cm. The small magnetic field between the coils was sufficient to prevent secondary electron emission from the Faraday cup collector. This was checked by biasing the collector with a positive potential of about 40V. This bias did not make any difference in the current measured by the Faraday cup collector. The measurements were usually done with one of the cups biased and the other unbiased. The electron free Faraday cup ion current signal is a unique feature of the annular diode.

Another way by which we checked the ion beam current and divergence was by a small pinhole camera using a CR-39 track detector. Etch pit counting gave us a rough estimate of the number of particles in the beam and the beam divergence. This also gave a picture of the negative ion emission intensity of the cathode surface. The pinhole camera was located about 10cm from the upper top of the beam annulus. We did try to put the camera at the center of the back flange of the vacuum system to see with it all the cathode area. But due to the chamber dimensions and limited beam divergence we were unable to get reasonable pictures with this camera configuration.

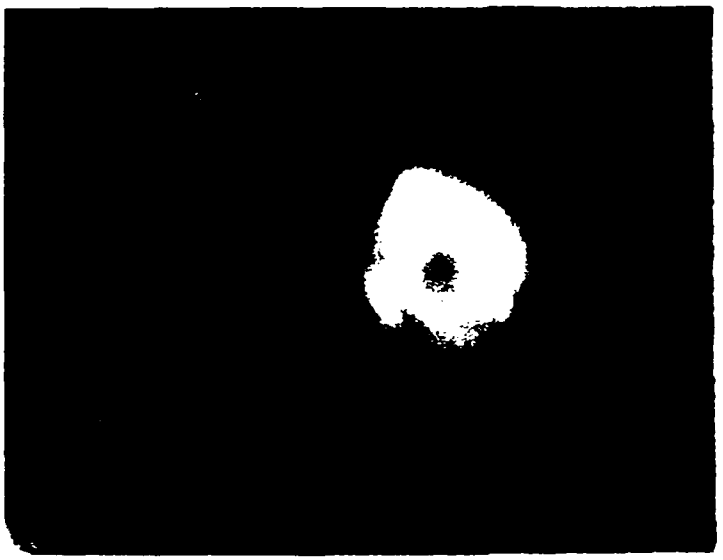

a: magnetic field=0 kGauss

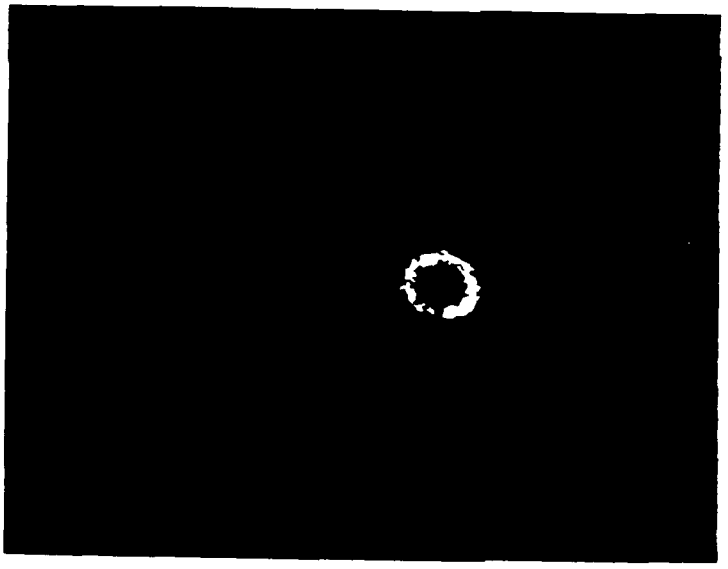

b: magnetic field =3.1 kGauss

Figure 7-4: Effect of magnetic field intensity on magnetic insulation.

7.2 Experiments with passive cathodes

7.2.1 Polyethelene cathodes

The polyethelene cathode consisted of a 2mm layer of polyethelene glued to an aluminum ring shaped piece (see figure 7–5). A few hundred 2mm holes were drilled in the polyethelene at distances of about 6mm from each other. The distance between cathode and anode ranged between 15mm to 25mm. Diode current was around 30kA. For smaller distances the diode current was about 50–60kA causing the voltage to drop substantialy.

A typical Faraday cup signal is shown in figure 7–6. The cup was located about 5cm from the cathode. Ion current has a wide broad shape with a width of about 100nsec. It seems that ions are emitted all along the high voltage pulse. The Faraday cup current signal has about the same width of the machine voltage signal. Currents measured reached $2A/cm^2$.

CR–39 pictures of the beam were taken by placing the film at the back side of the coil annulus. A typical picture is seen in figure 7–7. Electron damage is seen at the central part of the picture. Ion current looks homogeneous with a typical "turbine" shape (see figure 7–7). This shape is caused by the fact that ions emitted from the same cathode spot and accelerated by a varying voltage have a different azimuthal Hall deflection. We partially covered the CR–39 with $2.5\mu m$ thick mylar film. This did stop about 50% of the ions. The same film had a very small effect on the Faraday current, which means that probably most of the ions stopped by the film were low energy hydrogen ions.

Pinhole camera pictures showed the same hot spot behavior of ion emission discovered in the previous diode configurations. A typical picture is seen in figure 7–8. Some of the hot spot have a "tail" caused by the azimuthal Hall deflection of the ions in lower accelerating voltage. This means that These spots were active during the lower voltage parts of the pulse. It looks like these were the first spots created by the rising high voltage field stress on the cathode. The same spot is then active during the high voltage part of the signal, and

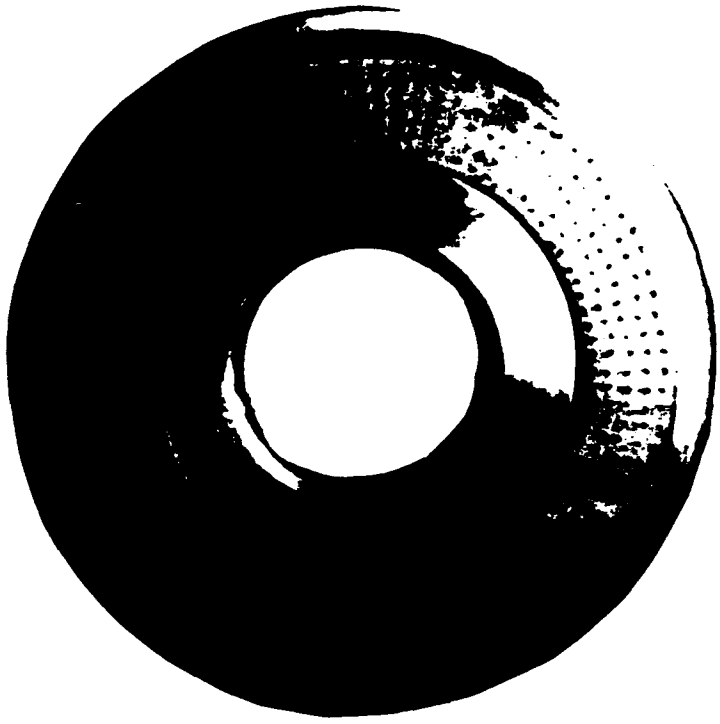

Figure 7–5: Polyethelene passive cathode.

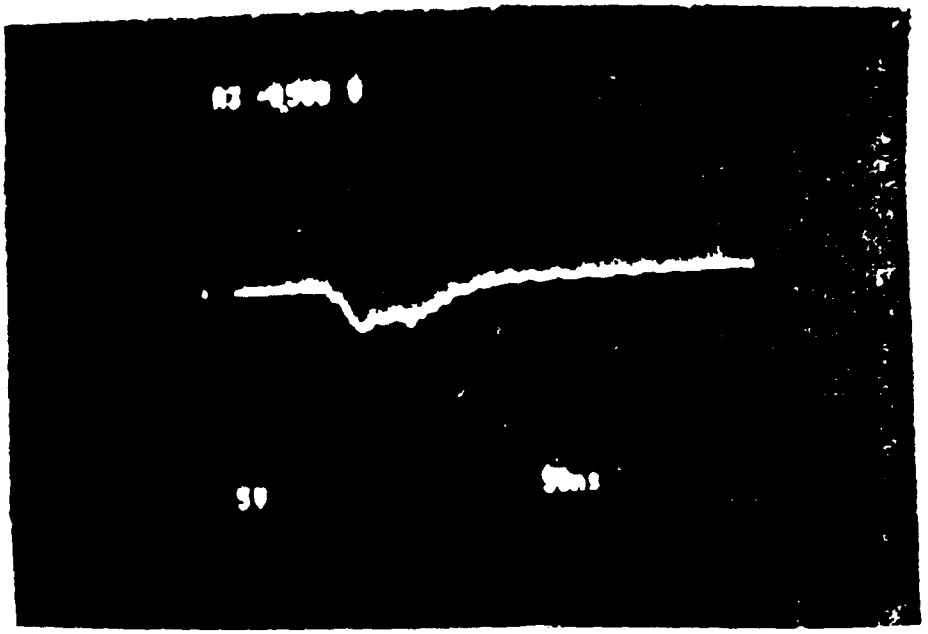

Figure 7–6: Faraday cup current signal from a polyethelene cathode.

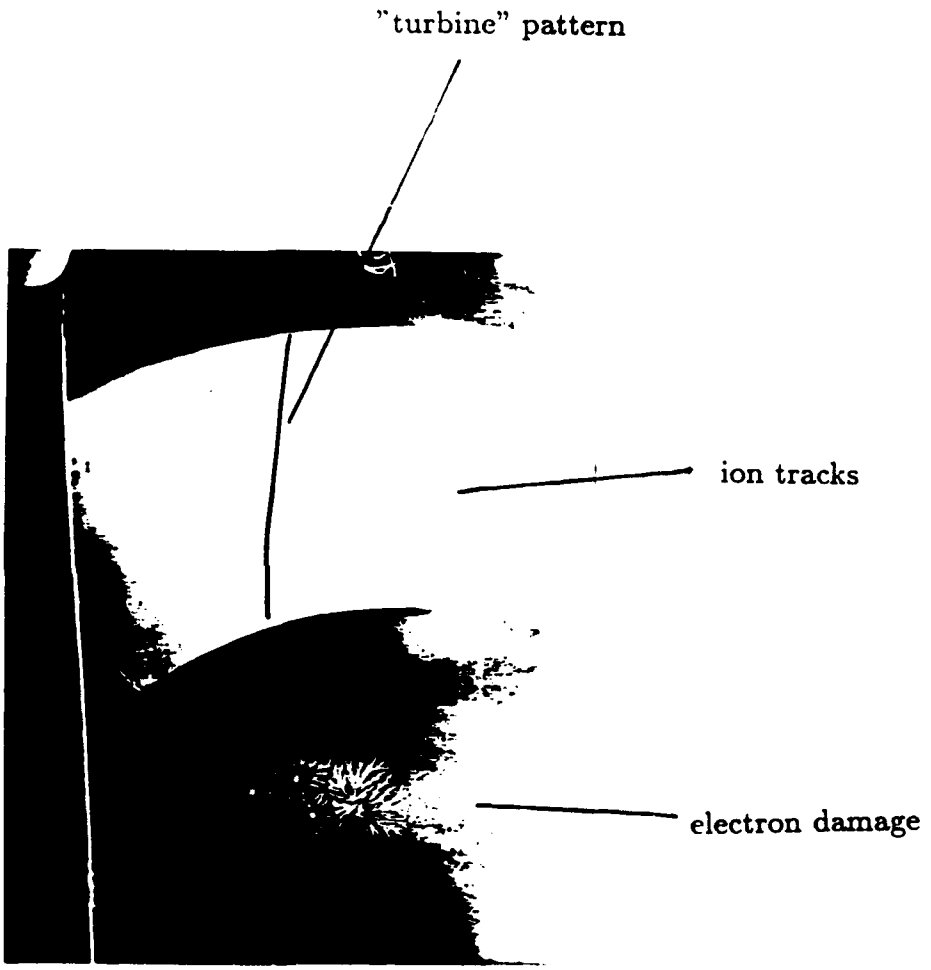

Figure 7–7: CR–39 picture of the ion beam with a polyethelene cathode.

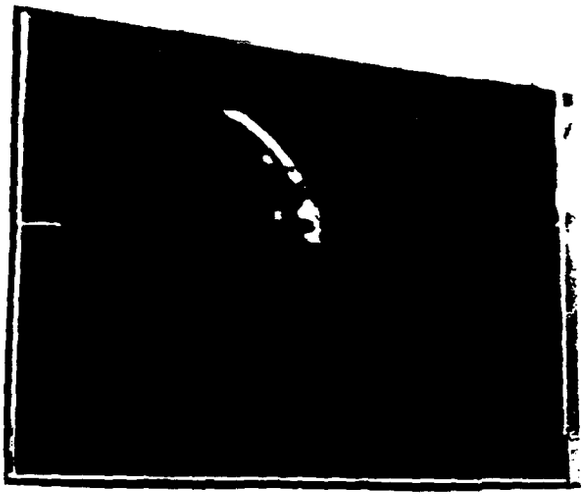

a: A picture with hot spot "tails"

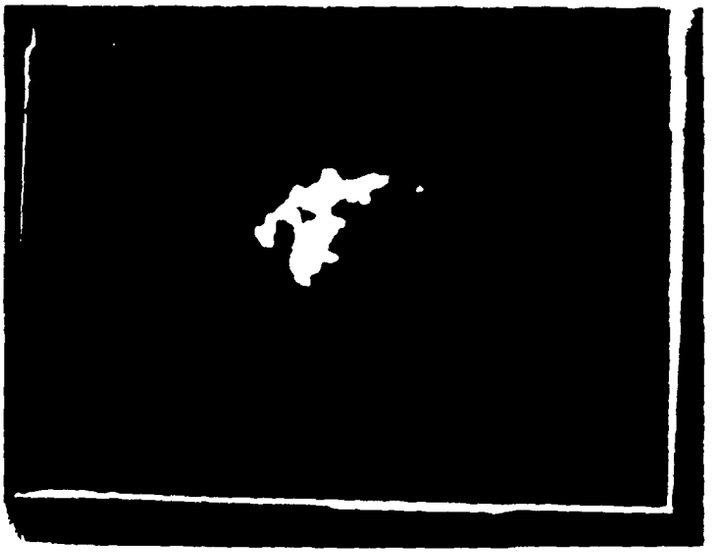

b: A typical picture

Figure 7-8: A typical pinhole camera CR-39 picture of a polyethelene cathode.

it seems there is no hot spots movement during the pulse. The phenomena of hot spots "moving" on the cathode surface is typical to electron emission from the cathode for low electron currents. When we put a 2.5μm thick mylar on the CR–39 film the hot spots tail disappeared proving again that this tail is caused by lower energy ions. Beam divergence was about 150 milliradians in the azimuthal direction. Each hot spot had a diameter of 3–5 mm. Taking this into account and counting the number of ions emitted from each hot spot we get a current density of about 15A/cm^2 from each spot. Since only part of the diode area is covered with spots this averages to the 2A/cm^2 current measured. The inhomogeneous emission of ions from cathode area is associated with an inhomogeneous cathode plasma. The plasma does not expand uniformly on the cathode surface because of the large magnetic field present. A transverse electric field appears near the cathode surface and is to be blamed for the large beam divergence.

7.2.2 Carbon brushes cathodes

The carbon brushes cathode was made of an aluminum ring with a few hundred small brushes stuck into holes drilled in it. The average distance between two brushes was about 10mm. The brushes were 7mm high (see figure 7–9). The distance between brushes edge and the anode was about 21mm.

A typical Faraday cup current trace is seen in figure 7–9. The ion current has the full width of the diode high voltage pulse. When we put 2.5μm thick mylar on the Faraday cup the current signal disappeared. Ion current measured was about 0.5A/cm^2.

CR–39 pictures of the back side of the diode annulus look homogeneous. Differences in beam intensity could not however be measured because of the overlap of ion tracks. When we put 2.5μm thick mylar on the CR–39 most of the tracks disappeared. This together with the Faraday cup measurements means that most of the negative ions measured consisted of carbon or heavier ions.

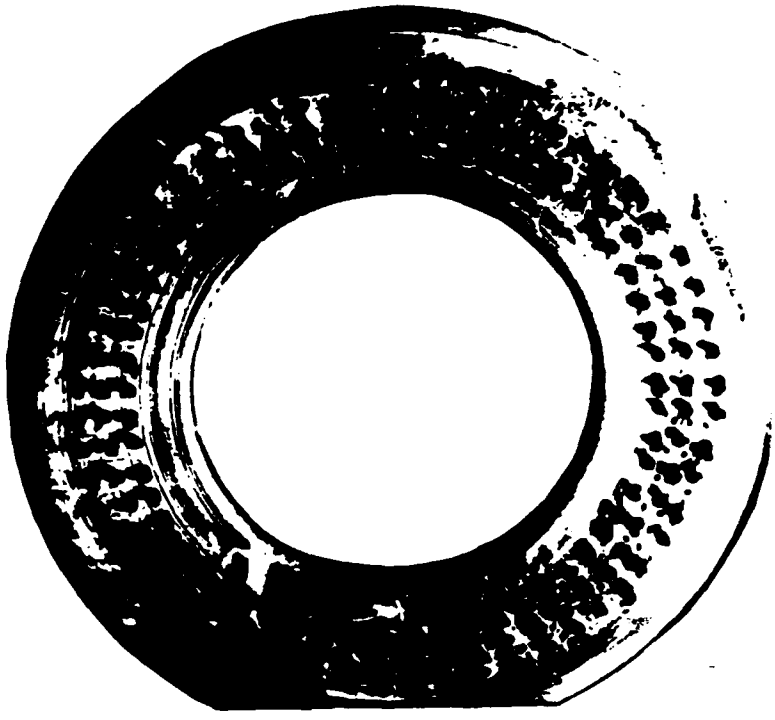

Figure 7–9: Carbon brushes cathode.

Pinhole camera showed the regular hot spot pattern. This time we used a three holes camera to have an estimate of the radial beam divergence (see figure 7–10). This divergence was about 200 milliradians with a 170 milliradians divergence in the azimuthal direction. Higher intensity hot spots are seen on a "background" of lower intensity spots. The spots follow a straight line "train" shape. It looks like a hot spot was created at one point. Electrons and ions from the plasma created would hit the cathode surface and initiate another spot, and so on. Spot size on the cathode is estimated to have a diameter of 6mm. When we covered one of the holes with a 2.5μm thick mylar most of the tracks of ions going through this hole disappeared. It is estimated that about 90% of the ions were carbon ions or heavier (like C_2^- or O^-).

7.2.3 Other passive cathodes

The first simple change we tried was to coat the carbon brushes cathode with parafine. The behavior was very similar to the pure carbon brushes cathode. Beam divergence and intensity were about the same. Ion current was a few hundred milliamperes/cm^2.

The second special cathode we tried was made of pure aluminum. Ion current was very low (a few tenths of milliamperes/cm^2). Hot spots covered the cathode only along a narrow train like path following the azimuthal direction having a similar shape to the spot "train" seen in figure 7–10.

We the tried a felt cathode. This cathode was constructed of a thin synthetic fiber felt cloth glued to an aluminum ring. Anode cathode distance was 25mm. Ion current was low (about 0.5A/cm^2). We changed the anode–cathode distance between 12–30mm with the same results. Pinhole camera picture show that only a very small area of the cathode surface (about 5%) was covered with hot spots. The number of spots was small, each having a diameter of about 5mm.

Figure 7–10: Pinhole camera (3 holes) picture of a carbon cathode.

7.3 Experiments with active cathodes

7.3.1 TiH_2 cathodes with low arc currents

The active cathode had the same basic design as the cathode used in the racetrack diode geometry case. It consisted of a 120 groves flashboard each filled with TiH_2 powder. The flashboard was described before in figures 4–7 and 4–9. The flashboard was placed inside two aluminum rings used for electrical field shaping (see figure 7–11). These electrodes also protect the flashboard from breakdowns inside the diode. We sometimes used longer metal rings to create a field free plasma expansion space. We also used the rings sometimes to support a fine metal screen put above the flashboard. This screen was used to lower the plasma density in the gap and to provide a flat extraction surface. Negative ion current was measured with two Faraday cups in the same way described above in chapter 7.1. Flashboard arc current and plasma conditions were described in chapter 4.

Faraday cup ion current signal show a broad peaked signal. This signal has about the same time duration as the diode voltage pulse (see figure 7–12). Diode currents were around 20kA for flashboard delay times of 2–4μsec. A plot of the measured ion current as a function of the delay is seen in figure 7–13 The current has a peak value of about 6A/cm^2 for delay times between 1–2μsec and goes down slowly as the delay becomes larger. No ions were measured for delay times smaller than 0.5μsec.

Pinhole camera pictures show that most of the cathode area was covered with hot spots (see figure 7–14). Beam divergence in the azimuthal direction is about 150 milliradians. Each hot spot had a diameter of about 7mm. Ion emission intensity from each spot was estimated to be about 30A/cm^2.

We tried a few more configurations with this plasma gun. First we tried the diode with longer field shaping electrodes. Instead of electrodes with 1cm hight above the flashboard surface, we used 3.5cm long electrodes. This made the electric field in the gun plasma expansion space much smaller. The results

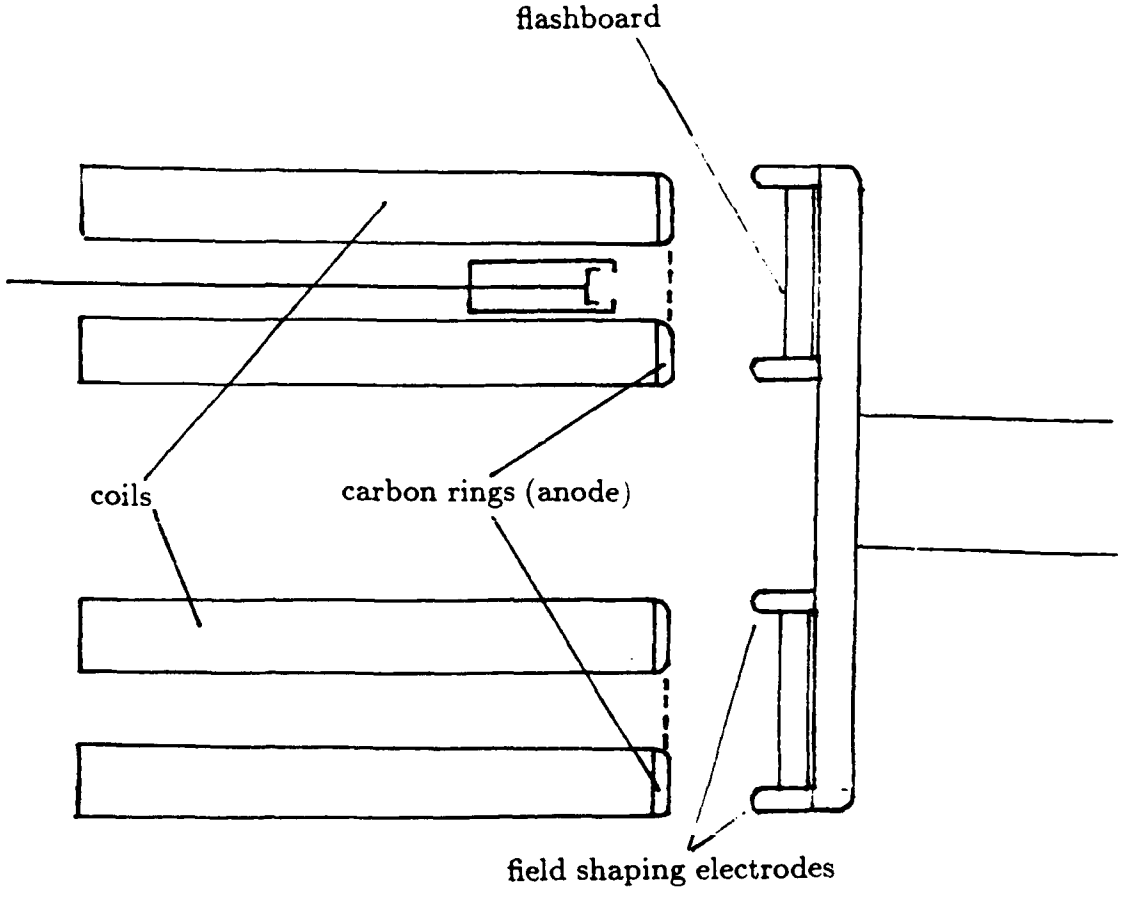

Figure 7-11: Active cathode experimental setup.

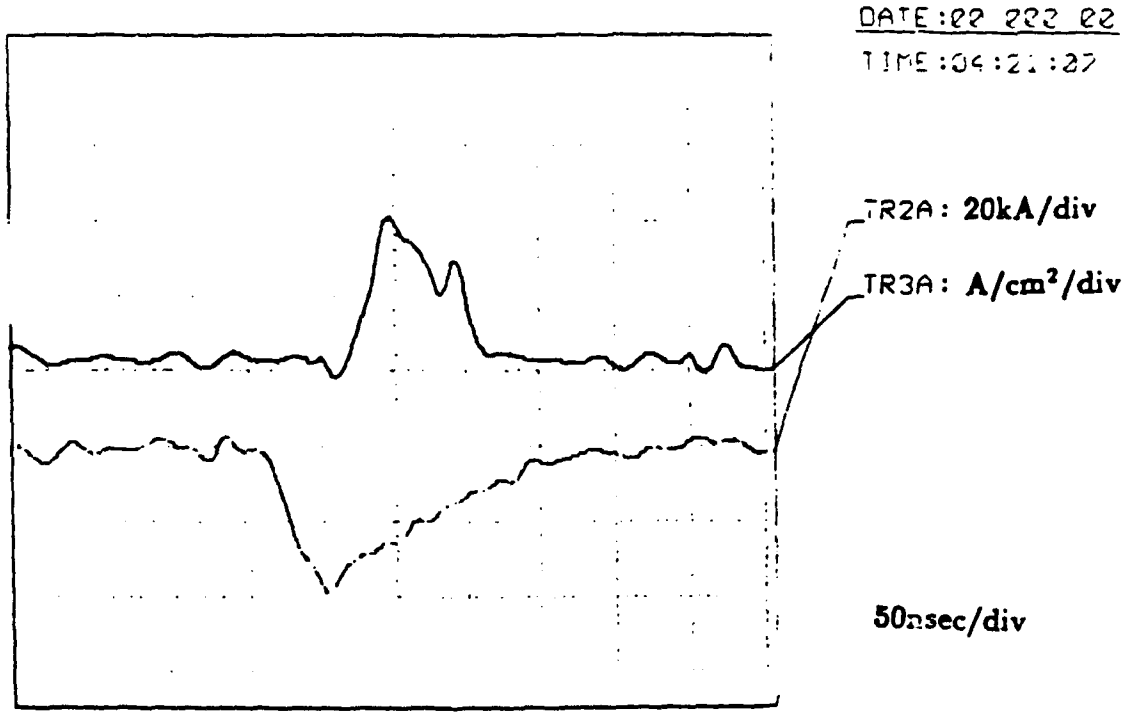

Figure 7–12: A typical ion current trace for a low current active cathode (with 2.5μm mylar on Faraday cup).

Figure 7-13: Faraday cup ion current as a function of flashboard delay time.

Figure 7–14: CR–39 pinhole camera picture of a low current annular active cathode.

were disappointing. Ion current was very low and could not be measured with a Faraday cup. Diode current was low (around 15kA). It looks like that the plasma density reaching the high voltage gap was too low.

The second configuration we tried was with a fine screen in front of the flashboard. The screen was made of stainless steel and had a transparency of about 30%. No ion current was measured with the Faraday cups under different delay conditions. Diode current was low, and again it looks like there is a very low density plasma in the gap.

7.3.2 TiH_2 cathodes with high arc currents

This experiment had the same diode geometry described in figure 7–11. The only difference was that the plasma gun was operated under high current conditions described before in chapter 4.

Diode voltage was about 700keV but dropped quickly. Diode current was about 50kA. Negative ion current was narrower than before and had a width of about 40 nsec (see figure 7–15). The ion current was a little smaller than before and reached values of $3A/cm^2$. The time delay behaviour was quite similar to what we saw in figure 7–13 with a broad maximum between 1–2μsec. The current dropped gradually for larger delay times. No ions were measured for delay times smaller than 0.5μsec.

CR–39 pinhole camera pictures show hot spots all over the cathode area. When delay time is larger the ion emission becomes much more homogeneous (see figure 7–16). Beam divergence was about 250 milliradians for delay times of about 2.5μsec.

We then put a fine metal screen on the flashboard. The screen had a transparency of about 40%. Diode current was 25kA and the voltage had the regular shape with a peak value of 700kV. Ion current was around $2A/cm^2$. Beam divergence was measured with a pinhole camera and was about 100 milliradians.

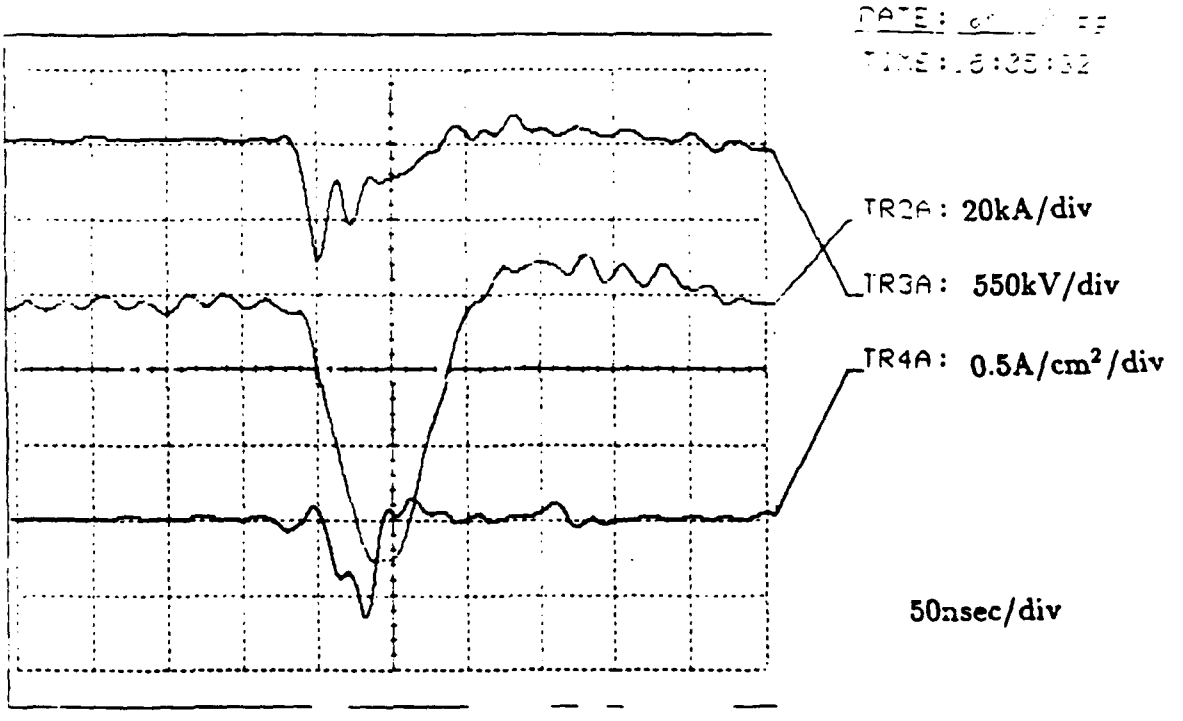

Figure 7-15: Typical ion current and diode voltage current traces for annular high current plasma gun cathode.

a: delay=2.1μsec

b: delay=7.2μsec

Figure 7-16: Pinhole camera pictures of an annular high current flashboard.

7.4 Summary

the conclusions which can be drawn from the experiments done on the annular diode geometry are:

- Ion current Faraday cup measurements were very easy to perform because most diode electrons drifted along magnetic field lines into the inner coil space.
- Ion currents of $2A/cm^2$ were extracted when we used a passive polyethelene cathode. The same typical hot spots phenomena seen in previous diodes appeared here. Beam divergence was around 150 milliradians in the azimuthal direction. Some spots have a low energy "tail". This could be explained by low energy ions ejected from the spots during the APEX pulse lower voltage parts. Such ions cause a "turbine" shaped ion beam.
- With a carbon brushes cathode we got ion currents of about $0.5A/cm^2$. Beam divergence was about 200 milliradians in the radial direction and about 150 milliradians in the azimuthal direction.
- Peak currents of $6A/cm^2$ were measured when we used a low current TiH_2 cathode. The ion current signal was broad with a width af about 90nsec. Most of the cathode area was covered with ion emitting hot spots. No ions were measured when we put a fine metal screen in front of the plasma gun.
- With high arcing current flashboard the ion current was not more than $3A/cm^2$. Diode load was high and the diode voltage dropped quickly. Ion current had a width of only 40nsec. With a fine metal screen in front of the the current voltage traces of the diode returned to normal, with an ion current of $2A/cm^2$.

The results obtained with the annular diode show the same typical behaviour found in previous diode configurations. Ions were emitted from hot spot areas on the cathode surface all along the high voltage pulse duration. The hot spot phenomena caused a large beam divergence. The situation was much better when we used an active plasma gun. Most of the cathode area was covered

with hot spots, and ion current intensity values reached were higher.

cathode material	current density (A/cm^2)	divergence (radians)	composition
C_2H_2	2	150	at least 50% H^-
carbon brushes	0.5	200	at most 10% H^-
active TiH_2 (low current)	6	150	
active TiH_2 (high current)	3	250	
active TiH_2 (fine screen)	2	100	

Table 7–1: summary of results with an annular diode configuration.

References

1. A. Fisher and N. Rostoker, Bull. Am. Phys. Soc., **21**, 1097(1976).

2. S. Humpheris, Jr., Nucl. Fusion, **20**, 1549 (1980).

3. J. H. Fink, 4^{th} Int. Symposium Production and Neutralization of Negative Ions and Beams, Brookhaven (1986), pp 618.

4. H. S. W. Massey, "Negative Ions", Cambridge university press, Cambridge, 1976.

5. B. M. Smirnov, "Negative Ions", McGrow–Hill, New–York, 1982.

6. see reference 4 pp 415.

7. C. E. Kuyatt, S.R Mielczarek and H.A. Simpson, Phys. Rev. Lett., **12**, 293(1964).

8. W. C. Linberger and T.A. Patterson, Chem Phys. Lett., **13**, 40(1972).

9. see reference 4 fig 10–8 pp 403.

10.K. W. Ehlers, Nucl. Inst. Meth., **32**, 309(1965).

11. R. L. York, K. W. Ehlers, M. Bacal, Rev. Sci. Inst., **55**, 681(1984).

12. J. R. Hiskes, Comments At Mol. Phys., **19**, 59(1987).

13. K. N. Leung and W. B. Kunkel, Phys. Rev. Lett. **59**, 787(1987).

14. J. M. Wadera and J. N. Bardsley, Phys. Rev. Lett. **41**, 1795(1978).

15. S. J. Smith and D. S. Burch, Phys. Rev., **116**, 1125(1972).

16. see reference 5 pp156.

17. see reference 4 fig 11–18.

18. see reference 4 fig 11–50

19. B. Peart and K. T. Dolder, J. Phys. **B3**, 1346(1970).

20. G. Poulaert et. al. , J. Phys., **B11**, L671(1978).

21. see reference 4 fig 13–8.

22. J. F. Williams, Phys. Rev. , **154**, 9(1967).

23. J. R. Hiskes, and A. M. Karo, 3^{rd} International Symposium on Production and Neutralization of Negative Ions an Beams, Brookaven (1983), pp 185.

24. K. N. Leung and K. W. Ehlers, 3^{rd} International Symposium on Production and Neutralization of Negative Ions an Beams, Brookaven (1983), pp265.

25. O. F. Hagena and P. R. W. Henkes, 4^{th} Int. Symposium Production and Neutralization of Negative Ions and Beams, Brookhaven (1986), pp 384.

26. J. R. Hiskes, 4^{th} Int. Symposium Production and Neutralization of Negative Ions and Beams, Brookhaven (1986), pp 2.

27. A. A. Agafonov, A.A.Kolomenski et. al. , Zh. Eksp. Teor. Fiz. ,**84**, 2040 (1983)., Sov. Phys. J. E. T. P. , **57**, 1188 (1983).

28. A. A. Kolomenski, A. N. Lebedev et. al. , Proc. of the 5^{th} Int. Conf. on High Power Particle Beams, San–Francisco (1983). **BEAMS 83**

29. A. A. Kolomenski, A. N. Lebedev et. al. , Proc. of the 6^{th} Int. Conf. on High Power Particle Beams, Kobe(1986). **BEAMS 86**

30. J. P. Vandevender, R. W. Stinnet and R. J. Andersom, Appl. Phys. Lett., **38**, 229(1981).

31. R. Stinnet and T. Stanley, J. Appl. Phys., **53**, 3819(1982).

32. R. Stinnet and M. T. Buttram, J. Fus. Ener., **3**, 253(1983).

33. R. W. Stinnet, M. Palmer, R. Spielman, Sandia Natl. Labs. report No. **SAND–82–1838C**.

34. R. W. Stinnet, G. R. Allen P. H. Davies et. al., Sandia Natl. Labs. report No. **SAND–83–2591C**

35. R. W. Stinnet, M. A. Palmer, R. B. Spielman and R. Bergston, IEEE Trans. Plas. Sci., **PS–11**, 216(1983).

36. S. Moustaizis, H. J. Doucet, H. Lamain and C. Rouille, Proc. of the 6^{th} Int. Conf. on High Power Particle Beams, Kobe(1986). **BEAMS 86**

37.V. M. Bistritsky, S. N. Volkov et. al., Proc. of the 6^{th} Int. Conf. on High Power Particle Beams, Kobe(1986). **BEAMS 86**

38. J. Nation, "Particle accelerators", **10**, 1(1979).

39. S. Winterberg, "Physics of high energy density", Academic Press, New–York, 1971.

40. J. F. Janni, Atomic Data, **27**, 147(1982).

41. C. D. Child, Phys. Rev. **32**, 492(1911).

42. I. Langmuir, Phys. Rev. **2**, 450, (1913).

43. P. Pellinen and V. Staggs, Rev. Sci. Inst., **44**, 46(1973).

44. P. Pellinen, Rev. Sci. Inst., **43**, 1654(1972).

45.Atomic data tables

46. B. G. Cartwright, E. K. Shirk and P. B. Price, Nucl. Inst. Meth., **153**, 457(1978).

47. G. Somogyi, "Solid State Nucl. Track Detectors, Proceedings of the 11^{th} Int. Conf., Bristol,sept. 1981", Pergamon–Press, Oxford 1982.

48. P. Dreike, C. Eichenberger, S. Humpheris Jr. and R. N. Sudan, J. Appl. Phys., **47**, 85(1976).

49. H. E. Tomaschke and D. Alpert, J. Vac. Sci. Tech., **4**, 192(1967).

50. E. W. Gray and R. W. Stinnet, J. Appl. Phys., **61**, 5222(1987.

51. S. P. Bugaev, E. A. Litvinov, G. A. Mesyates and D. J. Proskurovski, Sov. Phys. USP, **18**, 51(1975).

52. L. P. Harris in "Vacuum arcs", J. M. Lafferty editor, John Wiley, New–York, 1980.

53. F. F. Chen in "Plasma dignostics techniques", R. H. Huddlestone and S. L. Leonard editors, Academic Press, New–York, 1965.

54. W.H. Bostick, Phys. Rev., **104**, 292(1956).

55. F.M. Page and G.C. Goode, "Negative ions and the magnetron", Wiley Interscience,London, 1969.

56. S. J. Sackett, "EFFI, a code for calculating the electromagnetic field, force and inductance in coil systems of arbitrary geometry", UCRL report No. UCRL–52402 (1978).

57. F.F. Chen, "Plasma physics and controlled fusion", Plenum Press, New–York ,1984.

58. P. Dreike, C. Eichenberger, S. Humpheries Jr. and R. N. Sudan, J. Appl. Phys., **47**, 85(1976).

59. S. P. Bugaev, G. A. Mesyats and D. I. Proskurovskii, Sov. Phys. DOKLADY, **14**, 605(1969).

60. Hinshelwood, PhD thesis

61. S. Dushman, "Vacuum Technique", J. Wiley and sons, New–York, 1962.

62. R. Gomer in "Desorption Induced by Electronic Transitions DIET I", Proceedings of the First International Workshop, Williamsburg, Virginia 1982. N. H. Tolk, M. M. Traum, J. C. Tully and T. E. Madey –editors., Springer–Verlag, New–York, 1983.

63. I. Langmuir, Phys. Rev. **33**, 954(1929).

64. J. Maenchen, L. Wiley, S Humpheries, Jr., E. Peleg, R. N. Sudan, and D. A. Hammer, Phys. Fluids, **22**, 555(1979).

65. S. Humpheries, Jr., J. R. Freeman, J. Greenly, G. K. Kuswa, C. W. Mendel, J. W. Poukey, and D. M. Woodall, J. Appl. Phys., **51**, 1876(1980).

66. H. J. Doucet, H. Lamain, S. Moustaizis and C. Rouille, Proceed. Second European Workshop on the Production and Application of Light Negative Ions. Ecole Polytechnique, Palaiseau, march 1986.

67. J. T. Moseley, R. E. Olsen, J. R. Peterson, Case studies in Atomic Physics, **5**, 1(1975).

68. D. D. Hinshelwood, IEEE Trans. Plasma Science, **PS–11**, 188(1983).

69. Y. Maron, M. D. Coleman, D. A. Hammer and H. S. Peng, Phys. Rev. A, **36**,2818(1987).

70. D. S. Prono, H. Ishizuka, E. P. Lee, B. W. Stallard and W. C. Turner, J. Appl. Phys., **52**, 3004(1981).

71. C. Litwin and Y. Maron, "Role of neutrals in plasma expansion in ion diodes"–to be published.

72. C. Litwin and Y. Maron, "Ionization instability and magnetic insulation breakdown in ion diodes", to be published in J. Appl. Phys.

73. Y. Maron, L. Perlmutter, E. Sarid, M. E. Foord and M. Sarfati, "Spectroscopic determination of particle fluxes and charge–state distribution in pulsed–diode plasma", to be published.

74. Y. Maron, M. Sarfati, L. Perlmutter, O. Zehavi, M. E. Foord and E. Sarid, "Electron temperature and heating processes in a dynamic plasma of a high power diode", to be published.

75. Y. Maron and C. Litwin, Phys. Fluids, **30**, 1526(1987).

76. D. Menzel, Proceedings of the First International Workshop on Desorption Induced by electronic Transitions (DIET), Williamsburg, Virginia, USA (1982). Springer–Verlag , New–York 1983.

77. W. Jeland and D. Menzel, Chem. Phis. Lett., **21**, 178(1973).

78. J. Habritter, J. Appl. Phys., **53**, 6475(1982).

79. K. W. Struve, E. J. Lauer and F. W. Chambers, Proc. of the 5th Int. Conf. on High Power Particle Beams, san Francisco **BEAMS 83**, (1983).

80. Y. Maron, E. Sarid, O. Zahavi, L. Perlmutter, and M. Sarfaty, "Particle Velocity Distribution and Expansion of a Surface–Flashover Plasma in the Presence of Magnetic Fields", to be published

Chapter 8 NEGATIVE IONS PRODUCTION MODEL

8.1 Introduction

In this chapter we shall discuss the theoretical aspects of negative ion production in high voltage magnetically insulated diodes. The voltage in these diodes ranges between a few hundred volts and a few megavolts, with currents of tenths kiloamperes. The production of negative ions in this type of diodes is closely related to the properties and behavior of the cathode plasma. Unfortunately, most of the work done on plasma properties and behavior in high voltage magnetically insulated diodes was done on the anode plasm. This is because most of the research in ion beam production was aimed towards producing positive ion beams. As we shall see later the cathode plasma shows sometimes a similar behavior as the anode plasma. This applies for instance to its expansion velocity in the high insulating magnetic field. The cathode plasma should be confined by a field of a few kilogauss-but instead we measured an expansion velocity of about 1cm/μsec. A similar behavior was found with the anode plasma in positive ion diodes-and we shall discuss this later in this chapter. On the other hand we have found some plasma properties typical to low voltage discharge cathode plasma. This applies for instance to the *hot spot* phenomena. In low voltage discharge, electron emission is confined to a few hot spots on the cathode area. A similar behavior was found in some high voltage diodes [60, 68]. We found a similar behaviour for negative ion emission.

We shall start the chapter with a discussion of the conditions under which negative ions can exist in a plasma. We shall then go into the cathode plasma properties and how negative ions could be produced in the diode. We will discuss how negative ions are extracted from the plasma, despite the high electron negative space charge in the high voltage gap. At the end of the chapter we shall review the results we got from different diode configurations.

8.2 Existence of negative ions in a cathode plasma

In this chapter we shall discuss the various conditions under which negative ions can exist in a plasma under thermal equilibrium conditions. This is not the case in our experiment, but this discussion can throw light on the optimal conditions for negative ion production.

There are many unanswered questions about the mechanism of how negative ions are extracted from a cathode plasma producing current densities of a few ampers/cm^2. Such high current densities could not be extracted if the cathode plasma would be under thermal equilibrium conditions. The relative numbers of ions existing then in a plasma could be calculated from the Saha equation:

$$\frac{n_i}{n_n} \approx 2.4 \times 10^{21} \frac{T^{3/2}}{n_i} e^{-U_i/kT} \tag{8.1}$$

Where n_i and n_n are the densities (per m^3) of ionized atoms and neutrals respectively, T is the plasma temperature in °K, k is Boltzman's constant and U_i is the ionization energy of the gas. The "extra" n_i at the right side of the equation just reflects the fact that recombination rate is proportional to the electron density, which can be taken to be equal to n_i. Suppose we take a pure hydrogen plasma composed of electrons, positive and negative ions, and neutrals. Let us further assume that the plasma temperature is $T \approx 3eV$ and the ion density $n_i \approx 10^{16}/cm^3$. We shall see later that these are the numbers usually measured in the cathode plasma of a magnetically insulated diode. Putting these numbers in the Saha equation we get a neutral density of about 10^{12}/cm^3. The negative ion affinity is only 0.7eV which is small compared to U_i which is 13.6eV in our case. Negative ion density is therefore very close to the neutral density. Only about 10^{-2}% of the negative charges in a plasma under thermal equilibrium conditions are negative ions. This also justifies the fact that we approximated the number of electrons and positive ions to be equal.

The very small affinity also means that negative ions cannot exist in a plasma with density higher than $10^{14} - 10^{15}$/cm^3 [66]. Let us consider the case

where negative ions are destructed only by electron collisional detachment (see figure 2-5). The mean free path of an H^- ion produced in a plasma with electron density n_e is:

$$\lambda_{en} = \frac{1}{\sigma_{en} n_e} \tag{8.2}$$

For a plasma having an electron temperature of 3eV and a density of $10^{17}/\text{cm}^3$ the mean free path of an H^- ion is about 0.2mm. If the negative ions have the same temperature they will cross this distance in about 5nsec. This means that within a time scale of a few tenths of nanoseconds negative ions could not exist in a plasma with this density. For a plasma density of $10^{19}/\text{cm}^3$ the mean free path is about 1μ. in fact, for higher density the mean free path is about 100 times shorter [67]. In this calculation we ignored other negative ion destruction mechanisms. We also ignored negative ion production, since it is very much dependent on the amount of vibrationally excited molecules in the plasma. We shall go through a more detailed calculation later in this chapter, but it is quite clear that plasma density at which we can expect a reasonable number of negative ions to exist ranges at most between $10^{14} - 10^{15}/cm^3$.

Cathode plasma measurements were done by the Sandia group in a magnetically insulated transmission line using visible spectroscopy [31 – 35]. The plasma sheath extended 0.2cm from the cathode surface. It had a density of $10^{15} - 10^{16}/\text{cm}^3$ with a monotonically increasing density gradient from the edge of the cathode surface of $10^{17} - 10^{18}/\text{cm}^4$. Cathode plasma density was also measured by Hinshelwood using interferometric methods [60, 68]. The density was about $2 \times 10^{16}/\text{cm}^3$. Most negative ions formed in the high density part of the plasma near the cathode surface will therefore be destroyed before being able to be extracted. Only negative H^- ions produced in the lower density parts of the expanding plasma will be able to leave the plasma and be extracted by the applied electric field.

The maximum current density which can be extracted from the surface of

a uniform plasma in thermal equilibrium is given by [66]:

$$j_- = en_-(kT_-/2\pi M_-)^{1/2} \tag{8.3}$$

where T_- is the negative–ion temperature. If we assume that this temperature is about 1eV the maximum current density of H^- ions extracted from a region of the plasma where the density is $10^{14}/cm^3$, as given by the above equation is about $6A/cm^2$. For plasma densities much lower than $10^{14}/cm^3$, the negative ion current would be too small. But even if we have the plasma at the right temperature and density conditions we might get a very low negative ion current due to the Child–Langmuir limit discussed before. For an applied voltage of 1MV and diode gap of 1cm this limit is about $55A/cm^2$ for a pure hydrogen ion plasma. It is smaller if we have other ion species in the plasma, or if we have an electron negative space charge in the gap as is the case here.

Let us summarize the discussion of this chapter. We saw that the best conditions for negative ion existence in an equilibrium plasma are when plasma density is around $10^{14} - 10^{15}/cm^3$ if the ion temperature is a few eV. The maximum current could then range around a few A/cm^2 to a few tenths of A/cm^2

8.3 Creation of negative ions in a cathode plasma

We shall now propose a model for negative ion production in the cathode plasma. We saw in chapter 2 that the largest cross section for negative ion production by is electron attachment to a highly vibrationally excited molecule. So the best way to get negative ions is to have an area where we have a large amount of vibrationally excited molecules and electrons with energies of about 3eV. We saw in chapter 8.2 that under thermal equilibrium conditions we have a very small number of neutrals in a high density plasma with a temperature of a few eV. Actually, neutral numbers of about 10^{18} have been measured in a cathode plasma of a magnetically insulated diode [60, 68]. What we propose, is that some of these neutrals are in a molecular state (which could be

is due an expansion of hot neutrals. These hot neutrals are created, through multiple charge exchange processes, by ions emitted from the anode surface. The hot neutrals expand rapidly into the diode gap and create a layer which is subsequently ionized by energetic ions and an electron avalanche. A similar model has been suggested by Prono et. al. [70]. In addition to the hot neutrals, a cold neutral layer was observed to exist near the anode surface. The expected number of particles in this layer was $N \approx 10^{16} - 10^{17}/cm^2$, and the neutral temperature was about 1eV. In a later paper it was suggested that plasma expansion velocity was due to a lower hybrid drift instability caused by a large plasma pressure gradient [80]. This pressure is believed to be caused by the high ion temperature.

In experiments done on anode ([70 – 75]) or cathode plasma [68, 69], a high expansion velocity was observed despite the existence of the insulating magnetic field. In both cases a large number of neutrals was ejected from the dielectric surface into the gap. This particle flow from the metal surface goes on during and after the high voltage pulse. The mechanism of particle release from the dielectric surface are not well understood [71]. Particles can be released from the surface due to bombardment by plasma particles. Impact of plasma electrons of a few electron–volts may desorb neutrals from the surface with a yield of about unity [78]. These neutrals, however, will have a very low energy. The more energetic neutrals are probably produced by multiple charge exchange. As a matter of fact, most particles released in general from a surface by electron impact are neutrals [76]. Relative abundance measurements found in some cases that only a few percent of the particles were ions [77]. In some cases the neutrals were in an electronically excited state (this was observed for instance for desorption of CO from CO/Mo).

The cold neutral layer observed near the cathode surface, together with the existence of a drifting electron layer could create negative ions by electron detachment. Let us assume that part of the neutrals are in a molecular state. These molecular neutrals could be desorbed from the cathode surface, or be

created later by recombination processes of ionized material ejected from the cathode. Neutral molecules existing at the lower density part of the plasma, close to the negative drifting electron layer could be vibrationally excited and then create a negative ion by colliding with an electron in the negative charge layer. As we mentioned, the existence of a cathode plasma gradient layer was found in measurements done on a cathode plasma of a transmission line [31 – 35]. The cross section for a negative ion creation by dissociative attachment of a hydrogen molecule has a maximum at electron energies of a few eV. These energies were indeed measured in high voltage diode plasmas. Anode plasma electron temperature measurements in a racetrack diode gave numbers ranging around 7eV [74]. This plasma was also created by a surface flashover on a dielectric surface, as in our case. Cathode electron temperature was measured in a cathode plasma of a delay line and the numbers range around 2eV [31 – 35]. The cold neutral layer had a temperature of about 1eV and a density of about $10^{16}/cm^3$ [71]. Under these conditions of a cold neutral layer together with electrons at the right temperature, we could get negative ions. We have to remember that a current of about $1A/cm^2$ would be created over a pulse of 50nsec duration by $10^{11} - 10^{12}$ negative ions. If we really have a neutral density of about $10^{16}/cm^3$ then it is possible to have a negative ion density in the $10^{12} - 10^{13}/cm^3$ range. Negative ions could be destructed by colliding with electrons or heavier particles. We shall explain now why we think that this destruction processes have a low effect in our case.

The high voltage electric field penetrates the negative charge layer. Measurements done by Maron et. al. [69] showed that the electric field vanishes only at the cathode plasma. At the negative electron layer it just goes down slowly. This was also revealed by putting a vane on the anode. The vane edge created a negative drifting electron layer located at the same distance from the cathode as the edge. The electric field was then measured, and it was found that it dropped to zero only at the cathode plasma edge. Any negative ion created at the low density area near the negative charge layer, will be extracted into the

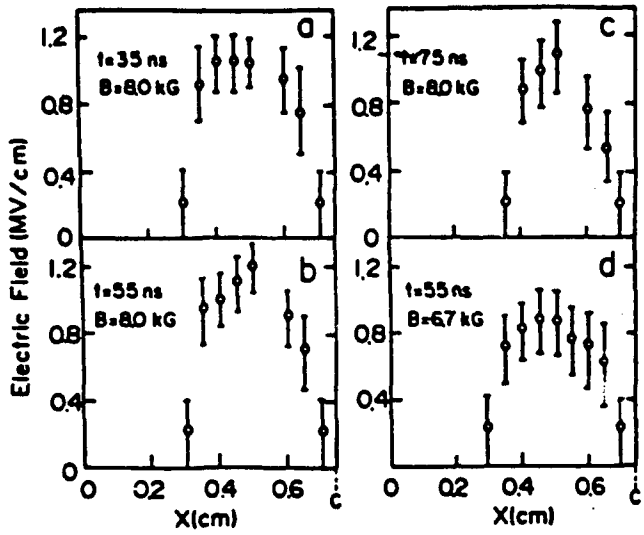

a: Electric field

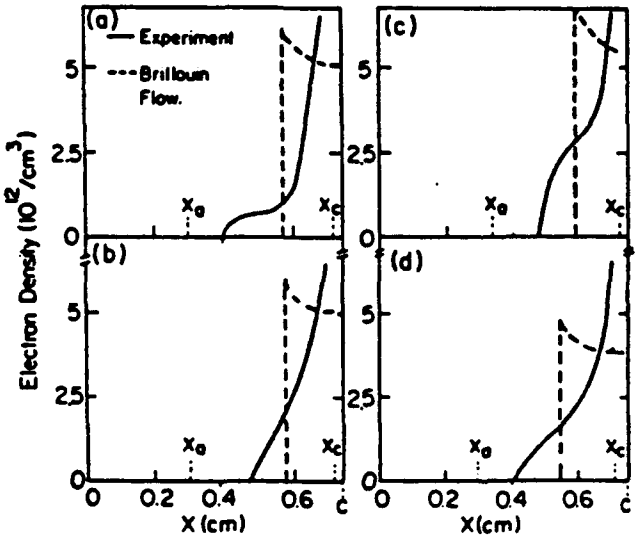

b: Inferred electron density

Figure 8.1: Measured electrical field and inferred electron density in a high voltage racetrack diod (after Maron et. al.[69]).

high voltage gap. This is because these ions are less affected by the insulating magnetic field. Negative ion destruction processes are therefore of low importance, since negative ions are extracted immediately. It looks therefore, that the conditions at the boundary area between the cathode plasma and the negative sheath layer are most important for negative ion production. The production mechanism we proposed is based on a very limited experimental data regarding the electric field, neutral density and cathode plasma measurements. It has to be then treated very cautiously. We do however believe that it is the most reasonable one.

8.4 Extraction of negative from the cathode plasma

Electrons ejected from the cathode plasma create a negative space charge in the high voltage gap of magnetically insulated diodes [69]. This space charge is responsible for the fact that positive ion currents, far above the Child–Langmuir limit have been extracted from these diodes. It is the same space charge which could prevent negative ions from being extracted from the cathode plasma. Once this electron layer is created it acts like a "virtual" cathode causing the extracting field on the plasma to be much smaller. As we did see in chapter 8.2, negative ions exist in this plasma probably only at the lower density front part of it. This is the area close to the electron sheath. This area is probably the most important in regards to negative ion production and extraction. The experimental results are not sufficient to support any theory regarding this questions. We shall try however to raise the problems concerned with the negative ion production and extraction in this layer.

The electrical field and charge distribution in a racetrack type magnetically insulated diode were measured by Maron et. al [69]. This was done by observing the Stark shift of line emission from ions accelerated in the diode. The measured electric field is shown in figure 8–1. While the electrode anode–cathode gap was 0.75cm, it turned out that the actual high voltage gap was only about 0.4cm long. The smallest measured value of the electric field was 0.4mV/cm observed

near the cathode and anode plasmas. The region between these points and the electrodes is occupied by the cathode plasma on one side, and an anode plasma on the other. Integration of the measured electric fields over the real gap distance gave values very close to the measured diode voltage.Comparison of the measured electric field with a calculated field using a one dimensional Brillouin–flow model (in which the real gap was used) show that an electron cloud is spread all over the high voltage gap. The electron cloud is not confined to a narrow sheath near the cathode; rather it migrates towards the anode.

This large electron negative space charge in the high voltage gap can prevent negative ions from being extracted from the cathode. Indeed, if we look at the electrical field measurements (figure 8–1) we can see that the electric field has a maximum at about the middle of the actual gap and then goes down slowly at the vicinity of the cathode. It is screened by the electron space charge. Taking into account the smaller field on the cathode surface (figure 8–1) the negative ion current extracted from the cathode would be only $5A/cm^2$ compared to about $30A/cm^2$ which is the Child–Langmuir.

On the other hand, one can see that the actual gap is about one half the electrode gap, and the electric field has a peak of about three times larger than the field we would get by dividing the applied voltage by the electrode gap (this number is about 0.5mV/cm compared to a peak measured value of 1.2mV/cm). These field measurements were taken with a polyethelene anode flashboard, while in our case we are dealing with a cathode plasma sources with no anode source. However, we always have some residual gas molecules on the anode which could be knocked out of the surface by fast electrons and create an anode plasma. We did in fact measure a small positive ion current of a few A/cm^2 (see chapter 5). We can therefore assume that the electric field in our case would have the same shape. The only difference could be the extension of the actual gap which might be a little larger because of the lower density anode plasma in our case. Taking the smaller actual gap and the smaller extracting field we get that the negative ion current extracted from the diode is about 20%

larger than the Child–Langmuir mechanical gap current limit.

8.5 Discussion of our experimental results

The high intensity emission of electrons from a few small areas on the cathode surface is very similar to what we observed in regards to negative ion emission. In all diode configurations checked by us we saw that emission of negative ions is confined to a few "hot–spots" on the cathode surface. This probably caused the high beam divergence measured. This divergence was between 100–300 milliradians in most of our measurements, and was about 200 milliradians in the positive ion case measured by Maron et. al. [75]. It is therefore possible that negative ions are emitted together with electrons from a few "hot–points" on the diode surface. If indeed this emission is Child–Langmuir current limited, and the electron current is about 1kA, then we should get a negative hydrogen current about 40 times smaller, which is about 25A for one burst. The current we got was estimated to be between 10–25A from one "hot spot" site, and averaged over the cathode area it was only a few A/cm^2. Despite the similarity between the electron bursts and negative ions "hot–spots" behavior, there are a few differences. We did not see negative ion emission in short timed bursts. Rather we measured negative ion emission all along the high voltage pulse, with quite a smooth shaped signal. The only exception was in the case of the racetrack diode where a short time high intensity negative ion signal was measured over a background of negative ions emitted all along the high voltage pulse duration.

When we used active plasma guns we got a much more homogeneous plasma with "hot spots" spread evenly on the cathode surface. When we use such a plasma gun–we do create plasma at 120 points spread evenly on the cathode surface. When , on the other hand, we use a passive plasma gun we cannot control where plasma is created on the cathode surface. Once we have a few "hot spots" created, a negative electron space charge builds up and lowers the field on the cathode surface. That is why we get only a small number of "hot–

spots". The "hot-spots" creation is a process which depends on the high voltage risetime. this was noticed also by Hinshelwood [68] who mentions that the cathode plasma is much more homogeneous for a fast risetime high voltage pulse.

The connection between our measurements, and measurements done on positive ion diodes is not straight foreword. The mechanisms we suggested here for creation and extraction of negative ions should therefore treated cautiously. More work has to be done, especially measurements of the cathode plasma behavior. This plasma is probably responsible for the transverse electrical fields existing in magnetically insulated diodes, and for the high electron leakage current in those diodes. Such measurements would also bring more knowledge to the subject of negative ion creation in this plasma.

Chapter 9 CONCLUSIONS

The work done by us showed that it is possible to produce negative ion beams of a few A/cm^2 from magnetically insulated diodes with divergence of not more than a few tenths milliradians. We were able to produce beams of negative hydrogen ions as well as negative carbon ions, depending upon the cathode used. During the research we developed a prepulsed plasma gun triggered by a light pulse, which was embedded in the cathode shank and was able to withstand the high voltage pulse on the cathode. We were able to control the gun parameters as well as plasma production time.

A few techniques were used for the first time for measuring negative ion beam properties. Negative ion beams were measured for the first time with a Faraday cup. We also used the insulating magnetic field for ion mass spectrometry. This gave us much information about the ion optics in the diode during the high voltage pulse. A computer code was written to simulate ion trajectories and compare them with the measured results.

The next step in this research area could be directed towards negative ion beam propagation studies. The possibility of producing a negative carbon beam looks attractive. It is very easy to produce a clean carbon cathode, so a pure carbon beam can be produced. The problem with negative ion beams is that it is impossible to produce a neutralized beam. A beam of positive ions drags electrons with it. This allows the beam to propagate with lower divergence across larger distances, and even across magnetic field lines. In order to solve this problem an idea used in connection with electron beam propagation can be used here. If a relativistic electron beam of line density N_b is launched on an ionized channel with N_i electrons within the beam radius, the N_i electrons will be expelled from the channel if $N_b > N_i$. If $N_i > N_b$ the number of electrons expelled will be N_b. The beam electrons then see only the field of the ions which focus the beam [79]. The plasma ions can be considered stationary for

the time of the order of an ion plasma oscillation period. A similar process can be applied to study H^- beam propagation. A plasma of density $n \approx 10^{11}$ can be placed in a drift tube through which the beam propagates. The plasma must be excluded from the diode, which can be done by injecting the plasma into the drift tube with a plasma gun. The H^- beam would expel the plasma electrons and be focused by the corresponding positive ions of the plasma. The mean free path for stripping the electrons from H^- ions would be $\lambda \approx (n\sigma)^{-1} \approx 100$m. Collisional scattering and energy loss should also be negligible over distances of up to 10m. The H^- ions are not relativistic so that self-fields do not cancel, but the self–magnetic field is unimportant due to the large mass of H^- and the self–electric field would be neutralized. The motion of the plasma ions cannot be neglected but the effects can be reduced by using a plasma ion that is much heavier than hydrogen.

Presented at BEAMS '88, Karlsruhe, Germany
July 4-7, 1988

H^- ION SOURCE AND HIGH FLUX NEUTRAL BEAMS

H. Lindenbaum, A. Fisher and N. Rostoker
Department of physics, University of California,
Irvine, California 92717

ABSTRACT

Conventional dc sources of H^- are limited to current densities of the order of 50 mA/cm^2 for sources with area larger than a few cm^2. Early work at UCI and more recent work at the Lebedev Institute have shown that pulsed magnetically insulated ion diodes can produce current densities larger by factors of the order 10^2 - 10^4. We studied the production of negative ion beams in the coaxial, racetrack and annular diode geometries. The experiments showed that when using a passive dielectric cathode negative ions are emitted mainly from a few "hot spots" located on the cathode surface. Large beam divergence (up to 300 milliradians) were measured with polyethelene cathodes, caused probably by transverse electric field in the gap due to the inhomogeneouty of the cathode plasma. We have built a TiH_2 plasma gun which produced a homogeneous cathode plasma. Negative ions with intensities of a few A/cm^2 and divergence of a few tens milliradians were produced with this gun. Results with different diode geometries are reported using passive cathodes, and the active plasma gun. Beam mass spectrometry showed that both H^- ions and C^- ions were produced.

1. INTRODUCTION

Power losses in magnetically insulated diodes led to the suggestion, that negative ions, produced in the cathode plasma are responsible for these losses. Preliminary experiments at UCI [1] showed negative ion currents of 10^{-3} times the space charge limited value. At Sandia National Labs., H^- production in magnetically insulated transmission lines (MITL) [2 – 4] was observed. A group at the Lebedev institute in Moscow reported [5 – 9] a series of experiments, in which H^- ion beams with current densities of $200A/cm^2$ and energy of a few hundred Kev were produced. They reported that a high voltage prepulse was necessary to get these high current densities. Independent efforts at at Ecole polytechnique in France [10, 11] and at Tomsk [12] had no success in producing high current densities. Following these experiments, the problem was investigated at UCI [13, 14].

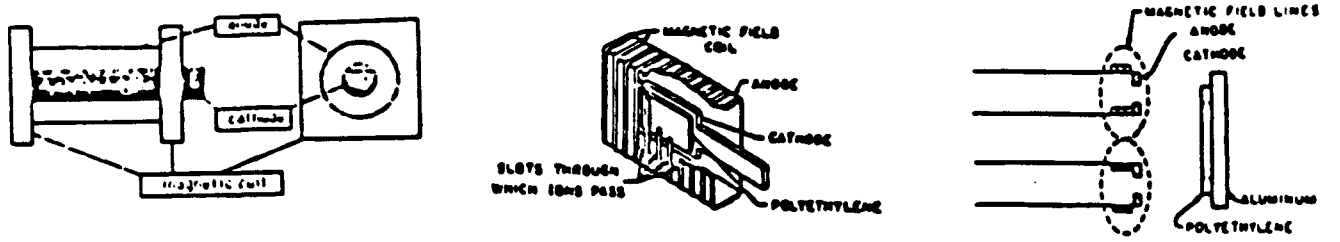

a: Cylindrically symmetric coaxial diode. b: Racetrack diode. c: Annular diode.

Figure 1: Different types of diodes used: (a)Coaxial diode; (b)Racetrack diode; (c)Annular diode.

2. EXPERIMENTS WITH PASSIVE CATHODES

2.1 Experiments with a coaxial diode

When a piece of dielectric insulator is put on the cathode surface, plasma is produced by "explosive emission" caused by the high electric field [15]. The coaxial diode, which we tried first, consisted of an inner cathode made of a conducting cylinder coated with a dielectric material and an outer wire mesh anode (see Figure 1a). The diode was driven by the UCI APEX pulse line of 1 Mv, 7Ω 50 nsec. A 14 kilogauss magnetic field was used for diode insulation. The same magnetic field was used for mass-spectrometry of the particles ejected from the diode (Figure 2). Ions emerging through a hole, were deflected by the insulating magnetic field and traced via a CR-39 track detector. Faraday cup measurements of the beam current were unsuccessful due to the beam divergence in the vertical direction. This diode is very useful for diagnostic purposes, but could not be used to produce an intense beam because of the beam spatial divergence.

With a polyethelene cathode beam intensity ranged between $1-5A/cm^2$ on the cathode surface. The beam consisted of H^- ions as well as C^- ions. Beam divergence in the azimuthal direction reached 0.3 radians at an energy of 100KeV and was about 70 milliradians at an energy of about 500 KeV. CR-39 pinhole pictures of the beam revealed the existence of hot spots on the cathode surface. Negative ion emission from those spots was higher-with a larger horizontal beam divergence. The existence of C^- ions together with H^- ions was verified by combining ion deflection in the magnetic field together with different thickness Mylar films.

The second cathode we tried consisted of bare aluminum. Negative ion currents of about $0.5A/cm^2$ at the cathode surface with a divergence of less then 40 milliradian in the azimuthal direction were produced. Both H^- ions and C^- ions were detected. Beam mass spectrometry showed about 10% H^- ions, about 45% C− ions and about 45% heavier ions (probably C_2^-).

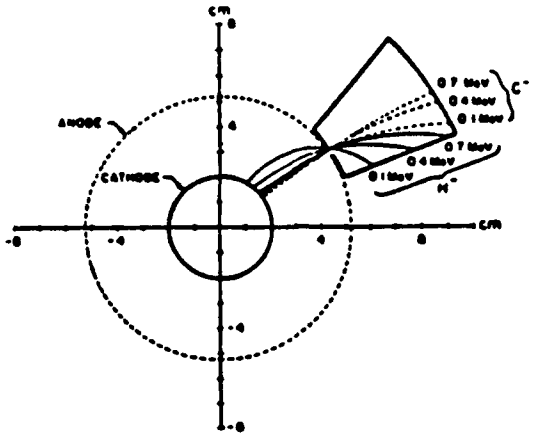

Figure 2: Ion mass spectrometry using the insulating magnetic field in the coaxial diode configuration.

The third cathode we tried was made of graphite which produced currents of 1-3 A/cm^2 with azimuthal beam divergence of 40 milliradians. The beam consisted of C^- ions, a comparable amount of C_2^- ions and about 10% H^- ions. No hot spots wre observed.

2.2 Experiments with a racetrack diode

Various types of cathodes were tried in the racetrack configuration (Figure 1b). Polyethelene covered cathode produced ion currents of $5A/cm^2$. Negative ions were emitted all along the high voltage pulse with a larger amount produced at the low energy part of the pulse (Figure 3a). When we put 2.5μm thick mylar film on the Faraday cup the ions were stripped and the Faraday cup collected a positive current (Figure 3 b). Only H^- ions with energies higher than 200keV could penetrate this thickness of mylar. The beam usually consisted of 70% H^- ions and 30% carbon ions. Hot spots with higher ion emission and larger beam divergence were identified on the cathode's surface. Beam divergence was about 0.1 radians in the azimuthal direction.

Another type of cathode was a paddle covered with carbon brushes. The current density of the brush cathode reached 8-10 A/cm^2. Beam divergence was about 0.3 radians in the azimuthal direction. The current collected by the Faraday cup is shown in Figure 3c. The bulk of the current was made of C^- ions. A small number of H^- ions (about $0.2A/cm^2$) was also measured.

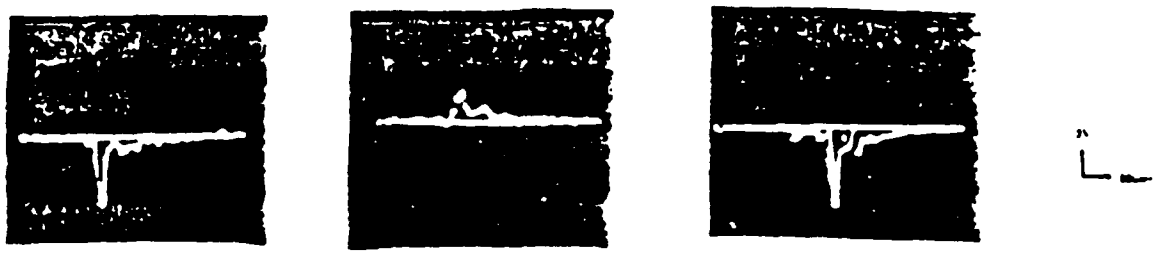

Figure 3: Faraday cup current: (a)with a polyethelene cathode; (b)with a polyethelene cathode and 2.5μ mylar on the cup; (c)with a carbon brushes cathode.

2.3 Experiments with an annular diode

Negative ion current in the annular configuration (Figure 1c) was measured with two Faraday cups placed between the two magnetic coils. With polyethelene cathodes we got ion densities of about 2A/cm^2 with divergence of 150 milliradians. When we used a carbon brushes cathode we got current intensities of 0.5 A/cm^2 with divergence of about 200 milliradians. Negative ions were emitted mainly from a few "hot spots" on the cathode surface.

3. EXPERIMENTS WITH ACTIVE CATHODES

3.1 The prepulsed plasma gun

The work reported by the Lebedev group reported that a prepulse is essential for getting measurable amounts of negative ions. Since in our case the APEX prepulse could not be controlled and the results of the passive cathodes used showed that plasma production is inhomogeneous and of random nature, we built an independent prepulse plasma producing gun. Plasma creation time as well as the density can be controlled. The gun consists of an electrical circuit embedded in the cathode shank, and a plasma producing flashboard. The circuit floats on the APEX high voltage producing an output voltage of a few kilovolts with currents of a few kiloampers.

The plasma gun circuit consists of a high voltage part, triggered by an external flashtube light signal. The high voltage is obtained by a DC to DC converter which is energized by rechargeable batteries and charges a capacitor to 3kV. The capacitor discharges through a spark gap to the primary of a transformer (1:2) the secondary of which is connected to the flashboard.

The flashboard was built from an array of 120 TiH_2 filled arcing groves and can be seen in Figure 4. The plasma gun was usually operated under two different conditions: under low current arc ($I \approx 500A; C = 0.25\mu F$), and under high current ($I \approx 3.2kA; C = 5\mu F$). Plasma parameters were measured in both cases with a double Langmuir probe. Assuming that

this was a pure hydrogen plasma one gets for the low current conditions a density of about $3 \times 10^{11}/cm^3$ with an electron temperature of 3.2eV, and for the high current conditions a density of $2 \times 10^{12}/cm^3$ with an electron temperature of 1.6eV. Plasma gun timing was measured with a fiber optics-photomultiplier system which measured the visible light emitted by the flashboard compared to the machine high voltage pulse timing.

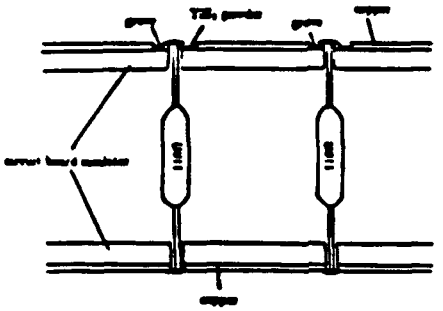

Figure 4: Plasma gun flashboard

3.2 Experiments with a racetrack diode

With a low current plasma gun in a racetrack geometry ion current densities reached were $2A/cm^2$. Maximum current densities were reached for delay times (between plasma gun and machine firing) of 1-2μsec and then decreased slowly as the delay became larger. Beam divergence was about 100 milliradians for a delay of 1.0μsec.

Under high flashboard arc current conditions negative ion beam intensities were too low to be measured with a Faraday cup. The behavior is probably due to the fact that negative ions cannot exist in a plasma with a too high density. We then put a 30% transparent screen in front of the plasma gun. Ion current density measured was $0.5A/cm^2$. Beam divergence in the azimuthal direction was in this case only about 10 milliradian when delay was 1.0 μsec. With a delay of 2.5 μsec the beam divergence grew up to 60 milliradians.

3.3 Experiments with an annular diode

With a low flashboard gun current in an annular diode geometry we got negative ion current densities of about $6A/cm^2$ with a total current of $\approx$ 1000A and beam divergence of 150 milliradians. The results had a good repeatability. Under high flashboaed current condition currents of about $3A/cm^2$ and divergence of 250 milliradians were observed. With a fine screen in front of the gun the current dropped to about $2A/cm^2$ with a divergence of 100 milliradians. No ions were measured with the Faraday cup for delay times smaller then 1μsec. Maximum current intensities were reached for delay times of 1-2μsec and then dropped slowly.

4. DISCUSSION

The results of measurements done on different diode geometries indicate that with passive cathodes negative ions are emitted from a few hot spots on the cathode surface. Beam divergence in these cases was large due probably to transverse electric field caused by the inhomogeneous cathode plasma. The same phenomena was observed in positive ion diodes in regards to electron emission [16]. This problem causes severe ion deflection and diode closure in any high voltage diode. The plasma gun we built works on the high voltage electrode and enables one to produce a homogeneous plasma and control it's production time and parameters. Perhaps the most important result we got we the gun, is that the experimental data is quite reproducible, unlike the case of the passive cathode.

Negative ions are probably produced by neutrals emitted from hot spots on the cathode surface. These neutrals with collide with electrons in the negative electron charge layer. Since the electric field penetrates this layer[17]–all negative ions are extracted and accelerated. negative ion destruction by collision with other particles does not occur.

9. REFERENCES

1) A. Fisher and N. Rostoker,*Bull. Am. Phys. Soc.*, 21, 1097 (1976).
2) J. P. Van Devender, R. W. Stinnet and R. J. Anderson,*Appl. Phys. Lett.* ,38, 229 (1981).
3) R. W. Stinnet and T. Stanley,*J. Appl. Phys.*, 53, 3819 (1982).
4) R. W. Stinnet and M. T. Buttram,*Journ. Fus. Energy*, 4, 253 (1983).
5) R. W. Stinnet, M. A. Palmer et. al.*IEEE Trans. Plasma Sci.*, PS-11, 216, (1983).
6) A. A. Agafonov, A. A. Kolomenski et. al.*Zh. Eksp.Teor. Fiz.*, 84, 2040, (1983).;*Sov. Phys. J. E. T. P.*,57, 1188 (1983).
7) A. A. Kolomenski, A. N. Lebedev et. al.*Proc. of the* 5^{th} *Int. Conf. on High Power Particle Beams*, San-Francisco (1983).**BEAMS 83**
8) A. A. Kolomenski, I. I. Logachev et. al.*Proc. of the* 2^{nd} *Euoropean Workshop on Production of Light Negative Ions*, Ecole Polytechnique,France (1986).
9) A. A. kolomenski, I. I. logachev et. al. 6^{th} *Int. Conf. on High Power Particle Beams*, Kobe (1986).**(BEAMS 86)**
10) S. Moustaises, H. J. Doucet et. al. 6^{th} Int. Conf. on High Power Particle Beams,Kobe (1986).**(BEAMS 86)**
11) H. Doucet, 4^{th} *Int. Symp. on Production and Neutralization of Negative ions and Beams*, Brookhaven, N.Y. (1986).
12)V.M. Bistritski, Ya. E. Matrienke et.al.6^{th} *Int. Conf. on High Power Particle beams*, Kobe (1986).**(BEAMS 86)**
13) A. Fisher, H. Lindenbaum and N. Rostoker, 6^{th} *Int. Conf. on High Power Particle beams*, Kobe (1986).**(BEAMS 86)**
14) A. Fisher, H. Lindenbaum and N. Rostoker, *Int. Soc. for Optical Engineers SPIE, Innovative Science and Technology Symposium, Los–Angeles*, (1988).
15)S. P. Bugaev, E. A. Litvinov et. al. ,*Sov. Phys. - USP*, 18, 551, (1975)
16)Y. Maron and C. Litwin, *Phys. Fluids*, 30, 1526(1987).
17)Y. Maron, M. D. Coleman, D. A. Hammer and H. S. Peng, *Phys. Rev. A*, 36, 2818(1987).

SPIE '88, Los Angeles, CA, January 10-15, 1988

H^- Ion Source and High Flux Neutral Beams

A. Fisher, H. Lindenbaum and N. Rostoker

University of California, Department of Physics
Irvine, California 92717

and

C. E. Wiswall, S. L. Cartier and J. C. Leader

McDonnell Douglas Corporation, St. Louis, MO 63166

ABSTRACT

Conventional dc sources of H^- are limited to current densities of the order of 50 mA/cm^2 for sources with area larger than a few cm^2. Early work at UCI and more recent work at the Lebedev Institute have shown that pulsed magnetically insulated ion diodes can produce current densities larger by factors of the order 10^2 - 10^4. The large current density and space charge required considerable development of diagnostics for reliable measurements of current density; the methods involve a biased Faraday cup, Etch pit counting on CR-39 film, and nuclear reactions. The diagnostic development was done mainly with a coaxial diode because most of the previous data, particularly from the Lebedev Institute was obtained for this diode design. Since this diode is not suitable for applications, several other types of magnetically insulated diodes have been developed and studied. For example, the annular and race-track diodes are suitable for an ion gun.

High current densities of H^- are obtained only when the cathode plasma is at suitable density and temperature. In previous experiments the plasma was produced by flashover of a dielectric surface driven by the pulse line prepulse. The H^- current density was quite sensitive to the magnitude and duration of the prepulse. The prepulse is a property of the machine design about which there is limited control in existing machines. We therefore developed a flash-board plasma source that is placed inside the cathode shank of the APEX generator and can be controlled independently of the pulse line. This paper will present the most recent results with this plasma source, and comparisons with the previous prepulse results.

1. INTRODUCTION

A great deal of effort has been put in the last few years in development of intense high energy positive ion beams. Ion-beam sources were built for use in inertial confinement fusion, magnetic confinement fusion and beam propagation studies. Most of these ion sources use magnetically insulated diodes. In these diodes a plasma is produced on the anode's surface and ions are extracted and accelerated by a high voltage pulse to produce a beam. Electrons are prevented from reaching the anode by applying a magnetic field in the high voltage gap, thus creating what is called a "magnetic insulation".

Power losses in magnetically insulated diodes led to the suggestion, which was first made by a group at UCI[1], that negative ions produced in the cathode's plasma are responsible for these losses. Preliminary experiments at UCI[1] showed negative ion currents of 10^{-3} times the space charge limited value. A detailed work followed by a group at Sandia National Labs who studied H^- production in magnetically insulated transmission lines (MITL)[2-4]. These works gave rise to the hope of producing intense beams of H^- ions in high power diodes. Following this approach a group at the Lebedev Institute in Moscow reported[5-9] a series of experiments in a cylindrical symmetric coaxial magnetically insulated diode, in which H^- ion beams with current densities of 200 A/cm^2 and energy of a few hundred keV were produced. They reported that a high voltage prepulse was necessary to get these high current densities. Independent efforts at Ecole Polytechnique in France[10,11] and at Tomsk[12] to reproduce and understand the Lebedev results have had no success in producing high current densities.

2. EXPERIMENTS WITH A COAXIAL DIODE

The first experiments were done on a cylindrically symmetric coaxial diode. The diode consists of an inner cathode made of a conducting cylinder coated with a dielectric material and an outer wire mesh anode (see Fig. 1). The cathode radius was 1/e of the anode radius. In the negative ion configuration the inner cylinder is pulsed negatively and the mesh is at ground potential. The diode was adapted to the UCI APEX pulse line that has a nominal output of 1 MV, 140 kA under matched conditions with a pulse length of 50 nsec.

When a high voltage is applied, a cathode plasma is created by explosive emission caused by the high electric fields.[13] Negative ions are extracted from the plasma, accelerated across the gap and out through the wire mesh. An axial magnetic field of 14 kilogauss prevents the electrons from crossing the gap. The same magnetic field was used for mass-spectrometry of the particles ejected from the diode (see Fig. 1). A box with a 0.5 mm hole in it was placed outside the wire-mesh anode. Ions emerging through the hole, and deflected by the insulating magnetic field were traced via a CR-39 track detector. Electrical measurements of the beam current were unsuccessful due to the beam divergence in the vertical direction. This diode is very useful for diagnostic purposes, but could not be used to produce an intense beam because of the beam's spatial divergence.

The first cathode we used was a thin sheet of polyethelene covering an aluminum rod. Beam intensity ranged between 1-5 A/cm^2 on the cathode surface. The beam consisted of H^- ions as well as C^- ions. Ions with energies ranging from 80 kV which was our lowest detection limit were detected. Beam divergence in the azimuthal direction reached 0.3 radians at an energy of 100 keV and was about 70 milliradians at an energy of about 500 keV. CR-39 pinhole pictures of the beam revealed the existence of hot spots on the cathode surface. Negative ion emission from those spots was higher with a larger horizontal beam divergence. The existence of C^- ions together with H^- ions was verified by combining ion deflection in the magnetic field together with different thickness Mylar films.

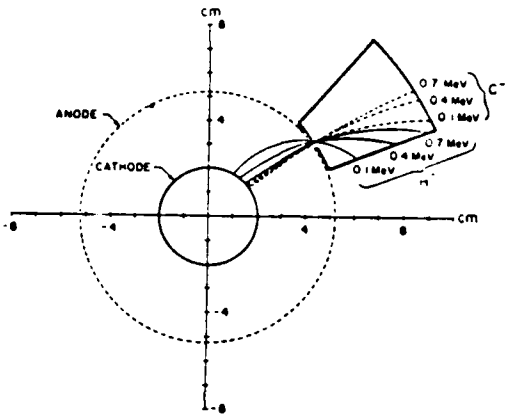

Figure 1. Coaxial diode with insulating magnetic field mass spectrometry

The second cathode we tried consisted of bare aluminum. In this cathode the role of absorbed gases on the metal surface was investigated. The cathode surface was sanded and washed thoroughly with propanol before being installed in the machine. Negative ion currents of about 0.5 A/cm^2 at the cathode surface with a divergence of less than 40 milliradians in the azimuthal direction were produced. Both H^- ions and C^- ions were detected. Tracks on a CR-39 film show that the plasma is very homogeneous in this case.

The third cathode we tried was made of graphite and produced currents of 1-3 A/cm^2 with azimuthal beam divergence of 40 milliradians. The beam consisted of C^- ions, a comparable amount of C_2^- ions and about 10% H^- ions. A carbon cathode can produce very clean beams with high intensity and low divergence.

3. EXPERIMENTS WITH A RACETRACK DIODE

The racetrack diode (see Fig. 2a) has a paddle shape and is located at the middle of a wire mesh box which serves as the anode. The same box is used to hold the magnetic field coil turns. This type of diode can produce a parallel ion beam if there were no insulating magnetic field. The Faraday cup is about 20 cm from the cathode. The voltage pulse is not constant and with the insulating magnetic field we usually get a beam with a very narrow divergence in the azimuthal direction, but with a large divergence in the vertical direction. Beam intensity measurements were done with a Faraday cup. Time of flight measurements with the Faraday cup revealed current peaks of H^-, C^-, and C_2^- ions. Current measurements were confirmed with etch pit counting on CR-39 film. Ion species identification was confirmed by measuring the ion current with a Faraday cup covered with Mylar films of different thickness.

Various types of cathodes were tried in this configuration. A polyethelene covered cathode produced ion currents of 5 A/cm^2. The beam usually consisted of 70% H^- ions and 30% carbon ions. Hot spots with higher ion emission and larger beam divergence were identified on the cathode's surface. Beam divergence was about 0.1 radians in the azimuthal direction.

Another type of cathode was a paddle covered with carbon brushes. The current density of the brush cathode reached 8-10 A/cm^2. Beam divergence was about 0.3 radians in the azimuthal direction. The bulk of the current was made of C^- and C_2^- with intensities of about 4-5 A/cm^2 of each species. A small number of H^- ions (about 0.2 A/cm^2) was measured.

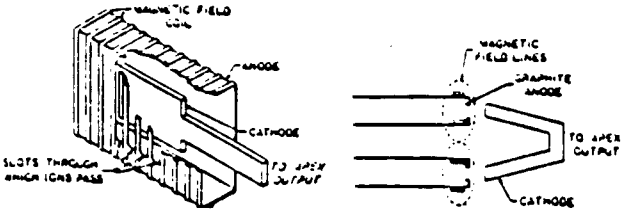

2a - Paddle type cathode 2b - Annular cathode

Figure 2. Magnetically insulated H^- cathodes

4. EXPERIMENTS WITH A PREPULSED FLASHOVER CATHODE

The highest negative ion currents were produced by a group at the Lebedev Institute. They reported that a high voltage prepulse was necessary to produce currents of 200 A/cm^2. This prepulse is caused by the capacitive coupling of the output switch. This prepulse was about 25% of the main pulse and a duration of 2 μsec. In their experiment the prepulse consists of a negative part and a positive part. The machine used in this experiment (APEX) has a prepulse of about 2% when using a resistive suppressor. With this prepulse we were not able to measure any negative ions. When we disconnected this resistor we got a prepulse of about 10% and only then were we able to make the measurements reported above. It is clear that a plasma has to be formed in the machine before the main pulse is applied. To investigate this we have built a prepulse plasma generator which produces plasma in the high voltage gap (see Fig. 3). The generator consists of a high voltage circuit embedded in the cathode shank and a plasma generating flashboard. The circuit has a few low voltage batteries connected to a dc to dc converter. The output of the converter is about 3 kV and it charges a high voltage capacitor. The capacitor is discharged through a krytron switch and a small low inductance transformer into the flashboard. The krytron is triggered by a photodiode which is triggered by an external light pulse produced by a flashtube. The flashboard consists of 120 grooves each filled with TiH_2 and connected through a 110 Ω resistor to the output of the circuit transformer. This resistor limits the current through each groove creating a more homogeneous plasma. A 60% transparent stainless steel wire mesh was put in front of the gun. With the wire mesh we got a much more homogeneous plasma and prevented arcing caused by the high density plasma in the gap. The timing of the plasma production was measured with a light collecting fiber optics and a photomultiplier system. Current densities were measured with a Faraday cup and checked with etch pit counting. With this plasma gun we will be able to control the plasma production time and its properties.

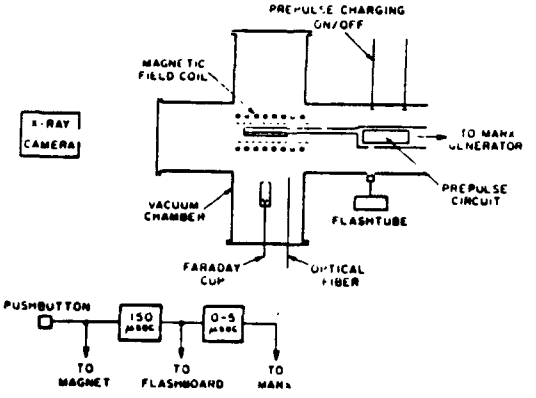

Figure 3. Prepulsed plasma gun configuration

Current densities reached were 2 A/cm^2. Beam divergence was a function of the delay between plasma creation and main voltage pulse. With a delay of about 1.0 μsec the beam divergence in the azimuthal direction was about 10 milliradians. With a delay of 2.5 μsec the beam divergence grew up to 60 milliradians. Without the wire mesh beam divergence was about 80 milliradians for a delay of about 1 μsec. Beam intensity was larger for small flashboard arc current. Beam intensities of 2 A/cm^2 were measured when current through each flashboard point was about 5 A. With arc current of 250 A beam intensities were too low to be measured with a Faraday cup. The behavior is probably due to the fact that negative ions

cannot exist in a plasma with a too high density.

The work with the prepulsed plasma gun has just begun. In the future we will investigate the production of negative ions at different prepulsed plasma temperature and density condition. We will try and measure the effects of a negative and positive prepulse which create high currents at the Lebedev Institute. We intend to see the effects of a negative prepulse by bombarding the cathode with electrons. The electrons will be produced by applying a negative pulse to carbon brushes close to the grounded wire-mesh. We also will study the same problem with an annular diode geometry (see Fig. 2b). This diode configuration gave the best results in positive ion experiments at Irvine.

5. DIODE PHYSICS EXPERIMENTS

The mechanism which yields a high production of H^- from a hydrogen plasma is not well understood. A separate investigation was conducted at McDonnell Douglas Corporation on the prepulse discharge itself with a goal of understanding the physical mechanisms involved and improving the H^- yield and emittance. This work centered on the use of a planar surface discharge as the prepulse discharge source. Following the basic design developed by Beverly[15], a diode was designed with a discharge formed across a hydrogen containing dielectric surface, e.g., polyethylene. This type of discharge has several characteristics which make it attractive as an ion source for this application; it produces a large homogenous flash with a shockwave of ablated material ejected perpendicular to the dielectric surface while holding the plasma against the surface. These are important for optimizing beam emittance and electron density near the surface.

Although the surface discharges used by Beverly were typically at atmospheric pressures or above, the guidelines developed for achieving uniform discharges under those conditions were used as the basis for designing a H^- source operating at relatively low gas pressures, below 10^{-4} Pa. The low pressures are desired in these tests to reduce the interference effects from the background gases as well as from surface contaminants. At such low pressures, however, the formation of a uniform discharge becomes difficult. Beverly specifies several criteria which affect the flash uniformity: the peak applied voltage, the rate of the initial voltage rise, the specific capacitance of the substrate, the background gas, and the type of substrate used. The use of a conducting backplane under the dielectric material, a voltage rise rate of 10^{10} V/s and the geometry of the electrodes were fixed by design, while the degree of overvoltage and discharge energy were left as test parameters.

A vacuum test chamber was prepared for these experiments using a 6-way glass cross to mount the source and provide access for diagnostic probes (Fig. 4). The cross is connected to a stainless steel, 150 mm dia., vacuum system which incorporates a quadrupole mass spectrometer. The system achieves a base pressure of 10^{-5} Pa with the largest mass spectrometer signal being water. The discharge diode is mounted on the end of a high voltage coaxial feed through (Fig. 5, side view) which can be rotated or translated to position the source. The discharge circuit consists of a capacitor bank with with a capacitance of 0.3 μF, a triggered sparkgap, and a water-$CuSO_4$ load resistor adjusted to give a single, noninverting discharge pulse. The metal backplane on the diode provides a distributed peaking capacitance of approximately 500 pf. As yet, the coils for the magnetic insulation have not been installed.

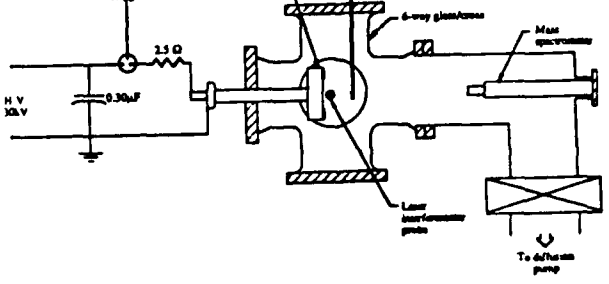

Figure 4. Experimental configuration for surface flash studies

Several electrode configurations were examined with the goal of achieving the best flash uniformity. These are shown in Fig. 5. In the first (Fig. 5a), two brass Rogowski electrodes separated by 5 cm were used to form a 5 cm wide discharge on a polyethylene substrate 0.16 cm thick. In Fig. 5b, the electrode separation is reduced to 2 cm. In Fig. 5c, a brass wire screen, (5.4 x 5.4 lines/cm; 0.025 cm dia. wire), was embedded in the

polyethylene substrate of the electrode configuration of Fig. 5a with just the crosses of the mesh exposed. This screen is intended to reduce surface electric fields and provide an electrode for H^- extraction. Fig. 5d shows pointed electrodes separated by 2 cm on polypropylene 0.32 cm thick.

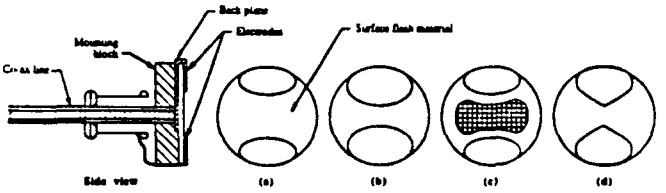

Figure 5. Surface flash electrode configurations and cut-away drawing of diode assembly. (a) Rogowski electrodes with 5 cm spacing, (b) Rogowski electrodes with 2 cm spacing, (c) brass wire screen embedded in polyethylene, (d) pointed electrodes.

Identification of ejected species is accomplished by optical and mass spectroscopy. The emission spectra is obtained by imaging a volume of the discharge plasma into a 1-meter Hilger-Engis monochromator which has been fitted with a Polaroid film holder to obtain time-integrated spectra. At low pressures, the emission spectrum is low in intensity and appears as a line spectrum with most of the emission at wavelengths less than 470 nm. In the spectra obtained by looking directly at discharges on hydrocarbon containing polymers, C II and H I emission lines are expected to be the most prominent. In this case, the line width of the Hα line (656.3 nm) can be used to obtain an electron density determination as it is the most intense line in the spectrum.[15] The series of C II line intensities can also be used by plotting them to determine the plasma electron temperature. The spectra obtained to date indicate the presence of copper from the brass electrodes but are not of sufficient quality to determine the derived quantities.

A mass spectrometer is used to determine the end products resulting from the discharge as well as changes in the background gases. The discharge pulse disrupts the mass spectrometer electronics enough that data cannot be obtained during a discharge. Therefore, the mass data is obtained by closing off the chamber and recording the spectra at a known gas pressure shortly after a discharge. The background spectra are obtained in the same way by recording the spectra when the chamber reaches the same pressure.

Direct measurements of ions emitted from the discharge were made using an apertured ion-collecting probe. This probe was constructed by exposing a short length of the center wire of a rigid coaxial conductor and wrapping tantalum foil around the wire to form a collector. This was enclosed in a metal shield cup, 4 mm in diameter, and the entire assembly was covered with Teflon shrink tubing to isolate the exposed grounded surfaces. A small orifice in the shield cup, 0.36 mm, through which the ions entered, made the probe directional. The ions were detected using a transformer to monitor the current drawn to the collector which was biased sufficiently negative, -45 V, to collect only positive ions. Also, the probe could be moved to provide spatial measurements of the discharge.

The formation of H^- is assumed to involve electron dissociative attachment with a hydrogen compound; although, surface effects may be an important factor. To understand the mechanisms involved,it is necessary to measure the electron plasma density near the surface with the magnetic insulation in place. To do this, we have constructed a laser interferometer which can probe the discharge volume to within a few millimeters of the diode surface without perturbing the discharge. A schematic of the system is shown in Fig. 6. A single mode He:Ne laser operating at 682.8 nm is used as the probe. This is a relatively short wavelength for electron density measurements, but it has the advantages of making the interferometer less sensitive to neutral particle densities and independent of plasma resonances even in the presence of kilogauss magnetic fields. A Mach-Zehnder interferometer was constructed using an Invar rod frame which can be moved relative to the vacuum chamber. A piezoelectric-driven cell containing mineral oil is added to the reference leg to allow a degree of compensation. Rather than using a fringe stabilization technique to remove mechanical vibration effects, a zero-crossing circuit is used to trigger the discharge at a time when the signal sensitivity is greatest. Since the laser signals are essentially constant for the microsecond time scales of the discharge, the problems associated with vibrations are eliminated.

The experimental system has been evaluated without magnetic insulation by measurements of electron density with the laser interferometer and positive ions with the mass spectrometer and ion collection probe. Observations to date have shown that although each electrode

configuration in Fig. 5 produced very uniform discharges at background gas pressures exceeding 0.1 Pa, discrete arcs formed across the surfaces at lower pressures. Over the mesh in Fig. 5c, however, and over an area between the electrodes in Fig. 5d of about 2 cm wide there was good uniformity.

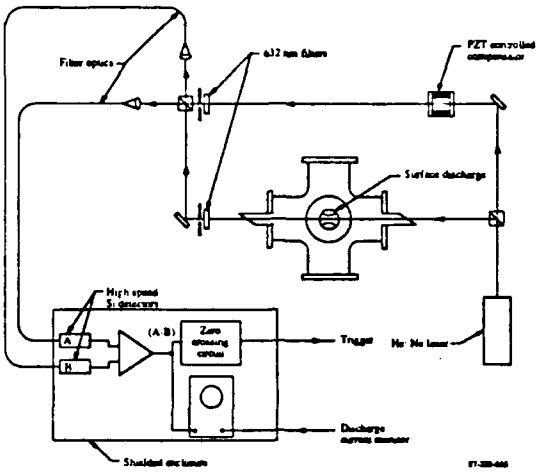

Figure 6. Mach-Zehnder interferometer system used for electron plasma density measurements

The mass spectrometer measurements confirm that following each discharge H^+, H_2^+, C^+, CH^+, CH_2^+, and higher hydrocarbons are produced in large quantities and that there is almost a complete loss of the background O_2 along with a reduction in H_2O. Polypropylene was found to evolve more H_2 than polyethylene and discharged more consistently. Also, the use of fluorinated solids for insulators and surface mounts should be avoided since evolved fluorine acts as an additional electron loss mechanism.

The integrated electron density inferred from multiple interferometer signals is shown in Fig. 7 as a function of distance from the surface for the electrode configuration of Fig. 5d. The rapid decrease in electron density implies a fairly rapid loss of electrons over the first few centimeters.

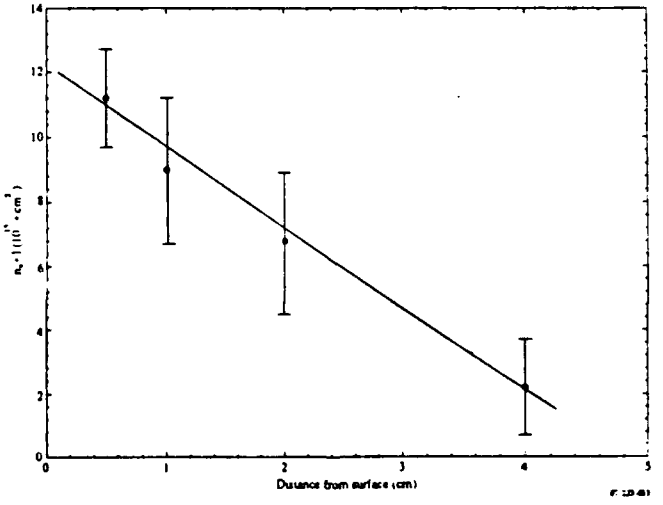

Figure 7. Line integrated electron density, $n_e \cdot l$, determined by laser interferometry as a function of the distance of the laser beam from a polypropylene discharge surface. The path length l = 2 cm.

The planar surface discharge appears promising as a large area, high emittance source of H^- ions based on the observed yield of hydrogen and on the measurements of the plasma density. Of course, the spatial distribution of the plasma will be greatly affected with the addition of a magnetic field, although this should actually lead to an increase in the plasma density found near the surface. The plasma density should then be high enough,

however, for a favorable production of H^- ions. In addition, the probe measurements indicate a small angle of divergence, although more specific measurements of the emittance will need to be made once H^- ions are extracted from a magnetically insulated diode. Polypropylene appears to be a better source material than polyethylene in terms of flash uniformity and H-atom production. It is no worse in terms of charring and channeling. Further comparison of plastic dielectric source materials and perhaps metal hydrides still needs to be done before a material is chosen for use.

6. BEAM PROPAGATION

If a relativistic electron beam of line density N_b is launched on an ionized channel with N_i electrons within the beam radius, the N_i electrons will be expelled from the channel if $N_b > N_i$. If $N_i > N_b$ the number of electrons expelled will be N_b. The beam electrons then see only the field of the ions which focus the beam.[16] The plasma ions can be considered stationary for a time of the order of an ion plasma oscillation period.[11] A similar process will be studied for H^- beam propagation. A plasma of density $n \sim 10^{11}$ cm^{-3} will be placed in a drift tube trough which the beam propagates. The plasma must be excluded from the diode which can be done by injecting the plasma into the drift tube with a plasma gun. The H^- beam would expel the plasma electrons and be focused by the corresponding positive ions of the plasma. The mean free path for stripping the electrons from H^- would be $\lambda = (n\sigma)^{-1} = 100$ m. Collisional scattering and energy loss should also be negligible over distances of up to 10 m. The H^- ions are not relativistic so that the self-fields do not cancel, but the self-magnetic field is unimportant due to the large mass of H^- and the self-electric field would be neutralized. The motion of the plasma ions cannot be neglected but the effects can be reduced by using a plasma ion that is much heavier than H^-.

7. DISCUSSION

We conclude that it is possible to develop magnetically insulated negative ion diodes. The plasma source from which H^- is extracted is very sensitive to prepulse which means that the plasma temperature and density must be controlled in order to achieve optimum results. The prepulsed flashboard described enabled us to investigate this problem by installing it in a magnetically insulated diode and making direct measurements of H^-,C^- extraction.

Since the formation and extraction of negative ions is not well understood a basic diode physics study has been initiated at M.D.C. The experimental systems and preliminary results are reported.

Negative ion beam diodes have a few advantages. A negative ion beam can easily be converted into a neutral beam. It is also easier to get a beam which consists of only one atomic species. In addition to producing intense H^- beams of 1-10 A/cm^2 we have shown that one can get a clean high intensity beam of carbon. It is very easy to make a carbon cathode - and the ion is heavy enough to be less sensitive to deflection by the insulating magnetic field.

Beams of positive ions drag electrons with them which neutralize the beam and enables it to propagate with a very small spatial divergence. A method to propagate intense negative ion beams has been proposed. If the problem of negative ion beam propagation can be solved-intense negative ion beams should find many applications in fusion research, as well as in directed energy beam systems.

8. ACKNOWLEDGEMENTS

This work was supported by the Office of Naval Research.

9. REFERENCES

1. A. Fisher and N. Rostoker, Bull. Am. Phys. Soc., 21, 1097 (1976).
2. J. P. VanDevender, R. W. Stinnet and R. J. Anderson, Appl. Phys. Lett. 38, 229 (1981).
3. R. W. Stinnet and T. Stanley, J. Appl. Phys. 53, 3819 (1982).
4. R. W. Stinnet and M. T. Buttram, Journ. Fus. Energy 4, 253 (1983).
5. R. W. Stinnet, M. A. Palmer, et al., IEEE Trans. Plasma Sci. PS-11, 216 (1983).
6. A. A. Agafonov, A. A. Kolomenski et al., Zh. Eksp. Teor. Fiz. 84, 2040 (1983); Sov. Phys J.E.T.P. 57, 1188 (1983).
7. A. A. Kolomenski, A. N. Lebedev et al., Proc. of the 5th Int. Conf. on High Power Particle Beams, San Francisco (BEAMS '83), (1983).
8. A. A. Kolomenski, I. I. Logachev et al., Proc. of the 2nd European Workshop on Production of Light Negative Ions, Ecole Polytechnique, France (1986).
9. A. A. Kolomenski, I. I. Logachev et al., 6th Int. Conf. on High Power Particle Beams, Kobe (BEAMS '86), (1986).
10. S. Moustaises, H. J. Doucet et al., 6th Int. Conf. on High Power Particle Beams, Kobe (BEAMS '86), (1986).

11. H. Doucet, 4th Int. Symp. on Production and Neutralization of Negative Ions and Beams, Brookhaven, N.Y. (1986).
12. V. M. Bistritski, Ya. E. Matrienke et al., 6th Int. Conf. on High Power Particle Beams, Kobe (BEAMS '86), (1986).
13. S. P. Bugaev, E. A. Litvinov et al., Sov. Phys. - USP 18, 551 (1975).
14. A. Fisher, H. Lindenbaum and N. Rostoker, 6th Int. Conf. on High Power Particle Beams, Kobe (BEAMS '86), (1986).
15. R. E. Beverly III, "Electrical, Gasdynamic, and Radiative Properties of Planar Surface Discharges," J. Appl. Phys. 60(1), (1 July 1986).
16. K. W. Struve, E. J. Lauer and F. W. Chambers, Proc. of the 5th Int. Conf. on High Power Particle Beams, San Francisco (BEAMS '83), (1983).

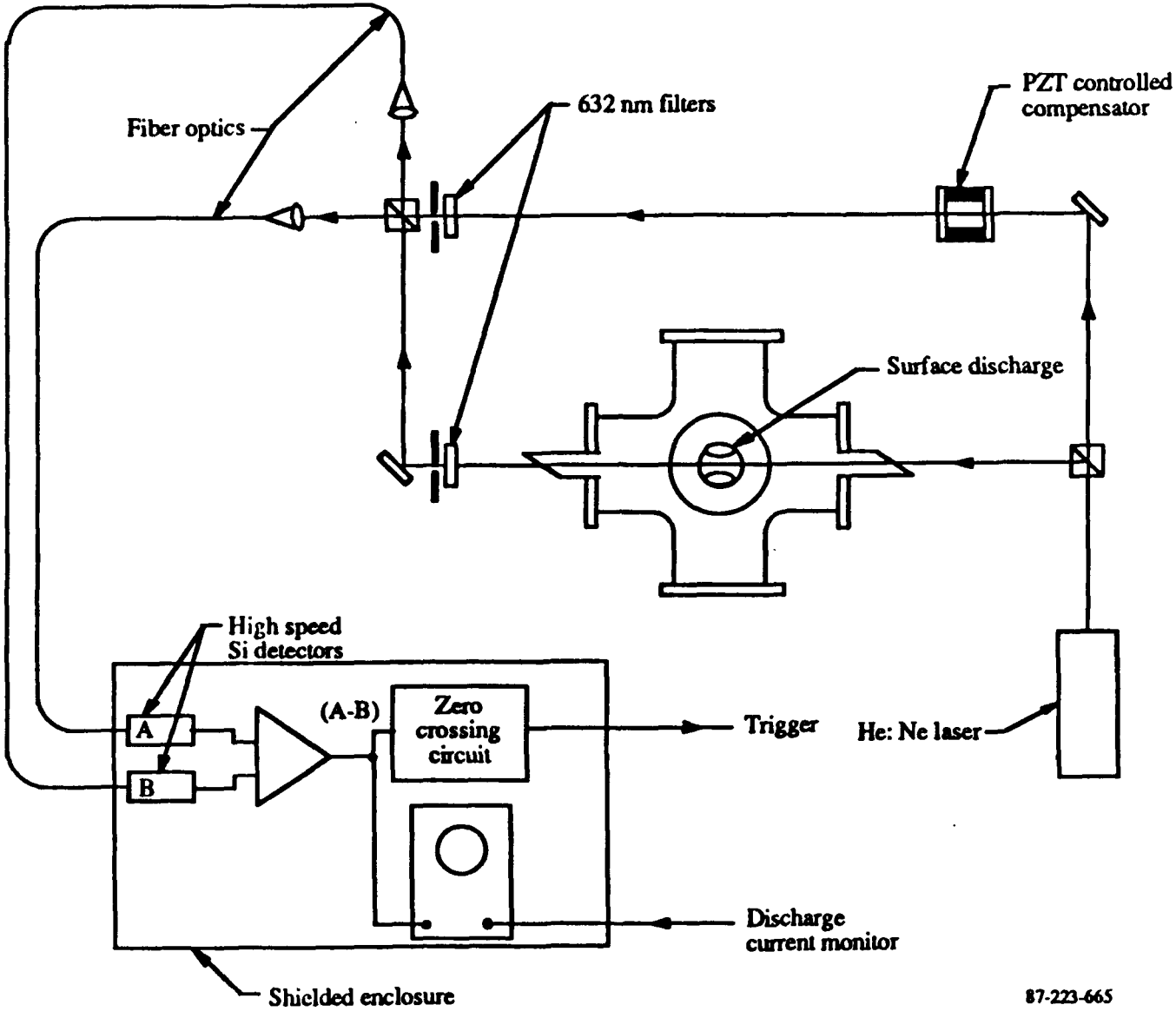
Fiber optics
632 nm filters
PZT controlled compensator
Surface discharge
High speed Si detectors
A
B
(A-B)
Zero crossing circuit
Trigger
He: Ne laser
Discharge current monitor
Shielded enclosure
87-223-665

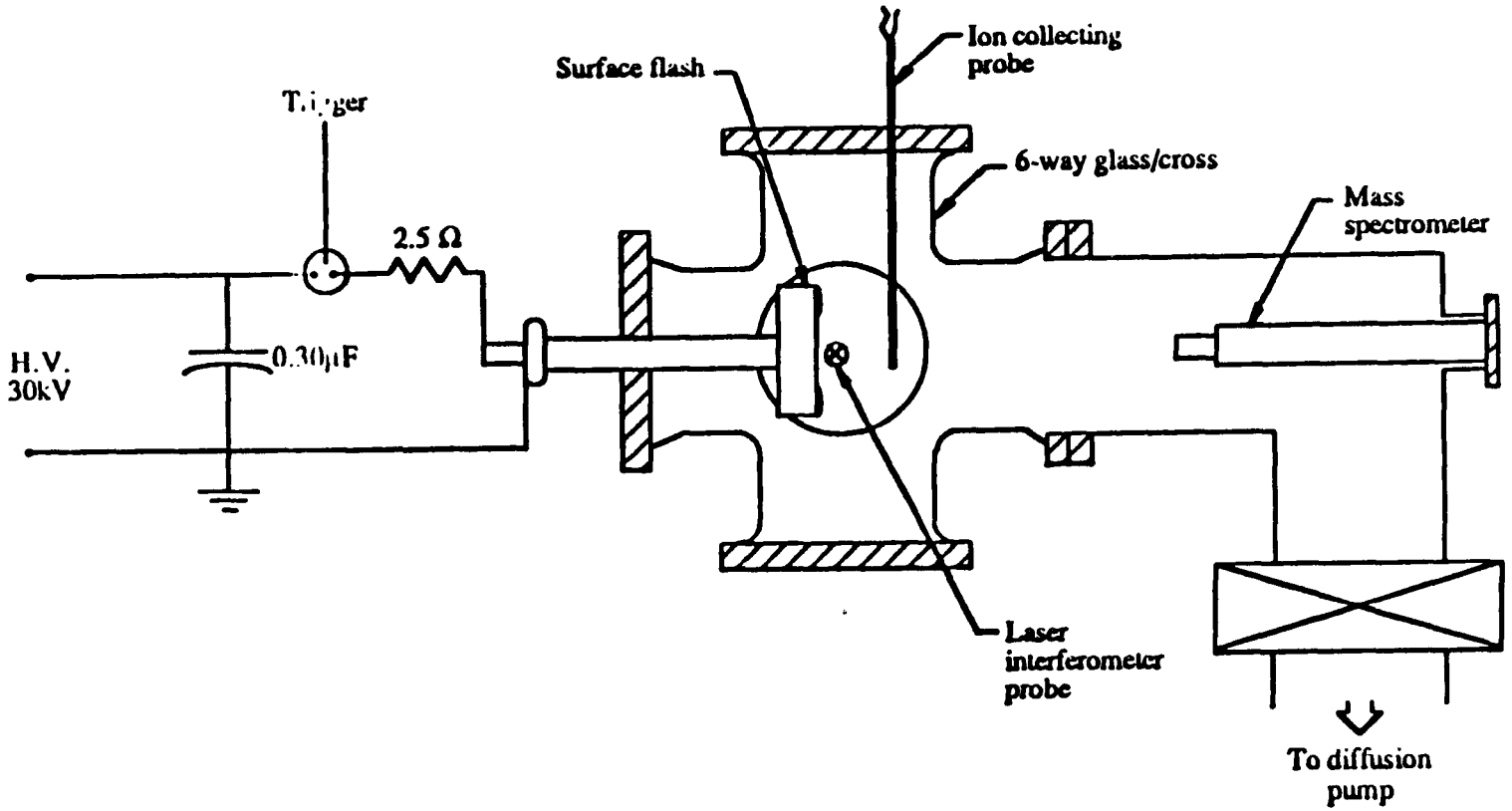
Surface flash
Ion collecting probe
Trigger
6-way glass/cross
Mass spectrometer
2.5 Ω
H.V. 30kV
0.30μF
Laser interferometer probe
To diffusion pump
87-223-664

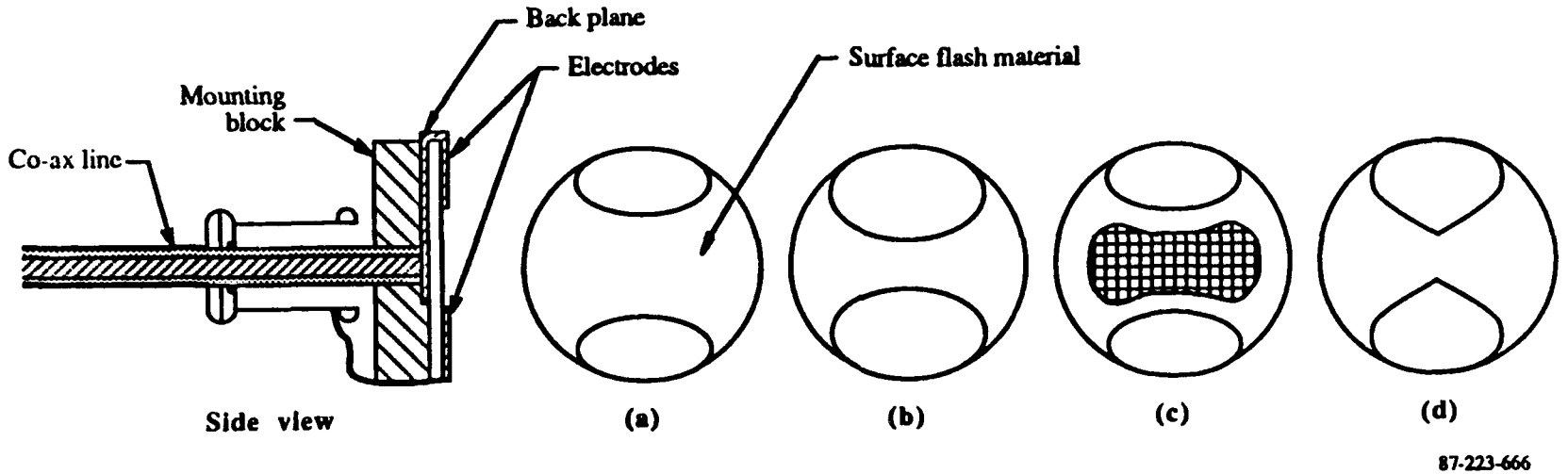
Back plane
Electrodes
Surface flash material
Mounting block
Co-ax line
Side view
(a)
(b)
(c)
(d)
87-223-666

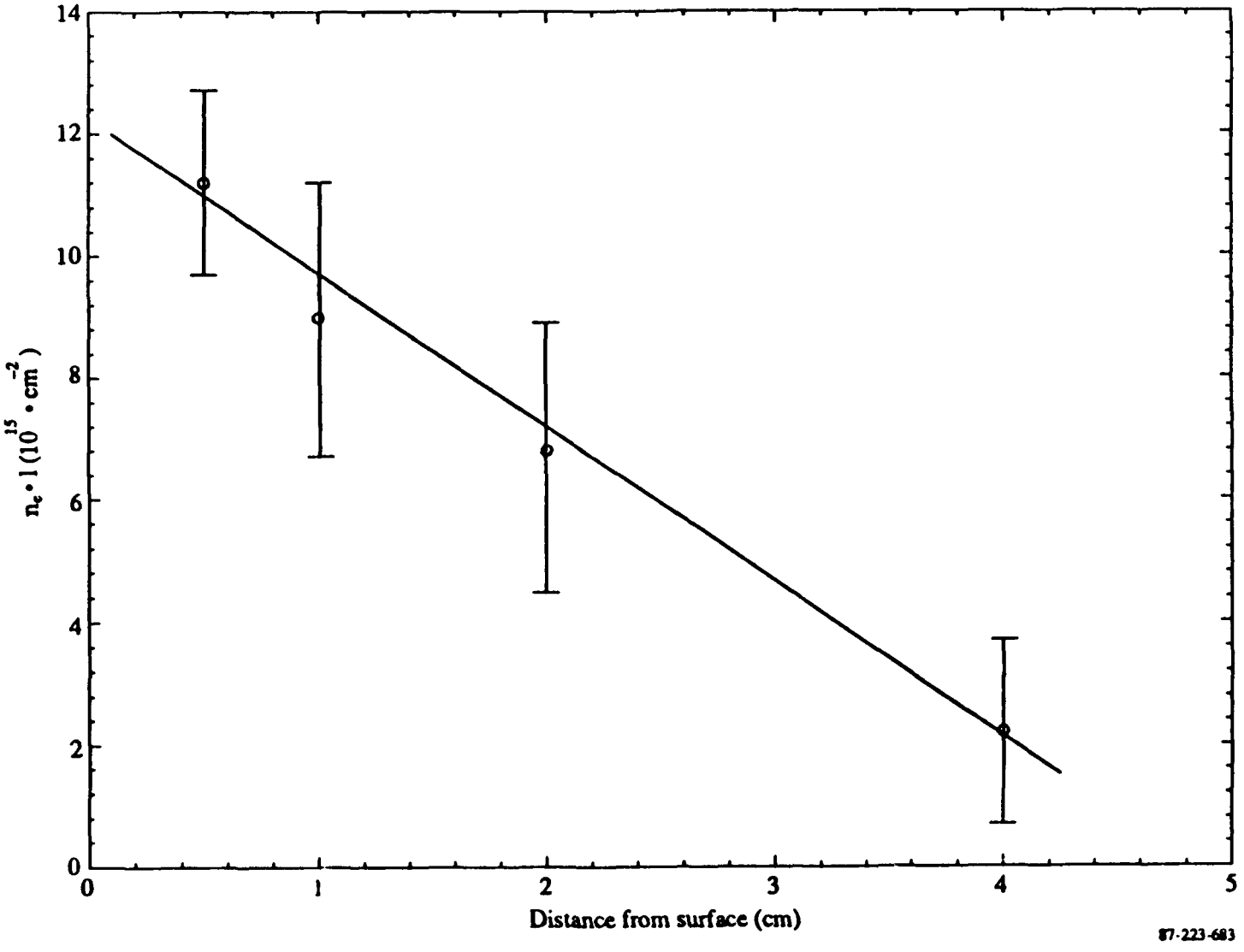
14
12
10
8
6
4
2
0
0
1
2
3
4
5
$n_e \cdot l\,(10^{15} \cdot cm^{-2})$
Distance from surface (cm)
87-223-683

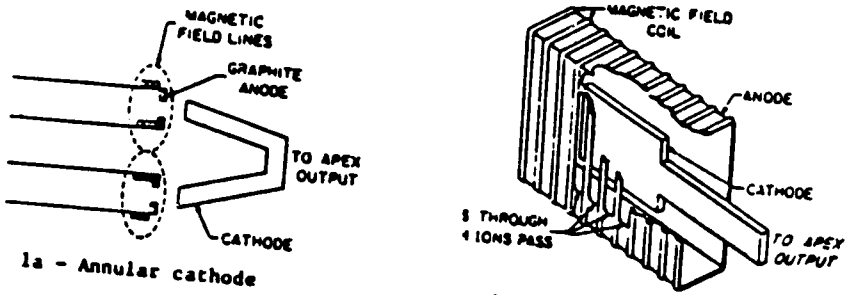

1a - Annular cathode

1b - Paddle type cathode

Fig. 1. Magnetically insulated H^- cathodes

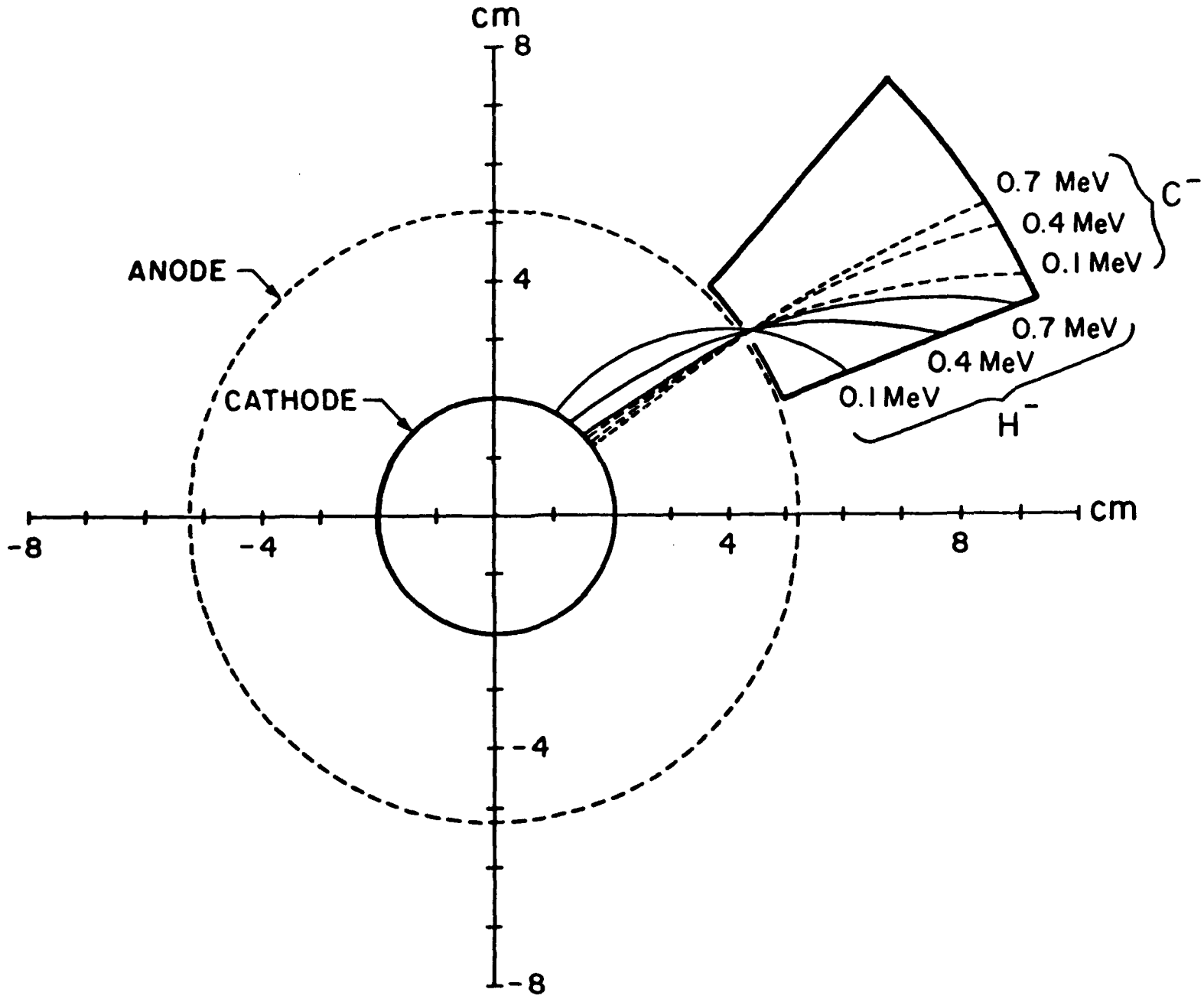
cm
8
4
-4
-8
-8
-4
4
8
cm
ANODE
CATHODE
0.7 MeV
0.4 MeV
0.1 MeV
C⁻
0.7 MeV
0.4 MeV
0.1 MeV
H⁻

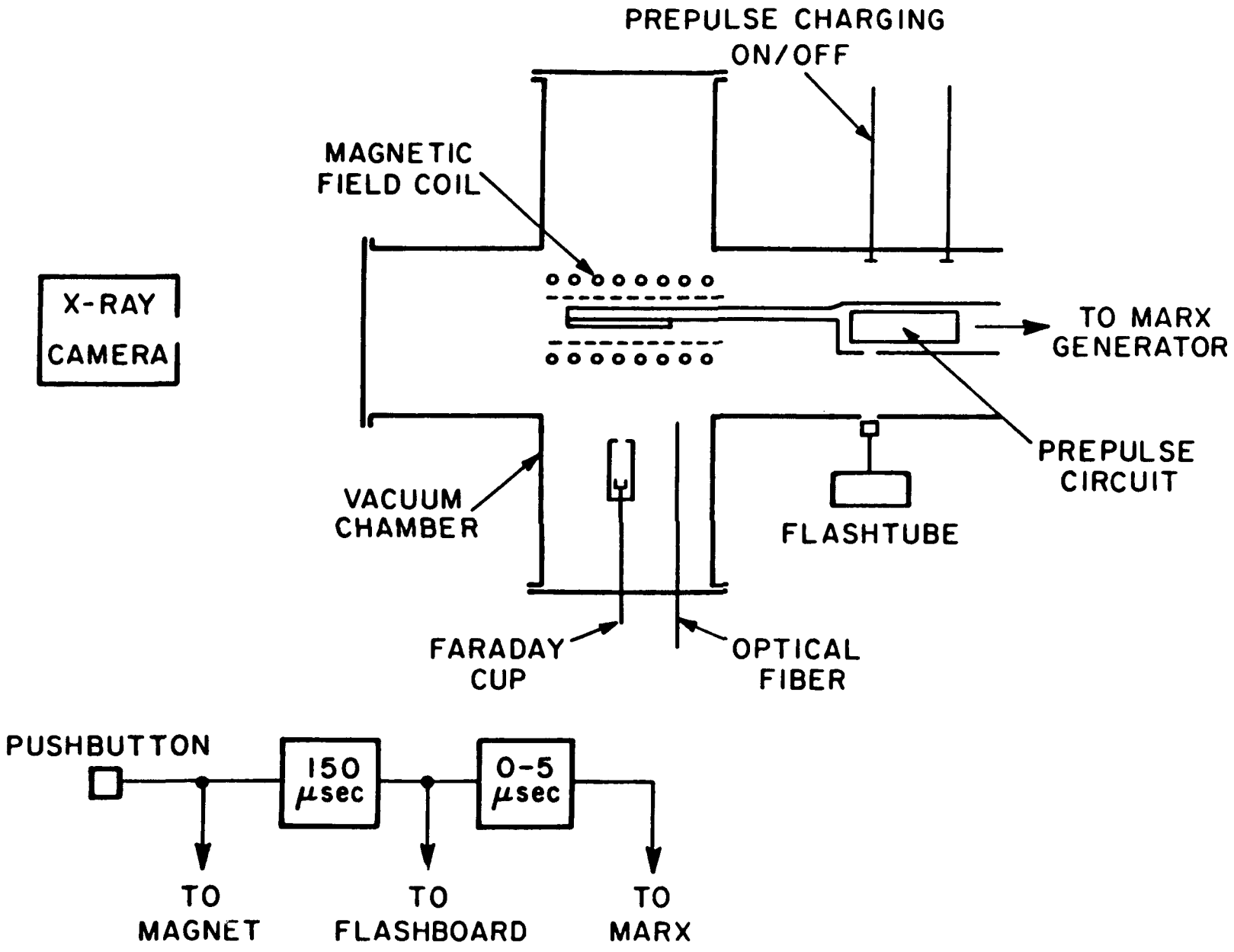
PREPULSE CHARGING
ON/OFF
MAGNETIC
FIELD COIL
X-RAY
CAMERA
TO MARX
GENERATOR
PREPULSE
CIRCUIT
VACUUM
CHAMBER
FLASHTUBE
FARADAY
CUP
OPTICAL
FIBER
PUSHBUTTON
150
μsec
0-5
μsec
TO
MAGNET
TO
FLASHBOARD
TO
MARX

SPIE '89, Los Angeles, California, January 15-20, 1989

H^- Ion Source and High Flux Neutral Beams

A. Fisher, H. Lindenbaum, and N. Rostoker

University of California, Department of Physics
Irvine, California 92717

and

S. L. Cartier and C. E. Wiswall

McDonnell Douglas Corporation, St. Louis, MO 63166

ABSTRACT

Conventional dc sources of H^- are limited to current densities of the order of 50 mA/cm^2 for sources with area larger than a few cm^2. Early work at UCI and more recent work at the Lebedev Institute have shown that pulsed magnetically insulated ion diodes can produce current densities larger by factors of the order 10^2 - 10^4. We studied the production of negative ion beams in the coaxial, racetrack and annular diode geometries. The experiments showed that when using a passive dielectric cathode negative ions are emitted mainly from a few "hot spots" located on the cathode surface. The angular divergence of the beam was about 300 milliradians. We have developed a TiH_2 plasma source that consists of 120 discharges on a flashboard. The resultant cathode plasma is quite homogeneous compared to typical polyethylene passive cathodes. H^- ions with a current density of 6 A/cm^2 and a divergence of 10 milliradians were observed with this source. The total current of H^- ions was about 1 kA. The current density is many orders of magnitude larger than would be expected from a thermal plasma source. A non-equilibrium model is advanced to explain this fact.

1. INTRODUCTION

Power losses in magnetically insulated diodes led to the suggestion that negative ions, produced in the cathode plasma, are responsible for these losses. Preliminary experiments at UCI[1] showed negative ion currents of 10^{-3} times the space charge limited value. At Sandia National Labs, H^- production in magnetically insulated transmission lines (MITL)[2-4] was observed. A group at the Lebedev Institute in Moscow reported[5-9] a series of experiments, in which H^- ion beams with current densities of 200 A/cm^2 and energy of a few hundred keV were produced. They reported that a high voltage prepulse was necessary to get these high current densities. Independent efforts at Ecole Polytechnique in France[10,11] and at Tomsk[12] had no success in producing high current densities. Following these experiments, the problem was investigated at UCI[13,14].

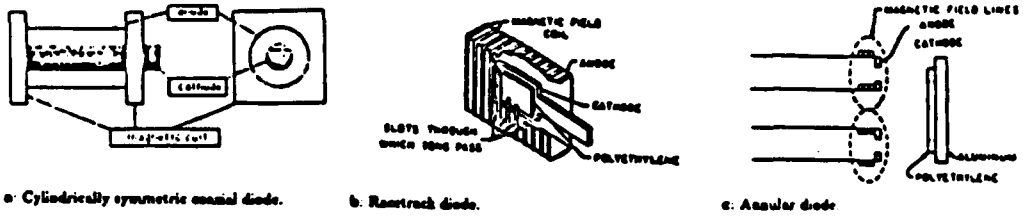

Figure 1. Different types of diodes used: (a) Coaxial diode; (b) Racetrack diode; (c) Annular diode.

2. EXPERIMENTS WITH PASSIVE CATHODES

2.1. Experiments with a coaxial diode

When a piece of dielectric insulator is put on the cathode surface, plasma is produced by "explosive emission" caused by the high electric field.[15] The coaxial diode, which we tried first, consisted of an inner cathode made of a conducting cylinder coated with a dielectric material and an outer wire mesh anode (see Figure 1a). The diode was driven by the UCI APEX pulse line of 1 mV, 7Ω, 50 nsec. A 14 kilogauss magnetic field was used for diode insulation. The same magnetic field was used for mass spectrometry of the particles ejected from the diode (Fig. 2). Ions emerging through a hole were deflected by the insulating magnetic field and traced via a CR-39 track detector. Faraday cup measurements of

the beam current were unsuccessful due to the beam divergence in the vertical direction. This diode is very useful for diagnostic purposes, but could not be used to produce an intense beam because of the beam spatial divergence.

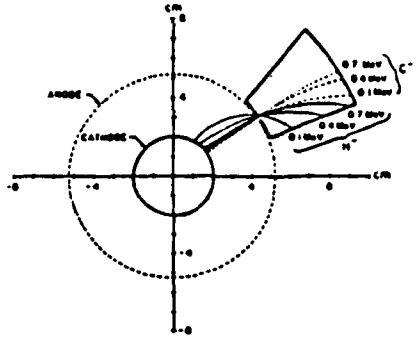

Figure 2. Ion mass spectrometry using the insulating magnetic field in the coaxial diode configuration.

With a polyethylene cathode beam intensity ranged between 1-5 A/cm^2 on the cathode surface. The beam consisted of H^- ions as well as C^- ions. Beam divergence in the azimuthal direction reached 0.3 radians at an energy of 100 keV and was about 70 milliradians at an energy of about 500 keV. CR-39 pinhole pictures of the beam revealed the existence of hot spots on the cathode surface. Negative ion emission from those spots was higher - with a larger horizontal beam divergence. The existence of C^- ions together with H^- ions was verified by combining ion deflection in the magnetic field together with different thickness Mylar films.

The second cathode we tried consisted of bare aluminum. Negative ion currents of about 0.5 A/cm^2 at the cathode surface with a divergence of less than 40 milliradian in the azimuthal direction were produced. Both H^- ions and C^- ions were detected. Beam mass spectrometry showed about 10% H^- ions, about 45% C^- ions, and about 45% heavier ions (probably C_2^-).

The third cathode we tried was made of graphite which produced currents of 1-3 A/cm^2 with azimuthal beam divergence of 40 milliradians. The beam consisted of C^- ions, a comparable amount of C_2^- ions and about 10% H^- ions. No hot spots were observed.

2.2. Experiments with a racetrack diode

Various types of cathodes were tried in the racetrack configuration (Figure 1b). Polyethylene covered cathode produced ion currents of 5 A/cm^2. Negative ions were emitted all along the high voltage pulse with a larger amount produced at the low energy part of the pulse When we put 2.5 μm thick mylar film on the Faraday cup the ions were stripped and the Faraday cup collected a positive current Only H^- ions with energies higher than 200 keV could penetrate this thickness of mylar. The beam usually consisted of 70% H^- ions and 30% carbon ions. Hot spots with higher ion emission and larger beam divergence were identified on the cathode's surface. Beam divergence was about 0.1 radians in the azimuthal direction.

Another type of cathode was a paddle covered with carbon brushes. The current density of the brush cathode reached 8-10 A/cm^2. Beam divergence was about 0.3 radians in the azimuthal direction.

2.3. Experiments with an annular diode

Negative ion current in the annular configuration (Figure 1c) was measured with two Faraday cups placed between the two magnetic coils. With polyethylene cathodes we got ion densities of about 2 A/cm^2 with divergence of 150 milliradians. When we used a carbon brushes cathode we got current intensities of 0.5 A/cm^2 with divergence of about 200 milliradians. Negative ions were emitted mainly from a few "hot spots" on the cathode surface.

3. EXPERIMENTS WITH ACTIVE CATHODES

3.1. The prepulsed plasma gun

The work reported by the Lebedev group reported that a prepulse is essential for getting measurable amounts of negative ions. Since in our case the APEX prepulse could not be controlled and the results of the passive cathodes used showed that plasma production is

inhomogeneous and of random nature, we built an independent prepulse plasma producing gun. Plasma creation time, as well as the density, can be controlled. The gun consists of an electrical circuit embedded in the cathode shank, and a plasma producing flashboard. The circuit floats on the APEX high voltage producing an output voltage of a few kilovolts with currents of a few kiloamperes.

The plasma gun circuit consists of a high voltage part, triggered by an external flash-tube light signal. The high voltage is obtained by a DC to DC converter which is energized by rechargeable batteries and charges a capacitor to 3 kV. The capacitor discharges through a spark gap to the primary of a transformer (1:2), the secondary of which is connected to the flashboard.

The flashboard was built from an array of 120 TiH_2 filled arcing groves and can be seen in Fig. 3. The plasma gun was usually operated under two different conditions: under low current arc (I ≈ 500 A; C = 0.25 μF), and under high current (I ≈ 3.2 kA; C = 5 μF). Plasma parameters were measured in both cases with a double Langmuir probe. Assuming that this was a pure hydrogen plasma one gets for the low current conditions a density of about $3 \times 10^{11}/cm^3$ with an electron temperature of 3.2 eV, and for the high current conditions a density of $2 \times 10^{12}/cm^3$ with an electron temperature of 1.6 eV. Plasma gun timing was measured with a fiber optics-photomultiplier system which measured the visible light emitted by the flashboard compared to the machine high voltage pulse timing.

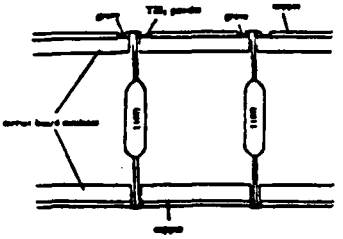

Figure 3. Plasma gun flashboard.

3.2. Experiments with a racetrack diode

With a low current plasma gun in a racetrack geometry ion current densities reached were 2 A/cm^2. Maximum current densities were reached for delay times (between plasma gun and machine firing) of 1-2 μsec and then decreased slowly as the delay became larger. Beam divergence was about 100 milliradians for a delay of 1.0 μsec.

Under high flashboard arc current conditions negative ion beam intensities were too low to be measured with a Faraday cup. The behavior is probably due to the fact that negative ions cannot exist in a plasma with a too high density. We then put a 30% transparent screen in front of the plasma gun. Ion current density measured was 0.5 A/cm^2. Beam divergence in the azimuthal direction was in this case only about 10 milliradian when delay was 1.0 μsec. With a delay of 2.5 μsec the beam divergence grew up to 60 milliradians.

3.3. Experiments with an annular diode

With a low flashboard gun current in an annular diode geometry we got negative ion current densities of about 6 A/cm^2 with a total current of ≈ 1000 A and beam divergence of 150 milliradians. The results had a good repeatability. Under high flashboard current conditions currents of about 3 A/cm^2 and divergence of 250 milliradians were observed. With a fine screen in front of the gun the current dropped to about 2 A/cm^2 with a divergence of 100 milliradians. No ions were measured with the Faraday cup for delay times smaller than 1 μsec. Maximum current intensities were reached for delay times of 1-2 μsec and then dropped slowly.

4. DIODE PHYSICS AT McDONNELL DOUGLAS

In a separate experiment conducted at the McDonnell Douglas Corporation, another pulsed magnetically insulated ion diode is being prepared. The facility is being used to investigate the formation of H^- ions in a working ion diode. This experiment follows from the work at UCI suggesting that pulsed magnetically insulated ion diodes may produce substantially greater H^- ion current densities than from conventional volume ionization sources.[19] An initiating discharge formed across a hydrogen containing dielectric (such as polyethylene or polypropylene sheets) placed on the cathode of the diode has been shown to be essential for obtaining the high current densities of H^- ions. The facility incorporates several diagnostics to study the physical mechanism involved in generation of high H^- yields. It also incorporates a cathode capable of generating uniform prepulsed surface discharges even

in a high vacuum.

The facility is shown schematically in Fig. 4. The diode, field coils, and necessary diagnostics are located in a cubical vacuum chamber measuring 41 cm on its side. The chamber has aluminum sides with electrically insulated feedthroughs to minimize pickup and ground loops. The base pressure of this chamber, $< 10^{-4}$ Pa, is sufficiently low that collisions of H^- ions with the background gases is not significant. The prepulse and extraction voltages are fed coaxially through a plexigas interface from a 61 cm long pressurized stainless steel chamber that also serves as the return for the extraction pulse line.

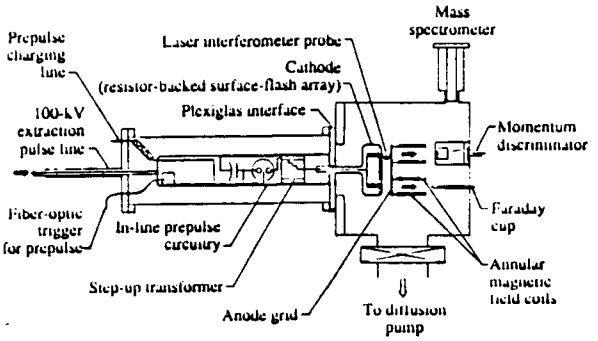

Figure 4. Surface-flashover facility

Incorporating the prepulse circuitry into the extraction line simplifies the connections made to the cathode. This in-line circuitry which comprises two 6 kV, 3 μF capacitors in parallel, a spark gap, a step-up autotransformer, and an optically fired trigger, is enclosed in a copper cylinder connected to the extraction pulse line. The circuit produces a 4 μsec, -20 kV pulse into 5 ohms and is triggered just before applying the extraction pulse, (100 kV, 100 nsec). A similar approach has been used at UCI to produce surface discharges over a TiH_2 substrate.[20] A brass screen attached with a 1 cm gap to a set annular magnetic field coils serves as the anode.

Uniformity of the preflashed discharges was a serious concern in designing the diode. One difficulty with using dielectric coverings over cathodes in a vacuum is that the preflash discharges frequently collapse into discrete arcs on the surface of the cathode. This results in poor beam uniformity and inconsistent shot-to-shot performance along with charring and channeling of the cathode surface. Such problems occurred especially in our investigations of cathode geometries with discharges forming over open dielectric surfaces in a vacuum. Such problems also impede the performance of measurements on the cathode, since the data from each shot must be treated individually and is not always reproducible.

A cathode usable in an ion diode that produces uniform prepulse discharges over its surface is being used in the facility. A schematic of the technique used is shown in a cross sectional view of the cathode in Fig. 5. An array of discharge tubes is created by drilling holes (3.2 mm in diam, 4 mm long) through a dielectric substrate placed behind a brass disk that serves both as an electrode for the array of discharge tubes as well as the cathode for the diode. Additional dielectric material may also be placed directly on the cathode. Resistors placed behind each tube distributes the prepulse evenly to all the tubes.

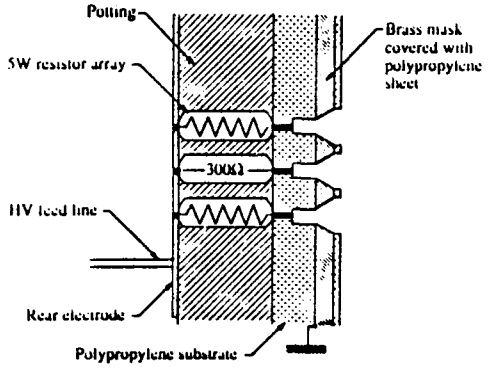

Figure 5. Cathode resistor array detail

Glow discharges form in each tube as dielectric material is evolved from the sides of the tube. The resulting plasma diffuses out onto the surface of the cathode. This technique may be used with a variety of dielectrics, although the prepulse requirement may vary.

Discharges more readily form over polypropylene than polyethylene. An array of 32 holes in polypropylene was successfully used for over 1300 shots with no observed charring. Open shutter photographs show that the discharges in this cathode fill each hole uniformly. The spectra of these discharges shows prominent hydrogen (particularly H_α) and carbon lines, while mass spectroscopic measurements of the residue gases following the discharges confirm that large quantities of H^+, H_2^+, C^+, CH_2^+, and higher hydrocarbons are produced. Also, preliminary measurements indicate that the quantity of mass evolved peaks at prepulse voltages between 20 and 25 kV. This may arise because the discharges contain too many runaway electrons which carry the bulk of the current without interacting with the walls. An annular array of 72 holes is currently being used in the cathode of the diode.

5. DISCUSSION

The results of measurements done on different diode geometries indicate that with passive cathodes negative ions are emitted from a few hot spots on the cathode surface. Beam divergence in these cases was largely due probably to transverse electric field caused by the inhomogeneous cathode plasma. The same phenomena was observed in positive ion diodes in regards to electron emission.[16] This problem causes severe ion deflection and diode closure in any high voltage diode. The plasma gun we built works on the high voltage electrode and enables one to produce a homogeneous plasma and control its production time and parameters. Perhaps the most important result we got with the gun is that the experimental data is quite reproducible, unlike the case of the passive cathode.

Negative ions are probably produced by neutrals emitted from the cathode surface. These neutrals collide with electrons in the negative electron charge layer. Since the electric field penetrates this layer[17] all negative ions are extracted and accelerated. Negative ion destruction by collision with other particles does not occur. The cathode plasma temperature should not exceed 1 eV. For 100 A/cm^2 negative ion current of a density of 5E14/cm^3 of H^- is required. Assuming a 10% population of H^- in the plasma and 1-10% total ionization we find that a density of 1E16-1E17/cm^3 is needed at the surface of the cathode. The mean free pass of the H^- in such an environment is about 50 micrometers and the lifetime is 2 ns. Russian work[18] indicated that a current of electrons of a few tens of kA/cm^2 is needed to maintain the production of the negative ions. The requirement of a sharp boundary of a 1E17 particles per cm^3 gas layer at the cathode is difficult to reach. The Russian work indicates that it can be done by a complicated sequence of prepulses or by a very large laser. We have had modest success with a low energy cathode plasma gun and in the near future we will try both an improved version of the plasma gun and a gas puff system that hopefully will give a better control on the neutrals.

6. ACKNOWLEDGEMENTS

This work was supported by SDIO/ONR.

7. REFERENCES

1. A. Fisher and N. Rostoker, Bull. Am. Phys. Soc. 21, 1097 (1976).
2. J. P. VanDevender, R. W. Stinnet, and R. J. Anderson, Appl. Phys. Lett. 38, 229 (1981).
3. R. W. Stinnet and T. Stanley, J. Appl. Phys. 53, 3819 (1982).
4. R. W. Stinnet and M. T. Buttram, Journ. Fus. Energy 4, 253 (1983).
5. R. W. Stinnet, M. A. Palmer, et al., IEEE Trans. Plasma Sci. PS-11, 216 (1983)
6. A. A. Agafonov, A. A. Kolomenski, et al., Zh. Eksp. Teor. Fiz. 84, 2040 (1983); Sov. Phys. J.E.T.P. 57, 1188 (1983).
7. A. A. Kolomenski, A. N. Lebedev, et al., Proc. of the 5th Int. Conf. on High Power Particle Beams (BEAMS '83), San Francisco (1983).
8. A. A. Kolomenski, I. I. Logachev, et al., Proc. of the 2nd European Workshop on Production of Light Negative Ions, Ecole Polytechnique, France (1986).
9. A. A. Kolomenski, I. I. Logachev, et al., 6th Int. Conf. on High Power Particle Beams (BEAMS '86), Kobe (1986).
10. S. Moustaises, H. J. Doucet, et al., 6th Int. Conf. on High Power Particle Beams (BEAMS '86), Kobe (1986).
11. H. Doucet, 4th Int. Symp. on Production and Neutralization of Negative Ions and Beams, Brookhaven, NY (1986).
12. V. M. Bistritski, Ya. E. Matrienke, et al., 6th Int. Conf. on High Power Particle Beams (BEAMS '86), Kobe (1986).
13. A. Fisher, H. Lindenbaum and N. Rostoker, 6th Int. Conf. on High Power Particle Beams (BEAMS '86), Kobe (1986).
14. A. Fisher, H. Lindenbaum and N. Rostoker, Int. Soc. for Optical Engineers Innovative Science and Technology Symposium (SPIE), Los Angeles (1988).
15. S. P. Bugaev, E. A. Litvinov, et al., Sov. Phys. USP 18, 551 (1975).
16. Y. Maron and C. Litwin, Phys. Fluids 30, 1526 (1987).
17. Y. Maron, M. D. Coleman, D. A. Hammer and H. S. Peng, Phys. Rev. A 36, 2818 (1987).

18. V. A. Papadichev, "Intense Negative Ion Propagation in High Power Diodes", 7th Int. Conf. on High Power Particle Beams (BEAMS '88), Karlsruhe (1988).
19. A. Fisher and N. Rostoker, Bull. Am. Phys. Soc. 21, 1097 (1976).
20. A. Fisher, H. Lindenbaum, N. Rostoker, C. E. Wiswall, S. L. Cartier, and J. C. Leader, Int. Soc. for Optical Engineers Innovative Science and Technology Symposium (SPIE), Los Angeles (1988).

SPIE '90, Los Angeles, California, January 14-19, 1990 1226-47

INTENSE H^- BEAM PRODUCTION IN A MAGNETICALLY INSULATED ION DIODE

A. Fisher, R. Prohaska, H. Lindenbaum, G. Sheperd and N. Rostoker

University of California
Department of Physics, Irvine, California 92717

ABSTRACT

Gas puff cathodes offer a flexible system to study the mechanism of the negative ion formation in a pulse power-driven cathode. A magnetically insulated gas puff diode has been built at UCI and the formation of H^- has been studied. Hydrogen, ammonia, butane and oxygen were investigated. Very low current less than 100 mA/cm^2 of H^- was measured when hydrogen or ammonia were puffed into the diode. Butane and oxygen produced at least ten times higher current density. Probably the negative ion production in the butane gas puff source and in the solid polyethylene cathode source is due to the interaction of electrons with long hydrocarbon chains. This mechanism doesn't require the formation of highly excited H_2, which is needed if one assumes the source of the H^- is molecular hydrogen interacting with electrons. Because oxygen is an electro-negative gas, it was expected that negative ions would be produced. These ions were used to test the negative ion diagnostic. The divergence of the ion beam coming from the gas puff cathode was about 10 mr. This is the lowest divergence that has ever been measured at UCI. Improved nozzles that will produce higher gas gradient between the cathode and the anode will be tested in the future.

1. INTRODUCTION

The production of neutral particle beams with energy over 100 kV requires starting with weakly bound negative ions which can be accelerated and then stripped to neutrals. Many workers[1] have studied the problem of producing negative ions, usually H^-, in steady state plasmas. We are investigating the use of transient plasmas and gas puffs in conjunction with magnetically insulated ion diodes to explore the possibility of obtaining high (kiloampere) currents of negative ions.

In plasmas H^- is produced most commonly by dissociative attachment in which a slow electron collides with and sticks to a molecule. The molecular ion then breaks into two or more fragments including the desired negative ion. Collisions between negative ions and the seed neutrals from which they are produced naturally eliminate negative ions and the current density obtained is always limited by the relative cross sections for attachment and detachment.

The probability of dissociative attachment depends strongly on the energy of the collision and is usually expressed as a cross section which has been tabulated[2] for a variety of (simple) molecules. Generally the optimum energy is not more than a few eV. Relatively little attention has been paid to polyatomic molecules of the kind which yield the best results in pulsed diodes.

The dissociative attachment cross section is on the order of ? x 10^{-20} for ground state H_2. The ionization cross section is a few orders of magnitude larger. The current density of steady state gas discharge (Penning) sources can be up to 1 A/cm^2 but the total area is small, usually less than 1 cm^2. Surface plasma sources, in which negative ions are formed in contact with a heated cesium loaded surface, give

on the order of .1 A/cm^2 with a total current of a few amperes. Vibrationally excited hydrogen is reported[3,4] to have several orders of magnitude larger cross section but the highly collisional conditions needed to cause the excitation result in prompt destruction of any negative ions formed.

The introduction of large density gradients in the cathode plasma minimizes the problem of destructive collisions. Usually the density gradients are produced by allowing a dielectric surface to flash over evaporating some of the dielectric into a thin, dense layer of neutrals and plasma. What negative ions form then have a reasonable chance of escaping through the cathode plasma.

2. PASSIVE CATHODES

Polyethelene is the most popular dielectric surface for making proton beams and is the best precursor for making negative ions. Carbon contamination is always a problem. Carbon forms stable negative ions with more binding energy than H^-; we used thin foils to stop the carbon selectively. A serious complaint is the difficulty in obtaining a uniform cathode plasma which is prerequisite to obtaining a well collimated beam. Normally a dielectric surface breaks down at a few points on the surface producing wildly diverging beamlets. Drilling arrays of holes in the dielectric surface tends to induce breakdown at each hole but large (megavolt) cathode potentials are required. The result is an array of hot spots which tends to produce a divergent beam.

Our work was inspired by Kolomensky's report[5] of more than 100 A/cm^2 negative hydrogen ion current from passive polyethelene cathodes in a cylindrical diode. We tried without success to confirm the report.

Prompt diagnostics consisted of a pair of Faraday cups biased to collect secondary electrons, one of which was covered with a 2μ mylar foil to strip H^- to H^+ and stop any high Z ions like C^-. The Faraday cups were carefully shielded and we could see currents down to about 1-2 mA/cm^2. Upon getting an ion signature (shown in Fig. 1 for the coil covered Faraday cup) we installed CR-39 track recording plastic either open (to count particle tracks) or in a pinhole camera to study cathode plasma uniformity and beam divergence. A single layer of 2μ mylar protected the CR-39 from C^-. A fiber optic and photomultiplier system measured the amount and timing of light emission from the cathode. Cathode voltage for ion extraction was provided by a 700 kV, 7 ohm 50 ns pulseline machine with the usual voltage, current and insulation field monitors.

The first experiments were basically a copy of the cylindrical diode experiments done at the Lebedev Institute. There was one important difference: Our machine had a negative prepulse of only about one percent, occurring shortly (250 ns) before the output pulse. The results were null: no H^- was seen.

Upon learning of the huge bipolar prepulse (15-30 percent, 1-2 μs) on the machine used for the early work we attempted to increase ours by removing the prepulse suppression resistor. This had the effect of increasing the prepulse to about 10 percent, but the timing was unchanged and the polarity was negative, in contrast to the positive and negative swing seen on the Russian machine. We observed about 10 A/cm^2 from cathode hot spots, with 1-2 A/cm^2 if we average over the entire cathode. The reproducibility was poor and the divergence varied from 100-300 mr.

These results fell far short of the promise of the initial report, but were not surprising given that we had a much smaller prepulse which occurred only a few hundred nanoseconds before the main pulse. In our experiments, the Faraday cup signals were in the form of short pulses, usually not more than 10 ns in duration at the start of the diode voltage pulse, implying that we were extracting an accumulated population of ions. The Russian workers used nuclear activation methods to monitor ion production, so the time dependence of the ion flow is not known. It seemed likely that we needed to form a cathode plasma, and then wait for an appreciable time (some microseconds) to give negative ions time to form before applying extraction voltage.

3. ACTIVE CATHODES

3.1. Plasma flashboards

It was decided to develop an active (self-powered, independently triggered) cathode[6] based on plasma sources we developed for other applications. That gave us independent control over the amount of energy invested in the cathode plasma and the timing of its creation.

If a spark is drawn between titanium hydride electrodes a relatively clean hydrogen plasma results, but the usual method is to apply tens of kilovolts to a single electrode which breaks down to form a point source of plasma. We have developed a flashboard plasma source capable of generating surface densities on the order of 10^{16} over 200 cm^2.

Titanium hydride powder is somewhat conductive, and if it is attached to an insulating surface with sodium silicate binder the resulting paint breaks down between grains at the application of only a few kilovolts. The discharge can be made uniform over an area of more than one square centimeter and the low voltage makes it easy to subdivide the flashboard coating into small cells with ballast resistors. The flashboard assembly for the annual diode is shown in Fig. 2.

The entire system consists of a copperclad circuit board which forms the substrate of the flashboard, a capacitor discharge circuit to deliver the needed energy and an optical trigger circuit (Fig. 3) to synchronize the flashboard to the beam generator. The flashboard is mounted on the face of the cathode, while the rest of the circuitry resides in the cathode shank. This arrangement was necessitated by the design of the beam generator, which uses an interface too thin to house isolation inductors or other electrical penetrations. For this reason it was decided to make the active cathode completely self-contained and electrically isolated.

A capacitor was charged to 2.7 kV by a DC to DC converter powered by NiCd batteries. A small ceramic metal spark gap switched the capacitor into an isolation transformer which then drove the individual cells of the flashboard through ballast resistors. The spark gap was triggered by a krytron triggered by an SCR triggered by a FET triggered by a photodiode. The delay from photodiode to flashboard was only a few microseconds, with about half a microsecond jitter.

Two modes of operation were used. In the high current mode the storage capacitor was 2 μF and the discharge current was 3.2 kA. In the low current mode a .25 μF capacitor was used, with a total discharge current of about 800 A.

The plasma production characteristics were studied using Langmuir probes and light output to determine the temporal and spatial evolution of the plasma. Measurements were made using a double probe in the racetrack diode configuration without insulation or accelerating fields. The plasma had a density of 3 to 13 x 10^{11}/cm^2 at a distance of 4-7 cm and an expansion velocity of 8 cm/μs. Application of a .3 T field effected complete confinement to the resolution of the probe (1 cm). Open shutter photographs demonstrated uniform breakdown of each section as shown in Fig. 4.

The plasma temperature appeared to be somewhere between 1 and 3 eV. The binding energy for H^- is only .6 eV while the ionization energy for H^+ is 13.6 eV. Obviously H^- is not a favored state, but we hoped to find something in the cold end of the distribution.

The active cathode system was tried in both racetrack and annular geometries, and performed about the same in both cases. The best results were 6 A/cm^2 (average over 100 cm^2) with about 10 mr divergence using the low current mode and 1.5 μs delay between the onset of plasma light and application of accelerating voltage. An illustrative Faraday cup trace is shown in Fig. 5.

3.2. Gas puff cathodes

Density gradients can also be made using a fast valve to create a gas puff with a risetime short compared to the gas transit time across the anode-cathode gap. The idea was to construct a cathode plasma in which dense cold gas expands through a region occupied by a swarm of trapped, slow electrons in the presence of a strong electric field. The applied field removes the ions as they form, before destructive collisions can occur. It is well known that fiber cathodes ignite uniformly at low fields, and we have incorporated carbon fibers as electron emitters into our ion diode designs. In its present form the gas is emitted from small apertures surrounding carbon fiber bundles which serve as cathodes. Figure 6 gives a sectional view of the cathode assembly and puff valve. Figure 7 shows the electrical circuit which operates the valve.

The choice of gas presents some difficult compromises. Hydrogen would be the cleanest source, but the dissociative attachment cross section in cold gas is only 2 x 10^{-20}. It has been reported that the dissociative attachment cross section is several orders of magnitude larger for hydrogen which is in a high state of vibrational excitation. The achievement of high vibrational excitation has been attempted[7] by passing the puffed gas through an arc at a few atmospheres, but it must then be allowed to expand freely: Wall collisions will de-excite it, and unless the density is lowered H^- has no chance for survival.

We made an attempt to measure H^- production from cold H_2 puffs but could measure no ions and decided to resort to more complex molecules which had larger published cross sections for dissociative attachment.

Ammonia would seem to be a good candidate with a large cross section(57 x 10^{-19} cm^2) and no contamination (there is no stable N^-) but it gave no measurable ion flux. We also tried loading the cathode fibers with borane ammonia, a complex of BH_3-NH_3, in the hope of seeing H^- derived either from the ammonia or borane. The attachment cross section for borane is not known but the published value[2] for silane SiH_4 is enormous; 2.2 x 10^3. No H^- was detected. We did not attempt to use silane gas because of its reportedly toxic and pyrophoric nature.

We decided to try a hydrocarbon puff to see if a long molecule worked better. It was speculated that large molecules with many internal vibrational modes could make less elastic collisions with electrons and exhibit higher cross section. Unfortunately we could find no published figures for molecules having more than 5 atoms.

Butane was the longest chain hydrocarbon which we could easily use in the valve. It gave about 10-20 mA/cm^2 of H^-. The resulting beam exhibited very good divergence of about 10 mr. The high molecular weight limited the mobility of the gas and we were able to puff in enough gas to load the diode without shorting it.

That butane worked better than ammonia or borane ammonia leads us to suspect that molecular structure is somehow important. The pressure in the gas puff was lower in the case of butane than any other, so we were working with less starting density. The density gradients were probably smaller than in the case of the borane ammonia loaded cathode fibers.

One of the persistent problems with gas puff diodes has been gas breakdown due either to gas reaching the electrical terminals or strong electric fields due to the rapid rise of the magnetic field. The result of any anode plasma formation in the diode is a short. We experimented briefly with a diode in which the anode was in the form of a solid plate of graphite in the hope that it would keep the gas away from high electric field regions and so avert any breakdown. Ions were to be extracted through a small number of ports in the plate. The result was a significant increase in electron leakage and a complete absence of negative ions.

4. SUMMARY

Three approaches to the production of intense H^- beams have been explored. Passive polyethelene cathodes give the highest current density but suffer from divergence and reproducibility problems. Titanium hydride flashboard cathodes give much better divergence and reproducibility with nearly comparable current density. Gas puff cathodes provide good divergence but the lowest current density. We expect that better results will come from other gases. A summary of results is given in Table 1.

We suspect that the quality of the magnetic insulation is important for much more than limiting the flow of leakage electrons. Any dissociative attachment process depends on having collision energies of no more than a few eV. If the magnetic insulation is leaky electrons gain energy temporarily as they gyrate through the cathode field. Energy transfer to the electrons of only a few parts per million is sufficient to ensure that collisions will be too violent to permit the formation or survival of negative ions.

Table 1.

Summary of Results for Various Cathodes

CATHODE TYPE	CURRENT DENSITY A/cm^2	COMMENTS
Polyethelene	10 A/cm2 peak (1-2 A/cm2 average)	large divergence poor reproducibility
Active titanium hydride	6 A/cm2 (average)	Good divergence and reproducibility
Hydrogen puff	<1 mA	
Butane puff	0.015	Good divergence (10 mr) and reproducibility
Borane Ammonia loaded fibers	<2 mA	
Ammonia puff	<2 mA	
Oxygen puff	0.1	Open Faraday cup

5. ACKNOWLEDGEMENT

This work was supported by the Office of Naval Research/SDIO.

6. REFERENCES

1. Production and Neutralization of Negative Ions and Beams. This is a series of symposia held every two years.

2. S. K. Srivatava, Present Status of the Measured Dissociative Attachment Cross Sections in Proceedings of the Fourth International Conf. on the Production and Neutralization of Negative Ions and Beams, Brookhaven, NY, 1986, p. 69.

3. K. N. Leung and W. B. Kunkel, Phys. Rev. Lett. 59, 787 (1987).

4. J. M. Wadera and J. N. Bardsley, Phys. Rev. Lett. 41, 1795 (1978).

5. A. A. Kolomensky, A. N. Lebedev et al., Proceedings of the Fifth International Conf. on High Power Particle Beams, San Francisco, 1983, p. 533.

6. Hayim Lindenbaum, Production of Intense Negative Ion Beams in Magnetically Insulated Diodes, PhD Thesis, University of California, Irvine, 1988.

7. R. J. Turnbull, S. R. Walther and J. L. Guttman, Generation of Vibrationally Excited Hydrogen for use in a Negative Ion Source in Proceedings of the Third International Symposium on the Production and Neutralization of Negative Ions and Beams, Brookhaven, [illegible], p. 132.

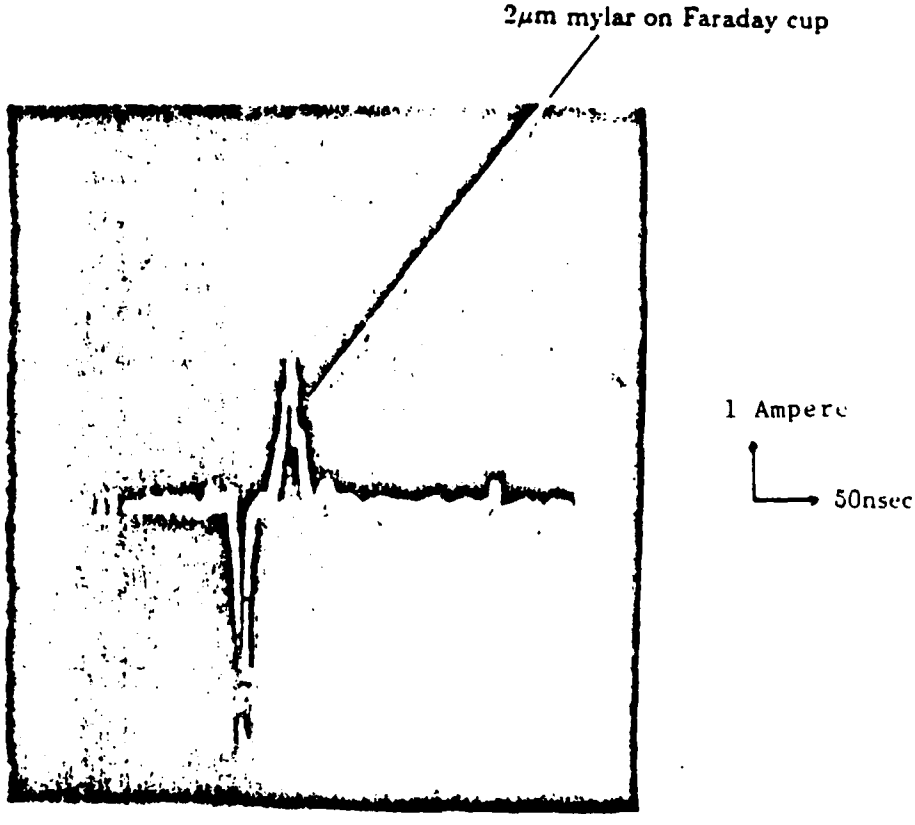

Figure 1. Ion signature on a foil covered Faraday cup from a passive polyethelene cathode.

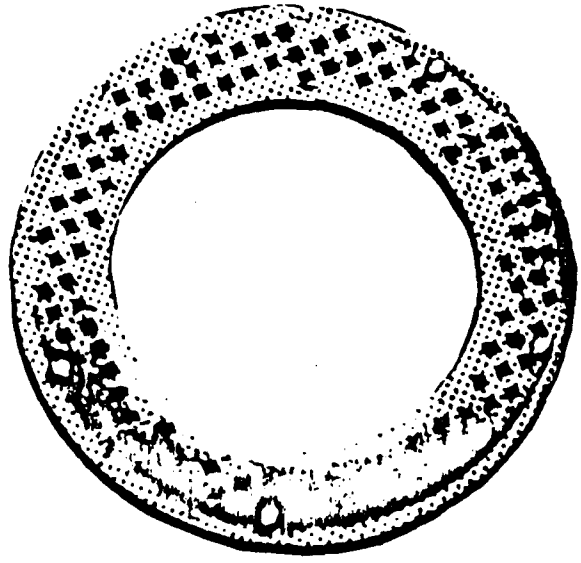

a: Flashboard front view.

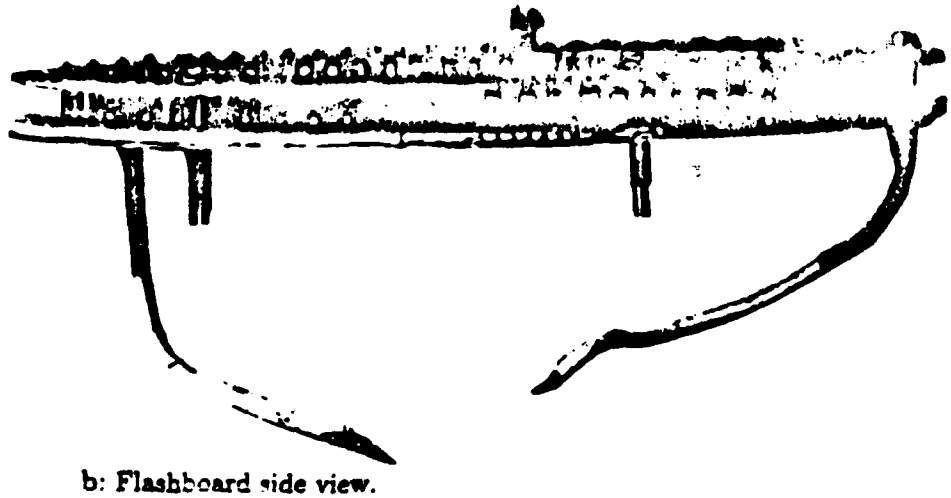

b: Flashboard side view.

Figure 2. Flashboard assembly for the annular diode

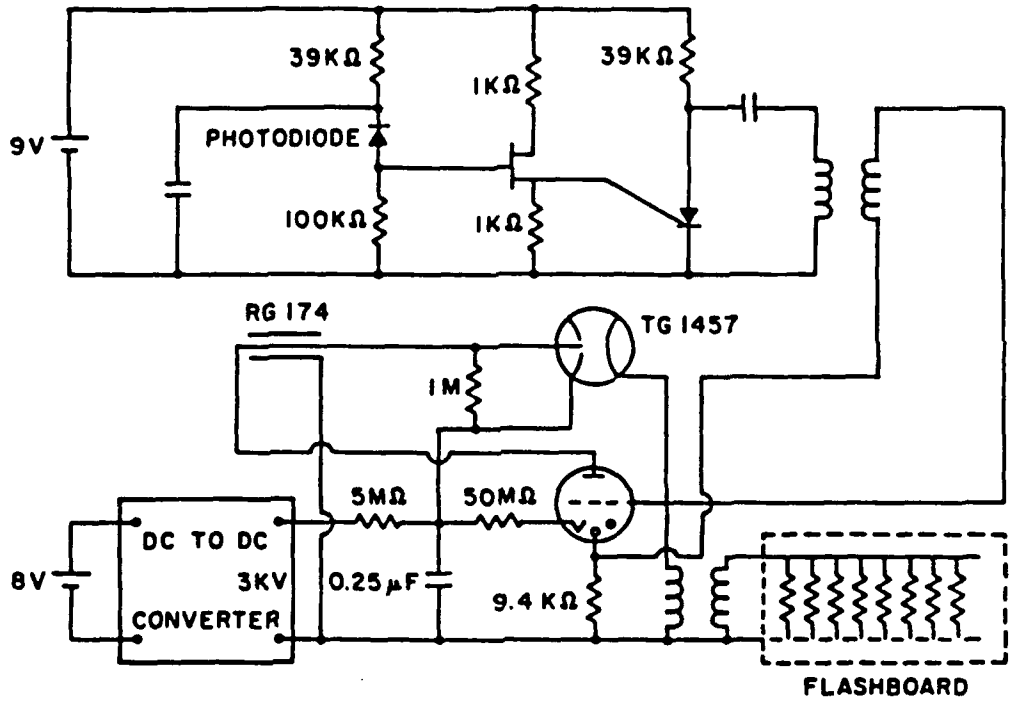

Figure 3. Capacitor discharge and optical trigger circuits for the flashboard cathode.

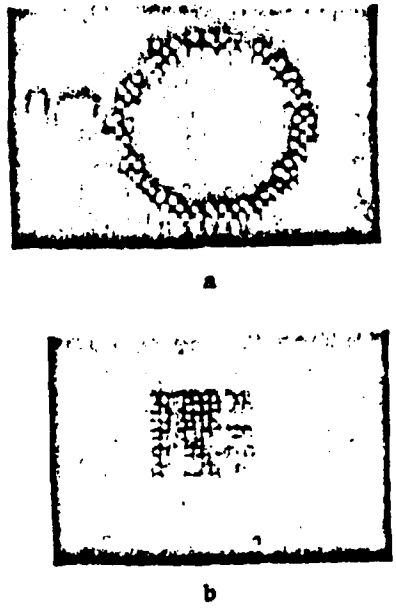

Figure 4. Open shutter photographs of flashboards in operation.

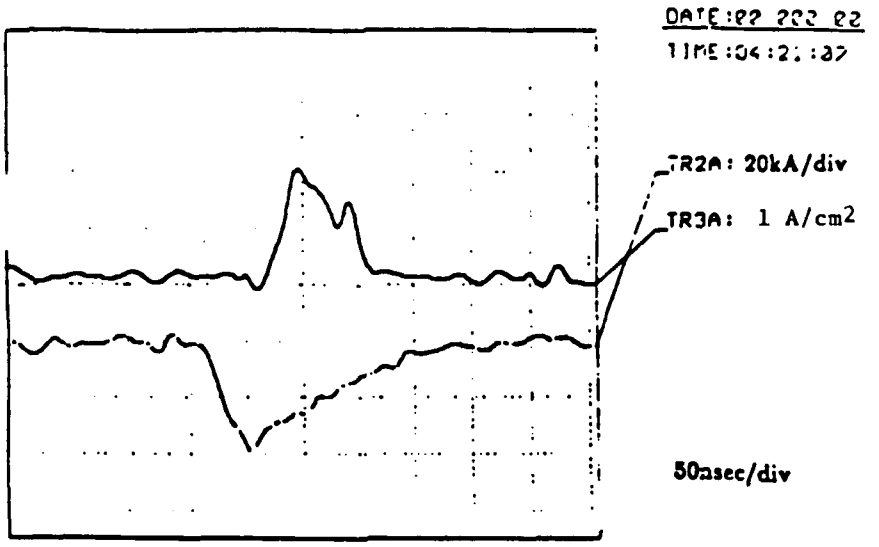

Figure 5. Ion current trace from a flashboard cathode.

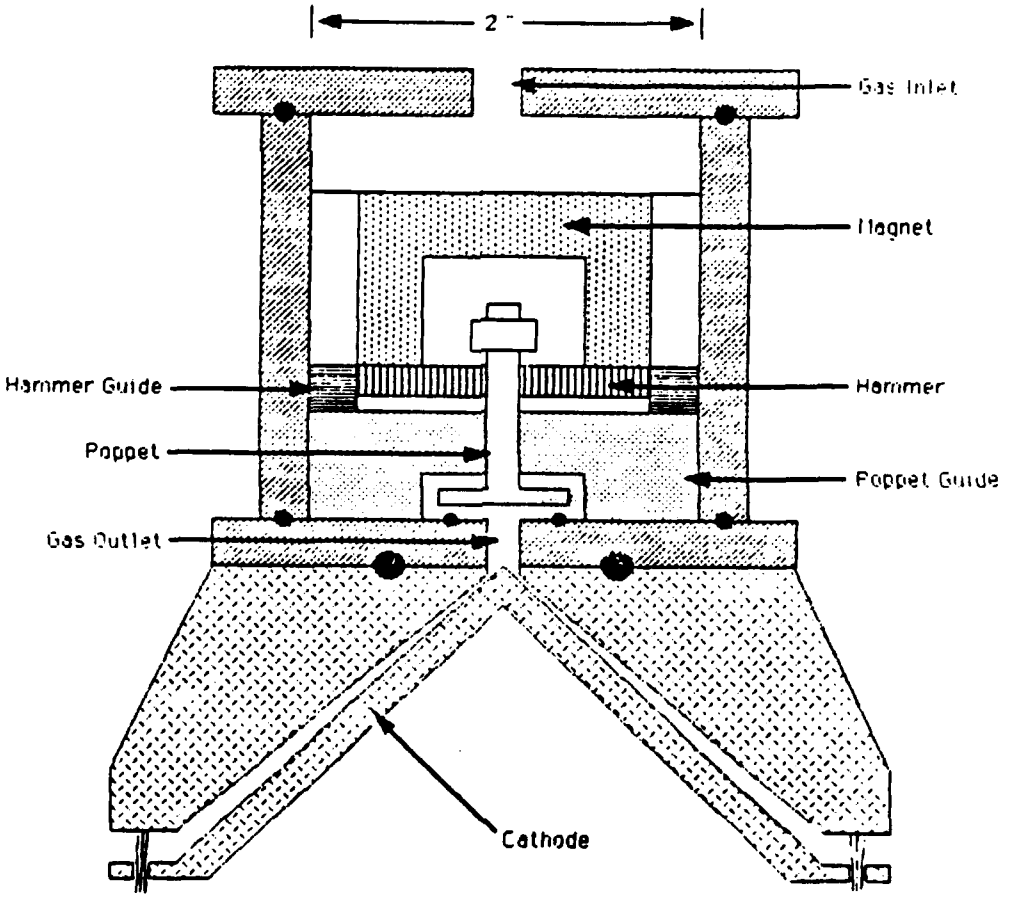

Figure 6. Gas puff cathode and valve.

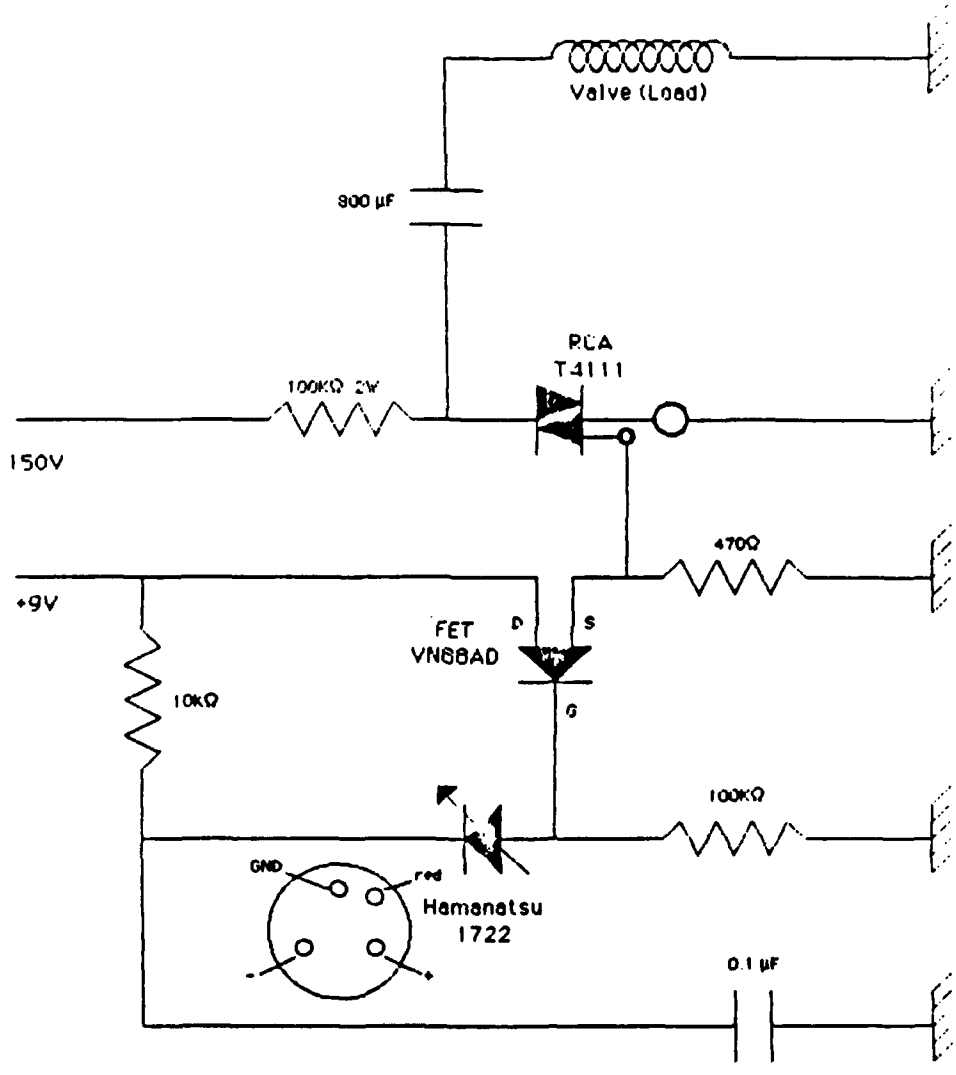

Figure 7. Control circuit for the puff valve.